International Journal of

Biology

and Chemistry

Al-Farabi Kazakh National University

EDITORIAL

The most significant achievements in the field of natural sciences are reached in joint collaboration, where important roles are taken by biology and chemistry. Therefore publication of a Journal, displaying results of current studies in the field of biology and chemistry, facilitates highlighting theoretical and practical issues and distribution of scientific discoveries.

One of the basic goals of the Journal is to promote the extensive exchange of information between the scientists from all over the world. We welcome publishing original papers and materials of biological and chemical conferences, held in different countries (by prior agreement, after the process of their subsequent selection).

Creation of International Journal of Biology and Chemistry is of great importance, since scientists worldwide, including other continents, might publish their articles, which will help to widen the geography of future collaboration.

The Journal aims to publish the results of the experimental and theoretical studies in the field of biology, biotechnology, chemistry and chemical technology. Among the emphasized subjects are: modern issues of technologies for organic synthesis; scientific basis of the production of biologically active preparations; modern issues of technologies for processing of raw materials; production of new materials and technologies; study on chemical and physical properties and structure of oil and coal; theoretical and practical issues in processing of hydrocarbons; modern achievements in the field of nanotechnology; results of studies in various branches of biology, chemistry and related technologies.

We hope to receive papers from the leading scientific centers, which are involved in the application of the scientific principles of biological and chemical sciences on practice and fundamental research, related to production of new materials, technologies well ecological issues.

U.N. Kapysheva [ID], Sh.K. Bakhtiyarova [ID], Y.K. Makashev [ID],
B.I. Zhaksymov * [ID], A.B. Junussova [ID], A.M. Kalekeshov [ID],
Y.Y. Makashev [ID] B.A. Mukhitdin [ID]

Institute of Genetics and Physiology, Almaty, Kazakhstan
*e-mail: bifara.66@mail.ru

Innovative approaches to improving the quality of feed base of farm animal to ensure competitiveness of animal products

Abstract. One of the most promising areas in Kazakhstan at present is the production of feed additives based on plant materials with mineral components. This article describes the use of a feed additive made from green plant materials obtained by growing the traditional cereal crop *Hordeum vulgare* (barley) from the family Poaceae, and the non-traditional fodder crop *Rumex confertus* (sorrel) from the family Polygonaceae, with the addition of locally produced montmorillonite and additional ingredients – calcium phosphate, potassium iodide and urea, which are necessary for metabolic processes in a growing organism and improve the nutritional qualities of milk and meat. The effect of a combination of plant components with the addition of mineral additives on the biochemical parameters of young sheep is shown. A significant (2-3 times) increase in concentration of protein, glucose, cellular enzymes alanine aminotransferase (ALT), aspartate aminotransferase (AST), bilirubin, alkaline phosphatase and urea was noted, which may indicate a high calorie content of the additive and the absence of factors contributing to pathological deviations in the development of animals.

Key words: feed, farm animals, biochemistry, feed mixture, rumen fluid, protein-carbohydrate metabolism, fat metabolism.

Introduction

The socio-political stability and food security of a country depend on the level of development of the agricultural sector as the most important branch of the state economy. Ensuring the country's food security in the context of the aggravated situation on world food markets requires an active regulatory role of the state. Kazakhstan, a country with historically strong agricultural traditions, can become a leading world producer of agricultural products in the current conditions of global economic instability, climate change and an unstable price system. The natural conditions of Kazakhstan and its biodiversity create significant potential for the development of animal husbandry. Traditionally, the republic is engaged in sheep, horse, camel and cattle breeding. Livestock and crop products are produced in state, cooperative and joint-stock agricultural enterprises, in peasant and peasant households, and on private subsidiary plots. However, the competitiveness of agricultural enterprises in the Republic of Kazakhstan is still significantly worse than the requirements of the time [1].

The lack of investment in agriculture hinders the widespread introduction of effective technologies, modern equipment and the use of scientific achievements. Only in recent years has the industry begun to actively focus on increasing the efficiency and competitiveness of domestic producers, reducing food dependence and providing the country's population with high-quality and safe agricultural products [2].

The development of livestock breeding in Kazakhstan is the main direction of the agro-industrial sector and provides more than half of the gross agricultural production. Despite the measures taken, domestic livestock products often cannot withstand competition from foreign producers. One of the main reasons for this is the weak feed base. Although Kazakhstan is a grain producer and one of the world's largest flour exporters, its feed milling industry is underdeveloped. The feed produced by the enterprises does not meet the quality requirements

of agro-industrial production. Feed mills are located in different regions of the country, and the lack of competition in this area makes them monopolists in the feed industry, which leads to higher prices for livestock products on farms [3].

Only in recent years, according to the Statistics Committee, the market for ready-made feed for farm animals, including feed production, has shown a gradual increase of 10-20% per year [4]. However, a major problem in the development of animal husbandry is the lack of nutrients in prepared feed, which disrupts the feeding conditions at different periods of the ontogenesis of farm animals [5]. The development of scientific approaches to the problems of industrial agriculture is often associated with the introduction of new technologies in feed production and an increase in productivity. For example, the acquisition of feed mixtures that promote more complete use of feed protein is of great importance [6].

The main objective of this study is to develop a cheap and cost-effective feed mixture based on the use of green mass of traditional and non-traditional forage plants, natural adsorbents, trace elements and vitamins that compensate for the lack of nutrients, activate the assimilation process and ensure the safety and quality of livestock products.

Materials and methods

Experimental material. The studies were conducted on 45 Degeres meat-and-wool fat-tailed sheep kept on fattening sites of 2 farms in the Karasai district of the Almaty region.

Design of the experiment. The rams were 5–6 months old, with an initial weight of 32–33 kg, and were divided into 2 groups: control (20) and experimental (25 rams). The control group was fed a standard daily diet, while the experimental group was supplemented with a standard feed supplemented with a granulated feed additive at a rate of 5-6 g per 1 kg of weight, an average of 180-200 g per day per sheep.

Obtaining feed additive. To obtain the feed mixture under laboratory conditions, we use the technology of using ionized water developed and tested by us, which allowed us to increase the germination of the plant mass of cultivated crops and quickly obtain green mass both in closed and open areas of farms. The main source of active compounds in the feed additive was the green mass obtained within 2-3 weeks from the germinated grain plant *Hordeum vulgare* (barley), Poaceae family, and the

non-traditional forage plant *Rumex confertus* (sorrel), Polygonaceae family, with a height of up to 40-50 cm. Green barley is characterized by a high content of macro and microelements, as well as vitamins of group B. Forage sorrel of the variety "Rumex-K-1" provides the feed mixture with a high content of protein, ascorbic acid and essential amino acids. The complex of these plants contains protein, micro and macroelements, essential amino acids necessary for the growing organism of animals in sufficient quantities.

To obtain the feed mixture, bentonite, dried and crushed green mass, dry crushed barley grain and additional ingredients were mixed: calcium phosphate, potassium iodide, urea, to improve the absorption and digestibility of plant feed. The ratio of additional components was 150 g – 500 g of ground dry barley grain, 30 g of bentonite, 300 g of green mass, 20 g of ingredients with active substances. The feed granules were prepared in a special container with constant stirring until a wide mass was formed and passed through an extruder. The resulting granules were then dried on special stands in the open air. The degree of maturity of the raw materials was determined by the following features: the granules should be hard, easily crushed and crumble into pieces with light pressure. When storing the feed additive in bags, sanitary and technical conditions were observed – room temperature, containers used, humidity, in accordance with the requirements of the regulations developed in the country [7,8].

Blood collection. The collected blood is stabilized with heparin (2-3 U/ml), centrifuged (10 min at 1500 rpm), and the plasma is separated from the erythrocytes. In the blood plasma samples in vivo, the level of lipid peroxidation is determined by the content of intermediate (diene conjugates), final (malonic dialdehyde) peroxidation products and catalase activity. Blood was collected before and after 21 and 42 days of feeding the sheep with the feed additive, biochemical parameters in the blood plasma were determined [9,10].

Spectrophotometric analysis of animal blood plasma. The assay was performed on a biochemical analyzer Biosystems A-25 (Biosystem S.A., Spain) using test kits. Albumin – reagent code 12547, total protein – reagent code 12500l, ALT reagent code 12533, AST reagent code 11830, creatinine (Jaffe method) – reagent code 12502, glucose – reagent code 11803, bilirubin – reagent code 11510, triglycerides – reagent code 12528, magnesium – reagent code 11797, phosphorus – reagent code

12508. These reagents were purchased from the company Biosystem S.A., Spain.

Analysis of oxidative stress reaction in animal blood. The reaction was determined by the content of the final product of the lipid peroxidation – malondialdehyde (MDA), by the reaction with 2-thiobarbituric acid (maximum absorption at 535 nm) and the intermediate product of lipid peroxidation – diene conjugates (DC) [11]. The state of the antioxidant system was determined by the activity of the key enzyme – erythrocyte catalase (EC), which is involved in interrupting the chain of free radical processes [12]. Statistical processing of the results was carried out using Microsoft Excel 2007, the significance of intergroup differences was assessed using Student's t-test for independent variables. Differences were considered statistically significant at $p<0.05$. The data is presented as follows: arithmetic means ± standard deviation (M±SD) [13].

Ethical approval. In studies on farm animals, we were guided by the decision of the Local Ethics Committee, Institute of Genetics and Physiology, Protocol No. 6 from November 3, 2022.

Results and discussion

The average weight of sheep in the control and experimental groups at the initial level fluctuated within 34.03±2.8 kg. On the 42nd day of the experiment, the weight of the control animals (n=20) fluctuated from 37.5 to 40.5 kg, in the experimental group (n=25) – from 40.1 kg to 43.8 kg, averaging 39.3±1.4 kg and 41.8±1.8 kg, respectively (Figure 1).
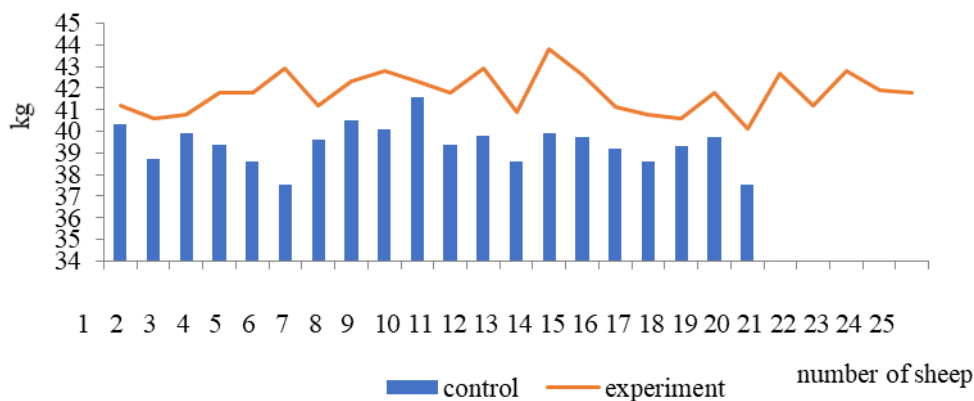

Figure 1 – Body weight growth of sheep in the control (n=20)
and experimental (n=25) groups on day 42

As can be seen from the results presented in Figure 1, the daily weight gain in the control group fluctuated within 125 g per sheep, in the experimental group the average weight gain was 18 per sheep.

The initial level of cellular fractions in the blood (leukocytes, lymphocytes, erythrocytes, hemoglobin) in the sheep of the control and experimental groups fluctuated within the physiological norm. After the introduction of the feed additive into the daily diet of animals for 42 days, in the experimental group of sheep the number of erythrocytes increased by 30%, and the concentration of hemoglobin increased by 10%, which indicates an improvement in the functions of the cardiovascular system. An increase in red blood cells provides a sufficient level of oxygen in muscles and tissues and promotes the active development

of adaptive mechanisms regulating metabolic processes during the growth of young farm animals [14,15].

The reaction of the rumen environment determines the state of enzymatic processes and the degree of absorption, with a neutral reaction pH = 7.0 units. In ruminants, pH fluctuates from 6.5 to 7.2 units, alkaline reaction – more than 7.0 units, acidic – less than 5.4 units [15].

The study of the rumen fluid of the control sheep showed a shift in pH to the acidic side (5.9 units), which is typical when feeding animals with easily digestible carbohydrates (grain concentrates). In the experimental sheep, on the 42nd day (validation is presented below) after adding the feed additive developed by us to the daily diet of the animals, some

animals showed a restoration of the neutral pH level to 6.6 units, while others had a shift to 7.1 units to the alkaline side. An increase in dry matter and ammonia in the rumen fluid of the experimental sheep by 10-12%, amylolytic (carbohydrate digestion) activity by 8-10%, an increase in protozoan and microbial mass by 4-5% were noted, compared with the data of the control group (Table 1).

Table 1 – Changes in rumen fluid of experimental sheep before and after the introduction of the feed additive into the daily diet of sheep

Indicator	Control	
	Control	
	42 days	42 day
pH	5.90±0.15	6.60±0.11
Dry matter, %	3.40+0.16	3.80±0.05
Degree of fermentation, cm^3/gas	1.16±0.26	1.11+0.09
Fiber digestibility, %	14.5+3.1	47.9±4.7*
Ammonia, mmol/l	40.0+1.9	44.3±0.7*
LFA, mEq/100 ml	14.5+1.0	15.4±0.6*
Proteolytic activity, %	14.6+3.6	30.3±3.5*
Amylotic activity, %	72.7±8.5	78.9±4.6*
Protozoan mass, mg	40.0±1.4	41.8±3.6
Microbial mass, mg	130.0+11.4	135.0±12.2

*Note: significant compared to control, $p<0.05$

In the rumen fluid of the control group of sheep, an increase in oxidative processes and fermentation activity, low digestibility of complex carbohydrates (fiber) and proteolytic (protein breakdown) activity are observed. In the experimental sheep, the pH was restored with a tendency to shift the pH to the alkaline side, the degree of fermentation decreased, and the ammonia level increased, which indicates an increase in proteolytic activity and absorption of ammonia into the blood. A slight increase in various microorganisms in the rumen of the experimental sheep indicates an increase in metabolism and synthesis of vital amino acids and vitamins [16].

The results of the studies of the sheep rumen fluid showed an improvement in amylolytic activity and an increase in microbial mass after using the

feed additive compared with the data of the control group. Blood biochemical studies in the control group of sheep fed with standard diet showed low levels of albumin (by 15-16%), glucose (by 20%) and creatinine (by 35%), which is below the average normal value for sheep [17].

A 2.3-fold increased level of the cellular enzyme AST and a 1.4-fold increased level of bilirubin were observed compared to the maximum normal values, indicating a tendency to develop pathological abnormalities of the hepatobiliary and cardiovascular systems [18]. An acute deficiency of trace elements – magnesium, phosphorus and vitamins – was also noted. In addition, the lack of proteins and fats in the standard feed was reflected in the level of triglycerides, alkaline phosphatase, urea and cholesterol, the values of which fluctuated at the level of the minimum limits of the physiological norm, which is associated with the low nutritional value of the feed used daily. After adding the feed additive to

the diet of the experimental sheep, the biochemical parameters of the blood of the animals showed a tendency to gradually restore the nutritional balance. An increase in the level of total protein due to the active growth of albumin in the blood by 15-16%, an increase in glucose concentration by 20%, creatinine, triglycerides and HDL cholesterol by 35%, a decrease in the enzymes LDL low density cholesterol, ALT, AST and the De Ritis coefficient to the average norm was noted [15, 17].

The level of triglycerides fluctuated at the level of the maximum norm, the level of alkaline phosphatase decreased, but remained 2 times higher than the maximum norm, the concentration of urea, reflecting the activity of protein metabolism and liver and kidney pathology, remained at the average physiological level, the concentration of trace elements magnesium and phosphorus reached the minimum level of the physiological norm (Figure 2).
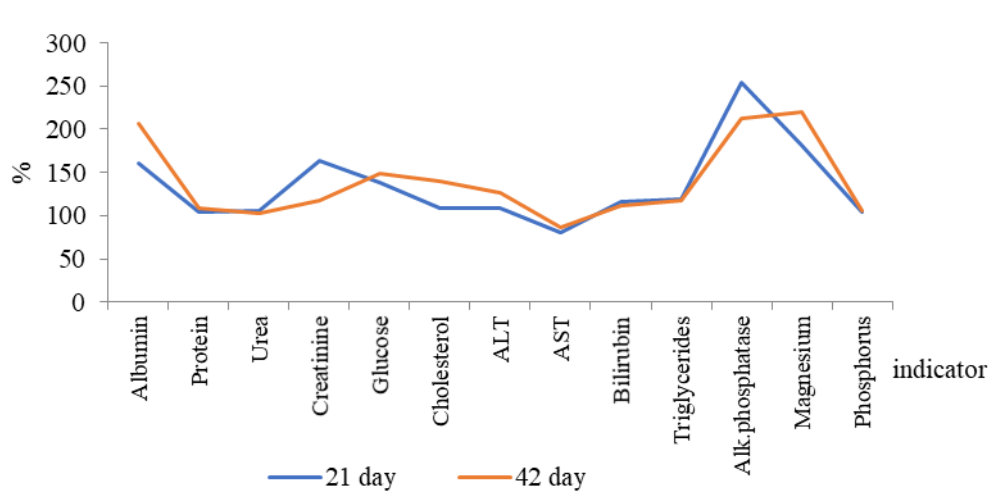
Figure 2 – Dynamics of changes in biochemical parameters (control – 100%)
in the blood of rams on days 21 and 42 after adding the feed additive to the daily diet

It should be noted that the level of creatinine, which reflects the energy supply of cells, in the blood of sheep of the control group was below the minimum norm, which is typical for a deficiency of protein-carbohydrate-fat components in the daily diet of animals. The urea/creatinine coefficient (the norm is below 0.08) is 0.09, which allows predicting the development of renal and hepatic failure with the possible development of hepatosis or cirrhosis [19]. The level of trace elements in the blood of control sheep was 45% below the minimum value for

magnesium concentration and within the minimum physiological norm for phosphorus level, which is typical for a deficiency of vitamin D and growth hormone [20].

Comparative analysis of biochemical data showed that the use of the feed additive provides protein saturation of the daily diet of sheep, increased metabolic processes in the liver and increased activity of excess cholesterol utilization. A tendency towards a stable increase in fat and muscle mass without the development of pathological abnormalities in

the functioning of the hepatobiliary system, such as fatty liver disease – hepatosis or cardiovascular insufficiency, which are the main cause of death of young animals during fattening, was shown.

The study of the oxidative activity of the blood showed an increase in antioxidant protection at the cellular level in the experimental group of sheep (Figure 3).

Figure 3 – Dynamics of changes in the indices of lipid peroxidation of plasma membranes of blood cells and enzymatic activity of blood plasma (%) after 21 and 42 days of introducing the feed additive.
Note: DK – diene conjugates, MDA – malonic dialdehyde, AC – catalase activity,
ALT – alanine aminotransferase, AST – aspartate aminotransferase

The indicators of primary and secondary peroxidation products were below the control values by 10-20%, which reflects the low level o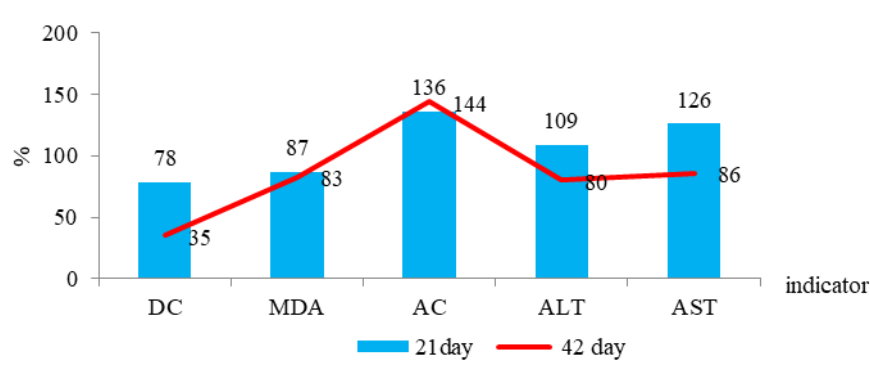f stress factors for the excitation of oxidative processes, and an increase in the catalase level by 12% ($p \leq 0.001$ compared to the control data) indicates pronounced protective antioxidant properties of the developed feed additive. Strengthening the antioxidant protection of blood cells is confirmed by a comparative analysis of data on lipid peroxidation and the enzymatic activity of ALT and AST.

A direct relationship is revealed between these indicators – a decrease in the level of diene conjugates as indicators of primary intoxication of the body and malonic dialdehyde – the final product of peroxidation, ensures a decrease in the concentration of cellular enzymes ALT and AST, that is, damage to the plasma membranes of hepatocytes and cardiomyocytes at a minimum.

An inverse relationship is also possible between enzymatic activity and an increase in the level of catalase in the blood, which prevents the development of oxidative stress.

To assume, raising young farm animals on fattening farms is associated with the nutritional value of the daily ration. At the final stage, the addition of feed additives enriched with proteins, fats and mineral and carbohydrate components improves the quality characteristics of animal products [21].

Biochemical blood tests of animals should be carried out as continuous monitoring.

Current study shows the effect of a feed additive obtained from the green mass of a well-known cereal crop (barley) and a widespread non-traditional forage crop (sorrel) with the addition of trace elements on the hematobiochemical parameters of animal blood. It was found that the addition of the feed mixture for 1.5 months has a positive effect on the growth and development of animals and ensures the adequacy of the daily diet. Biochemical studies create the basis for expanding the feed base to compensate for the lack of nutrients in the daily diet. According to the latest literature data, the assessment of biochemical parameters shows the influence of the environment, pesticide load and the value of various types of feeding with the inclusion of various biologically active additives on the productivity of farm animals [22, 23].

A recent biochemical study described the dependence of heavy metal concentration in the blood of sheep on the grazing season, which must be taken into account when feeding animals in fattening farms [24]. Based on the biochemical analysis of sheep blood, the use of an unconventional forage plant, daylily, as a partial replacement for traditional corn silage as a feed resource for sheep is recommended [25]. The use of licorice extract as a feed source of antioxidants is described, biochemical parameters

were studied, which showed a positive effect of the extract on growth, nutrient digestibility, humoral immunity and antioxidant activity in cattle [26].

In recent years, prophylactic agents have been actively developed to prevent hepatosis and cardiovascular diseases in humans and animals, based on betaine, a glycine derivative obtained from grain [26].

The inclusion of young barley greens and sorrel in our feed additive provides the animal body with the necessary amount of glycine, antioxidants necessary for the growth and development of animals. In this work, biochemical parameters of blood plasma of sheep in the control group showed the presence of imbalance and deficiency of proteins, carbohydrates, fats and trace elements in the daily diet of fattening rams. A tendency to liver and bile insufficiency was noted, low creatinine levels indicate a lack of muscle mass in animals [27].

A study of the microelement composition of the blood of the control group of sheep revealed a deficiency of potassium, sodium, calcium, phosphorus, chlorine and especially magnesium, which slows down the growth and development of animals. The use of the feed additive developed by us for 42 days showed the restoration of the balance of nutrients in the daily diet, an increase in total protein, glucose and triglycerides, as well as a decrease in the De-Ritis coefficient, which reflects an increase in the activity of protein, carbohydrate, fat and mineral metabolism.

The shelf life of the feed additive from the green mass of rumex and barley at the initial stages of vegetation – stem formation, is short-term and, like other green fodder, does not exceed 2 months, after which a loss of the nutritional properties of the forage crops is noted [28-30]. The period of maximum biological value of the feed additive has been selected.

After 42 days, the level of lipid metabolism – both HDL and LDL cholesterol and creatinine – reflected the sufficient water supply of the body and moderate activity of protein-fat metabolism, which ensures a stable increase in muscle mass.

The level of triglycerides fluctuated at the level of the maximum norm, the level of alkaline phosphatase decreased, but remained twice the maximum norm, and the concentration of urea, reflecting the activity of protein metabolism, as well as liver and kidney pathology, remained at an average physiological level, and the concentration of trace elements magnesium and phosphorus reached the minimum level of the physiological norm.

Restoring the balance of nutrients is associated with the introduction of a new feed additive into the diet, which, in addition to the green mass of sprouted grain crops and sorrel, includes bentonite, calcium phosphate, urea and potassium iodide, the ions of which enter the blood through the gastrointestinal tract and are included in the metabolic processes in the body.

The study of lipid peroxidation on plasma cell membranes showed a consistently low level of oxidative processes in the blood after the use of the feed additive, which suggests a high antioxidant and protective effect of the compound feed. The introduction of the feed additive developed by us into the diet of farm animals will give farmers certain opportunities to obtain high-quality meat products from healthy animals.

Conclusion

The organization of a full-fledged diet for farm animals is the most important condition for increasing their productivity. Standard diets for farm animals are balanced in many respects, but the most important of them is protein content. In ruminants, protein is additionally supplied by microorganisms that synthesize protein from non-protein nitrogen compounds during digestion. For this, nitrogen compounds must be supplied daily in sufficient quantities with feed. In this regard, urea, which contains 42-49% nitrogen, is introduced into the composition of feed additives. The main advantage of urea is that it is readily available and much cheaper than natural protein. The difficulty of its use in animal feed is the formation of ammonia during its hydrolysis in the rumen of ruminants [31].

Rations containing green fodder, other concentrates and urea increase the ammonia content in the rumen and blood plasma, changing the ratio of essential and interchangeable amino acids [32].

The inclusion of urea in the diet of sheep, as well as green mass from germinated cereal plants, reduces the acidity and the amount of dry matter in the rumen fluid, which indicates increased fermentation of feed nutrients in the forestomachs. High-quality feed determines the profitability of production and high productivity of livestock farming.

The feed additive developed by us is based on dry and green mass of sprouted grain crop *Hordeum vulgare* (barley), family Poaceae, and non-traditional feed crop *Rumex confertus* (horse sorrel), family Polygonaceae, with the addition of bentonite,

calcium phosphate, urea and potassium iodide in the ratio of 500 g of mixture – 150 g of ground dry barley grain, green mass of barley and sorrel – 300 g, ingredients with active substances 50 g; – after using the feed additive, biochemical analysis of the animals' blood showed an increase in the concentration of protein, fat, indicators of mineral-carbohydrate metabolism, a consistently low level of oxidative processes in the blood, which indicates a high nutritional, antioxidant and protective effect of this plant mixture and can be recommended for growing animals in fattening areas.

Acknowledgments

Conflict of interest

All authors are aware of the article's content and declare no conflict of interest.

References

1. On approval of the national project for the development of the agro-industrial complex of the Republic of Kazakhstan for 2021-2025. Resolution of the Government of the Republic of Kazakhstan from October 12, 2021 [Ob utverzhdenii nacional'nogo proekta po razvitiyu agropromyshlennogo kompleksa Respubliki Kazahstan na 2021-2025 gody. Postanovlenie Pravitel'stva Respubliki Kazahstan ot 12 oktyabrya 2021 goda] No. 732. https://adilet.zan.kz/rus/docs/P2100000960

2. Government Resolution No. 423 on July 12, 2018 "On approval of the State program for the development of the agro-industrial complex of the Republic of Kazakhstan for 2017-2021 [Postanovlenie Pravitel'stva № 423 ot 12.07.2018 «Ob utverzhdenii Gosudarstvennoj programmy razvitiya agropromyshlennogo kompleksa Respubliki Kazahstan na 2017-2021 gody]

3. Kekchebayev E., Zhakupova G. (2021) Marketing research of agriculture. Analysis of investment attractiveness of the market [Marketingovye issledovaniya sel'skogo hozyajstva. Analiz investicionnoj privlekatel'nosti rynka] Institute of Marketing and Sociological Research Elim, Kazdata.kz. https://marketingcenter.kz/20/rynok-selskoe-khoziaistvo-kazakhstan.html, date posted 04.15.2021

4. Smagulova Sh.A. (2020) Measures to improve state regulation of agriculture in Kazakhstan [Mery po sovershenstvovaniyu gosudarstvennogo regulirovaniya sel'skogo hozyajstva Kazahstana] Narxoz. Law and state policy, 1(1), pp. 79-87.

5. Seisekenova M., Kasseinova M., Abdykalyk S., Assanova Zh. (2021) Ensuring food security in Kazakhstan: theory, methodology and practice of agribusiness development [Obespechenie prodovol'stvennoj bezopasnosti v Kazahstane: teoriya, metodologiya i praktika razvitiya agrobiznesa] Statistics, accounting and audit, 2 (81), pp. 47-53

6. Gridneva E.E., Kaliakparova G.Sh., Emy E.V. (2020) Ensuring innovative development of the agro-industrial complex of Kazakhstan: problems and solutions [Obespechenie innovacionnogo razvitiya APK Kazahstana: problemy i puti resheniya] Eur. J. Econ. Manag. Sci., 1(1), pp. 42-44.

7. On approval of veterinary (veterinary and sanitary) requirements for organizations producing, storing and selling veterinary drugs, feed and feed additives [Ob utverzhdenii veterinarnyh (veterinarno-sanitarnyh) trebovanij k organizaciyam po proizvodstvu, hraneniyu i realizacii veterinarnyh preparatov, kormov i kormovyh dobavok]. Order of the Minister of Agriculture of the Republic of Kazakhstan No. 7-1/848 from September 23, 2015.

8. On approval of the technical regulations "Requirements for the safety of feed and feed additives [Ob utverzhdenii tekhnicheskogo reglamenta «Trebovaniya k bezopasnosti kormov i kormovyh dobavok] Resolution of the Government of the Republic of Kazakhstan No. 263 from March 18, 2008

9. Kondrakhin I.P., Arkhipov A.V., Levchenko V.I., Talanov G.A., Frolova L.A., Novikov V.E. (2004) Methods of veterinary clinical laboratory diagnostics [Metody veterinarnoj klinicheskoj laboratornoj diagnostiki]. – M.: Kolos, 520 p., ISBN 5-9532-0165-6

10. Kosolapov V.M., Chuikov V.A., Khudyakova H.K., Kosolapova V.G. (2019) Mineral elements in feed and methods of their analysis [Mineral'nye elementy v kormah i metody ih analiza]. M.: Ugreshskaya printing house, 272 p., ISBN 978-5-91850-037-8

11. Burlakova E.B. (1975) Bioantioxidants in radiation damage and malignant growth [Bioantioksidanty v luchevom porazhenii i zlokachestvennom roste]. – Nauka, Moscow p.210., ISBN 14384085

12. Babenko G.A., Goynatsky M.N. (1976) Determination of catalase activity in erythrocytes and serum by iodometric method Lab.delo [Opredelenie aktivnosti katalazy v eritrocitah i syvorotke jodometricheskim metodom]. – P. 157-158.

13. Ivanter E.V., Korosov A. (2010) Elementary biometrics [Elementarnaya biometriya]. 2nd ed., Petrozavodsk: Publishing house of PetrSU – 104 p. ISBN 978-5-8021-1112-3

14. Adylkanova Sh.R., Kim G.L., Sadykulov T.S., Koishibaev A.M., Baimazhi E., Dolgopolova S.Yu. (2019) Polymorphic blood systems of Degeres sheep and their use in breeding [Polimorfnye sistemy krovi degersskih ovec i ih ispol'zovanie v selekcii]. *Orig. res.*, 9 (11), pp. 5-11.

15. Vasilyeva V.A. (1982) Clinical biochemistry of farm animals. [Klinicheskaya biohimiya sel'skohozjstvennyh zhivotnyh]. M.: Rosselkhozizdat,254 p.

16. Fomichev Yu.P., Bogolyubova N.V., Rom anov V.N., Kolodina E.N. (2020) Comparative assessment of natural feed additives for functional effect on digestion processes and rumen microbiota in sheep (*Ovis aries*) [Sravnitel'naya ocenka prirodnyh kormovyh dobavok po funkcional'nomu dejstviyu na processy pishchevareniya i mikrobiotu rubca u ovec (*Ovis aries*)] Agric. biol., 55(4), pp. 770-783.

17. Mishurov A.V., Bogolyubova N.V., Romanov V.N. (2018) Features of digestive and metabolic processes in sheep using various protein sources [Osobennosti pishchevaritel'nyh i obmennyh processov u ovec pri ispol'zovanii razlichnyh istochnikov proteina] Achievements of science and technology of the agro-industrial complex, 32(8), pp. 66-69.

18. Pogodaev V.A., Sergeeva N.V., Marchenko V.V. (2018) Growth dynamics and biochemical blood parameters of crossbreeds obtained from crossing Kalmyk fat-tailed ewes with Dor-Per rams [Dinamika rosta i biohimicheskie pokazateli krovi pomesej, poluchennyh ot skreshchivaniya matok kalmyckoj kurdyuchnoj porody s baranami porody Dor-Per] Agric. sci., 9, pp. 40-44.

19. Simpraga M., Smuc, T., Matanovic K., Radin L., Shek-Vugrovecki A., Ljubicic I., Vojta A. (2013) Reference intervals for organically raised sheep: effects of breed, location and season on hematological and biochemical parameters. *Small Rum. Res.*, 112, 1-6.

20. Bhat S.A., Mir M.R., Reshi A.A., Ahmad S.B., Husain I., Bashir S., Khan H.M. (2014) Impact of age and gender on some blood biochemical parameters of apparently healthy small ruminants of sheep and goats in Kashmir valley India. *Int. J. Agric. Sci.*, 2, pp. 22-27.

21. Ramalan S.M, Adama T.Z, Alemede I.C, Tsado D.N, Zaifada A.U, Alagbe J.O, Hassan D.I., Tanimomo B.K. (2022) Haematological and serum biochemical parameters of yankasa ewes fed varying levels of localand industrial supplemented premix. *Am. J. Appl. Sci.*, 1, pp. 64-75.

22. Bessonova N.M., Zykovich S.N., Petruseva N.S. (2013) The influence of the bioactive feed additive "Rumexan" on the morphological and biochemical composition of the blood of the Altai-Sayan breed of marals [Vliyanie bioaktivnoj kormovoj dobavki «Rumeksan» na morfologicheskij i biohimicheskij sostav krovi Altae-Sayanskoj porody maralov]. *Bull. Altai State Agrar. Univ.*, 10(108), pp. 80-82.

23. Paulina M., Katarzyna S. (2018) The role of probiotics, prebiotics and synbiotics in animal nutrition. *Gut. Pathogens*. 10(21), p. 1186.

24. Anton K., Julius A., Eva T., Lubos H., Eva T., Katarina Z., Peter C., Stefania A., Jan T., Peter M. (2017) Seasonal variations in the blood concentration of selected heavy metals in sheep and their effects on the biochemical and hematological parameters. *Chemosphere*, 168, pp. 365-371. https://doi.org/10.1016/j.chemosphere. 2016.10.090

25. Junli Zh., Fen L., Rina N., Xue B., Yanfen M., et al. (2023) The effect of replacing whole-plant corn silage with daylily on the growth performance, slaughtering performance, muscle amino acid composition, and blood composition of tan sheep. *Animals*, 13(22), p. 3493 https://doi.org/10.3390 /ani13223493

26. Sunzhen L., Jinzhu M., Zining T., et al. (2024) Licorice extract supplementation benefits growth performance, blood biochemistry and hormones, immune antioxidant status, hindgut fecal microbial community, and metabolism in beef cattle. *Vet. Sci.*, 11(8), p. 356, https://doi.org/10.3390/vetsci11080356

27. Yu C., Mingtian D., Qifan Zh., Zifei L., Liang W., Wenwen Sh., Yanli Zh., Peihua Y., Ziyu W., Feng W. (2021) Effects of dietary betaine supplementation on biochemical parameters of blood and testicular oxidative stress in Hu sheep. *Theriogenology*, 164, pp. 65-73. https://doi.org/10.1016/j.theriogenology

28. Fakhratov Zh.O., Batanov S.D., Kislyakva E.M. (2005) Patent RU2005119753A, Protein-carbohydrate granules based on green fodder Rumex K-1 [Belkovo-uglevodnye granuly na osnove zelenogo korma Rumeks K-1]

29. Algazin D.N., Ivanov V.N., Vorobyov D.A., Zabudskiy A.I. (2016) Possibilities of using green fodder in feeding farm animals [Vozmozhnosti ispol`zovaniya zelenogo korma v kormlenii sel`skoxozyajstvenny`x zhivotny`x] Electronic scientific and methodological journal of Omsk State Agrarian University, 4 (7), ISSN 2413-4066

30. Melnikov S., Manankina E. (2010) Use of chlorella in feeding farm animals [Ispol'zovanie hlorelly v kormlenii sel'skohozyajstvennyh zhivotnyh] *In the world of science*, 8(90), pp. 40-43.

31. Mishurov A.V. (2021) The influence of biologically active substances on rumen metabolism in sheep [Vliyanie biologicheski aktivnyh veshchestv na rubcovyj metabolizm ovec] *Bulletin of P.A. Kostychev Ryazan State Agrotechnical University*, 13(2), pp. 35-41.

32. Kostin O.V., Tishkina T.N., Velmatova L.N., Erofeev V.I. (2019) Influence of aminotransferase enzymes on the growth energy of bulls of different body types [Vliyanie fermentov aminotransferaz na energiyu rosta bychkov raznyh tipov teloslozheniya] Proc. 15th international scientific-practical conference dedicated to the memory of S.A. Lapshin "Resource-saving environmentally friendly technologies for the production and processing of agricultural products". Saransk: NIMGU, pp. 63-66.

Information about authors:

Kapysheva Unzira Nayrzbayevna – Doctor of Biological Sciences, Professor, Chief Researcher of the Laboratory of Ecological Physiology of Humans and Animals, Institute of Genetics and Physiology, Almaty, Kazakhstan, e-mail: unzira@inbox.ru

Bakhtiyarova Sholpan Kadirbaevna – Candidate of Biological Sciences, Head of the Laboratory of Ecological Physiology of Humans and Animals, Institute of Genetics and Physiology, Almaty, Kazakhstan, e-mail: bifara.66@mail.ru

Makashev Yerbulat Kapanovich – Doctor of Biological Sciences, Professor, Head of the Digestion Laboratory, Institute of Genetics and Physiology, Almaty, Kazakhstan, e-mail: e_makashev@mail.ru

Zhaksymov Bolatbek Isauly – Master of Science, Senior Researcher, Laboratory of Ecological Physiology of Humans and Animals, Institute of Genetics and Physiology, Almaty, Kazakhstan, e-mail: bolat_kaz@inbox.ru

Junussova Ainur Bolatovna – Master of Science, Junior Researcher, Laboratory of Ecological Physiology of Humans and Animals, Institute of Genetics and Physiology, Almaty, Kazakhstan, e-mail: ainur.a1988@mail.ru

Kalekeshov Askar Maralovich – Candidate of Biological Sciences, Leading Researcher at the Laboratory of Digestion, Institute of Genetics and Physiology, Almaty, Kazakhstan, e-mail: akan.maralov@mail.ru

Makashev Yerlan Yerbolatovich – Researcher at the Digestion Laboratory, Institute of Genetics and Physiology, Almaty, Kazakhstan, e-mail: erlan_makashev@mail.ru

Mukhitdin Beibarys Azamatuly – Senior laboratory assistant of the laboratory of ecological physiology of humans and animals, Institute of Genetics and Physiology, Almaty, Kazakhstan, e-mail: mukhitdin00beibarys@gmail.com

N.F.S. Rosely* ⓘ , N.N. Saimi ⓘ ,
M.R. Midin ⓘ , M.F. Karim ⓘ

International Islamic University Malaysia, Pahang, Malaysia
*e-mail: mfauzihan@iium.edu.my

Acclimation to drought stress improves root physiology and cell mitotic index, leave pigments and water status in *Oryza sativa* L.

Abstract. Drought is a prominent abiotic stressor that critically impairs rice productivity by disrupting fundamental physiological processes and diminishing yield potential. This study investigates the effects of continuous and alternating drought stress on cell mitotic index and physiological responses in selected traditional and domestically grown rice varieties. Drought stress was imposed for approximately 9 days, a condition visibly marked by the rolling of leaves. In the alternating drought treatment, plants were exposed to identical drought conditions but were rehydrated to normal water levels on the 10th day, with this cycle of drought and rehydration repeated twice. Continuous drought stress led to a significant reduction in root cell mitotic activity, with a decrease ranging from 23.6% to 67% compared to control conditions. Additionally, drought stress adversely impacted leaf physiology, evidenced by reductions in total chlorophyll content, Fv/Fm ratios, and relative leaf water status. In contrast, the severity of these physiological disruptions was less pronounced in plants subjected to alternating drought stress. In addition, while acclimated plants exhibited elevated levels of root electrolyte leakage (REL) and malondialdehyde (MDA) compared to controls, these levels were substantially lower than those observed under continuous drought stress. These findings suggest that while drought negatively affects most physiological parameters, its impact can be mitigated through intermittent watering and the use of drought-tolerant rice varieties.

Key words: Rice, drought stress, mitotic index, root electrolyte leakage, malondialdehyde.

Introduction

Rice or *Oryza sativa* L., is known to be one of the most consumed staple foods worldwide [1]. It plays a critical role in ensuring food security, preserving cultural heritage, and shaping governmental policies in developing nations [2,3]. Projections anticipate that the world population will reach approximately 9.8 billion by 2050, leading to a projected doubling in demand for rice [4]. Presently, rice constitutes a primary dietary staple for about half of the world's population, with Asia contributing nearly 90% to its global production. The required volume of rice to meet future demands has escalated by 70% due to the expanding population in Asia [5]. Despite these trends, approximately 35% of rice-growing regions worldwide are experiencing production stagnation [6,7].

Meanwhile, plants inherently fixed in the soil, are inevitably exposed to a wide range of potentially detrimental environmental conditions, including drought stress [8]. Drought, characterized by a prolonged period of water scarcity leading to soil moisture falling below saturation levels to completely convey the yield capacity [9,10]. Globally, drought substantially reduces cereal production by 9 to 10%, profoundly impacting plant growth, physiology, and grain development [11-14]. Drought stands as the foremost factor affecting agricultural productivity and thereby poses a significant threat to global food security [15,16].

Plant growth is primarily driven by processes such as cell division, cell growth, and differentiation. Drought stress, like other abiotic stressors, is reported to suppress the mitotic index [17,18], resulting in compromised growth due to impaired cell elongation and mitosis [19]. The lack of turgor pressure under drought conditions significantly hinders cell growth and development, making cell growth one of the most vulnerable physiological processes to drought [19-21]. Even mild drought stress has been suggested to negatively affect cellular development, potentially

leading to cell death under prolonged and severe drought conditions. This disturbance in metabolism further impacts physiological functions [22,23].

Drought conditions are classified into two primary types: intermittent and terminal [24]. Terminal drought is characterized by a significant reduction in the water available for plant uptake, leading to severe drought stress and ultimately resulting in plant mortality. In contrast, intermittent drought conditions, which may occur either in discrete episodes or repeatedly throughout the growing season, adversely affect plant development when there is insufficient irrigation or rainfall. Unlike terminal drought, intermittent drought is typically not lethal. The capacity of plants to survive and maintain functionality under both intermittent and extreme drought conditions is indicative of their drought tolerance or resistance mechanisms [25]. Therefore, the aim of this study was to investigate the effects of two different types of drought, continuous and alternating, on the root mitotic activity and physiological responses of rice plants.

Materials and methods

Field preparation and treatments. This study was conducted at the Department of Plant Science, International Islamic University Malaysia with six varieties; UPM Putra 2, Kuku Belang, Jarum Mas, Dular, Huma Wangi Lenggong (HWL) and a homozygous breeding Line 541 (L541) were compared to a susceptible but domestically grown MR297. Rice seedlings were cultivated in 9 cm x 12 cm polybags containing 100% topsoil. The polybags were then placed in containers and subsequently filled with water to submerge the basal part of the plants. All plants were organized following to a completely randomised design with five replications for each treatment. Throughout the experiments, standard rice cultivation practices, including fertilization, were followed. After 28 DAS, drought stress was initiated by withholding water for approximately 9 days, indicated by the appearance of rolled leaves in plants. Meanwhile, the alternate drought treatment, was implemented under identical conditions, with the exception that plants were rehydrated back to normal water levels on day 10. This cycle of alternating drought was done twice.

Mitotic index analysis. Nuclei were isolated from the terminal 1.0 mm segment of root tips using a sharp sterile scalpel blade. The chopping procedure was performed in 0.8 ml of a slightly modified LBOI buffer (15 mM Tris, 2 mM EDTA, 80 mM KCl, 20 mM

NaCl, 0.5 mM spermine, 15 mM mercaptoethanol, 0.1% Triton X-100, pH 7.5), following the method described by [26]. The suspension was subsequently filtered through a 40 μm cell strainer. Post-filtration, 50 μl of Propidium Iodide (PI) was added for DNA staining, along with 50 μl of RNase, and allowed to incubate for 10 minutes. The nuclei suspension was then analyzed using a Muse® Cell Analyzer flow cytometer. The percentage of cells in the G2/M phase was determined from the data extracted from the Muse® Cell Analyzer (Merck Millipore, Darmstadt, Germany).

Measurement of chlorophyll fluorescence. Chlorophyll fluorescence was measured on a fully grown leaf using a portable chlorophyll fluorometer PAM-2500 (Heinz Walz GmbH). Prior to measurements, the leaf was subjected to dark adaptation for approximately 30 minutes. The ratio of variable to maximum fluorescence (Fv / Fm), indicative of the maximum quantum yield of Photosystem II (PS II), was recorded following the method described by [27].

Leaf total chlorophylls and carotenoids content. Total chlorophyll content was determined following the procedures by [28] with minor adjustments. A known weight of fresh leaves was homogenized in 3 ml of 80% acetone using a mortar and pestle. The extracts were then centrifuged at 13.3g for 5 minutes, and the supernatants were collected. Total chlorophylls were quantified using a spectrophotometer at 663.6 nm, 646.6 nm, and 750 nm.

Meanwhile, carotenoid content was analysed by homogenizing a known weight of fresh leaves with 3 ml of 80% acetone following the method by [29]. The pigment concentrations were determined spectrophotometrically at 645 nm, 663 nm, and 480 nm with 80% acetone used as blank.

Relative water content (RWC). Leaf relative water content (RWC) was assessed using a known weight of fresh leaves. The samples were hydrated in distilled water for 4 hours in a petri dish to reach a maximum turgor capacity. Subsequently, the leaves were gently dried with tissue paper before measuring their turgor weight. Following this, the samples were dried in an oven at 60°C for three days until a constant weight was achieved for leaf dry weight (DW).

Measurement of root electrolyte leakage (REL). A modified method measuring REL on fine roots was employed based on the procedures by [30-32]. Root samples weighing between 100 and 500 mg were placed in 16 ml of distilled or deionized water within 28-ml universal glass bottles, achieving a tissue-to-water ratio of approximately 1:20. The bottles were

sealed, shaken continuously, and incubated at room temperature for 12 hours. The initial conductivity (C1) of the solution was measured using an electrical conductivity (EC) meter. Subsequently, the samples were autoclaved at 110°C for 10 minutes, cooled to room temperature, and the second conductivity measurement (C2) was recorded. REL was calculated using the following formula:

$$REL = (C_1/C_2) \times 100$$

Measurement of lipid peroxidation. Lipid peroxidation was assessed by measuring malondialdehyde (MDA) production following the protoco by [33] with some modifications. Approximately 0.2-0.4 g fresh weight of roots were homogenised in 4 ml of 0.1% (w/v) trichloroacetic acid (TCA, followed by centrifugation at 10 000 G for 10 minutes. A 750 µL aliquot was taken and mixed vigorously with same amount of (A) +TBA solution containing 20% (w/v) TCA and 0.5% (w/v) thiobarbituric acid (TBA), and (B) –TBA containing only 20% (w/v) TCA. The samples were then heated at 95°C for 25 minutes in a water bath and subsequently cooled down to room temperature prior to centrifugation at 10 000 G for 10 minutes. The absorbance at 440, 532 and 600 nm were recorded. MDA in each sample was calculated as follows:

$$(Abs\ 532\ +TBA - Abs\ 600\ +TBA) - $$
$$- (Abs\ 532\ -TBA - Abs\ 600\ -TBA) = A$$
$$(Abs\ 440\ +TBA - Abs\ 600\ +TBA)\ x\ 0.0571 = B$$
$$MDA\ (nmol.mL^{-1}) = [(A-B)\ /\ 157000]\ *\ 1x10^6$$

Statistical analysis. All the data were analyzed using GraphPad Prism Version 9 and one-way ANOVA was performed to test significance differences ($p \leq 0.05$) among the treatment means. The overall effects of different paddy varieties and drought treatments and their interactions on growth, physiological and biochemical parameters were determined by comparing treatments means with a two-way ANOVA at $p \leq 0.05$.

Results and discussion

Effect of drought and alternate drought on roots mitotic activity. The present study aimed to assess the resilience of root cell cycle dynamics under drought and alternating drought conditions (Figure 1).
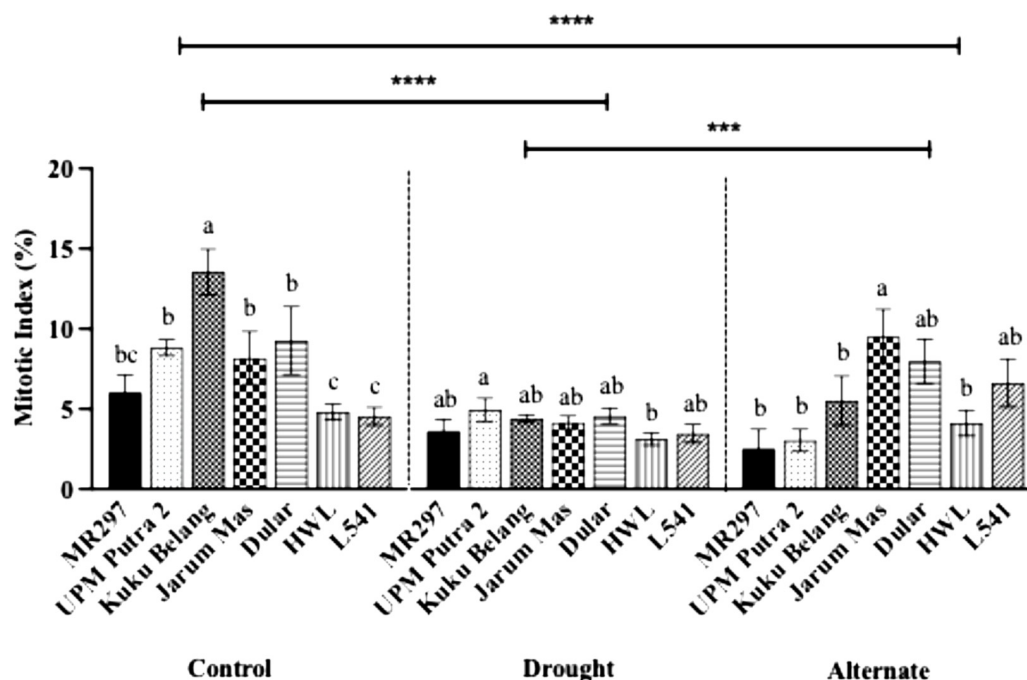
Figure 1 – Mitotic index in rice seedlings subjected to normal irrigation, drought and alternate drought stress. Data was analysed using one way ANOVA to assess the significance level between means ± SE of n = 5 (p≤0.05). Comparison was done amongst varieties within the same treatment and values are not sharing common letters differ significantly. Meanwhile, values are not sharing a common superscript (*, **, ***) differ significantly at p≤0.05, p≤0.001 and p≤0.001 (LSD), respectively

In the control condition, it was assumed that mitotic activities would align with the inherent characteristics of respective plant varieties. Notably, the Kuku Belang cultivar exhibited the highest mitotic activity at 13.6%, followed significantly by MR297, UPM Putra 2, Jarum Mas, Dular, HWL, and L541. However, under drought conditions, a significant reduction in mitotic activity was observed across all examined varieties. This reduction displayed variability among varieties with 39.8%, 43.9%, 67.5%, 49.2%, 50.7%, 35.2%, and 23.6% reduction compared to their respective control conditions. Further analysis also shows that alternating drought treatment yielded higher root mitotic activity in certain varieties than in continuous drought, particularly in Jarum Mas and Dular.

The regulation of the cell cycle is intricately dependent on a complex interplay of intrinsic and extrinsic factors, including hormonal signaling and environmental cues [34]. Previous research by [35] demonstrated that water stress led to a substantial reduction, approximately 90%, in endosperm cell division, accompanied by decreased thymidine incorporation into DNA and a concurrent attenuation of the endoreduplication process. This investigation suggests that certain rice varieties subjected to alternating drought conditions exhibit enhanced mitotic activity compared to those under continuous drought, indicating potential acclimation mechanisms that increase a plant's resilience to drought-induced stress, as evidenced by cellular mitotic activity.

Effect of drought and alternate drought stress on the leaf photosynthetic components. Changes in leaf physiology serve as key indicators of a plant's response to environmental conditions, particularly evidenced by alterations in photosynthetic-related components such as proteins and molecules during abiotic stress [36]. One crucial metric for assessing the impact of drought stress is the ratio of variable to maximum fluorescence, Fv/Fm, which represents the maximum photochemical quantum yield of photosystem II (PSII) under the theoretical condition where all reaction centers are open [37]. In the present investigation, plants subjected to controlled irrigation consistently exhibited Fv/Fm values exceeding 0.8, indicating the absence of stress-induced effects (Table 1).

Table 1 – Comparison of Fv/Fm, total chlorophyll and carotenoid content in different variety of rice within the same treatment subjected to drought and alternate drought stress. Data was analysed using a one-way ANOVA followed by LSD's post hoc test to assess the significance between means ($p \leq 0.05$). Values represent the mean ±SE of n = 4

	Control	Drought	Alternate drought
		Fv/Fm	
MR297	0.805[b]	0.7432[b]	0.7590[c]
UPM Putra 2	0.808[b]	0.7692[a]	0.7680[b]
Kuku Belang	0.814[a]	0.7646[a]	0.7964[a]
Jarum Mas	0.810[ab]	0.7682[a]	0.7950[a]
Dular	0.802[b]	0.7714[a]	0.7766[b]
HWL	0.803[b]	0.7682[a]	0.7808[b]
L541	0.807[b]	0.7716[a]	0.7914[a]
		Total chlorophyll content (?	
MR297	1.46[ab]	0.59[b]	1.27[b]
UPM Putra 2	1.74[a]	0.47[b]	1.37[b]
Kuku Belang	1.36[ab]	0.89[a]	2.14[a]
Jarum Mas	1.89[a]	0.66[a]	2.03[a]
Dular	1.55[a]	0.71[a]	1.57[ab]

Continuation of the table

	Control	Drought	Alternate drought
HWL	0.92[b]	0.67[a]	1.89[a]
L541	1.76[a]	0.36[b]	1.92[a]
	Carotenoid content (ug/ml)		
MR297	8.94[a]	16.54[c]	12.40[c]
UPM Putra 2	5.96[b]	15.12[c]	8.96[c]
Kuku Belang	5.92[b]	39.78[a]	18.28[b]
Jarum Mas	9.97[a]	20.72[bc]	26.82[a]
Dular	6.96[ab]	20.95[bc]	16.08[b]
HWL	6.40[ab]	24.47[b]	13.84[bc]
L541	4.82[b]	17.48[bc]	15.11[b]

However, under drought stress conditions, all plants recorded values below 0.8, with MR297 showing the highest susceptibility compared to other varieties. Conversely, under alternating drought conditions, Kuku Belang, Jarum Mas, and L541 exhibited significantly higher Fv/Fm values, approaching 0.8. Despite being commercially cultivated, MR297 demonstrated the lowest Fv/Fm value. It is worth noting that Fv/Fm values in the range of 0.79 to 0.84 represent the approximate optimal range for many plant species, with lower values indicating photoinhibition of PSII and subsequent reduction in photosynthetic activity [38, 27]. According to [39], F_v/F_m in rice was severely affected at panicle initiation, flowering and ripening stages under drought condition. Meanwhile, according to [40] there was a positive correlation between Fv/Fm and drought.

The analysis of chlorophyll pigments demonstrated significant variations in the total chlorophyll content across different rice varieties. Under controlled irrigation conditions, Jarum Mas exhibited the highest natural chlorophyll content, followed sequentially by UPM Putra and Dular. However, the imposition of drought stress resulted in a reduction of chlorophyll content across all varieties, with MR297, UPM Putra 2, and L541 experiencing particularly greater decreases compared to Kuku Belang, Jarum Mas, Dular, and HWL. Interestingly, except for MR297 and UPM Putra 2, all plants showed a significant increase in total chlorophyll pigments under alternating drought conditions compared to their respective controls.

Chlorophyll is a critical component of the photosynthetic process, with the photosynthetic rate being shown to have a linear correlation with chlorophyll content [41]. The decline in chlorophyll levels is primarily attributed to the overproduction of reactive oxygen species (O2- and H2O2), which can induce lipid peroxidation of the chloroplast membrane during drought conditions. This lipid peroxidation impairs membrane stability and leads to the degradation of chlorophylls [42]. Additionally, abiotic stressors can cause damage to the chloroplast ultrastructure, resulting in reduced chlorophyll levels and consequently diminished photosynthetic activity [43].

The impact of continuous and alternate drought on carotenoid content was assessed and presented in Table 1. The carotenoid concentration was observed to be at its lowest under normal irrigation conditions. However, a significant increase in concentration was recorded in all plants following continuous drought exposure, in comparison to their respective varieties under control and alternate drought conditions. Previously, improved Fv/Fm ratios were attributed in part to efficient non-photochemical quenching (NPQ) mechanisms [45].

However, correlation analyses conducted in this study between Fv/Fm and both chlorophylls and carotenoid content revealed no significant differences. In contrast, a significant positive correlation was found between total chlorophylls and carotenoid content (r = 0.5885****). This suggests that the efficient dissipation of excess energy by carotenoids may contribute to the preservation of chlorophylls, particularly chlorophyll a, from degradation [44].

Effect of drought and alternate drought on leaf relative water content. Irrigation treatments was observed to have affected the relative water status in plants (Figure 2).
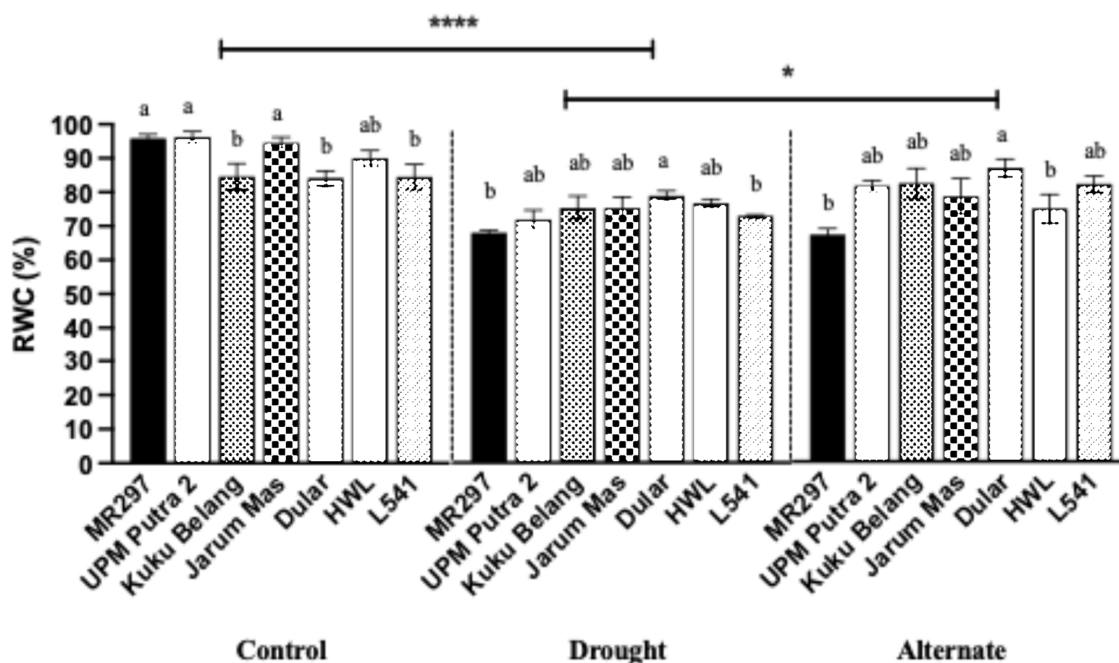
Figure 2 – Relative water content in rice seedlings subjected to normal irrigation, drought and alternate drought stress.
Data was analysed using one way ANOVA to assess the significance level between means ± SE of n = 5 (p≤0.05).
Comparison was done amongst varieties within the same treatment and values are not sharing common letters
differ significantly. Meanwhile, values are not sharing a common superscript (*, **, ***) differ significantly
at p≤0.05, p≤0.001 and p≤0.001 (LSD), respectively.

Under control irrigation conditions, all plants exhibited RWC values above 80%, indicative of normal leaf water status. In contrast, both continuous (p ≤ 0.0001) and alternate drought treatments (p ≤ 0.001) led to a significant reduction in RWC. Among the varieties studied, MR297 consistently displayed the lowest RWC under both drought conditions. Notably, plants subjected to alternate drought showed higher RWC compared to those under continuous drought stress. Drought stress typically results in a decrease in leaf RWC, often ranging from 60% to 80% [45]. However, the severity of this reduction depends on the plant's ability to mitigate stress through physiological adaptations such as stomatal regulation, acclimation in photosynthesis, and the accumulation of osmoprotectants to enhance cellular water conservation [38,46]. Acclimated plants do not only maintain higher RWC under drought stress but also exhibit resilience under other abiotic stress such as salinity and high temperatures [47,48,49]. In addition, studies also found higher accumulation of osmolytes including increased levels of amino acids, sugars, and ions as part of acclimation process [50,51]. The accumulation of these osmolytes was positively correlated with RWC and is associated with enhanced drought tolerance in plants [46].

Effect of drought and alternate drought on root physiology. Drought stress significantly increased MDA levels in rice compared to both control conditions and alternate drought stress (p ≤ 0.001***), with the highest accumulation observed in MR297 (Figure 3).

Although plants subjected to alternate drought exhibited higher MDA content compared to the control, the severity was significantly lower than that observed in continuously drought-stressed plants. This suggests that exposing rice plants to a sequence of drought events may enhance the physiological resilience of roots against the adverse effects of drought stress. MDA is a byproduct of lipid peroxidation caused by increased reactive oxygen species under stress condition [52,53]. This oxidative damage can lead to alterations in membrane-associated proteins, ionic channels, or receptors, thereby affecting their functionality [54]. Additionally, the release of phospholipid degradation enzymes, such as phospholipases, may further compromise membrane integrity [55].
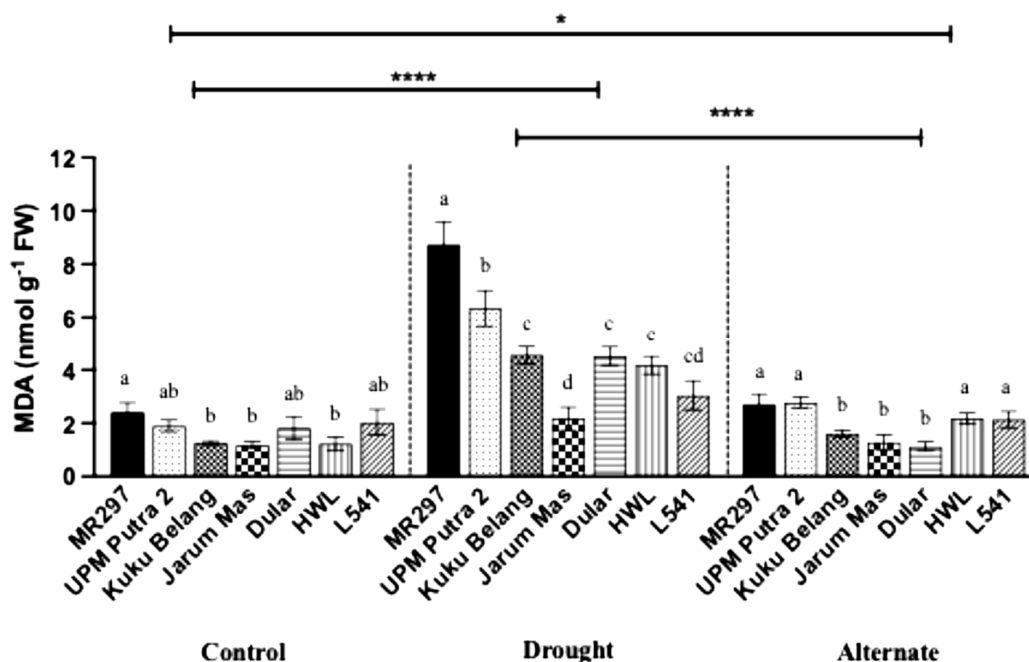
Figure 3 – MDA content in rice seedlings subjected to normal irrigation, drought and alternate drought stress. Data was analysed using one way ANOVA to assess the significance level between means ± SE of n = 5 (p≤0.05). Comparison was done amongst varieties within the same treatment and values are not sharing common letters differ significantly. Meanwhile, values are not sharing a common superscript (*, **, ***) differ significantly at p≤0.05, p≤0.001 and p≤0.001 (LSD), respectively.

The increase in REL was found to correlate with a significant rise in MDA levels under drought stress conditions. A two-way ANOVA analysis indicated that both continuous and alternate drought treatments significantly influenced REL (Figure 4).

Under control conditions, all plant varieties exhibited REL values ranging from 15% to 26%, indicating minimal membrane damage. In contrast, the imposition of drought conditions significantly elevated REL compared to both control and alternate drought treatments, with HWL and L541 showing the lowest REL values among the treatments. Drought-treated plants exhibited REL values ranging from 48% to 73%, while acclimated plants showed lower REL values between 29% and 44%. Plants exposed to alternate drought condition exhibited REL of less than 50%, a value higher than that observed in the control group. Nonetheless, this impact was comparatively less severe than the effects observed under continuous drought stress. As reported by previous studies [56], REL serves as an indicator of root injury, reflecting the health and functionality of root cell membranes.

There is no definitive standard value for REL; however, typical ranges between 10% to 40%, with values potentially reaching up to 80% were reported in previous studies [56-58]. Nonetheless, plants with acclimated roots to drought stress showed significantly lower root leakage compared to those experiencing acute drought stress exhibiting the importance of root acclimatization in mitigating cellular damage [57]. Both REL and MDA reflect membrane health status, with MDA specifically indicating lipid peroxidation, while REL measuring conductivity due to ion efflux due to damage in cell membranes. In our study, a positive correlation between root REL and MDA levels was observed (r = 0.3475**), which is consistent with previous findings that reported a similar relationship in rice subjected to drought stress [59,60]. This correlation portrayed the interconnectedness of lipid peroxidation and membrane integrity under drought conditions, suggesting that both parameters are crucial for assessing plant health and resilience in response to drought.
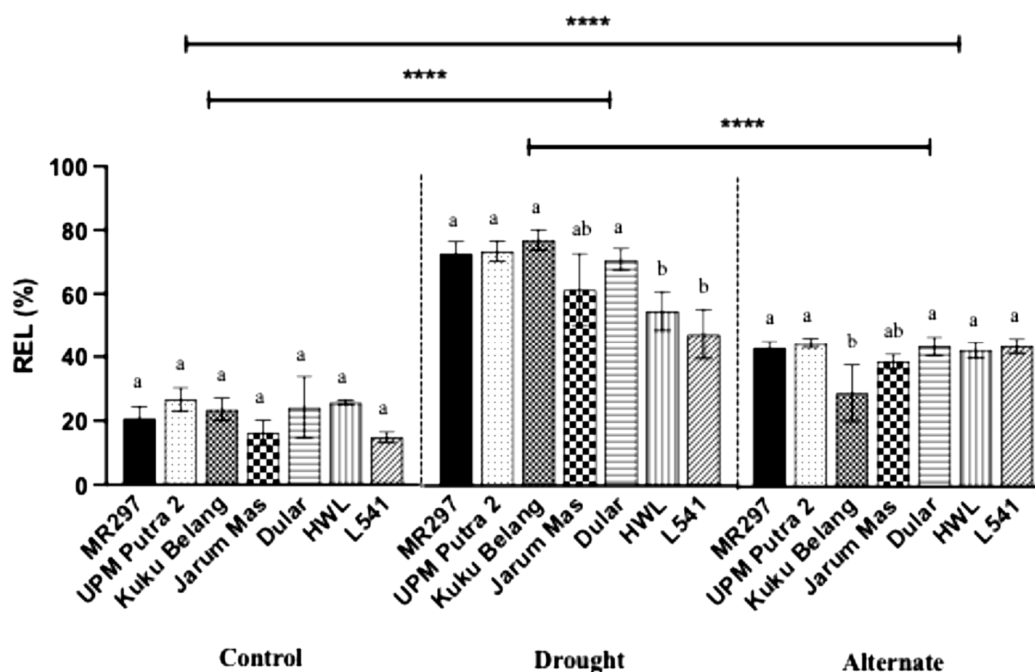
Figure 4 – REL in rice seedlings subjected to normal irrigation, drought and alternate drought stress. Data was analysed using one way ANOVA to assess the significance level between means ± SE of n = 5 (p≤0.05). Comparison was done amongst varieties within the same treatment and values are not sharing common letters differ significantly. Meanwhile, values are not sharing a common superscript (*, **, ***) differ significantly at p≤0.05, p≤0.001 and p≤0.001 (LSD), respectively.

Conclusion

This study observed that drought conditions led to a decrease in cellular mitotic activity and impaired leaf physiology, as evidenced by reductions in Fv/Fm, total chlorophylls, and total carotenoid content. Additionally, drought induced lipid peroxidation and increased root electrolyte leakage, indicating significant membrane damage. Rice plants subjected to alternating drought treatments, although exhibiting lower values compared to the control, demonstrated enhanced responses across all parameters relative to continuous drought stress. This suggests that acclimation strategies implemented during periods of drought and subsequent rehydration improved the plants' ability to tolerate the typical effects of drought. Furthermore, among the varieties assessed, Kuku Belang and Jarum Mas were identified as possessing superior tolerance traits despite showing an increased root electrolyte leakage.

Conflict of interest

All authors are aware of the article's content and declare no conflict of interest.

References

1. Priya T.S.R., Nelson A.R.L.E., Ravichandran K., Antony U. (2019) Nutritional and functional properties of coloured rice varieties of South India: a review. *J. Ethnic Foods.*, 6(1). https://doi.org/10.1186/s42779-019-0017-3
2. Omar S.C., Shaharudin A., Tumin S.A. (2019) The status of the paddy and rice industry in Malaysia. Malaysia: Khazanah Research Institute. 220 p. ISBN 978-967-16335-7-1.
3. Shah S., Bhat, J. A. (2019) Ethnomedicinal knowledge of indigenous communities and pharmaceutical potential of rainforest ecosystems in Fiji Islands. *J. Integr. Med.*, 17(4), pp. 244-249. https://doi.org/10.1016/j.joim.2019.04.006.
4. Islam S.F., Karim Z. (2019) Sustainable agricultural management practices and enterprise development for coping with global climate change. *Intech Open eBooks*. https://doi.org/10.5772/intechopen.87000

5.   Papademetriou M.K. (2000) Rice production in the Asia-Pacific region: Issues and perspectives. Bridging the rice yield gap in the Asia-Pacific region, p. 220. x6905e

6.   Khoury C.K., Bjorkman A.D., Dempewolf H., Ramirez-Villegas J., Guarino L., Jarvis A., Rieseberg L.H., Struik P.C. (2014) Increasing homogeneity in global food supplies and the implications for food security. *P. Natl. Acad. Sci.,* 111(11), pp. 4001-4006. https://doi.org/10.1073/pnas.1313490111

7.   Zhu C., Kobayashi K., Loladze I., Zhu J., Jiang Q., Xu X., Liu G., Seneweera S., Ebi K.L., Drewnowski A., Fukagawa N.K., Ziska L.H. (2018) Carbon dioxide (CO_2) levels this century will alter the protein, micronutrients, and vitamin content of rice grains with potential health consequences for the poorest rice-dependent countries. *Sci. Adv.,* 4(5). https://doi.org/10.1126/sciadv.aaq1012

8.   Singhal R., Kuma S., Kumar V. (2019) Drought tolerance mechanism in plant system. *Ind. J. Crop Ecol.,* 3(4), pp. 23-32.

9.   Blum A. (2011) Drought resistance – is it really a complex trait? *Funct. Plant Biol.,* 38(10), pp. 753. https://doi.org/10.1071/fp11101

10.   Ceccarelli S., Grando S., Baum M. (2007) Participatory plant breeding in water-limited environments. *Exp. Agric.*, 43(4), pp. 411-435. https://doi.org/10.1017/s0014479707005327

11.   Farooq M., Hussain M., Siddique K.H. (2014) Drought stress in wheat during flowering and grain-filling periods. *Crit. Rev. Plant Sci.,* 33(4), pp. 331-349. https://doi.org/10.1080/07352689.2014.875291

12.   Lesk C., Rowhani P., Ramankutty N. (2016) Influence of extreme weather disasters on global crop production. *Nature,* 529(7584), pp. 84-87. https://doi.org/10.1038/nature16467

13.   Matiu M., Ankerst D.P., Menzel A. (2017) Interactions between temperature and drought in global and regional crop yield variability during 1961-2014. *Plos One*, 12(5), pp. e178339. https://doi.org/10.1371/journal.pone.0178339

14.   Fahad S., Bajwa A.A., Nazir U., Anjum S.A., Farooq A., Zohaib A., Sadia S., Nasim W., Adkins S., Saud S., Ihsan M. Z., Alharby H., Wu C., Wang D., Huang J. (2017) Crop production under drought and heat stress: plant responses and management options. *Front. Plant Sci.,* 8. https://doi.org/10.3389/fpls.2017.01147

15.   Parry M.L., Canziani O.F., Palutikof J.P., Van Der Linden P.J., Hanson C.E. (2007) Climate change 2007: Impacts, adaptation and vulnerability. Contribution of working group II to the fourth assessment report of the intergovernmental panel on climate change. United Kingdom: Cambridge University Press, 3 p. ISBN 978 0521 88010-7

16.   Daryanto S., Wang L., Jacinthe P. A. (2015) Global synthesis of drought effects on food legume production. *Plos One*, 10(6), e0127401. https://doi.org/10.1371/journal.pone.0127401

17.   Ozmen S., Tabur S., Oney-Birol S., Ozmen, S. (2022) Molecular responses of exogenous polyamines under drought stress in the barley plants. *Cytologia*, 87(1), pp. 7-15. https://doi.org/10.1508/cytologia.87.7

18.   Radic S., Prolic M., Pavlica M., Pevalek-Kozlina B. (2005) Cytogenetic effects of osmotic stress on the root meristem cells of *Centaurea ragusina* L. *Env. Exp. Bot.*, 54(3), pp. 213-218. https://doi.org/10.1016/j.envexpbot.2004.07.007

19.   Hussain M., Malik M.A., Farooq M., Ashraf M.Y., Cheema M.A. (2008) Improving drought tolerance by exogenous application of glycinebetaine and salicylic acid in sunflower. *J. Agron. Crop Sci.,* 194(3), pp. 193-199. https://doi.org/10.1111/j.1439-037x.2008.00305.x

20.   Taiz L., Zeiger E. (2010) Responses and adaptations to abiotic stress, Sunderland, MA: Sinauer Associates, pp. 755-778.

21.   Jaleel C.A., Manivannan P., Wahid A., Farooq M., Al-Juburi H.J., Somasundaram R., Panneerselvam R. (2009) Drought stress in plants: a review on morphological characteristics and pigments composition. *Int. J. Agric. Biol.*, 11(1), pp. 100-105.

22.   Alves A.A., Setter T.L. (2004) Response of cassava leaf area expansion to water deficit: Cell proliferation, cell expansion and delayed development. *Ann. Bot.,* 94(4), pp. 605-613. https://doi.org/10.1093/aob/mch179

23.   Apel K., Hirt, H. (2004) Reactive oxygen species: Metabolism, oxidative stress, and signalling transduction. *Ann. Rev. Plant Biol.,* 55, p. 373. https://doi.org/10.1146/annurev.arplant.55.031903.141701

24.   Polania J., Rao I.M., Cajiao C., Grajales M., Rivera M., Velasquez F., Raatz B., Beebe S.E. (2017) Shoot and root traits contribute to drought resistance in recombinant inbred lines of MD 23–24× SEA 5 of common bean. *Front. Plant Sci.*, 8, p. 296. https://doi.org/10.3389/fpls.2017.00296

25.   Oladosu Y., Rafii M.Y., Samuel C., Fatai A., Magaji U., Kareem I., Kamarudin Z.S., Muhammad I., Kolapo, K. (2019) Drought resistance in rice from conventional to molecular breeding: a review. *Int J Mol. Sci.,* 20(14), p. 3519. https://doi.org/10.3390/ijms20143519

26.   Dolezel J., Bartos J., Voglmayr, H. (1992) Improved method of preparing plant material for analysis of nuclear DNA content by flow cytometry. *Biol. Plant,* 34(2), pp. 245-249.

27.   Maxwell K., Johnson, G. N. (2000) Chlorophyll fluorescence – a practical guide. *J. Exp. Bot.*, 51(345), pp. 659-668. https://doi.org/10.1093/jexbot/51.345.659

28.   Porra R.J., Thompson W.A., Kriedemann P.E. (1989) Determination of accurate extinction coefficients and simultaneous equations for assaying chlorophylls a and b extracted with four different solvents: verification of the concentration of chlorophyll standards by atomic absorption spectroscopy. *BBA-Bioenergetics*, 975(3), pp. 384-394. https://doi.org/10.1016/S0005-2728(89)80347-0

29.   Arnon D.I. (1949) Copper enzymes in isolated chloroplasts. Polyphenoloxidase in *Beta vulgaris. Plant Physiol.*, 24(1), pp. 1-15. https://doi.org/10.1104/pp.24.1.1

30.   Wilner J. (1955) Results of laboratory tests for winter hardiness of woody plants by electrolyte methods. *Proceed. Amer. Hortic. Sci.,* 66, pp. 93-99.

31. McKay H. M. (1992) Electrolyte leakage from fine roots of conifer seedlings: a rapid index of plant vitality following cold storage. *Canadian J. Forest Res.,* 22(9), pp. 1371-1377. https://doi.org/10.1139/x92-182

32. McKay H.M. (1998) Root electrolyte leakage and root growth potential as indicators of spruce and larch establishment. *Silva Fenn.*, 32(3), pp. 241-252. https://doi.org/10.14214/sf.684

33. Hodges D.M., DeLong J.M., Forney C.F., Prange R.K. (1999) Improving the thiobarbituric acid-reactive-substances assay for estimating lipid peroxidation in plant tissues containing anthocyanin and other interfering compounds. *Planta*, 207(4), pp. 604-611. https://doi.org/10.1007/s004250050524

34. Shimotohno A., Aki S.S., Takahashi N., Umeda M. (2021) Regulation of the plant cell cycle in response to hormones and the environment. *Ann. Rev. Plant Biol.*, 72(1), pp. 273-296. https://doi.org/10.1146/annurev-arplant-080720-103739

35. Setter T.L., Flannigan B.A. (2001) Water deficit inhibits cell division and expression of transcripts involved in cell proliferation and endoreduplication in maize endosperm, *J. Exp. Bot.*, 52, pp. 1401-1408. https://doi.org/10.1093/jexbot/52.360.1401

36. Miller M.A.E, O'Cualain R., Selley J., Knight D., Karim M.F., Hubbard S.J., Johnson G.N. (2017) Dynamic acclimation to high light in *Arabidopsis thaliana* involves widespread reengineering of the leaf proteome. *Front. Plant Sci.*, 8, https://doi.org/10.3389/fpls.2017.01239

37. Lang Y., Wang M., Xia J., Zhao Q. (2018) Effects of soil drought stress on photosynthetic gas exchange traits and chlorophyll fluorescence in *Forsythia suspensa. J. Forestry Res.*, 29(1), pp. 45-53. https://doi.org/10.1007/s11676-017-0420-9

38. Karim M.F., Johnson G.N. (2021) Acclimation of photosynthesis to changes in the environment results in decrease of oxidative stress in *Arabidopsis thaliana*. *Front. Plant Sci.,* 12. https://doi.org/10.3389/fpls.2021.683986

39. Zaman N.K., Abdullah M.Y., Othman S., Zaman N.K. (2018) Growth and physiological performance of aerobic and lowland rice as affected by water stress at selected growth stages. *Rice Sci.*, 25(2), pp. 82-93, https://doi.org/10.1016/j.rsci.2018.02.001

40. Zhuang J., Wang Y., Chi Y., Zhou L., Chen J., Zhou W., Song J., Zhao N., Ding J. (2020) Drought stress strengthens the link between chlorophyll fluorescence parameters and photosynthetic traits. *Peer J.*, 8, https://doi.org/10.7717/peerj.10046

41. Li R.H., Guo P.G., Michael B., Stefania G., Salvatore C. (2006) Evaluation of chlorophyll content and fluorescence parameters as indicators of drought tolerance in barley. *Agric. Sci. China*, 5(10), pp. 751-757. https://doi.org/10.1016/S1671-2927(06)60120-X

42. Gupta B., Huang B. (2014) Mechanism of salinity tolerance in plants: Physiological, biochemical, and molecular characterization. *Int. J. Genom.,* 2014, pp. 1-18. https://doi.org/10.1155/2014/701596

43. Sidhu G.P.S., Singh H.P., Batish D.R., Kohli R.K. (2017). Alterations in photosynthetic pigments, protein, and carbohydrate metabolism in a wild plant *Coronopus didymus* L. (Brassicaceae) under lead stress. *Acta Physiol. Plantarum*, 39(8), pp. 1-9. https://doi.org/10.1007/s11738-017-2476-8

44. Ruban A.V. (2016) Nonphotochemical chlorophyll fluorescence quenching: mechanism and effectiveness in protecting plants from photodamage. *Plant Physiol.*, 170(4), pp. 1903-1916. https://doi.org/10.1104/pp.15.01935

45. Singh R., Pandey N., Naskar J., Shirke P.A. (2015) Physiological performance and differential expression profiling of genes associated with drought tolerance in contrasting varieties of two *Gossypium* species. *Protoplasma.* 252(2), pp. 423-438. https://doi.org/10.1007/s00709-014-0686-0

46. Karimi S., Rahemi M., Rostami A.A., Sedaghat S. (2018) Drought effects on growth, water content and osmoprotectants in four olive cultivars with different drought tolerance. *Acta Hortic.*, 18(3). pp 254-267. https://doi.org/10.1080/15538362.2018.1438328

47. Shaukat M., Wu J., Fan M., Hussain S., Yao J., Serafim M.E. (2019) Acclimation improves salinity tolerance capacity of pea by modulating potassium ions sequestration. *Sci. Hortic.*, 254, pp. 193-198. https://doi.org/10.1016/j.scienta.2019.05.013

48. Veena P., Alok S. (2015) Acclimation and tolerance strategies of rice under drought stress. *Rice Sci.*, 22(4), pp. 147-161. https://doi.org/10.1016/S1672-6308(14)60289-4

49. Xu S., Li J., Zhang X., Wei H., Cui, L. (2006) Effects of heat acclimation pretreatment on changes of membrane lipid peroxidation, antioxidant metabolites, and ultrastructure of chloroplasts in two cool-season turfgrass species under heat stress. *Environ. Exp. Bot.,* 56(3), pp. 274-285. https://doi.org/10.1016/j.envexpbot.2005.03.002

50. Gosh U.T., Islam M.N., Siddiqui Md.N., Khan M.A.R. (2021) Understanding the roles of osmolytes for acclimatizing plants to changing environment: a review of potential mechanism. *Plant Sign. Behav.*, 16(8), pp. 1-13. https://doi.org/10.1080/15592324.2021.1913306

51. Ma Y., Dias M.C., Freitas H. (2020) Drought and salinity stress responses and microbe-induced tolerance in plants. *Front. Plant Sci.*, 11, https://doi.org/10.3389/fpls.2020.591911

52. Mihaljevic I., Vuletic M.V., Simic D., Tomas V., Horvat D., Josipovic M., Zdunic Z., Dugalic K., Vukovic D. (2021) Comparative study of drought stress effects on traditional and modern apple cultivars. *Plants*, 10(3), p. 561. https://doi.org/10.3390/plants10030561

53. Janku M.L., Luhov A., Petrivalsky M. (2019) On the origin and fate of reactive oxygen species in plant cell compartments. *Antioxid.*, 8, p. 105. https://doi: 10.3390/antiox8040105

54. Garcia J.J., Reiter R.J., Guerrero J.M., Escames G., Yu B.P., Oh C.S., Munoz- Hoyos A. (1997) Melatonin prevents changes in microsomal membrane fluidity during induced lipid peroxidation, *Febs Lett.*, 8(3), pp. 297-300. https://doi.org/10.1016/s0014-5793(97)00447-x

55. Pivtoraiko V.N., Stone S.L., Roth K.A., Shacka J.J. (2009) Oxidative stress and autophagy in the regulation of lysosome-dependent neuron death, *Antioxid. Redox Sign.*, 11(3), pp. 481-496. https://doi.org/10.1089/ars.2008.2263

56. Khan Z., Jan R., Asif S., Farooq M., Jang Y.H., Kim E.G., Kim N., Kim K.M. (2024) Exogenous melatonin induces salt and drought stress tolerance in rice by promoting plant growth and defense system. *Sci. Rep.*, 14(1), p. 1214. https://doi.org/10.1038/s41598-024-51369-0

57. Karimi A., Tabari M., Javanmard Z., Bader M.F. (2022) Drought effects on morpho-physiological and biochemical traits in Persian oak and black poplar seedlings. *Forests*, 13(3), p. 399. https://doi.org/10.3390/f13030399

58. Piacentini D., Della R.F., Sofo A., Fattorini L., Falasca G., Altamura M.M (2020) Nitric oxide cooperates with auxin to mitigate the alterations in the root system caused by cadmium and arsenic. *Front. Plant Sci.*, 11(1182), pp. 1-16. https://doi.org/10.3389/fpls.2020.01182

59. Bui L.T., Ella E.S., Dionisio-Sese M.L., Ismail A.M. (2019) Morpho-physiological changes in roots of rice seedling upon submergence. *Rice Science*, 26(3), pp. 167-177. https://doi.org/10.1016/j.rsci.2019.04.003

60. Xu Y., Burgess P., Zhang X., Huang B. (2016) Enhancing cytokinin synthesis by overexpressing ipt alleviated drought inhibition of root growth through activating ROS-scavenging systems in *Agrostis stolonifera. J. Exp. Bot.*, 67(6), pp. 1979-1992. https://doi.org/10.1093/jxb/erw019

Information about authors:

Nur Farah Suhada Rosely – MS, Department of Plant Science, Kulliyyah of Science, International Islamic University Malaysia, 25200 Pahang, Malaysia, email: suhadarosely@gmail.com

Nur Nazifah Saimi – Postgraduate, Department of Plant Science, Kulliyyah of Science, International Islamic University Malaysia, 25200 Pahang, Malaysia, email: nazifahsaimi@gmail.com

Mohd Razik Midin – PhD, Lecturer, Sustainable Agriculture and Green Technology Research Group (AG-TECH), Kulliyyah of Science, International Islamic University Malaysia, 25200 Pahang, Malaysia, Department of Plant Science, Kulliyyah of Science, International Islamic University Malaysia, 25200 Pahang, Malaysia, email: mohdrazik@iium.edu.my

Mohd Fauzihan Karim – (corresponding author) – PhD, Lecturer, Sustainable Agriculture and Green Technology Research Group (AG-TECH), Kulliyyah of Science, International Islamic University Malaysia, 25200 Pahang, Malaysia, Department of Plant Science, Kulliyyah of Science, International Islamic University Malaysia, 25200 Pahang, Malaysia, email: mfauzihan@iium.edu.my

E.S. Jafarov [1*] , A.A. Tagiyev [2] , I.Ch. Zeynalova [2] ,

M.Z. Velijanova [1] , A.E. Jafarov [1]

[1]Institute of Radiation Problems of the Ministry of Science and Education
of the Republic of Azerbaijan, Baku, Azerbaijan
[2]Scientific Research Institute of Plant Protection and Technical Plants
of the Ministry of Agriculture of the Republic of Azerbaijan, Ganja, Azerbaijan
*e-mail: elimkhan.jafarov@gmail.com

Comparative analysis of inheritable and modified variations induced by gamma irradiation in the first and second generation of cotton varieties Ganja-160, Ganja-182 and Ganja-183

Abstract. The main goal of the conducted research was to obtain cotton genotypes resistant to extreme environmental factors and various diseases, since high doses of γ-irradiation is a mutagenic factor. At the initial stage, before sowing, 1100 samples of plants whose seeds were treated with γ-rays in different doses were cultivated (in four parallel versions), the characteristics of the growing plants were studied, and the plants with changed signs were identified. At the end of the growing season, the raw cotton of 850 plants was collected by individual sampling and the transformed and untransformed plants in M1 were separated, their seeds were collected individually, stored and used for sowing as a family in the next planting (in M2). Changes in vegetation duration, main stem height, number of sympodial branches and number of bolls per bush of both M1 and M2 lineages were evaluated as the main criteria for determining the effectiveness of the mutation. In addition, the main economic characteristics and quality indicators such as the productivity of a bush, fiber yield, and fiber length, mass of raw cotton per boll were determined. It became clear that radiation can create certain changes in the first generation of all three varieties, some of which can be preserved in the second generation. In order to clarify whether the changes observed in the I and II generations are genetic (mutagenic) or just modification changes, the listed parameters are also planned to be studied in the next generations of plants.

Key words: Pre-sowing gamma irradiation of seeds, M1 and M2 generations of cotton varieties, economic characteristics and quality indicators.

Introduction

Today, there is a great demand for new cotton varieties that are productive, fast-growing, resistant to diseases and pests, and have high fiber quality. From this point of view, the creation of new cotton varieties that can provide an intensive increase in cotton productivity and their application in farms is not only an urgent practical issue, but also a matter of scientific importance.

As it is known, one of the most effective methods for obtaining economically valuable starting material in cotton farming is experimental mutagenesis. Experimental mutagenesis is a methodical approach to create cotton varieties with desirable traits and is the best tool to intensify breeding efforts.

It is known that mutation, as well as modification variability, is a characteristic feature of all living things. Mutation can occur in any organism (including plants) even in natural conditions. Mutational variability can also be caused by external influence, more precisely, by changing the influence of external conditions on the organism. For this reason, types of mutagenesis are distinguished, such as natural (or spontaneous) and artificial (or induced).

Today, for obtaining plant genotypes resistant to pests and various extreme factors of the environment, as well as with better quality indicators, selection methods based on artificial, i.e., induced mutations are more preferred [1-4].

This method, called mutation selection, is significantly different in terms of time and cost from

mutations obtained through genetic engineering and allows to create targeted genetic changes. For example, since γ-irradiation accelerates the natural genetic mutation process, the time required for this process is significantly shorter [5]. Besides the vital role in plant breeding programs, a new role of induced mutations in releasing of gene silencing in transgenic plants has been reported [6].

Mutagenesis is known to be a powerful tool for creating new germplasm resources and elucidating the function of plant genes [7, 8]. Artificial mutagenic methods, such as T-DNA insertion mutations and various physical mutagens, have been widely used to create mutations in many types of plants [4].

Until recent years, breeders have preferred to obtain resistant plant forms (hybrids, lines and varieties) based on the use of chemical mutagens. Although these methods give good results, the substances used in some cases have toxic properties, require a lot of labor, and the process is expensive.

It is known that today radiation technologies are widely used in all fields of the national economy, including agriculture. This is due to such advantages as ease of use of radiation technologies, low cost, environmental friendliness, stimulating effect in small doses, high degree of neutralization of planting material, the absence of lethal outcome, minimization of damage to seeds during processing, absence of induced radiation, and reduced energy consumption, etc. For example, exposure of seed to ionizing radiations and the irradiation treatment of male pollen with low doses of gamma rays before cross-pollination resulted in the development of new genetic changes/variability in different crop species [3, 9, 10].

It is believed that one of the main and most common methods for producing mutant varieties is radiation-induced mutagenesis [3, 11, 12].

Gamma rays have both higher linear energy transfer and can transmit more energy to greater depths. For generating mutants, this type of irradiation also has several advantages, such as high mutation efficiency and a wide range of mutations [13].

Radiation mutagenesis is also widely used in cotton breeding. For example, cottonseeds irradiated by γ-rays have been used to obtain heat-resistant and early- maturing mutants [14]. Tong [15] tested cotton mutants for glyphosate resistance through ^{60}Co-γ-ray mutation. In addition, Mu et al. [16] identified cotton mutants with chicken-foot leaves or gossypol-free glands, using ^{60}Co-γ-ray radiation. Chen and Liu [17] found that laser processing of cotton can promote

growth, increase yield, and improve cotton fiber quality.

Because γ-irradiation is a mutagenic factor in high doses, we started research together with well-known cotton growers of our country to buy cotton genotypes that are resistant to adverse conditions and various diseases.

The aim of our research was to obtain mutant cotton lines resistant to various diseases and extreme environmental factors, based on radiation mutagenesis, and use them as a new starting material for selection.

Materials and methods

Ganja-160, Ganja-182 and Ganja-183 cotton varieties, regionalized by the Republican Agrarian Services Agency, were used as research objects.

Before sowing, cottonseeds were irradiated with Co-60 isotope in doses of 5, 10, 50, 100, 200, 300, 400 Gy (dose rate was 0.342 Rad/sec) in the RUXUND-20000 (Russia) device at the "Isotope Sources of Radiation" Scientific-experimental complex. Non-irradiated seeds of these varieties were used as control options.

Irradiated cotton seeds were sown together with non-irradiated ones (control) in Ganja Regional Agrarian Science and Innovation Center's Samukh experimental base in open field conditions in 90 x 10 cm scheme in 4 replication options (Figure 1).

Considering that experimental mutagenesis did not allow dilution, a limited number of seeds (2 units) were sown in each nest. It is known that dilution in the field violates the percentage of mutation yield and can also destroy plants that have changed in a positive direction, which is important for breeding process. In total, 100 seeds were used for each variant.

During the study, the effect of gamma radiation at different doses on the growth and development of cotton plants was studied by measuring 25 plants in each variant during the phases of mass budding, flowering, and maturation. At the end of the vegetation, the viability of plants was also studied.

Systematic phenological observations were made on plants during the entire vegetation period. At the end of the vegetation, altered plants were recorded in each variant, which differed from the original varieties in terms of phenotypic characteristics. Also, sterile, fertile, etc. forms of the plants have been identified. The collection of raw cotton began with the collection of samples. For this purpose, raw cotton of 20 bolls was collected from I and II places of II-V

bar branches of all plants on each repetition. After the raw cotton of the samples was collected, the modified and unchanged plants were collected as an individual sample. To determine the frequency of mutations, the number of mutations occurring in 100 families in M2 of a 100-count sample in M1 was studied. Biometric analysis of all indicators, obtained in the study, was calculated according to Dospekhov [18].

Figure 1 – Visibility of the experimental area

Results and discussion

At the initial stage (in M1) before sowing, plant seeds treated with different doses of γ-rays were cultivated in field conditions; phenological observations and biometric measurements were carried out during the vegetation period. The bio morphological characteristics of the plants were studied, and the plants with changed characteristics were identified. Changes in vegetation duration, main stem height, sympodial branches and the number of bolls per bush are known to be the main criteria that determine the effectiveness of the mutation. Based on what has been said, these parameters, as well as the main economic characteristics and quality indicators, such as the productivity of a bush, cotton fiber yield, fiber length, and the mass of raw cotton per boll, have been determined.

In total, raw cotton of 1100 plants was collected by individual selection, and seeds of transformed and untransformed plants in M1 were collected separately, stored under special conditions and sown as a family in the next planting (in M2). In order to clarify whether the changes observed in M1 are genetic – mutagenic or simply modification changes, it is planned to study the plants not only in M2, but also in the subsequent generations.

We started the research by determining the bio morphological indicators, such as the vegetation period, the length of the plants, the number of bolls and sympodial branches on the bush of the first generation of all three cotton varieties.

The results obtained regarding the duration of vegetation, the length of the plants, the number of bolls and sympodial branches in one bush are reflected in Table 1.

From the results, the first thing that attracts attention is that for all three plants, at doses higher than 200 Gy, the duration of vegetation was about 5-6 days longer compared to the control. It can be considered that radioactive radiation in these doses had an inhibitory effect on the development of plants and slowed down their development.

Of particular interest are the results on plant height. Medium doses of radiation caused the height of plants to increase. On the contrary, high doses of radiation caused them to become shorter.

The number of sympodial branches and the number of bolls per bush also showed a significant dependence on the radiation dose. Apart from minor deviations, it can be considered that the treatment of seeds at high radiation doses (200 Gy and greater) led to an increase in both sympodial branches and the number of bolls per bush. To be more precise, the number of bolls per bush at the radiation doses of 300 and 400 Gy was on average 5 more for Ganja-160, 4 for Ganja-182, and 3 more for Ganja-183 varieties compared to the control.

It was established that plants at higher doses also grew sparsely and developed a large number of side branches from the main stem. At high doses, plants were also characterized by a lack of chlorophyll.

Table 1 – Dose-dependent change in the bio morphological characteristics of the M1 generation plants whose seeds were subjected to pre-sowing γ-irradiation.

Name of the variety	Radiation doses, Gy	Vegetation period, day	Plant height, cm	Number of sympodial branches	The number of bolls in one bush
GANJA-160	0(C)	122	114.6	13.4	21.1
	5	121	120.3	12.9	21.3
	10	121	117.6	12.8	20.2
	50	120	123.1	12.6	20.5
	100	123	120.8	12.4	19.7
	200	125	120.2	14.3	23.8
	300	128	117.1	15.4	23.7
	400	127	114.4	15.5	26.1
GANJA – 182	0(C)	119	114.6	14.1	19.4
	5	120	104.8	14.4	18.1
	10	119	109.1	13.7	18.5
	50	118	115.1	14.8	21.8
	100	120	118.2	14.6	20.4
	200	121	109.1	14.7	25.1
	300	124	103.1	15.6	24.2
	400	125	103.1	15.5	23.1
GANJA – 183	0(C)	120	112.1	12.8	19.5
	5	119	107.4	11.5	20.1
	10	120	110.1	12.1	19.6
	50	118	123.4	10.7	19.7
	100	122	106.6	11.7	20.2
	200	121	104.6	13.3	23.4
	300	124	100.2	13.4	23.9
	400	126	101.1	13.3	22.8

In general, it was not possible to find any regularity in the change of the height of the main stem and the number of sympodial branches, depending on the radiation dose. Simply, the phenological observations we conducted on cotton varieties showed that despite the normal development of all three varieties at low doses, at doses above 200 Gy the growth of plants slowed down, and they could not give normal output.

Our studies have shown that among the plants changed in M1 at high doses of radiation, there are fast – growing plants, plants with elongated oval, multi-lobed cones, as well as plants with fruiting organs of 3, 4 and even 5 bolls arranged in a cluster. In the first generation of plants at high doses of radiation, plants with a changed shape were also found, in which the development of the main stem stopped, the lateral branches lengthened, the stem was weak and densely pubescent, the leaves were deeply lobed and heart-shaped, the bush was spreading, the distance between the joints was reduced (Figure 2).

Figure 2 – The shape of the fruiting organ of plants

Gamma radiation also affected the shape of plant bushes. In fact, at high doses both compact and scattered plants were formed, as well as plants with a strong and branched trunk. At the same time, there were plants with fascinated branches and low-growing plants. At high doses there was a definite change in the shape and number of bolls. Thus, we were able to register plants with grape-shaped, large and small bolls. The effect of gamma radiation on the number and shape of bolls in fruiting organs at high doses has been recorded. Bolls with a hairy, elongated ovoid body and sharp spouts were found at various radiation doses, mainly at doses above 200 Gy.

At the end of the vegetation, in the M1 generation, the changed plants, which differ from the initial varieties in terms of their phenotypic characteristics, were recorded and the sterile, fertile, etc. forms of the plants were determined. Twelve visible phenotypic mutants were observed.

The results of these changes recorded in the M1 generation of cotton varieties treated with γ-rays, as well as the number of late-maturing, early maturing, sterile and semi-sterile plants, are presented in Table 2.

It is clear from the presented results that γ-irradiation can produce different types of variability at different doses.

The effect of γ-radiation on the shape of the bush in plants is more noticeable. Scattered bushy plants are observed in all three cotton varieties at doses of 200 Gy and higher. A radiation dose of 300 Gy in this case produces plants that are more scattered. Plants with strong, branching stems are also preferred at these doses.

It is interesting that if at low doses of γ-irradiation (up to 100 Gy) compact plants were obtained, at high doses (200 Gy and above) both sparsely bushy and highly branched plants were observed.

Plants with branch fasciation were also mostly found at relatively high doses. Such doses, in addition to producing large boll plants, formed clustered boll plants. It has become clear that sterile and semi-sterile plants are also more common in variants corresponding to high values of γ-irradiation dose (doses of 200 Gy and higher). High doses of radiation could also affect the maturity of plants. Therefore, in these doses, the plants matured later.

We believe that the presence of sterile, semi-sterile and chlorophyll-less plants among the changed plants in M1 can be considered a sign of change. Plants with compact form, zero, first and pyramidal branching, as well as fast-growing, high-yielding forms are of special interest for practical selection.

The variability in M1 is assumed to be mainly modification variability. Thus, it is possible to detect rare dominant mutations in M1. Recessive mutations can be observed in M2 after self-pollination. In M1, the seeds of both transformed and untransformed plants, as we already mentioned, were collected separately by individual selection and used for the next planting (for M2). At the end of vegetation, transformed and untransformed plants were also determined for M2 generation plants. In other words, the relevant mutants were screened in M2 generation.

The results (in absolute number and percentage) for the total number of families studied and the number of families changed in both M1 and M2 are presented together in Table 3 for comparison.

Table 2 – Results on the number and type of variation recorded in the M1 generation of γ-irradiated cotton varieties

The name of the variety	Radiation dose, Gy	Type and number (in pieces) of variation in M1 plants											
		Bush shape					Boll shape			Growing up		Sterile	Semi-sterile
		Compact	Scattered	Plants with strong, branched stems.	Branch fasciation	Short stature	A plant with a cluster-shaped boll	Large	Small	Late growing	Fast growing		
GANJA – 160	0(C)												
	5	1									1		
	10	2			1				1		1		
	50	3											
	100	3			1				1		3		
	200	2	2	5	7			1			5		
	300		4	5	4	2	3	4		3		3	1
	400		3	1			4	5		5		4	3
GANJA – 182	0(C)												
	5	1											
	10	1									2		
	50	2							1		3		
	100	4		2					1		3		
	200	1	3	7	5	3		5		4		1	
	300		4	6				3		3		5	2
	400		1	1	3	3		2		3		3	1
GANJA – 183	0(C)												
	5	2									1		
	10	1							1		2		
	50	2			1		1		3		5		
	100		3		3	2	4	4		3		1	1
	200	1	2	5	2	2		6		5		4	2
	300		3	4	3		3	4				1	
	400		1	1		1	2	2		2		3	2

From the data on the changes caused by gamma irradiation in two consecutive generations of cotton plants, it is clear that the number of changed plants in the M1 generation of plants prevails at high radiation doses. For example, the number of modified plants at irradiation doses of 300 and 400 Gy is 28-42%, 22-33% and 35-70% of the total number of plants for the varieties Ganja-160, Ganja-182 and Ganja-183, respectively.

Some of the changes that occurred in the first generation of plants were also present in their second generation. It is clear from the results that 16 out of 22 plants changed in M1 in Ganja-160 varieties of cotton, according to the radiation dose of 200 Gy kept their changed form in M2. 23 out of 28 plants that changed in M1 in the variant corresponding to 300 Gy radiation dose of this variety and 18 out of 25 plants in the variant corresponding to 400 Gy radiation dose kept their changed form in the next generation.

For Ganja – 182 cotton variety, those figures are 28(21), 23(19) and 17(13) at 200, 300, and 400 Gy radiation doses, respectively, and for Ganja-183 cotton variety, those numbers are again, respectively, 29(21), 21(15) and 14(10).

Table 3 – Data on the number of changes caused by gamma radiation in M1 and M2 generation plants of cotton varieties

Gamma-radiation dose, Gy	Number of studied families, pieces	Number of families changed in M1		Number of families changed in M2	
		Absolute number	%, $(x \pm S_x)$	Absolute number	%, $(x \pm S_x)$
GANJA-160					
0 (C)	316	-	-	-	-
5	296	2	0.67 ± 0.47	1	0.34 ± 0.3
10	292	5	1.71 ± 0.76	3	0.68 ± 0.5
50	292	6	2.05 ± 0.83	4	0.68 ± 0.5
100	268	8	2.98 ± 1.04	5	1.12 ± 0.6
200	220	22	10.0 ± 2.02	16	3.18 ± 1.2
300	100	28	28.0 ± 4.49	23	15.0 ± 3.6
400	60	25	41.7 ± 6.36	18	13.3 ± 4.4
GANJA-182					
0 (C)	356	-	-	-	-
5	352	1	0.40 ± 0.34	1	0.28 ± 0.3
10	336	3	0.89 ± 0.51	2	0.42 ± 0.3
50	292	6	2.05 ± 0.83	5	0.68 ± 0.5
100	288	10	3.47 ± 1.08	7	1.04 ± 0.6
200	272	28	10.3 ± 1.84	21	4.41 ± 1.2
300	104	23	22.1 ± 4.07	19	8.65 ± 2.8
400	52	17	32.7 ± 6.50	13	11.5 ± 4.4
GANJA-183					
0 (C)	336	-	-	-	-
5	308	3	0.97 ± 0.56	2	0.32 ± 0.3
10	316	4	1.26 ± 0.63	2	0.63 ± 0.4
50	276	12	4.35 ± 1.23	7	1.09 ± 0.6
100	240	21	8.75 ± 1.82	15	3.33 ± 1.2
200	224	29	12.9 ± 2.24	21	6.70 ± 1.7
300	60	21	35.0 ± 6.16	15	13.3 ± 4.4
400	20	14	70.0 ± 10.25	10	20.0 ± 8.9

The plants that kept their changed shapes in M2 were also observed for Ganja-182 and Ganja-183 varieties at the radiation dose of 100 Gy. At this radiation dose, the number of plants that retained the altered form in the next generation was 10(7) and 21(15), respectively.

The results show that, in some variants, it was possible to detect the same type of altered plants, recorded in the first generation, in the second generation of plants. A certain part of them was initially assumed to be hereditary. These variations are recorded as mutational variations. The modified cultivar seeds will be used for planting in M3, and the nature of the variations will be determined. For this reason, those plants were collected separately, according to variants; their number was determined; and it was planned to study them in the third generation to determine whether the variation is hereditary.

The presence of variations in new traits was also found in the second-generation plants. The seeds of the plants with variations in the new traits were also collected separately, and it was planned to use them for planting in M3 and to determine the nature of the variations.

Taking into account that the productivity of one bush, the mass of raw cotton in one boll, fiber yield,

fiber length and strength are important quantitative and qualitative indicators of cotton, we clarified the effect of γ-irradiation on the quantitative and qualitative indicators of both generations of the studied cotton varieties. At the same time, it was also considered that the mentioned indicators may change depending on agro technical measures, abiotic and mutagenic factors. For this purpose, raw cotton of 20 bolls from the I and II places of the second to fifth sympodial branches at the end of vegetation for both generations of plants was collected by individual sampling, and parameters, such as yield of one bush, mass of raw cotton in one cone, fiber yield, fiber length, were determined.

Table 4 presents the results of the quantitative and qualitative changes observed in the M1 and M2 generations of cotton varieties whose seeds were treated with γ-rays.

Table 4 – Quantitative and qualitative changes observed in M1 and M2 generations of cotton varieties whose seeds were treated with γ-rays

The name of the variety	Radiation dose, Gy	Productivity of one bush, g		The mass of raw cotton in one boll, g		Fiber yield, %		Fiber length, mm	
		M1	M2	M1	M2	M1	M2	M1	M2
GANJA – 160	0(C)	132.9	126.6	6.3	6.0	34.2	35.0	34.6	33.5
	5	129.9	121.4	6.1	5.7	36.7	36.4	34.9	34.2
	10	127.3	129.3	6.3	6.4	36.4	36.6	33.8	34.0
	50	131.2	125.1	6.4	6.1	36.2	36.6	34.5	32.4
	100	128.1	112.3	6.5	5.7	35.9	34.6	33.6	31.4
	200	145.2	133.3	6.1	5.6	36.5	37.8	33.3	31.6
	300	161.2	146.9	6.8	6.2	35.5	38.3	33.6	31.4
	400	177.5	140.9	6.8	5.4	36.5	38.5	32.3	31.5
GANJA – 182	0(C)	126.1	116.4	6.5	6.0	34.5	35.4	34.1	33.7
	5	119.5	126.7	6.6	6.1	34.8	35.8	34.1	34.4
	10	114.7	112.9	6.2	6.1	34.6	34.9	33.5	33.7
	50	128.6	135.2	5.9	6.2	37.2	37.1	33.7	34.2
	100	126.5	126.5	6.2	6,2	35.4	37.6	33.2	32.5
	200	163.2	130.5	6.5	5.2	34.0	40.2	33.9	32.0
	300	159.7	140.4	6.6	5.8	34.9	39.2	33.4	31.2
	400	143.2	138.6	6.2	6,0	34.0	39.0	34.1	31.3
GANJA – 183	0(C)	126.8	115.1	6.5	5.9	36.6	36.8	34.2	34.5
	5	126.6	116.6	6.3	5.8	37.9	37.7	33.2	32.1
	10	131.3	111.7	6.7	5.7	37.2	38.9	32.6	30.2
	50	130.0	108.4	6.6	5.5	35.7	37.0	33.4	28.4
	100	123.2	123.2	6.1	6.1	34.9	37.2	32.4	30.4
	200	154.4	135.7	6.6	5.8	34.6	32.6	31.7	31.6
	300	153.0	133.8	6.4	5.6	33.7	34.5	33.0	28.7
	400	143.6	125.4	6.3	5.5	33.5	33.1	31.9	31.5

It is clear from the results that the treatment of seeds with γ-rays before sowing can cause certain quantitative and qualitative changes in the M1 generation of cotton, and some of these changes can be preserved in the next generation. A change (increase) in the productivity of a bush is mainly observed at high doses. For example, if the average yield of one bush was 132.9 g in the control variant of the M1 generation of the Ganja-160 cotton variety, the yield increased at doses of 200, 300 and 400 Gy, and became 145.2, 161.2 and 177.5 g, respectively.

It is interesting that the increase in the productivity of a bush at high radiation doses was preserved in the II generation of this variety. Simply, the difference was that in this case the magnitude of the increase was relatively small.

Another interesting fact is that similar dependence on radiation dose was observed for Ganja-182 and Ganja-183 varieties. In the first generation of the Ganja-182 variety, the mass of cotton per bush was 163.2, 159.7, and 143.2 g at doses of 200, 300, and 400 Gy, respectively (the yield of the control sample was 126.1 g), and the productivity of the Ganja-183 variety at those doses was 154.4, 153.0, and 143.6 g, respectively (the yield of the control sample was 126.8 g). The high yield of cotton in doses of 200, 300 and 400 Gy was maintained in the II generation of these varieties with a slight difference.

In their studies, Muthusamy and Narayanasamy [2] also exposed two varieties of cotton to different doses of γ-rays (at doses of 100, 200, 300, 400 and 500 Gy). Moreover, the selected traits of each mutant also showed higher yield traits in each generation than the parental varieties.

A large number of phenotypic variations was observed in the studies of Zhao et al. [19]. The authors examined three successive generations of cotton and identified variations, including changes in cotton fiber color, plant dwarfing, significant improvements in yields, and increased susceptibility to *Verticillium* wilt. These results indicate that radiation mutagenesis is an effective and feasible method for generating plant mutant libraries.

The high productivity of mutant cotton, obtained as a result of radiation mutagenesis, was also confirmed in the studies of Aslam et al. [3].

Now let's clarify the results we got about the mass of raw cotton of a boll. It is known that the most valuable part of the cotton plant is raw cotton. That is, when we say raw cotton, we understand the cotton seed and the complex of fibers covering it.

The general picture in our results regarding the mass of raw cotton per boll is that for all three cotton varieties, there were no significant changes in the dependence of this parameter on the radiation dose, except for small deviations. Only in one case, a significant increase in the mass of raw cotton of a boll was observed for Ganja-160 variety at 300 and 400 Gy irradiation doses. In these doses, the mentioned parameter was 0.5 g more than the control.

In the second generation of cotton varieties, there was no change in the mass of raw cotton per boll, depending on the radiation dose. In other words, the mass change that occurred in the I generation was not maintained in the II generation.

Like the mass of raw cotton per boll, fiber yield (the part of the raw cotton that has been separated from the seed) is also an important economic indicator of cotton.

From the results presented in the table, it is clear that the dependence of fiber yield on the radiation dose in the M1 generation is different in different cotton varieties. In fact, fiber yield for Ganja-160 variety was about 1.5-2.5% more than the control at all irradiation doses. In the II generation of this variety, the fiber yield increased more, and the increase was 2.8, 3.3 and 3.5%, respectively, at 200, 300 and 400 Gy irradiation doses compared to the control.

Our results show that there is no significant dependence of the fiber yield of the experimental I generation varieties of the Ganja-182 variety on the irradiation dose. In only one variant (dose 50 Gy), the fiber yield was 2.7% higher than in the control. This result can be considered an experimental error. However, in the II generation of this variety, an increase in approximately the same amount of fiber yield at the same dose gives reason to believe that in this case there may be a stimulating effect. It is interesting that at doses of 200 Gy and higher, there was no obvious dependence of the fiber yield on the radiation dose for the I generation of Ganja-182 variety, but a significant increase in the fiber yield of the II generation of this variety was observed at appropriate doses. More precisely, fiber yield was 4.8, 3.8, and 3.6% higher at 200, 300, and 400 Gy doses than the control, respectively.

The dependence of fiber yield on irradiation dose was completely different for Ganja-183 variety. In fact, in this case, the increase in radiation dose in the first generation of the plant caused a small-scale increase in fiber yield, and then, on the contrary, a decrease. The tendency of fiber output to change in this form was also maintained in the II generation of this variety.

It should be noted that the length of the fiber is one of the most important economically valuable technological characteristics of the cotton plant, and the quality of the fiber is mainly determined by this characteristic. In the textile industry, as a raw material for various types of fabric products, fiber is evaluated according to this indicator.

Like cotton fiber yield, fiber length can also vary under the influence of various agro ecological factors. Changes in water and nutrient regimes, disruption of the agro technological process, and various mutagenic

factors can affect fiber length. The length of the fiber can vary depending on both the variety and the layers of the bolls on the plant.

Table 4, which we present, also shows the results on the dependence of the fiber length on the radiation dose for both generations of all three cotton varieties.

It can be seen from the table that in the first generation of the Ganja-160 variety, there was no change in the dependence of the length of the fiber on the radiation dose in the dose range of 0-50 Gy while a slight decrease trend was observed in the dose range of 100-400 Gy. A similar change occurred in the II generation of this variety. Simply put, the decrease in fiber length was relatively large in this generation. Thus, if in the M1 generation the decrease in fiber length was 1.0, 1.3 and 2.3 mm at doses of 200, 300 and 400 Gy, respectively, then in the M2 generation this decrease was 1.9, 2.0 and 2.1 mm.

Except for small deviations in the length of the fiber of the M1 generation of the Ganja-182 and Ganja-183 varieties, which are within the error of the experiment, almost no change has occurred. However, in the second generation of these cotton varieties, fiber length was shortened at doses of 300 and 400 Gy.

Changes in parameters, such as fiber yield and fiber length in mutant forms of cotton obtained based on the use of radiation technologies, have been confirmed in other works [3, 20-23].

Current work is continuation of research results of which were previously broadcasted in the journal [24].

Conclusion

Visible phenotypic variations in the amount of 850 plants were selected from 1100 M1 populations at the end of the growing season, using individual selection. Individual selection is of particular importance for the source material, on the basis of which the selection of economically valuable mutant forms will be carried out in subsequent generations.

Seeds of stably inherited mutants were saved for sowing the next generation of M3 cotton. It is also planned to study the M4 and M5 generations of these plants in order to obtain resistant forms to various diseases and environmental stress factors. In other words, we continue our strategy of detecting phenotypic changes. We hope that radiation mutagenesis, which is an effective and feasible method for creating libraries of plant mutants, will make it possible to obtain cotton mutants with stable heritable traits.

The selection of more valuable forms will be carried out by studying the observation of a single mutant trait or a complex of positive traits in a hybrid generation. Selected mutant hybrids will be studied for their breeding and agricultural value. According to the characteristics of mutation selection, stable mutants with one or more selection characteristics preserved in subsequent generations will be crossed with the original varieties (or with each other). That is, hybridization will be carried out according to the accepted method.

It is clear that the creation of mutant forms of cotton is of great practical importance since this allows for genetic improvement of cotton and the creation of new varieties. It should be noted that although traditional breeding methods have made a great contribution to the cultivation of cotton varieties, they have led to significant loss of genetic potential and increased susceptibility to pests [25]. Therefore, expansion of the genetic background through mutations can diversify functional genes, create new traits, and generate more germplasm resources [26]. In addition, a library of mutants is of great importance for studying gene function since acquired traits, such as fiber length, stem height, harvest quantity, leaf morphology, fiber color and other mutants, can greatly contribute to genetic breeding and basic research in cotton [19].

Summarizing the data we obtained from two generations of cotton, we can conclude that, in general, radiation produced many types of mutants, some of which had positive traits. We suggest that these forms can be used as germplasm to improve the properties of cotton.

Acknowledgements

Conflict of interest

All authors are aware of the article's content and declare no conflict of interest.

References

1. Aslam M.Z. (2002). Evolution of high yielding, early maturing and CLCuV resistant mutant of cotton NIAB-98, through the use of pollen irradiation approach. *Plant Pathology Journal*, 1(1), pp. 27-31. https://doi:10.3923/ppj.2002.27.31.

2. Muthusamy A., Narayanasamy J. (2005). Induced high yielding mutant in cotton (*Gossypium hirsutum* L.). *Mutation Breeding Newsletter and Reviews,* 1(1), pp. 6-8. https://www.researchgate.net/publication/235766382.

3. Aslam M.Z., Haq M.A., Bandesha A.A., Haidar S. (2018). NIAB-846: high yielding and better quality cotton mutant developed through pollen irradiation technique. *Pakistan Journal of Agricultural,* 55(4), pp. 767-776. https://doi: 10.21162/PAKJAS/18.5133.

4. Liu J., Zhao G., Geng J., Geng Zh., Dou H. et al. (2023). Genome-wide analysis of mutations induced by carbon ion beam irradiation in cotton. *Frontiers in Plant Science Front (Sec. Plant Breeding),* 14. https://doi.org/10.3389/fpls.2023.1056662.

5. Maluszynski M. (1990). Gene manipulation in plant improvement. II. (Gustafsson J.P., ed.), New York. Plenum press, 438 p.

6. Bhatia C.R. (1999). Release of gene silencing in transgenics – a new role for induced mutations. *Mutation Breeding Newsletter & Reviews,* 44, pp. 3-5.

7. Holme I. B., Gregersen P. L., Brinch-Pedersen H. (2019). Induced genetic variation in crop plants by random or targeted mutagenesis: Convergence and differences. *Frontiers in Plant Science,* 10. https://doi: 10.3389/fpls.2019.01468.

8. Bhoi A., Yadu B., Chandra J., Keshavkant S. (2022). Mutagenesis: A coherent technique to develop biotic stress resistant plants. *Plant Stress,* 3 (100053). https://doi: 10.1016/j.stress.2021.100053.

9. Iqbal R.M.S., Chaudhry M.B., Aslam M. and Bendasha A.A. (1994). Development of a high yielding cotton mutant NIAB-92 through the use of induced mutations. *Pakistan Journal of Botany,* 26, pp. 99-104.

10. Maluszynski M., Ahloowalia B.S. and Sigurbjornsson B. (1995) Application of in Vivo and in Vitro Mutation Techniques for Crop Improvement. *Euphytica*, 85, pp. 303-315. https://doi.org/10.1007/BF00023960.

11. Ishikawa S., Ishimaru Y., Igura M., Kuramata M., Abe T. et al. (2012). Ion-beam irradiation, gene identification, and marker-assisted breeding in the development of low-cadmium rice. *Proceedings of the National Academy of Sciences*, 109(47), pp. 19166-19171. https://doi: 10.1073/pnas.1211132109.

12. Kazama Y., Hirano T., Nishihara K., Ohbu S., Shirakawa Y., Abe T. (2013). Effect of high-LET Fe-ion beam irradiation on mutation induction in *Arabidopsis thaliana*. *Genes & Genetic Systems*, 88(3), pp. 189-197. https://doi: 10.1266/ggs.88.189.

13. Permata T.B.M., Sato H., Gu W., Kakoti S., Uchihara Y. et al. (2021). High linear energy transfer carbon-ion irradiation up regulates PD-L1 expression more significantly than X-rays in human osteosarcoma U2OS cells. J*ournal of Radiation Research*, 62(5), pp. 773-781. https://doi: 10.1093/jrr/rrab050.

14. Toker C., Yadav S.S., Solanki İ. (2007). Mutation Breeding (In book: Lentil), pp. 209-224. https://doi: 10.1007/978-1-4020-6313-8_13.

15. Tong X. H. (2021). Selection and Mechanisms of Glyphosate to Lerant Mutant R0198. Zhejiang University.

16. Mu G.J. (2008). Creation and Molecular Genetical Identification of the Beneficial Mutants in Upland Cotton (*Gossypium hirsutum* L.). Hebei Agricultural University.

17. Chen Z.G., Liu X.G. (1993). Effect of CO_2 laser water pretreatment on isolated cotyledon culture of cotton. *Journal of Anhui Agricultural University*, 20(1), p.3.

18. Dospekhov B. A. (1985). Field experiment method [Metod polevogo opyta]. M.: Agropromizdat, 352 p.

19. Zhao Z., Liu Z., Zhou Y., Wang J., Zhang Y. et al. (2022). Creation of cotton mutant library based on linear electron accelerator radiation mutation. *Biochemistry and Biophysics Reports,* 30, 101228. https://doi.org/10.1016/j.bbrep.2022.101228.

20. Muthusamy A. and Jayabalan N. (2011). In vitro induction of mutation in cotton (*Gossypium hirsutum Linnaeus*) and isolation of mutants with improved yield and fibre characters. *Acta Physiologiae Plantarum,* 33, pp. 1793-1801. https://doi.org/10.1007/s 11738-011-0718-8.

21. Muhammad A., Wazir S.M., Ullah H. and Afridi S. (2015). Effect of Selected -Irradiated Cotton Varieties on Fiber Quality During M2 Generation under Rainfed Condition. *American-Eurasian Journal of Agricultural & Environmental Sciences,* 15(2). pp. 191-196. https://doi: 10.5829/idosi.aejaes. 2015.15.2.12511.

22. Haidar S., Aslam M. and Haq M.A. (2016). NIAB-852: Anew high yielding and better quality cotton mutant developed through pollen irradiation technique. *Pakistan Journal of Botany*, 48(6), pp. 2297-2305. https://www.researchgate.net/publication/312495225.

23. Orabi M.H., El-Hoseiny H.A., Abd-El-Rahman Y. Sh., Khater M. S. (2017). The Effect of Gamma Rays on Cotton Yield, Yield Components and Fiber Quality Characters. *Journal of Plant Production*, 8(12), pp. 1277-1284. https://doi: 10.21608/JPP.2017.41981.

24. Zeynalova I.C., Tagiyev A.A., Gojayeva G.A., Jafarov E.S. (2022). types and economically valuable features of change produced by the gamma radiation before sowing the seeds by the M1 generation of the cotton plant". *International Journal of Biology and Chemistry,* 15(2), pp. 40-46. doi.org/10.26577/İjbch.2022.V15.İ2.06.

25. Aslam U., Cheema H., Sheraz A., Khan, I.A., Waqas M., Khan A.A. (2016). COTIP: cotton-TILLING platform, a resource for plant improvement and reverse genetic studies. *Frontiers in Plant Science,* 7, 1863. https://doi: 10.3389/fpls.2016.01863.

26. Xu T., Bian N., Wen M., Xiao J., Yuan C. et al. (2017). Characterization of a common wheat (*Triticum aestivum* L.) high-tillering dwarf mutant. *Theoretical and Applied Genetics*, 130, pp. 483-494.

Information about authors:

Elimkhan Jafarov – (corresponding author) – Doctor of Science, Professor, Institute of Radiation Problems of the Ministry of Science and Education of the Republic of Azerbaijan, Baku, Azerbaijan, e-mail: elimkhan.jafarov@gmail.com

Aladdin Tagiyev – Doctor of Science, Professor, Scientific Research Institute of Plant Protection and Technical Plants of the Ministry of Agriculture of the Republic of Azerbaijan, Ganja, Azerbaijan, e-mail: t.eleddin@mail.ru

Intizar Zeynalova – Associate Professor, Scientific Research Institute of Plant Protection and Technical Plants of the Ministry of Agriculture of the Republic of Azerbaijan, Ganja, Azerbaijan, e-mail: z-va.tarana@mail.ru

Mehriban Velijanova – PhD, Associate Professor, Institute of Radiation Problems of the Ministry of Science and Education of the Republic of Azerbaijan, Baku, Azerbaijan, e-mail: mehriban.velijanova@gmail.com

Anar Jafarov – Associate Professor, Institute of Radiation Problems of the Ministry of Science and Education of the Republic of Azerbaijan, Baku, Azerbaijan, e-mail: anar_jafarov@internet.ru

K.S. Utegenova [1,3] ⒾⒹ , S.S. Bakiyev [1,2] ⒾⒹ , D.S. Mambetova [1,3] ⒾⒹ ,

A.Zh. Kauysbekov [1,3] ⒾⒹ , A.K. Bissenbaev[1,3*] ⒾⒹ

[1]A-Farabi Kazakh National University, Almaty, Kazakhstan
[2]Makhambet Utemisov West Kazakhstan University, Uralsk, Kazakhstan
[3]Scientific Research Institute of Biology and Biotechnology Problems, Almaty, Kazakhstan
*e-mail: amangeldy.bisenbaev@kaznu.kz

Biochemical and molecular genetic identification of the bacterial pathogen – *Aeromonas bestiarum* from a diseased Siberian sturgeon (*Acipenser baerii*)

Abstract. The article presents the results of isolation and identification of the bacterium *Aeromonas bestiarum* from diseased individuals of Siberian sturgeon (*Acipenser baerii*) reared in recirculating aquaculture system (RAS). As a result of biochemical studies, the isolated strain *A. bestiarum* AB002 is characterized as: a Gram-negative, non-motile oxidase-positive bacillus capable of growing in a wide temperature range from 13 to 42 ºC. In addition, strain AB002 is characterized by the hydrolysis of gelatin and esculin, forming H_2S and indole, and exhibits arginine dihydrolase activity. The analysis of bacterial resistance to antibiotics revealed that strain AB002 is resistant to multiple groups of antibiotics, including Penicillins (Oxacillin, Penicillin G, Ampicillin, Amoxicillin); Cephalosporins (Cefazolin); Macrolides (Erythromycin); Lincomycins (Lincomycin); Rifamycins (Rifampicin); Coumarins (Novobiocin). The analysis of virulence factors revealed that the pathogenic strain *A. bestiarum* AB002 is characterized by the presence of 6 virulence genes out of 10 studied, among which lipase (*pla*), cytotonic enterotoxin (*alt*), serine protease (*ahe2*), DNAase (*nucl*), cholesterol acyltransferase (*gcaT*), aerolysin (*aerA*) were identified.
Key words: *Acipenser baerii*, *Aeromonas bestiarum*, biochemical characteristics, 16S rRNA gene, *gyr*B gene.

Introduction

Bacteria of the genus *Aeromonas* are ubiquitous and represent a large community in the ecosystem [1]. The bacteria of the genus *Aeromonas* have a wide distribution in water and aquatic environments. Their ability to move across the ecosystem is facilitated by the presence of flagella [2]. Similar to numerous Gram-negative bacteria, the *Aeromonas* genus is capable of causing disease in animals [3], and certain members of the genus can potentially cause disease in humans under specific conditions [4, 5]. In addition, sturgeon fish are no exception and are also susceptible to diseases caused by bacteria of the *Aeromonas* genus [6]. The most common pathogenic representatives of bacteria of the genus *Aeromonas* are *A. hydrophila*, *A. salmonicida*, *A. veronii*, which can cause death of fish in aquaculture conditions [7-9]. The main virulence factors in bacteria of the genus *Aeromonas* include: haemolysin, aerolysin, elastase, and cytolytic enterotoxins [10]. Through the presence of virulence factors, bacteria of the genus *Aeromonas* cause numerous hemorrhages on the body, boils, branchial ischemia, and catarrhal and hemorrhagic inflammation of internal organs in fish [11, 12]. At the same time, many members of the genus *Aeromonas* have recently shown multiple resistance to the antibiotics used against them, which causes a serious risk. *Aeromonas bestiarum* is one of the representatives of pathogenic bacteria of the genus *Aeromonas*. As a result of *A. bestiarum* infection, the following clinical signs are observed in fish: necrosis of the fins, numerous hemorrhages on the body [13, 14]. However, information on the representative of *A. bestiarum* is very limited. In this regard, the conducted studies provide a comprehensive understanding of the biology of *A. bestiarum*. The results include detailed information on the biochemical and physiological characteristics of the bacterium, as well as analyses of the presence of virulence and antibiotic resistance genes. These findings will be crucial for enhancing measures to protect and prevent diseases caused by this bacterium.

Materials and methods

Biological specimens were obtained from the ulcers and internal organs of diseased Siberian sturgeons (*A. baerii*) reared under industrial aquaculture conditions. The obtained biological materials were inoculated into both liquid and solid nutrient media, specifically Lisogenic Broth (LB) and LB agar, respectively. Bacterial colonies were grown at a temperature of 37 ℃ in a thermostat within 16 hours. Isolated colonies were selected for further research. The morphological properties of bacterial colonies were determined. Biochemical identification was performed according to Bergey's manual [15] using the following biochemical tests: oxidase test, methyl red test, oxidative-fermentative (OF) test, Voges-Proskauer reaction, amino acid decarboxylation and hydrolysis tests, gelatin and esculin hydrolysis test, formation of acids from carbohydrates [15-17]. Bacterial DNA was isolated using the boiling method [18] and the Easy Pure Bacteria Genomic DNA Kit (Trans Gen Biotech, China). Molecular genetic identification of the bacterium was performed using the following 16S rRNA gene primers: 27F: 5'-AGAGTTTGATCCTG-GCTCAG-3' and 1492R: 5'-GGCTACCTTGT-TACGACTT-3' [19]. Primers used for the *gyr*B gene, *gyr*B-F: 5'-TCCGGGGCGGTCTGCACGGC-GT-3' and *gyr*B-R: 5'-TTGTCCGGGGGTTGTTG-TACTCGTC-3' [20]. The nucleotide sequence was determined using the Sanger method. The obtained sequences of the 16S rRNA and *gyr*B genes of the *A. bestiarum* strain were used to construct phylogenetic trees. Sequence searches were performed using BLAST through the NCBI website. Phylogenetic trees were constructed using the neighbour-joining method in MEGA XI software according to Han et al. (2017) [21]. The primers of the following genes were used to analyse virulence factors: haemolysin (*hlyA*), aerolysin (*aerB* and *aerA*), cytotonic enterotoxins (*alt* and *ast*), elastase (*ahpB*), cholesterol acyltransferase (*gcaT*), lipase (*pla*), DNAase (*nucl*), serine protease (*ahe2*) presented in Table 1.

Table 1 – Sequences of primers used to determine the presence of virulence genes

Primers	DNA sequence (5'-3')	Amplicon (b.p.)	Source
AH-aerAF	CAAGAACAAGTTCAAGTGGCCA	309	[22]
AH-aerAR	ACGAAGGTGTGGTTCCAGT		
hlyA-F	GGCCGGTGGCCCGAAGATACGGG	595	[23]
hlyA-R	GGCGGCGCCGGACGAGACGGG		
Aer-F	CCGGAAGATGAACCAGAATAAGAG	451	[24]
Aer-R	CTTGTCGCCACATACCTCCTGGCC		
Ast-F	TCTCCATGCTTCCCTTCCACT	331	[25]
Ast-R	GTGTAGGGATTGAAGAAGCCG		
Pla-F	ATCTTCTCCGACTGGTTCGG	382	[25]
Pla-R	CCGTGCCAGGACTGGGTCTT		
AhpB-F	ACACGGTCAAGGAGATCAAC	513	[25]
AhpB-R	CGCTGGTGTTGGCCAGCAGG		
Alt-F	TGACCCAGTCCTGG	442	[26]
Alt-R	GGTGATCGATCACC		
Ahe2-F	ACGGGGTGCGTTCTTCCTACTCCAG	211	[27]
Ahe2-R	CCGTTCATCACGCCGTTATAGTCG		
ExN-F	CAGGATCTGAACCGCCTCTATCAGG	504	[27]
ExN-R	GTCCCAAGCTTCGAACAGTTTACGC		
gcaT-F	CTCCTGGAATCCCAAGTATCAG	237	[28]
gcaT-R	GGCAGGTTGAACAGCAGTATCT		

The following 19 antibiotics (Condalab, Spain) were used to determine antibiotic resistance: oxacillin (1 µg), rifampicin (5 µg), enrofloxacin (5 µg), ampicillin (10 µg), amoxicillin (10 µg), penicillin G (10 µg), norfloxacin (10 µg), gentamicin (10 µg), streptomycin (10 µg), chloramphenicol (10 µg), lincomycin (10 µg), erythromycin (15 µg), trimethoprim + sulfamethoxazole (25 µg), cefazolin (30 µg), tetracycline (30 µg), oxytetracycline (30 µg), novobiocin (30 µg), florfenicol (30 µg), nitrofurantoin (300 µg). The antibiotic resistance of microorganisms was assessed using disc diffusion method according to relevant guidelines [29, 30].

Results and discussion

The isolated bacterial colonies were characterized as small, rounded with even edges, translucent beige in color, up to 1.5 mm in size, with a smooth, soft slightly slimy surface. Bacterial colonies appear as bulging masses on the surface of a dense nutrient medium. The isolate AB002 is a Gram-negative, non-motile, oxidase-positive bacillus (Table 2).

Table 2 – Results of biochemical and physiological characteristics of *A. bestiarum* AB002

№	Characteristics	AB002	№	Characteristics	AB002
1	Gram stain	-	14	Arginine dihydrolase	+
2	Morphology	rod	15	ONPG	+
3	Motility	-		Acid formation from:	
4	Oxidase	+	16	Sucrose	+
5	Methyl red	+	17	Trehalose	+
6	Voges-Proskauer test	+	18	D-xylose	-
7	O/F test	F	19	Lactose	-
8	Hydrolysis of gelatine	+		Growth under conditions:	
9	Hydrolysis of esculin	+	20	0-4% NaCl	+
10	H_2S formation	+	21	5% NaCl	-
11	Indole formation	+	22	13, 27, 32, 37, 42°C	+
12	Lysine decarboxylase	-	23	pH 3.0	-
13	Ornithine decarboxylase	-	24	pH 5.0-9.0	+

Note: «+» – positive, «−» – negative, « F» – fermentative

The results of the studies demonstrated that strain AB002 was capable to grow in a wide range of NaCl concentrations from 0 to 4% and at temperatures from 13-42 ºC and pH values from 5.0 to 9.0. It exhibited a positive reaction in methyl red test, Voges-Proskauer test, and was also capable of hydrolyzing gelatin and esculin, forming H_2S and indole. A negative reaction was observed in the lysine decarboxylase and ornithine decarboxylase tests and in the D-xylose and lactose tests.

Meanwhile, strain AB002 exhibits arginine dihydrolase activity and forms acids from sucrose and trehalose. Thus, the obtained results of biochemical characteristics of strain AB002 corresponded to bacteria of the genus *Aeromonas* [11, 12].

To determine the species identity of strain AB002 within the genus *Aeromonas*, sequencing of full-length 16S rRNA and *gyr*B genes was performed. Analysis of the PCR products by electrophoresis in 1% agarose gel showed single specific bands of about 1000 and 1500 bp in length (Figure 1).

Sequencing of full-size 16S rRNA and *gyr*B genes of the AB002 strain with subsequent phylogenetic tree construction has identified the *gyr*B gene with a high level of homology of up to 99% as a species of *Aeromonas bestiarum* (Figure 2).

According to the obtained results of antibiotic resistance studies of the isolated strain, AB002 was shown to exhibit multiple resistance to different groups of antibiotics, including β-lactams (Table 3).
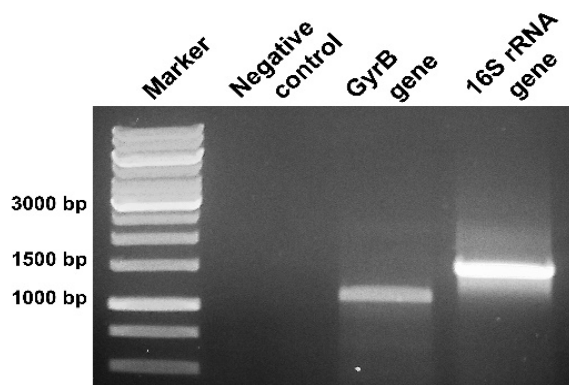
Figure 1 – Agarose gel electrophoresis of PCR products
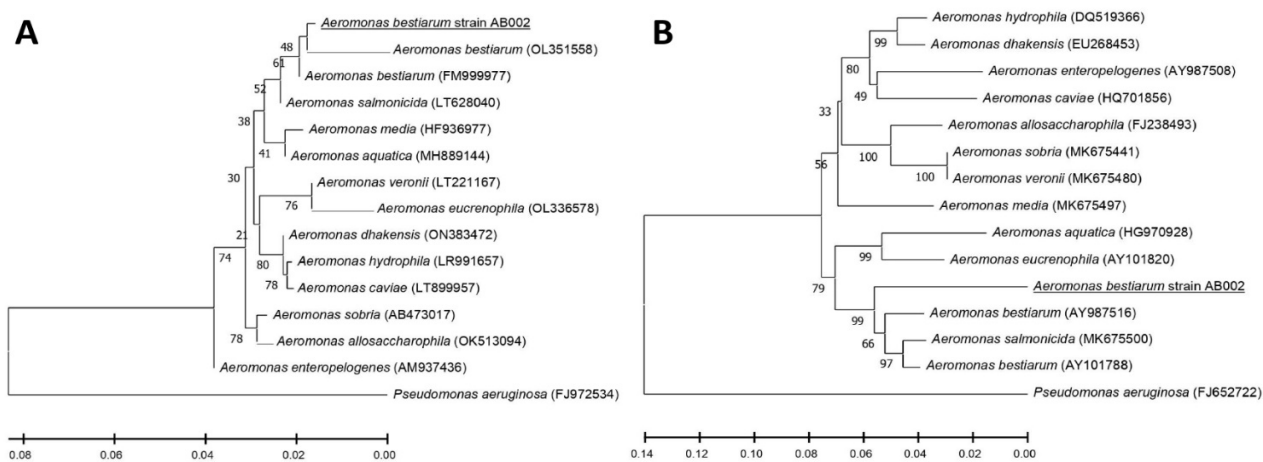of the 16S rRNA and *gyr*B genes

Figure 2 – Phylogenetic trees of the isolated strain *A. bestiarum* AB002 based on
16S rRNA (A) and *gyr*B (B) gene sequences with known bacteria of the genus *Aeromonas*

Table 3 – Results of antibiotic resistance analysis of the isolated AB002 strain

Group	Antibiotic	Disk Content (μg)	AB002	
			Sensitivity	Zone diameter (mm)
Penicillins	Oxacillin	1	R	0
	Penicillin G	10	R	0
	Ampicillin	10	R	0
	Amoxicillin	10	R	0
Quinolones	Enrofloxacin	5	S	27
	Norfloxacin	10	S	28±1
Cephalosporins	Cefazolin	30	R	0
Aminoglycosides	Gentamicin	10	S	20.3±1.5
	Streptomycin	10	S	17.7±0.6
Nitrofurans	Nitrofurantoin	300	S	18±1

Continuation of the table

Group	Antibiotic	Disk Content (µg)	AB002	
			Sensitivity	Zone diameter (mm)
Tetracyclines	Tetracycline	30	S	23.3±0.6
	Oxytetracycline	30	I	21.7±0.6
Macrolides	Erythromycin	15	R	13.2±0.3
Lincomycins	Lincomycin	10	R	7.7±1.2
Rifamycins	Rifampicin	5	R	9.3±0.6
Coumarins	Novobiocin	30	R	9.2±0.3
Amphenicols	Chloramphenicol	10	S	24.3±0.6
	Florfenicol	30	S	25.3±1.5
Folic acid synthesis inhibitors	Trimethoprim + sulfamethoxazole	25	S	16.5±0.9
Note: R – resistant, I – intermediate, S – sensitive				

The strain AB002 has been found to be resistant to several antibiotic groups, including penicillins (oxacillin, 1 µg, ampicillin, 10 µg, amoxicillin, 10 µg, penicillin, 10 µg), cephalosporins (cefazolin, 30 µg), macrolides (erythromycin, 15 µg), lincomycins (lincomycin, 10 µg), rifamycins (rifampicin, 5 µg), and coumarins (novobiocin, 30 µg). The sensitivity of strain AB002 to the following antibiotics was found: enrofloxacin (5 µg), norfloxacin (10 µg), gentamicin (10 µg), streptomycin (10 µg), nitrofurantoin (300 µg), tetracycline (30 µg), chloramphenicol (10 µg), florfenicol (30 µg), and trimethoprim + sulfamethoxazole (25 µg). The results showed that the strain had an intermediate sensitivity to oxytetracycline (30 µg). The analysis of antibiotic resistance revealed that strain AB002 is resistant to 9 out of 19 antibiotics tested, indicating that *A. bestiarum* is a multi-drug-resistant strain. For instance, resistance to β-lactams (penicillins, cephalosporins and carbapenems) is a common occurrence in *Aeromonas* bacteria [11, 31-33]. The resistance to a wide range of antibiotics may be attributed to their extensive use in prophylactic veterinary practices in aquaculture fish production. However, despite the multidrug resistance, the study also found that *A. bestiarum* is sensitive to several antibiotics, including quinolones, aminoglycosides, nitrofurans, amphenicols, and inhibitors of folic acid synthesis.

Assessing the pathogenicity and toxicity of pathogenic bacteria relies heavily on their virulence factors [34]. The study also examined the presence of virulence factors in the isolated strain AB002, as shown in (Figure 3).
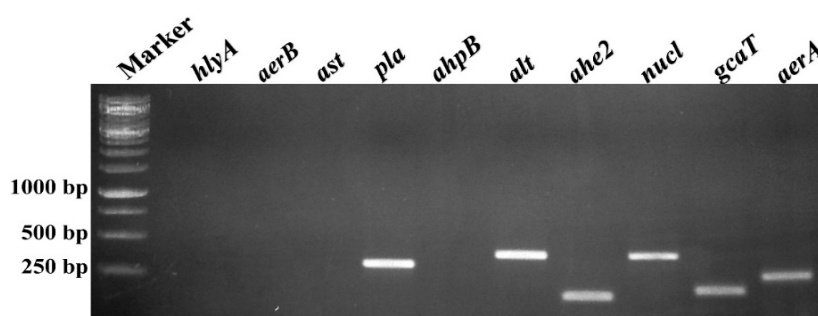

Figure 3 – Agarose gel electrophoresis of the amplicons of virulence genes of isolate AB002

The study identified several virulence factors in strain AB002, including lipase (*pla*), cytotonic enterotoxin (*alt*), serine protease (*ahe2*), DNAase (*nucl*), cholesterol acyltransferase (*gcaT*), and aerolysin (*aerA*). Notably, strain AB002 possesses a complex of serine protease and aerolysin, which is known to increase the bacterium's overall pathogenicity [35].

Conclusion

AB002 was isolated as a result of the conducted studies. The study provides the findings of the biochemical and physiological characteristics of strain AB002, which was identified as an oxidase-positive, non-motile, Gram-negative bacillus capable of growing over a wide temperature range from 13 to 42 ºC. As a result of molecular genetic analysis of the nucleotide sequences of 16S rRNA and *gyr*B genes, strain AB002 was identified as a species of *A. bestiarum*. The isolated strain AB002 is characterized as multi-drug resistant, showing resistance to 9 and 19 antibiotics tested. In addition, 6 virulence factors were detected in strain AB002 out of 10 tested, indicating that the isolated strain exhibits pathogenicity. The research results provide new insights into the biology of the pathogenic bacterium *A. bestiarum*, including its antibiotic resistance and virulence factors. These findings can be used to develop control measures against pathogenesis caused by *A. bestiarum*.

Acknowledgments

Conflict of interest

All authors are aware of the article's content and declare no conflict of interest.

References

1. Fernández-Bravo A., Figueras M.J. (2020). An update on the genus Aeromonas: taxonomy, epidemiology, and pathogenicity. *Microorganisms*, 8(1), pp. 1-39. https://doi.org/10.3390/microorganisms8010129

2. Kirov S.M., Tassell B.C., Semmler A.B., O'Donovan L.A., Rabaan A.A., Shaw J.G. (2002). Lateral flagella and swarming motility in *Aeromonas* species. *J bact.*, 184(2), pp. 547–555. https://doi.org/10.1128/JB.184.2.547-555.2002

3. Roges E.M., Gonçalves V.D., Cardoso M.D., Festivo M.L., Siciliano S., Berto L.H., Pereira V.L.A., Rodrigues D.D.P., de Aquino M.H.C. (2020). Virulence-associated genes and antimicrobial resistance of *Aeromonas hydrophila* isolates from animal, food, and human sources in Brazil. *BioMed research international*, 2020, pp. 1-8. https://doi.org/10.1155/2020/1052607

4. Altwegg M., Steigerwalt A.G., Altwegg-Bissig R., Lüthy-Hottenstein J., Brenner D.J. (1990). Biochemical identification of Aeromonas genospecies isolated from humans. *J. Clin. Microbiol*, 28(2), pp. 258-264. https://doi.org/10.1128/jcm.28.2.258-264.1990

5. Pessoa R.B.G., de Oliveira W.F., Correia M.T.D.S., Fontes A., Coelho L.C.B.B. (2022). Aeromonas and Human Health Disorders: Clinical Approaches. *Front Microbiol*, 13, pp. 1-15. https://doi.org/10.3389/fmicb.2022.868890

6. Bakiyev S.S., Bissenbaev A.K. (2021). Diseases caused by bacteria of the Aeromonas and Pseudomonas genus when reared fish in controlled systems [Zabolevanija, vyzyvaemye bakterijami rodov Aeromonas i Pseudomonas pri vyrashhivanii ryb v uslovijah reguliruemyh sistem]. *Al-Farabi KazNU Exp. Biol,* 87(2), pp. 4-16. https://doi.org/10.26577/eb.2021.v87.i2.01

7. Guz L., Kozińska A. (2004). Antibiotic susceptibility of *Aeromonas hydrophila* and *A. sobria* isolated from farmed carp (*Cyprinus carpio* L.). *Bull. Vet. Inst. Pulawy*, 48(4), pp. 391-395.

8. Chen F., Sun J., Han Z., Yang X., Xian J.A., Lv A., Hu X., Shi H. (2019). Isolation, identification and characteristics of *Aeromonas veronii* from diseased crucian carp (*Carassius auratus* gibelio). *Front. Microbiol,* vol. 10, pp. 1-10. https://doi.org/10.3389/fmicb.2019.02742

9. Lian Z., Bai J., Hu X., Lü A., Sun J., Guo Y., Song Y. (2020). Detection and characterization of *Aeromonas salmonicida subsp. salmonicida* infection in crucian carp *Carassius auratus*. *Vet. Res. Commun.*, 44(2), pp 61-72. https://doi.org/10.1007/s11259-020-09773-0

10. Ahangarzadeh M., Ghorbanpour Najafabadi, M., Peyghan R., Houshmand H., Sharif Rohani M., Soltani M. (2022). Detection and distribution of virulence genes in Aeromonas hydrophila isolates causing infection in cultured carps. *Vet. Res. Forum*, 13(1), pp. 55-60. https://doi.org/10.30466%2Fvrf.2020.115998.2761

11. Bakiyev S., Smekenov I., Zharkova I., Kobegenova S., Sergaliyev N., Absatirov G., Bissenbaev A. (2022). Isolation, identification, and characterization of pathogenic *Aeromonas hydrophila* from critically endangered *Acipenser baerii. Aquac. Rep,* 26(6), pp. 1-11. http://dx.doi.org/10.1016/j.aqrep.2022.101293

12. Bakiyev S., Smekenov I., Zharkova I., Kobegenova S., Sergaliyev N., Absatirov G., Bissenbaev A. (2023). Characterization of atypical pathogenic *Aeromonas salmonicida* isolated from a diseased Siberian sturgeon (*Acipenser baerii*). *Heliyon*, 9(7), pp. 1-17. https://doi.org/10.1016/j.heliyon.2023.e17775

13. Pieters N., Brunt J., Austin B., Lyndon A.R. (2008). Efficacy of in-feed probiotics against *Aeromonas bestiarum* and *Ichthyophthirius multifiliis* skin infections in rainbow trout (*Oncorhynchus mykiss*, Walbaum). *J Appl. Microb.*, 105(3), pp. 723-732. https://doi.org/10.1111/j.1365-2672.2008.03817.x

14. Fuentes-Valencia M.A., Osornio-Esquivel J.L., Martínez Palacios C.A., et al. (2022). Bacterial and parasite co-infection in Mexican golden trout (*Oncorhynchus chrysogaster*) by *Aeromonas bestiarum, Aeromonas sobria, Plesiomonas shigelloides* and *Ichthyobodo necator*. *BMC Vet Res.*, 18(137), pp. 1-11. https://doi.org/10.1186/s12917-022-03208-5

15. Holt J., Kriga N., Snita P., Staley J., Williams S. (1997). Bergey's Manual determinative bacteriology: in 2 vol., [Opredelitel' bakterij Berdzhi: v 2-h tomah]. M.: Mir, 432 p.

16. El-Barbary M., Hal A. (2016). Isolation and molecular characterization of some bacterial pathogens in El-Serw fish farm, Egypt. *Egyp. J. Aqua. Bio. Fish,* 20(4), pp. 115-127. http://dx.doi.org/10.21608/ejabf.2016.11183

17. Gufe C., Hodobo T.C., Mbonjani B., Majonga O., Marumure J., Musari S., Gilbert J., Pious V.M., Jairus M. (2019). Antimicrobial profiling of bacteria isolated from fish sold at informal market in Mufakose, Zimbabwe. *Int. J. Microbiol.*, 2019, pp. 1-7. https://doi.org/10.1155/2019/8759636

18. Scarpellini M., Franzetti L., Galli A. (2004). Development of PCR assay to identify *Pseudomonas fluorescens* and its biotype. *FEMS Microbiol. Lett.*, 236(2), pp. 257-260. https://doi.org/10.1016/j.femsle.2004.05.043

19. Lane D.J. (1991). 16S/23S rRNA sequencing. In Nucleic acid techniques in bacterial systematics. Ed. by E. Stackebrandt, M. Goodfellow. John Wiley and Sons, Chichester, UK, pp. 177-203.

20. Hu M., Wang N., Pan Z.H., Lu C.P., Liu Y.J. (2012). Identity and virulence properties of Aeromonas isolates from diseased fish, healthy controls and water environment in China. *Lett. Appl. Microbiol*, 55(3), pp. 224-233. https://doi.org/10.1111/j.1472-765x.2012.03281.x

21. Han Z., Sun J., Lv A., Sung Y., Shi H., Hu X., Xing K. (2017). Isolation, identification and characterization of Shewanella algae from reared tongue sole, *Cynoglossus semilaevis* Günther. *Aquac*, 468, pp. 356-362. https://doi.org/10.1016/j.aquaculture.2016.10.038

22. Wang G., Clark C.G., Liu C., Pucknell C., Munro C.K., Kruk T.M., Caldeira R., Woodward D.L., Rodgers F.G. (2003). Detection and characterization of the hemolysin genes in *Aeromonas hydrophila* and *Aeromonas sobria* by multiplex PCR. *J. Clin. Microbiol.*, 41(3), pp. 1048-1054. https://doi.org/10.1128/jcm.41.3.1048-1054.2003

23. Zhu D., Aihua L., Jianguo W., Ming L., Taozhen C., Jing H. (2007). Correlation between the distribution pattern of virulence genes and virulence of *Aeromonas hydrophila* strains. *Front. Biol. China*, 2(2), pp. 176-179. https://doi.org/10.1007/s11515-007-0024-4

24. Falcón R., d'Albuquerque T., Luna M. das G., Freitas-Almeida A., Yano T., Adley C. (2006). Detection of hemolysins in Aeromonas spp. *M. Biotech. F.-B. Pathogens. M. Prot.*, 21, pp. 1-13. https://doi.org/10.1385/1-59259-990-7:003

25. Sen K., Rodgers M. (2004). Distribution of six virulence factors in *Aeromonas* species isolated from US drinking water utilities: a PCR identification. *J. Appl. Microbiol*, vol. 97(5), pp. 1077-1086. https://doi.org/10.1111/j.1365-2672.2004.02398.x

26. Li J., Ni X.D., Liu Y.J., Lu C.P. (2011). Detection of three virulence genes alt, ahp and aerA in *Aeromonas hydrophila* and their relationship with actual virulence to zebrafish. *J. Appl. Microbiol*, 110(3), pp. 823-830. https://doi.org/10.1111/j.1365-2672.2011.04944.x

27. Nam I.Y., Joh K. (2007). Rapid detection of virulence factors of *Aeromonas* isolated from a trout farm by hexaplex-PCR. *J. Microbiol*, 45(4), pp. 297-304.

28. Thornton J., Howard S.P., Buckley J.T. (1988). Molecular cloning of a phospholipid-cholesterol acyltransferase from Aeromonas hydrophila: Sequence homologies with lecithin-cholesterol acyltransferase and other lipases. *Biochim. Biophys,* 959(2), pp. 153-159. https://doi.org/10.1016/0005-2760(88)90026-4

29. Hudzicki J. (2009). Kirby-Bauer disk diffusion susceptibility test protocol. American Society for Microbiology, pp. 1-23.

30. CLSI supplement M100-Ed32 (2022). Performance standards for antimicrobial susceptibility testing. Clinical and laboratory standards institute, USA.

31. Ramadan H., Ibrahim N., Samir M., Abd El-Moaty A., Gad T. *Aeromonas hydrophila* from marketed mullet (*Mugil cephalus*) in Egypt: PCR characterization of β-lactam resistance and virulence genes. *J. Appl. Microbiol*, 124(6), pp. 1629-1637. https://doi.org/10.1111/jam.13734

32. Lupiola-Gómez P.A., González-Lama Z., Tejedor-Junco M.T., González-Martín M., Martín-Barrasa J.L. (2003). Group 1 β-lactamases of *Aeromonas caviae* and their resistance to β-lactam antibiotics. *Can. J. Microbiol*, 49(3), pp. 207-215. https://doi.org/10.1139/w03-030

33. Bakken J.S., Sanders C.C., Clark R.B., Hori M. (1988). Beta-lactam resistance in *Aeromonas* spp. caused by inducible beta-lactamases active against penicillins, cephalosporins, and carbapenems. *Antimicrob. A. Chemot.*, 32(9), pp. 1314-1319. https://doi.org/10.1128/aac.32.9.1314

34. Gao T., Ding Y., Wu Q., Wang J., Zhang J., Yu S., Yu P., Liu C., Kong L., Feng Z., Chen M., Wu S., Zeng H., Wu H. (2018). Prevalence, virulence genes, antimicrobial susceptibility, and genetic diversity of *Bacillus cereus* isolated from pasteurized milk in China. *Front. Microbiol.*, 9. pp. 1-11. https://doi.org/10.3389/fmicb.2018.00533

35. Abrami L., Fivaz M., Decroly E., Seidah N.G., Jean F., Thomas G., Leppla S.H., Buckley J.T., van der Goot F.G. (1998). The pore-forming toxin proaerolysin is activated by furin. *J. Biol. Chem,* 273(49), pp. 32656-32661. https://doi.org/10.1074/jbc.273.49.32656

Information about authors:

Utegenova Kalamkas – PhD student, Department of Biophysics, Biomedicine and Neuroscience, Al-Farabi Kazakh National University, researcher, Scientific Research Institute of Biology and Biotechnology Problems, Almaty, Kazakhstan, e-mail: kalamkas.utegenova@yandex.kz

Bakiyev Serik – PhD, Senior lecturer, Makhambet Utemisov West Kazakhstan University, Uralsk, Kazakhstan, researcher, Scientific Research Institute of Biology and Biotechnology Problems, Almaty, Kazakhstan, e-mail: serik_2595@mail.ru

Mambetova Dana – master's student, Department of Biodiversity and Bioresources, Al-Farabi Kazakh National University, Almaty, Kazakhstan, researcher, Scientific Research Institute of Biology and Biotechnology Problems, Almaty, Kazakhstan, e-mail: dana.mambetova.01@gmail.com

Kauysbekov Almas – master's degree, Department of Molecular Biology and Genetics, Al-Farabi Kazakh National University, Almaty, Kazakhstan, researcher, Scientific Research Institute of Biology and Biotechnology Problems, Almaty, Kazakhstan, e-mail: almas.kauysbekov@bk.ru

Bissenbaev Amangeldy – (corresponding author) – Doctor of Biological Sciences, Professor, Academician, Department of Molecular Biology and Genetics, Head of Scientific Research Institute of Biology and Biotechnology Problems, Al-Farabi Kazakh National University, Almaty, Kazakhstan, e-mail: amangeldy.bisenbaev@kaznu.kz

I. Owais [1*] , N. Koondhar [2] , N.A. Rajput [3] ,
M.A. Khanzada [4] , N. Khanzada [4] , S. Zaman [4]

[1]Yunnan Agricultural University, Kunming, China
[2]Lasbela University of Agriculture Water and Marine Sciences, Balochistan, Pakistan
[3]University of Agriculture, Faisalabad, Pakistan
[4]Sindh Agriculture University, Tando Jam, Pakistan
*e-mail: owais.iqbal.918@gmail.com

Comparative effectiveness of some novel fungicides and different biocontrol agents against two *Colletotrichum musae* isolates under laboratory condition

Abstract. *Colletotrichum musae*, is aggressive and devastating threat and causing huge losses in banana production globally. The use of various fungicides and as well as biocontrol agents can help to manage the crop. However, five different fungicides, namely., Antracol, Defeater plus, Ridomil gold, Kocide, and Topsin M at five different concentrations viz., 10 ppm, 100 ppm, 200 ppm, 500 ppm, and 1,000 ppm were used to check the growth inhibition of the two isolates (CM02 and CM11) of *C. musae* by food poison technique. The topsin M fungicide at all concentrations (10-1,000 ppm) was highly effective, which yielded 72-98% inhibition, followed by Ridomil gold 1,000 ppm caused 82.11% and 79% inhibition of both isolates. Ridomil gold at 500 ppm causes 75.13% and 69.44% mycelial growth inhibition of CM02 and CM11. In comparison, Kocide at 1,000 ppm caused more than 60% inhibition of both strains. However, we observed that, as the concentration decreased the mycelial growth of the pathogen increased. Furthermore, during the present investigation, three biocontrol agents, viz., *Trichoderma harzianum*, *Trichoderma polysporum* and *Paecilomyces variotii* were used for their antifungal activity against (CM02 and CM11) by dual assay test. *T. harzianum* proved highly effective biocontrol agents and cause (18.88% and 20.11%) mycelial inhibition of both strains, followed by *T. polysporum* (13.33% and 15%) and *P. variotii* (9.11% and 8.75%) on 3rd, 4th and 7th day of inoculation by dual assay test. In conclusion, among all tested fungicides, Topsin M was found highly effective against both strains of *Colletotrichum musae*. Therefore, biological control especially with *Trichoderma* species are promising method to control this pathogen quickly. Both isolates of *C. musae* showed high sensitivity against Trichoderma species on the third and fourth day of inoculation.
Key words: Banana, anthracnose, *Colletotrichum musae*, fungicides, biocontrol agents.

Introduction

Banana (*Musa spp*), members of the Musaceae family, are a major commercial fruit crop cultivated in many parts of the world [1]. Many species of big herbaceous blooming plants in the genus *Musa* yield an edible fruit known as a banana. The fruit may vary in size, colour, shape and firmness, but is frequently elongated and bent [2]. It has a starchy, juicy interior covered by thin skin that turns various colors when mature. It is the fourth-largest food crop consumed in the globe after wheat, rice and maize and also considers the fourth most valuable food after rice, meat, and milk [3, 4]. In Pakistan, banana fruit about 34.8 thousand hectares with annual production is 154.8 thousand tons, whereas Sindh province contributes 87% of the total banana production of the country [5]. Due to the absence of agrochemical and biocontrol applications and the extended time between harvesting and reaching the market, organic bananas are more prone to postharvest diseases, which can degrade their quality when compared to conventional banana crops [6]. Postharvest disease caused by fungal pathogens is most important and aggressive factor, which cause huge economically losses in the globe [7, 8]. Among them, anthracnose rot caused by *Colletotrichum (C.) musae* is a huge problem in bananas production, which affect the

fruit quality and commercial viability worldwide [9]. The fungus cause brown to black lesions appearing symptoms on banana, which are usually diamond-shaped. Symptoms of the disease appear when the banana is still green. Orange or salmon-colored rings consisting of fungal spores may pronounce in the latter stage around the lesions, and the lesion appears more sunken than orange-colored masses of spores [10]. Many postharvest disease including, anthracnose rot are managed through agrochemicals, which available in the market [11, 12]. Therefore, the continued application of these fungicides has led to the emergence of *C. musae* strains that have developed resistance to them [13]. Nowadays, consumers demand chemical-free fresh fruits and look for substitute approaches for managing diseases [9, 14].

Biological control has emerged as one of the most promising strategies for preventing and reducing postharvest losses. Especially when disease resistance or chemical control options are unavailable [15]. For the last few years, many researchers are showing interest in controlling plant disease through biological control [16]. Plant pathogen populations can be hidden from view by biological control, a method used to combat plant diseases [17]. Many *Trichoderma* species are valuable against plant diseases [18, 19]. Therefore, the present study was aimed to evaluate the five fungicides at five different doses and three biocontrol agents against two isolates of *C. musae* causing anthracnose rot disease in bananas.

Materials and methods

Collection, isolation, and identification of pathogens. To isolate the fungal pathogen, anthracnose-affected banana fruits were collected from different banana orchards in the district Matiari of Sindh province, Pakistan. Collected samples were kept in paper bags with location tags and carried out into the laboratory to isolate fungi associated with banana fruit. The sample was rinsed with tap water to cleanse the fruits from any adhering soil particles. The infected parts of the banana fruit skin having the disease were cut into small pieces (1 cm) with the help of a sterilized scalpers knife. They were surface sterilized for 1-2 minutes with 5% NaClO solution, rinsed three times with distilled sterilized water (DSW), and then put on PDA Petri plates amended with streptomycin sulfate and penicillin at 1 ml/L. Five pieces of banana fruit skin were placed in each Petri plate and incubated at 28°C for 3-4 days. The strains of *C. musae* were identified based on mycelial characters, color, size, and shape described by [20] and [21].

In vitro screening of fungicides against two isolates of C. musae. Five different fungicides viz., Antracol, Defeater plus, Ridomil gold, Kocide and Topsin M were used at five different doses viz., 10 ppm, 100 ppm, 200 ppm, 500 ppm and 1,000 ppm against two isolates (CM02 and CM11) of *C. musae* by food poisoned technique [22]. The details of fungicides, including brand names, active ingredients, chemical groups and distribution in Pakistan, are shown in (Table 1).

Table 1 – Details of different fungicides which are used in this experiment

Trade name	Active ingredients	Chemical group	Manufacturer/ Distributor in Pakistan
Antracol	Propineb	Dithiocarbamates	Bayer Crop Science
Defeater plus	Flumorph+fosetyl aluminium	Ethyl phosphate	Kanzo Ag Pharma
Ridomil gold	Mancozeb+mefenoxam	Dithiocarbamates& Acylalanines	Syngenta Pakistan Limited
Kocide	Copper hydroxyde	Inorganic	FMC Corporation
Topsin M	Thiophanate methyl	Thiophanates	Arysta Life Science Pakistan

Before pouring, the required concentrations were mixed in a PDA medium. Fungicide-free mediums were used as control. After PDA solidifying, a 5 mm disk of seven days old culture was placed to the centre of the Petri plate. Each treatment was depend on four replications and mean values were calculated. After

inoculations, the petri plates were incubated at 27ºC for seven days. To evaluate the mycelial growth of the fungi, two perpendicular lines were drawn on the backside of the Petri plates and crossed in the centre of the plate. The colony growth (mm) was measured using a scale every 24 hours until the control plate

was filled in any treatment. The mycelial growth inhibition percentage was recorded through formula as given by [23]

$$PI = \frac{(R-S)}{R} \times 100,$$

where: PI – percent inhibition of fungal mycelial growth;

R – fungal mycelial growth in control plates;

S – fungal mycelial growth in treated plates.

Collection of fungal biocontrol agents. Three fungal biocontrol agents viz., two species of *Trichoderma* (*T. harzianum* and *T. polysporum*) and one *Paecilomyces variotii* were retrieved from the Department of Plant Protection, Sindh Agriculture University, Tando Jam, Pakistan to check the sensitivity of *Colletotrichum* isolates (CM02 and CM11) by dual assay method.

In vitro screening of biocontrol agents against *C. musae.* Three biocontrol agents, viz., *Trichoderma harzianum, Trichoderma polysporum*, and *Paecilomyces variotii*, were used for their antagonistic activity against *C. musae* isolates through a dual assay test [24].

A 5 mm agar disc was cut from 5-day-old pure cultures of fungal biocontrol agents were placed on one side on PDA-containing plates. On the opposite side, at the end of the same plate, a 5 mm agar disc of 7-day-old pure culture of each isolates of *C. musae* was also placed. Each biocontrol agent was tested separately in the same manner. The plates were incubated at $(25 + 2^0C)$ for 3-4 days. Each treatment was divided into four replications with control and mean values recorded. One straight line was drawn at the center on the backside of the Petri plates. The colony growth (mm) was measured using a scale every 24 hours until the control plate was filled in any treatment. The mycelial growth inhibition percentage was recorded through a formula as given by [25]:

$$PI = \frac{(P1–P2)}{P1} \times 100,$$

where: percent inhibition of fungal mycelial growth;

P1 – Covered area by the fungal mycelial growth in control plate;

P2 – Covered area by the fungal mycelial growth in dual culture plate.

DNA extraction. For the extraction of DNA, a CTAB method developed by Doyle and Doyle (1987) was utilized with some adjustments from banana anthracnose causal agent *C. musae* [26]. To determine the DNA concentration and purity, the Li et al., (2006) method was used for performing a Nano-drop [27]. Furthermore, a 1% agarose gel was utilized to analyse the DNA concentration and purity by running the samples for 30 minutes.

PCR based detection. The Polymerase Chain Reaction (PCR) stands as a potent molecular technique, enabling the targeted amplification of distinct DNA sequences. Two primers, ITS1 and ITS4 were evaluate to amplify a specific sequence region [28]. The PCR reactions were conducted with a fixed amount of reagents, including 1.5 μl of each primer, 7 μl of master mix, and 0.5 μl of Platinum Taq-polymerase, in a total volume of 12.5 μl of reaction. An automated thermal cycler was employed to conduct the PCR amplification with a protocol consisting of an initial denaturation at 96°C for 9 min, followed by 40 cycles of denaturation at 96°C for 30 sec and annealing at 53°C for 1 min. The final extension was carried out at 72°C for 7 min. The amplified products were detected on a 1.5% agarose gel containing ethidium bromide [27]. This method finds extensive employment in molecular biology investigations, fundamentally transforming our capacity to scrutinize and manage DNA sequences with exceptional precision and sensitivity.

Characterization of the strains. The manufacturer's recommendations (Bio Product) were followed in sequencing the PCR-amplified products that were positive. A BioEdit v7.2 version software was used for the analysed to attained 16S rDNA sequences and (NCBI) blast tool was utilized for compared to those retrieved [29]. After that, the sequence was uploaded to MEGA-7 software and align with the help of ClustalW program. A phylogenetic tree was construct with the help of neighbor joining method with 1,000 bootstrap value and Tamura 3-parameter model. By employing this approach, we were able to discern connections among diverse sequences, yielding a profoundly enlightening and influential analysis that unveils novel insights into the intricate interplay among these vital genetic components.

Data analysis. The experiments were carried out Completely randomized design (CRD). The least significant difference test (LSD) was used to compare mean values at p = 0.05. The data was analyzed by Statistix 8.1 version computer software. The Graphpad prism 8 software was used for graphs.

Results and diacussion

Colonial appearance and morphological characters. The pathogen grown in isolation displayed a copious amount of white aerial mycelium lacking a distinct pattern. The colonies typically appear as fluffy and cottony. The mycelium was septate. The conidia are one-celled and slightly curved, with a tapering base and a rounded or slightly pointed tip and size 12-14 µm in length. Conidiophores structures are simple or branched.

Molecular characterization. In phylogenetic analysis, we included 09 closest sequences of *C. musae* revealed in the BLAST search along with representative sequences of other members of clade, namely *C. gloeosporiodes, C. siamense and C. fragariae.* In the ITS sequence analysis, our two sequences (OQ8917591 and OQ8917601) of *C. musae* was found to be 99.8% identical to the rest of the GenBank sequences of *C. musae* we used, except for Ok0415151 and MT3511141, which showed 99.2% and 99.5% sequence homology to our isolate, respectively. Moreover, our isolate showed only 98.7% and 98.8% sequence similarity with *C. gloeosporiodes* HM0158521 and *C. siamense* MZ0404911 and MT5974041, respectively. The other members of clade, such as *C. fragariae* MT5974041, was distantly related to our isolate, showing only 93.6 sequence homology (Figure 1).

In vitro sensitivity of CM02 and CM11 against different fungicides. Five fungicides at different doses were used to check growth inhibition of the two isolates of *C musae.* At all concentrations (10-1,000 ppm), Topsin M appeared highly effective, which yielded 85-98% inhibition, followed by Redomil gold 1,000 ppm caused 82.11% inhibition of CM02. Redomil gold at 200 and 500 ppm causes 75.13% and 69.44% inhibition of mycelial growth. In comparison, Kocide at 1,000 ppm caused 63.22% inhibition. While Antracol 10-1,000 ppm, Defeater plus 200-1,000 ppm, and Kocide 100-500 ppm showed more than 50% inhibition, followed by Redomil gold 100 ppm caused 43.11%, and Defeater plus 10-100 ppm reduced the 37.33%-40% mycelial growth of CM02, respectively (Figure 2).
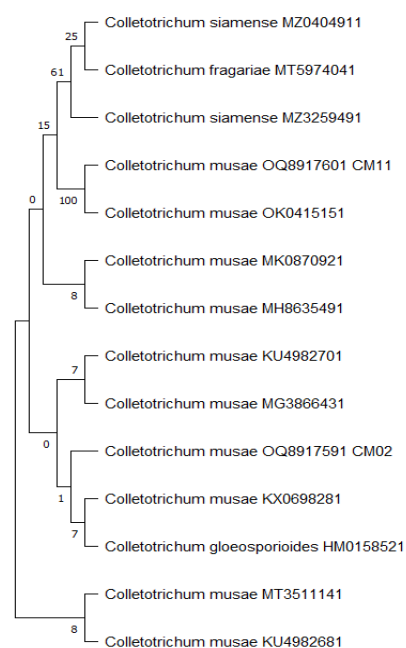

Figure 1 – Phylogenetic relationship of two sequence of *Colletotrichum musae* with NCBI BLAST search sequences, constructed with neighbor joining method based of partial sequence of ITS region
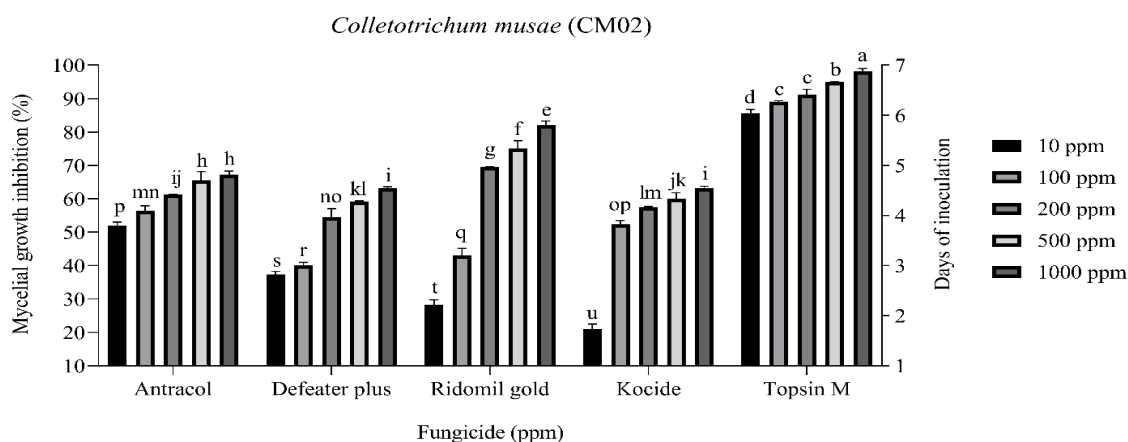

Figure 2 – Response of *Colletotrichum musae* strain (CM02) against five different fungicides in seven days of inoculation by food poison technique. The error bars and alphabetic letters show significant values of LSD (p>0.005) among each other

Against CM11, also Topsin M was found most effective which leading 72-95% mycelial growth inhibition at al dosses followed by Ridomil gold cause 79% and Antracol cause 73.22% mycelial growth inhibition at 1,000 ppm of tested patogen. In comparision, Kocide at 500-1,000 ppm, Ridomil gold 200-500 ppm, Antracol 200-500 ppm and Defaeter plus 500-1,000 ppm were showed moderately highly effective, leading more than 60% mycelial growth inhibition of CM11.

Therefore, Antracol 10-100 ppm, Defeater plus 200 ppm and Kocide 100-200 ppm showed moderately effective and cause 50-59% growth inhibition of CM11. However, Ridomil gold 10-100 ppm, Defeater plus 10-1,000 ppm and Kocide at 10 ppm were show least effective and cause 20-45% colony growth inhibition of tested fungus, respectively (Figure 3).

Antifungal activity of various fungal biocontrol agents. Three different fungal bio-control agents, including two species of *Trichoderma* (*T. harzianum* and *T. polysporum*) and one *Paecilomyces variotii* were used against two strains of *C. musae* by dual plate assay. Both *Trichoderma* species were found highly effective against (CM02 and CM11) and reached on the fungal mycelial growth in 3rd and 4th days. The *P. variotii* showed moderately effective and reached on the mycelial growth of the pathogen in 7th days. On 3rd day *T. harzianum* showed 18.88% inhibition of CM02 followed by 20.11% CM11 mycelial growth inhibition percentage of CM11. At 4th day of inoculation, *T. polysporum* cause 13.33% growth inhibition of CM02 followed by 15% CM11. The *P. variotii* growing slow and cause 9.11% of CM02 followed by 8.75% growth inhibition of CM11 on 7th day of inoculation (Table 2).
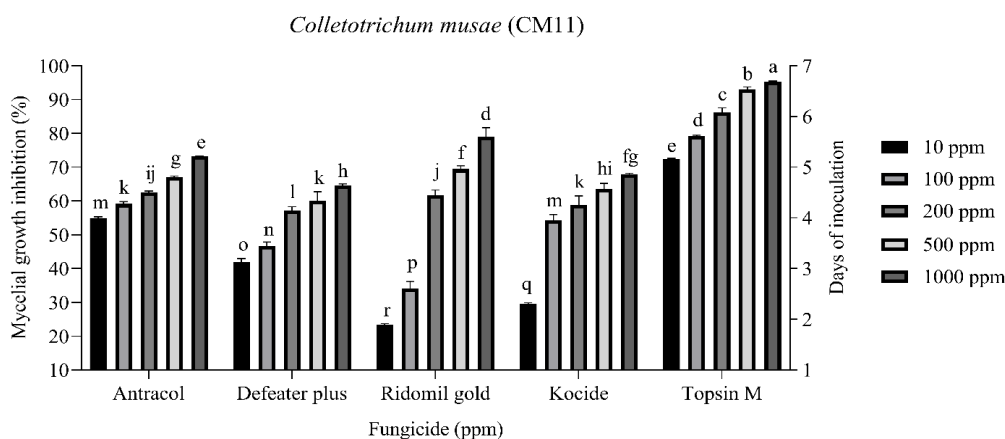

Figure 3 – Response of *Colletotrichum musae* strain (CM11) against five different fungicides in seven days of inoculation by food poison technique. The error bars and alphabetic letters show significant values of LSD (p>0.005) among each other.

Table 2 – Effect of three different fungal biocontrol agents against two isolates of *Colletotrichum musae* (CM02 and CM11) on mycelial growth by dual assay method. The + sign show the standard deviation and alphabetic letters show significant LSD (p>0.005) values among each other

Biocontrol agents	Inhibition pencentage (%) of *Colletotrichum musae* isolates					
	3rd day		4th day		7th day	
	CMO2	CM11	CMO2	CM11	CMO2	CM11
Trichoderma harzianum	18.88+1.462 a	20.11+2.588 a	-	-	-	-
	-	-	13.33+1.005 b	15+1.178 b	-	-
	-	-	-	-	9.11+2.007 c	8.75+1.558 c

C. musae is a devastating threat and causes considerable losses in banana crops worldwide. Using fungicides and biocontrol agents against *C. musae* is simple and can help manage the crop. Various agropesticides and fungicides are available in markets that control anthracnose rot disease of bananas but continuous application of these fungicides were hazards for human health and the environment [11-13].

However, during the present study, five different fungicides viz., Antracol (Propineb), Defeater plus (Flumorph + Fosetyl Aluminium), Ridomil gold (Mefenoxam + Mancozeb), Kocide (Copper Hydroxide), and Topsin M (Thiophanate-methyl) with five different concentrations viz., 10 ppm, 100 ppm, 200 ppm, 500 ppm, and 1,000 ppm were used against *C. musae*. All fungicides showed highly and moderately effective against both strains and cause significant mycelial growth inhibition. In addition, both isolates show highly sensitivity against Topsin M (Thiophanate-methyl) at all concentrations (10-1,000 ppm), leading 72-98% colony growth inhibition. In comparision, Ridomil gold show moderately effective and cause 61-82% growth inhibtion of both strains.

Similarly, Vieira et al. [30] reported that thiophanate methyl (Topsin M) is more effective against *C. musae*. In recent study, Mancozab and cupper oxychloride was found effective with 70% growth inhibition at high dosses against *Fusarium solani* causal pathogen of root rot disease in faba bean crop [31]. *Lasiodiplodia theobromae* causal agent of banana fruit rot disease was found most sensitive against four fungicides including Mancozab at 2,500 ppm [32]. The lowest doses (10-100 ppm) of two fungicides were found least effective which lead 21-43% growth inhibition followed by Kocide at 10 ppm cause 21.11% and 29.56% mycelial growth inhibition of CM02 and CM11. We observed that both strains rapidly grow on the lowest doses of various fungicides. Therefore, biological control is one of the most promising alternative methods of fungicides to control postharvest disease and reduce the economical losses, especially when pathogen show resistance against chemical fungicides [15, 33, 34].

Furthermore, three different biocontrol agents, namely, *Trichoderma harzianum*, *Trichoderma polysporum*, and *Paecilomyces variotii* were used for their antifungal activity against *C. musae* under laboratory conditions. Among biocontrol agents, *T. harzianum* was found highly effective and cause 18.88% and 20.11% mycelial growth inhibition percentage of CM02 and CM11 on 3rd day of inoculation followed by *T. polysporum* on 4th day cause 13.33% and 15% growth inhibition of CM02 and CM11. The *P. variotii* was found least effective. According to Tongsri et al. [35] *Trichoderma* spp. has been effective control against many phytopathogens including, *Phytopatora capsici* and *Colletotrichum gloeosporioides* [36], *Colletotrichum dematium* [37], *Lasiodiplodia theobromae* [38], *C. musae* [19, 39], *Fusarium oxysporum* [40], *Cladosporium spherospermum*, *Aspergillus niger* and *Fusarium oxysporum* [41] and *Fusarium solani* [42]. Out of 6 strains of *Trichoderma*, three strains were found highly effective against three pathogens viz., *Sclerotium rolfsii*, *Rhizoctonia solani* and *Fusarium solani*, leading 60-100% mycelial growth inhibition by dual assay test [18]. Our results indicated that, as compared to fungicides, the pathogen was quickly control through biocontrol agents especially *Trichoderma* species.

Conclusion

Among all tested fungicides, Topsin M was found highly effective at all concentrations (10-1,000 ppm) against *C. musae* isolates (CM02 and CM11), which led to 72-98% mycelial growth inhibition. After that, Ridomil gold was found moderately effective against both strains. However, we observed that, as the concentration decreased the mycelial growth of the pathogen increased. Biological control especially with Trichoderma species are promising method to control this pathogen quickly. Both isolates of *C. musae* showed high sensitivity against Trichoderma species on the third and fourth day of inoculation.

Acknowledgement

Conflict of interest

All authors are aware of the article's content and declare no conflict of interest.

References

1.   Shuai L., Li L., Sun J., Liao L., Duan Z., Li C., He X. (2020) Role of phospholipase C in banana in response to anthracnose infection. *Food Science & Nutrition*, 8, 1038-1045.

2.   Larada J.I., Pojas G.J., Ferrer L.V.V. (2018) Postharvest classification of banana (Musa acuminata) using tier-based machine learning. *Postharvest biology and technology*, 145, 93-100.

3.   Ambisa Z., Tesfa B., Olani T., Abdeta D. (2019) Review on the production and marketing of banana in Ethiopia. *World Journal of Agriculture and Soil Science*, 2, 1-9.

4.   Mohanty S., Das M.P., Surabhi G.-K. (2017) 'OMICS'-approach to regulate ripening and enhance fruit shelf-life in banana: an important fruit crop for food security. *Canadian Journal of Biotechnology*, 1, 289.

5.   Memon I.N., Wagan H., Noonari S., Lakhio M.H., Lanjar B.A. (2016) Economic analysis of banana production under contract farming in Sindh Pakistan. *Economic Analysis*, 21.

6.   Almutairi M., Alsaleem T., Al Herbish H., Al Sayari A.A., Alowaifeer A.M. (2021) LC-MS/MS and GC-MS/MS analysis of pesticide residues in Ecuadorian and Filipino Cavendish bananas imported into Saudi Arabia. *Food Additives & Contaminants: Part A*, 38, 1376-1385.

7.   Mari M., Bautista-Banos S., Sivakumar D. (2016) Decay control in the postharvest system: role of microbial and plant volatile organic compounds. *Postharvest Biology and Technology*, 122, 70-81.

8.   Palou L., Ali A., Fallik E., Romanazzi G. (2016) GRAS, plant-and animal-derived compounds as alternatives to conventional fungicides for the control of postharvest diseases of fresh horticultural produce. *Postharvest Biology and Technology*, 122, 41-52.

9.   Jagana D., Hegde Y.R., Lella R. (2017) Green nanoparticles: a novel approach for the management of banana anthracnose caused by *Colletotrichum musae*. *Int. J. Curr. Microbiol. Appl. Sci*, 6, 1749-1756.

10. Abd-Elsalam K.A., Roshdy S., Amin O., Rabani M. (2010) First morphogenetic identification of the fungal pathogen *Colletotrichum musae* (Phyllachoraceae) from imported bananas in Saudi Arabia. *Genetics and Molecular Research*, 9, 2335-2342.

11. Ayón-Reyna L.E., López-Valenzuela J.Á., Delgado-Vargas F., López-López M.E., Molina-Corral F.J., Carrillo-López A., Vega-García M.O. (2017) Effect of the combination hot water-calcium chloride on the in vitro growth of *Colletotrichum gloeosporioides* and the postharvest quality of infected papaya. *The Plant Pathology Journal*, 33, 572.

12.   Mirshekari A., Ding P., Kadir J., Ghazali H.M. (2012). Effect of hot water dip treatment on postharvest anthracnose of banana var. Berangan. *African Journal of Agricultural Research*, 7, 6-10.

13. Alakonya, A., Kimunye, J., Mahuku, G., Amah, D., Uwimana, B., Brown, A., Swennen, R. (2018) Progress in understanding Pseudocercospora banana pathogens and the development of resistant Musa germplasm. *Plant Pathology*, 67, 759-770.

14.   Mahajan B.V.C., Tandon R., Kapoor S., Sidh M.K. (2018) Natural coatings for shelf-life enhancement and quality maintenance of fresh fruits and vegetables – a review. *J. Postharvest Technol*, 6, 12-26.

15.   Collinge D.B., Jensen D.F., Rabiey M., Sarrocco S., Shaw M.W., Shaw R.H. (2022) Biological control of plant diseases – What has been achieved and what is the direction? *Plant Pathology*, 71, 1024-1047.

16. Samuelian S. (2016) Potential of *Trichoderma harzianum* for control of banana leaf fungal pathogens when applied with a food source and an organic adjuvant. *Biotech*, 6, 1-11.

17.   Tariq M., Khan A., Asif M., Khan F., Ansari T., Shariq M., Siddiqui M.A. (2020) Biological control: a sustainable and practical approach for plant disease management. *Acta Agriculturae Scandinavica, Section B-Soil & Plant Science*, 70, 507-524.

18.   Bastakoti S., Belbase S., Manandhar S., Arjyal C. (2017) *Trichoderma* species as biocontrol agent against soil borne fungal pathogens. *Nepal Journal of Biotechnology*, 5, 39-45.

19.   Bhale U.N. (2020) Antagonistic conflict of *Trichoderma harzianum* against fruit rots pathogens. *African Journal of Biological Sciences*, 2, 92-98.

20.   Sutton B., Waterston J. (1970) *Colletotrichum musae*. [Descriptions of Fungi and Bacteria]. Descriptions of Fungi and Bacteria, Sheet 222.

21. Lim J., Lim T.H., Cha B. (2002) Isolation and identification of *Colletotrichum musae* from imported bananas. *Plant Pathology Journal*, 18, 161-164.

22. Schmitz H. (1930) Food poisoned technique. *Industrial Engineering Chemical Analyst Education*, pp. 361-363.

23. Vincent J. (1947) Distortion of fungal hyphae in the presence of certain inhibitors. *Nature*, 159, 850-850.

24.   Whipps J.M. (1987) Effect of media on growth and interactions between a range of soil□borne glasshouse pathogens and antagonistic fungi. *New phytologist*, 107, 127-142.

25.   Melgarejo P., Carrillo R., Sagasta E. (1985) Mycoflora of peach twigs and flowers and its possible significance in biological control of *Monilinia laxa*. *Transactions of the British Mycological Society*, 85, 313-317.

26.   Doyle J.J., Doyle J.L. (1987) A rapid DNA isolation procedure for small quantities of fresh leaf tissue. *Phytochemical bulletin*.

27. Li W., Hartung J.S., Levy L. (2006) Quantitative real-time PCR for detection and identification of *Candidatus Liberibacter* species associated with citrus huanglongbing. *Journal of microbiological methods*, 66, 104-115.

28.   White T. (1990) PCR protocols: a guide to methods and applications. (No Title), 315.

29.   Hall T.A. (1999) BioEdit: a user-friendly biological sequence alignment editor and analysis program for Windows 95/98/NT. In: Nucleic acids symposium series, 41, Oxford, pp. 95-98.

30. Vieira W.A.d.S., Lima W.G., Nascimento E.S., Michereff S.J., Reis A., Doyle V.P., Câmara M.P.S. (2017) Thiophanate-methyl resistance and fitness components of *Colletotrichum musae* isolates from banana in Brazil. *Plant disease*, 101, 1659-1665.

31.   Dugassa A., Alemu T., Woldehawariat, Y. (2021) In-vitro compatibility assay of indigenous *Trichoderma* and *Pseudomonas* species and their antagonistic activities against black root rot disease (*Fusarium solani*) of faba bean (*Vicia faba* L.). *BMC microbiology*, 21, 1-11.

32.   Nath K., Solanky K., Kumawat G. (2014) Effective approaches of potential bioagent, phytoextract, fungicide and cultural practice for management of banana fruit rot disease. *J Plant Pathol Microb*, 5, 2.

33.   Iqbal O., Li C., Lodhi A.M. Antagonistic Pseudomonas: alternative to chemical fungicides for the management of phytopathogens. In: Biofungicides: Eco-Safety and Future Trends, CRC Press, pp. 216-246.

34. Iqbal O., Li C., Rajput N.A., Lodhi A.M. (2023) Management of phytopathogens by antagonistic *Bacillus* spp. in tomato crop.

35.   Tongsri V., Sanosomneng K., Umrung S., Montri N. Antagonistic activity of Candida utilis SCKU1 yeast against crown rot disease of 'Hom Thong'Banana (*Musa acuminata*, AAA group).

36.   De la Cruz-Quiroz R., Roussos S., Rodríguez-Herrera R., Hernandez-Castillo D., Aguilar C.N. (2018) Growth inhibition of *Colletotrichum gloeosporioides* and *Phytophthora capsici* by native Mexican *Trichoderma* strains. *Karbala International Journal of Modern Science*, 4, 237-243.

37.   Shovan L., Bhuiyan M., Begum J., Pervez Z. (2008) *In vitro* control of Colletotrichum dematium causing anthracnose of soybean by fungicides, plant extracts and *Trichoderma harzianum*. Int. J. Sustain. *Crop Prod*, 3, 10-17.

38.   Mortuza M.G., Ilag L.L. (1999) Potential for biocontrol of Lasiodiplodia theobromae (Pat.) Griff. & Maubl. in banana fruits by *Trichoderma* species. *Biological Control*, 15, 235-240.

39.   Zhang H., Kong N., Liu B., Yang Y., Li C., Qi J., Ma Y., Ji S., Liu Z. (2022) Biocontrol potential of *Trichoderma harzianum* CGMCC20739 (Tha739) against postharvest bitter rot of apples. *Microbiol. Res.*, 265, 127182.

40.   Bunbury-Blanchette A.L., Walker A.K. (2019). Trichoderma species show biocontrol potential in dual culture and greenhouse bioassays against *Fusarium* basal rot of onion. *Biological Control*, 130, 127-135.

41.   Lone M.A., Wani M.R., Sheikh S.A., Sahay S., Dar M.S. (2012). Antagonistic potentiality of *Trichoderma harzianum* against *Cladosporium spherospermum, Aspergillus niger* and *Fusarium oxysporum*. *Journal Biology, Agriculture and Healthcare*, 2224-3208.2222.

42.   Amira M.B., Lopez D., Mohamed A.T., Khouaja A., Chaar H., Fumanal B., Gousset-Dupont A., Bonhomme L., Label P., Goupil P. (2017) Beneficial effect of *Trichoderma harzianum* strain Ths97 in biocontrolling Fusarium solani causal agent of root rot disease in olive trees. Biological Control, *110*, 70-78.

Information about authors:

Owais Iqbal – (corresponding author) – PhD Student, Key Laboratory of Agro-Biodiversity and Pest Management of Education Ministry of China, Yunnan Agricultural University, Kunming, China, e-mail: owaisiqbalrajput786@yahoo.com

Naimatullah Koondhar – PhD, Assistant Professor, Department of Plant Pathology, Faculty of Agriculture, Lasbela University of Agriculture Water and Marine Sciences, Balochistan, Pakistan, e-mail: koondhar.naimat@gmail.com

Nasir Ahmed Rajput – PhD, Associate Professor, Department of Plant Pathology, University of Agriculture Faisalabad, Pakistan, e-mail: nasirrajput81@gmail.com

Muhammad Ali Khanzada – PhD, Associate Professor, Department of Plant Protection, Faculty of Crop Protection, Sindh Agriculture University, Tando Jam, Pakistan, e-mail: malikhanzada@sau.edu.pk

Nimra Khanzada – PhD student, Department of Plant Protection, Faculty of Crop Protection, Sindh Agriculture University, Tando Jam, Pakistan, e-mail: nimrak62@gmail.com

Sumbal Zaman – PhD student, Department of Plant Protection, Faculty of Crop Protection, Sindh Agriculture University, Tando Jam, Pakistan, e-mail: szaman2k12@gmail.com

N.K. Altynova [1]*, S.S. Tokmurzina[1], A.M. Kassymbekova [1],

T.N. Kereyev [1,2], L.Z. Musralina [1,2], L.P. Lebedeva [1],

L.B. Djansugurova [1,2]

[1]Institute of Genetics and Physiology, Almaty, Kazakhstan
[2]Al-Farabi Kazakh National University, Almaty, Kazakhstan
*e-mail: naz10.79@mail.ru

Genetic markers of sports performance, interpretation of individual genotypes in the athlete's genetic passport

Abstract. Identifying and studying genetic polymorphisms that determine the phenotypes of elite athletes is a highly relevant and significant task in sports science. This research forms the foundational basis for developing what are known as sports genetic passports, which have the potential to revolutionize athlete training and performance through personalized genetic insights. The aim of this review was to analyze genetic markers associated with the development of key athletic qualities – specifically strength, power, speed, and endurance – by conducting a selective systematic review of the existing literature. Through this comprehensive review, we were able to select single nucleotide polymorphisms (SNPs) that are associated with specific athletic traits by examining the functions of their corresponding gene products. This approach offers a valuable framework for interpreting sports genetic markers within genetic passports. These genetic markers can provide scientists and practitioners in the fields of physical culture and sports medicine with the latest and most compelling evidence in exercise genomics, thereby facilitating more personalized and effective training strategies. As a result, we have compiled a set of 40 widely recognized genetic markers linked to athletic performance–strength, speed, and endurance. This compilation serves as a crucial resource for further research and practical applications aimed at optimizing athletic potential and enhancing performance.

Key words: sports, genetic markers, endurance genes, speed-related genes, muscle fibers, single nucleotide polymorphism, sports medicine, GWAS, strength, genetic passports.

Introduction

Sports genetics provides insights into an individual's capacity for specific types of exercise, shaped by both task demands and genetic factors. An athlete's genotype strongly influences traits like strength, endurance, muscle fiber composition, muscle mass, flexibility, neuromuscular coordination, and reaction speed [1]. Genetic testing of both professional and amateur athletes can provide initial information on optimal physical loads for an individual based on their muscle fiber composition and metabolic characteristics. This testing also aids in selecting appropriate sports and optimizing nutrition, training regimens, and recovery processes [2]. According to O.S. Glotov, when considering trait heritability, it's important to acknowledge that the development and expression of physical qualities result from a complex interplay between genetic and environmental factors. Thus, in early sports specialization, identifying genetic predispositions toward sports where success relies on highly heritable traits – like explosive power, speed, and flexibility – is essential [3].

In sports genetics, two types of methods are used for detailed analysis of genetic features: candidate gene studies and genome-wide association studies (GWAS). Case-control studies continue to be the predominant research approach in sports genetics [4-7]. At the same time, the advent of GWAS has enabled the analysis of entire genomes and the identification of multiple mutations or polymorphisms simultaneously [8]. Furthermore, the overall effect of polymorphisms on an athlete's status can be measured through meta-analysis [9]. Advances in GWAS methodologies may broaden the spectrum

of genetic variants linked to elite athletic status and other attributes critical for athletic success, including susceptibility to performance-limiting injuries and individual responses to training and nutrition [5].

The field of sports genomics emerged in the early 2000s after the human genome was decoded and the first DNA polymorphisms linked to athletic performance were discovered (such as variations in the *ACE, ACTN3, AMPD1, PPARD*, and *PPARGC1A* genes) [10]. According to recent data from Akhmetov, 149 genetic marker variants are associated with various physical activity traits (42 of which are genome-wide significant), and 253 variants are linked to athlete status (115 related to endurance, 96 to strength) [6].

Although the relationship between the ACTN3 and ACE genes and athletic performance has been extensively studied [11], the list of candidate genes is updated annually and continues to expand [12-14]. Modern genetic tests examine several well-known variants thought to be related to athletic abilities (e.g., the *ACTN3, ACE*, and *NOS3* genes) or injury susceptibility (e.g., the *COL5A1, COL1A1*, and *MMP3* genes). A review of the literature suggests that some of these genetic associations with specific physical predispositions can be reasonably confirmed. For example, the *ACE* gene is linked to endurance, while *ACTN3* is associated with strength. However, genetic test results for athletes should be interpreted cautiously, as each genetic variant explains only a small portion of performance, with factors like training volume, organization, nutrition, daily routine, and other environmental factors playing a much larger role [15].

In this review, we aim to analyze the genetic markers associated with athletic qualities and the functions of these gene products based on the available literature. We also propose an interpretation of the sports markers related to strength, speed, and endurance for use in genetic passports.

Materials and methods

This literature review aims to comprehensively summarize relevant information from publications on genetic markers responsible for athletic performance. By analyzing a broad range of studies, we seek to identify key genes and polymorphisms that influence traits such as strength, endurance, speed, and muscle fiber composition. Understanding these genetic factors is crucial for advancing personalized training programs, improving athletic performance, and potentially reducing the risk of injury among athletes.

The articles reviewed in this paper were published between 2003 and 2023 and were sourced from online search engines and library databases, including Web of Science, NCBI, and PubMed. The primary search terms used were "sports genetics," "genes associated with athletic performance," "candidate genes," "endurance genes," "speed genes," "muscle fibers," among others. We employed both individual terms and combinations thereof to ensure a comprehensive search. The search process also involved reviewing the bibliographies of the retrieved articles to extract additional relevant publications. Inclusion criteria focused on peer-reviewed articles that provided significant insights into the genetic aspects of athletic performance.

In addition, we utilized the program STRING: functional protein association networks, Version 12.0, as a primary data resource. Identified by the Global Biodata Coalition and ELIXIR, this tool allowed us to explore protein-protein interactions and functional associations between the genetic markers of interest. Data was accessed on May 9, 2024. The use of STRING facilitated a deeper understanding of the biological pathways and networks involved in athletic performance, thereby enriching the analysis and interpretation of the genetic data collected.

Results and discussion

Numerous data, including findings from recent studies, confirm that polymorphisms in certain genes impact an athlete's physical traits, such as strength, speed, and endurance, thereby influencing the body's predisposition toward strength or endurance training [10,16]. In this review, we based our findings on a large body of scientific research to present candidate genes for athletic qualities. Expanding this list of genetic polymorphisms that determine the phenotype of an elite athlete is a highly relevant task, as it serves as the basis for developing so-called sports genetic passports. A sports genetic passport assesses the cumulative contribution of genotypes and gene alleles in determining hereditary predisposition to physical activity and developing professional pathologies in athletes. Below is a panel of 40 of the most prevalent genetic markers selected from scientific articles associated with athletic activities. The presented table provides a list of genes proven to influence human athletic qualities (Appendix, Table 1).

Markers of strength and endurance. *ACE* is the most extensively studied gene in physical activity genetics [17-20]. The *ACE* I allele is linked to a

predisposition for endurance sports and resistance to hypoxia in high-altitude environments. The *ACE* gene encodes Angiotensin-Converting Enzyme, a zinc-containing protease that catalyzes the conversion of angiotensin-1 to angiotensin-II (AT-II). The *ACE* gene contains 26 exons, and in the 16th intron, there is a deletion of a specific DNA sequence (Alu repeat 287 bp). There is also considerable evidence linking the *ACE* gene polymorphism (specifically the D allele) with an increased risk of conditions such as myocardial infarction, hypertension, left ventricular hypertrophy (LVH), hypertrophic cardiomyopathy, obesity, kidney disease, and vascular complications of type 2 diabetes, even among athletes [21-24]. Research results on the influence of the *ACE* gene on the strength and speed qualities of professional athletes are contradictory. In addition to positive associations affecting sprinting qualities, there are also negative associations. For example, a research group led by Scott et al. conducted studies on Kenyan, Ethiopian, Jamaican, and African-American populations and refuted the influence of *ACE* genotypes on the predisposition to sprinting abilities. They found that *ACE*'s DD and GG genotypes do not contribute to endurance development in athletes [25].

The *AGT* gene, which consists of five exons, encodes angiotensinogen, a serum protein in the α-globulin fraction, primarily produced by the liver and adipocytes in adipose tissue. The synthesis of this protein is regulated by estrogens, glucocorticoids, and thyroid hormones. Literature suggests that the rs699 polymorphism in the *AGT* gene is associated with the status of strength athletes but not with endurance-trained athletes [26,27]. Additionally, GWAS studies on sprint performance in elite youth soccer players with various genetic polymorphisms highlight a connection between the rs699 SNP of the *AGT* gene and sprint test outcomes [28].

The *GALNTL6* gene has 21 exons and encodes a membrane-bound protein N-acetylgalactosaminyltransferase type 6, predominantly expressed in the testes, brain, spinal cord, cerebellum, and skeletal muscles of adults. It plays a significant role in the glycosylation pathway of proteins, which is a part of the post-translational modification of polypeptides [29]. The C/T polymorphism (rs558129) in the *GALNTL6* gene, located in the last intron, is positively associated with athletic performance [30-32].

The *NR1H3* gene encodes a nuclear receptor involved in regulating macrophage function, lipid homeostasis, and inflammation [33]. The association of rs7120118 with high endurance may indicate a strong linkage disequilibrium (r2 = 0.89, P < 0.0001) between rs7120118 TT and the potentially functional

rs1052373 GG. This link might also be connected to increased synthesis of the testosterone precursor 5alpha-androstane-3alpha,17alpha-diol disulfate, as *NR1H3* regulates hypothalamic-pituitary-adrenal steroidogenesis [34]. Al-Khelaifi F et al. found that athletes with high endurance display elevated levels of several sex hormones involved in testosterone synthesis [35]. However, the functional significance of these associations still requires further validation.

Research by Akhmetov et al. demonstrated that the C allele of *NFIA-AS2* rs1572312 and the *TSHR* rs7144481 allele are indicators of elite endurance athlete status, including in marathon runners [36].

The *NOS3* gene encodes the endothelial NO synthase enzyme, which catalyzes nitric oxide (NO) formation from L-arginine. The G allele (Glu298, rs1799983) is a marker of predisposition to endurance development, associated with the functions of the vascular and respiratory systems and insulin sensitivity in liver and skeletal muscle cells [37]. Sorokina et al. identified associations of polymorphic variants of the *ADRB2*, *NOS3*, and *PPARGC1A* genes associated with endurance in judo and freestyle wrestling athletes with different sports qualifications [38,39].

The *KCNJ11* gene encodes a potassium channel protein. The substitution of cytosine (C) with thymine (T) at position 67 of the nucleotide sequence leads to the replacement of the amino acid lysine with glutamine (Lys23Gln), which alters the protein structure, prevents the closure of the channels and results in reduced insulin secretion from beta cells and impaired blood sugar control. *KCNJ11* is involved in carbohydrate metabolism and is expressed in various tissues, including the myocardium and skeletal muscles. It is frequently studied to identify genetic predisposition to type 2 diabetes and assess the cardiovascular system's adaptation to physical exercise and stress. In the work of Gonzalez et al., a sample of Spanish marathon runners showed a higher frequency of the *KCNJ11* 23Gln allele than the control group [40]. Akhmetov considers the *KCNJ11* Gln23 allele a potential genetic marker for endurance development [41].

The *GABPβ1* gene, which encodes a subunit of the beta one transcription factor GA-binding protein (also known as nuclear respiratory factor 2, NRF2), is associated with athletic status. The minor alleles G (rs7181866) and T (rs8031031) are overrepresented in athletes (P < 0.003), particularly among world-class athletes (P < 0.0002), and may enhance the likelihood of an individual becoming a combat sports athlete, potentially due to an improved mitochondrial response to intermittent exercise [42,43]. No

association was found between genotypes and relative aerobic capacity, nor between *GNB3* genotypes and blood pressure, BMI, and fat percentage [44].

Georgios I. Tsianos et al. studied the association of polymorphisms in eight genes related to muscles or metabolism with endurance performance in participants of the Olympus marathon. They showed that among 316 male athletes who identified running as their favorite sport, *BDKRB2* rs1799722 (P = 0.018) and *ADRB2* rs1042713 had a significant association with faster times for the minor alleles, with the fastest time on record (P = 0.01) [45].

Cytokines are important mediators of various aspects of health and disease, including appetite, glucose and lipid metabolism, insulin sensitivity, and the hypertrophy and atrophy of skeletal muscles [46]. Interleukin-6 (*IL-6*) is a functional protein with a cytokine structure. It is especially effective in the immune system, providing pro/anti-inflammatory responses and muscle tissue hypertrophy and recovery. A study by Turkish scientists aimed at studying the distribution of the *IL-6* rs1800795 polymorphism in national cross-country skiers and determining the preferred genotype for endurance performance showed that the GC genotype is more advantageous than the GG genotype in skiers [47].

The *ADRB3* gene plays a role in energy expenditure by participating in lipolysis, which affects body composition and performance [48]. An important polymorphism involved in the genetics of physical fitness is rs4994, which consists of the substitution of cytosine for thymine at codon 64 of the *ADRB3* gene, resulting in the conversion of tryptophan to arginine (Trp64Arg) in the amino acid sequence. Santiago, Catalina, and colleagues demonstrated that heterozygosity for the *ADRB3* Trp64Arg polymorphism is linked to elite endurance performance. At the same time, other variants of β-adrenergic receptor genes do not appear to provide a good result in high-level athletic performance, at least among athletes of Spanish descent [49].

Markers of speed-strength abilities and muscle mass gain. *ACTN3* (alpha-actinin-3) is recognized as one of the most significant genes related to physical fitness (both aerobic and anaerobic), playing a key role in the development and function of muscle fiber structure. Individuals with two functional copies of the reference variant (RR) of the *ACTN3* gene typically exhibit a better ability to develop muscle strength and speed activity, as alpha-actinin-3 accelerates muscle contraction [9,50,51]. A genotype effect exists among female sprinters and endurance

athletes: a higher-than-expected number of 577RX heterozygotes among sprinters and a lower-than-expected number among endurance athletes. The absence of a similar effect in men suggests that the *ACTN3* genotype affects athletic performance differently in men and women [51]. However, other similar studies indicate the opposite. For example, Gentil P et al. reported that the R577X polymorphism in the *ACTN3* gene was not associated with muscle strength at rest and the muscle strength response to resistance training [52].

The *AMPD1* gene encodes adenosine monophosphate deaminase-1, crucial in adenosine and adenosine monophosphate (AMP) metabolism. Mutations in the *AMPD1* gene can be associated with various hereditary diseases, such as mild myopathy, which may manifest as muscle weakness and fatigue. Additionally, variations in the *AMPD1* gene can affect physical endurance and the risk of developing various metabolic and muscle function-related diseases. Restriction fragment length polymorphism analysis showed a notably lower frequency of T allele and TT genotype in the *AMPD1* among athletes participating in speed and strength sports (N=305) compared to non-athletes (N=499). Thus, the C34T polymorphism of the *AMPD1* gene can be considered a marker of predisposition to high-speed and strength muscle activities [52]. However, publication results indicate ambiguous findings among elite athletes and controls. For example, Ginevičienė et al. considered the *AMPD1* C allele a marker associated with sprint and strength performance. In contrast, the T allele is seen as an unfavorable factor for strength-related athletics [53].

The *AQP1* gene encodes a protein known as aquaporin-1 (*AQP1*), a member of the aquaporin family of proteins. *AQP1* expression is observed in various tissues, namely red blood cells, endothelial cells, as well as smooth, skeletal, and cardiac muscles. *AQP1* regulates water permeability in the heart's capillary network, ensuring water flows through the endothelial layer into the blood. Additionally, aquaporin-1 may play a role in various physiological processes, such as cell volume regulation, water transport in the lungs and other organs, and influencing the function of the nervous system and circulation [54].

Muscle fiber type and endurance. The *PPARGC1A* gene ensures muscle tissue's morphology and energy metabolism. The G482S G>A polymorphism leads to reduced oxidative processes and impaired mitochondrial formation.

Research has demonstrated that individuals with the G allele exhibit an increased proportion of slow-twitch muscle fibers and enhanced aerobic capacity, both in athletes and non-athletes. In contrast, the A allele is linked to a higher risk of hypertension in people under 50 years old, obesity, and type 2 diabetes [55]. Therefore, the presence of the G allele favors the development of endurance. Carrying the *PPARG* 12Ala allele increases muscle tissue sensitivity to insulin and enhances its anabolic effects on skeletal muscles, predisposing individuals to develop and display speed-strength qualities [56].

Individuals carrying the G allele of the *PPARA* gene exhibit a predominance of aerobic metabolism and increased content of slow-twitch muscle fibers, giving them an advantage in the development and manifestation of endurance. Such a genotype contributes to success in cyclic sports activities [57,58].

The *TTN* gene encodes the third myofilament, titin, which plays a structural, mechanical, regulatory, and ontogenetic role in sarcomeres. The most well-known variation in the *TTN* gene is the C>T polymorphism (rs10497520), which results in the transformation of lysine (Lys) into glutamic acid (Glu), which may influence the variability of isoform expression in muscle tissue [60].

Muscle strength. A group of researchers demonstrated a strong association between *ACVR1B* genotypes and the strength of knee extensors, with rs2854464 being the most promising candidate polymorphism, where the A allele (allele frequency 0.73) was associated with higher muscle strength [61]. Additionally, it was shown that the phenotype-genotype relationship may depend on ethnic background; for example, the *ACVR1B* rs2854464 A allele is associated with sprinting/strength performance in Caucasians but not in Brazilian athletes [62]. Genome-wide association studies (GWAS) identified *FTO* as a gene that contributes to obesity and maximizes BMI variability in Europeans and Asians [63]. Rut Loos and her colleagues reported the results of a meta-analysis of numerous studies investigating how physical activity mitigates the impact of a specific *FTO* gene variant on obesity in adults and children. They reported a significant attenuation of the influence of this genetic variant on obesity risk in adults due to physical activity by approximately 30% [64].

Endurance under anaerobic conditions. The hypoxia-inducible factor alpha (*HIF1A*) gene encodes a transcription factor that facilitates cellular adaptation to low-oxygen environments. *HIF1A* is among the genes studied in the context of genetics and athletic performance [65,66]. Pickering, Craig, et al. conducted a genome-wide association study to identify genetic variants associated with sprint test results in elite young football players using a "case-control" scheme, where they identified 2 SNPs in *ADRB2* as markers associated with footballer status [67]. The T/C polymorphism in *NOS3* (rs2070744) is a candidate for explaining individual differences in phenotypes. Comparing the results of 100 world-class endurance athletes, 53 elite strength athletes, and 100 sedentary, healthy men of Spanish origin associated with sports, significant differences in genotype frequencies among footballers, athletes in the control group, endurance athletes, and strength athletes (all P <0.02) were shown. It was demonstrated that the -786C allele is associated with elite footballer status [68]. Henderson, Jennifer, et al. reported that *EPAS1* haplotypes might provide a more sensitive metabolic response in determining the aerobic and anaerobic contributions to endurance sports [69].

Endurance under aerobic conditions. The *UCP2* gene plays a role in thermogenesis, regulation of lipid and energy metabolism, protection against reactive oxygen species, influence on insulin secretion, and possesses neuroprotective effects. It has been established that the expression of *UCP2* increases in human skeletal muscles in response to aerobic training [70]. By inhibiting insulin production in pancreatic cells, the product of the *UCP2* gene promotes lipolysis–the utilization of fatty acids as an energy source–thereby enhancing the body's efficiency and endurance [71]. However, the results of existing publications indicate ambiguous results. For example, Petr M et al. found no correlation between tested strength/power parameters and *UCP2* Ala55Val genotypes in elite football players [72]. The *GSTP1* gene encodes glutathione S-transferase P1, important in detoxification and antioxidant protection. There is some evidence suggesting that the *GSTP1* c.313A>G polymorphism may positively influence physical activity. The G allele of the *GSTP1* c.313A>G single nucleotide polymorphism is associated with improved endurance performance due to better elimination of exercise-induced reactive oxygen species [73]. The *HFE* gene regulates blood iron levels and hepcidin expression in the liver, affecting iron availability. Thakkar, Drishti, et al. showed associations between *HFE* risk genotypes and endurance performance, suggesting that individuals with *HFE* genotypes of moderate or high

risk (rs1800562 and rs1799945) outperform those with low-risk genotypes in a 10-kilometer cycling workout [74].

Endurance and features of the vascular system. The *VEGFA* gene, encoding the *VEGF-A* protein, regulates erythropoiesis, angiogenesis, and muscle blood flow. This gene's specific SNP variants (rs2010963) are associated with human endurance. Boidin et al. found that these SNPs are linked to adaptation to four-week resistance and endurance training. Heterozygotes for the C allele in rs2010963 adapt better to endurance, while homozygotes for the G allele demonstrate less endurance adaptation [76]. Akhmetov et al. reported an association between polymorphisms of the *VEGFR2* gene and aerobic power and muscle fiber type [77].

Predisposition to combat sports. In the study by Krzysztof Chmielowiec et al., a connection between the polymorphism of the dopamine receptor gene and the personality traits of athletes practicing martial arts was demonstrated. In athletes, a lower score on the reward dependence scale was associated with the *DRD2* rs1799732 polymorphism compared to the control group [78].

Fighting characteristics and qualities of a strength athlete. Success in combat sports has been associated with three polymorphisms (*SLC6A2* rs2242446, *HTR1B* rs11568817, and *ADRA2A* rs521674) encoding components of the serotonergic and catecholaminergic systems. A single nucleotide polymorphism (SNP) in the promoter region of the norepinephrine transporter gene *SLC6A2* (rs2242446) has been associated with panic disorder. Scientists suggest that this SNP may be associated with anxious arousal in individuals who have experienced trauma [79]. The results of Peplonska, Beata et al.'s research confirm the hypothesis that genetic variants potentially influence mental processes and emotions, particularly the serotonin pathway, and also affect predisposition to sporting achievements [80]. The dopamine transporter gene *SLC6A3* has also been proposed as a candidate gene for attention-deficit/hyperactivity disorder syndrome [81].

Endurance of an athlete fighter. Between 20% and 60% of athletes experience stress due to excessive physical exertion and inadequate recovery [82]. The prevalence of stress is higher in endurance sports such as swimming, rowing, cycling, triathlon, and to some extent, long-distance running, where athletes train for 4–6 hours a day, six days a week, for several weeks without a break from intensive workouts [83]. Therefore, the genes *TPH2* and *NR3C2* were chosen as genetic markers of endurance in combat sports athletes. Upon entering the central nervous system, L-tryptophan is converted by tryptophan hydroxylase (*TPH*) into 5-hydroxytryptophan (*5-HTP*), the rate-limiting step in serotonin synthesis in the brain. This compound is rapidly decarboxylated by aromatic amino acid decarboxylase to form cytosolic serotonin. This process may reflect adaptation to different needs for regulating serotonin production in the brain and peripheral organs [84]. The *NR3C2* gene encodes the mineralocorticoid receptor, which mediates the action of aldosterone on salt and water balance in target cells. Defects in this gene are also associated with early-onset hypertension. Homozygosity for the G allele of the *MR-2G/G* gene polymorphism is associated with higher cortisol levels in healthy adults, especially during peak cortisol secretion in the morning. This polymorphism may contribute to interindividual variability in stress response and may be involved in the development of stress-related disorders [85].

Marathon runner's endurance. The brain's serotonin receptors (*5-HTR*) are located on neurons innervating cortical and limbic areas involved in cognitive and emotional regulation. Among the fourteen subtypes of *5-HTR*, *5-HT1AR* and 5-HT7R are associated with the development of anxiety, depression, and mental functions [86]. The findings of Haslacher H et al. suggest that the *5-HT1A* receptor may mediate the positive effects of physical exercise on depressive mood, and the protective effect is enhanced by the C allele of the rs6295 variant [87].

Speed indicators. The *COL6A1* gene encodes one of the subtypes of collagen type VI, an essential extracellular matrix component. It plays a crucial role in maintaining the structural integrity of various tissues, including skin, muscles, and connective structures. Studies have shown that the variant of the *COL6A1* gene, rs35796750, is a marker of endurance performance in cycling during a 180-kilometer cycling stage and a 226-kilometer South African triathlon and is associated with changes in tissue composition (muscles and tendons) [88]. However, in other similar studies, the results indicate the opposite. No significant differences in genotypes were found for *COL3A1* (P = 0.828), *COL6A1* (P = 0.300), or *COL12A1* (P = 0.120) genotypes between the EAMC and NON groups [89].

Conclusion

Active research is being conducted in many countries worldwide to develop methods for identifying promising candidates for various sports. Thanks to the continually improving methods of molecular biology and genetics and the significant experience accumulated by international colleagues, it has become possible to determine athletic potential from birth, significantly increasing the chances of choosing the optimal sport.

This review is based on the analysis of genetic profiles of professional athletes from a comprehensive search of literature data, identification of key candidate genes, determination of each gene's contribution to traits such as speed, muscle strength, and endurance, and evaluation of variations across different populations. Based on our new inclusion criteria and using the STRING program, our literature search revealed interaction networks between genes, their experimental determination, co-expression, co-occurrence in scientific texts, and scientific evidence for at least 40 genetic markers potentially associated with athletic qualities (Appendix, Table 1).

We acknowledge the limitations of this review, as it does not include all psychogenetic characteristics of athletes (e.g., stress response, leadership qualities, team-playing ability, attention, tactics, strategy, risk-taking propensity) or metabolic characteristics affecting athletic capabilities and performance (e.g., hormonal balance, vitamin and micronutrient sufficiency, bone strength). Additionally, predispositions to injuries and diseases due to high physical load (e.g., cardiovascular system features, muscle fiber type, ligament elasticity, fracture risk, inflammatory response, tissue regeneration capability) were not covered. Although many other genetic factors remain undiscovered, our results highlight the association between genetic profiles derived from 40 markers and athletic qualities (genes *ACE* (rs4363 – alleles A, G, C); *AGT* (rs699 – alleles A, G); *GALNTL6* (rs558129 – alleles A, G); *NR1H3* (rs7120118 – alleles T, C); *NFIA*-AS2 (rs1572312 – alleles G, T); *NOS3* (rs1799983 – alleles T, G, A); *KCNJ11* (rs5219 – alleles T, C, A, G); *GABPB1* (rs7181866 – alleles A, G); *GNB3* (rs5443 – alleles T, C); *BDKRB2* (rs1799722 – alleles C, T, G); *IL6* (rs1800795 – alleles C, G, T); *ADRB3* (rs4994 – alleles A, G); *ACTN3* (rs1815739 – alleles C, A, T); *AMPD1* (rs17602729 – alleles G, A, T); *AQP1* (rs1049305 – alleles G, A, C); *PPARGC1A* (rs8192678 – alleles G, A); *PPARG* (rs1801282 – alleles C, G, T); *PPARA*

(rs4253778 – alleles G, C, T); *TTN* (rs10497520 – alleles T, C, A); ACVR1B (rs2854464 – alleles A, C, G); FTO (rs9939609 – alleles T, A); HIF1A (rs11549465 – alleles C, T); ADRB2 (rs1042713 – alleles G, A, C); NOS3 (rs2070744 – alleles T, C); *EPAS1* (rs1867785 – alleles A, G); *UCP2* (rs660339 – alleles G, A); *GSTP1* (rs1695 – alleles A, G, T); *HFE* (rs1799945 – alleles C, G, T); *ACE* (rs4311 – alleles T, C); *ADRB2* (rs1042713 – alleles G, A, C); *VEGFA* (rs2010963 – alleles C, G, T); *VEGFR2* (rs1870377 – alleles T, A); *DRD2* (rs1079597 – alleles C, T); *HTR1B* (rs11568817 – alleles A, C); *SLC6A2* (rs2242446 – alleles C, G, A, T); *TPH2* (rs7305115 – alleles A, G, C, T); *NR3C2* (rs2070951 – alleles G, A, C, T); *5HT1A* (rs6295 – alleles C, G, A); *COL6A1* (rs35796750 – alleles T, C, G), based on scientifically validated results.

The genetic panel of genes responsible for strength, speed, and endurance represents an innovative approach to optimizing athletic training. With its rich history and cultural heritage, Kazakhstan has unique national sports essential to Kazakh identity and traditions. Statistics have shown that boxing, Greco-Roman wrestling, weightlifting, and judo are the most practiced sports in Kazakhstan. Popular national sports include Kokpar, Audaryspak, Tenge Ilu, Zhamby Atu, Alaman Baiga, Asyk Atu, Togyz Kumalak, and others. Future research on genetic markers associated with Kazakh national sports will provide deeper insights into the physical characteristics and heritability of physical abilities in this population. This can aid in developing individualized approaches to training, selecting sports disciplines, and optimizing performance in these sports.

Acknowledgements

Conflict of interest

All authors are aware of the article's content and declare no conflict of interest.

References

1. Ponomareva O.V. (2018) Genetika v sovremennom sporte: nauchnye tehnologii dlja novyh dostizhenij [Genetics in modern sport: scientific technologies for new achievements], Nauka molodyh [Eruditio Juvenium], 6(4), pp. 569-581.

2. Mosse I.B. (2012) Sravnenie genotipov sportsmenov raznoj specializacii po kompleksu genov sportivnoj uspeshnosti [Comparison of genotypes of athletes of different specializations by a set of sports success genes]', in Kil'chevskiy, A.V. (ed.) Molekuljarnaja i prikladnaja genetika: sbornik nauchnyh trudov [Molecular and Applied Genetics: Collection of Scientific Papers], Minsk: Pravo i Ekonomika, 13, pp. 19-24.

3. Glotov O.S., Glotov A.S., Pakin V.S., Baranov V.S. (2013) 'Monitoring zdorovya cheloveka – vozmojnosti sovremennoi genetiki [Human health monitoring – possibilities of modern genetics]', Vestnik Sankt-Peterburgskogo universiteta [St. Petersburg University Bulletin], ser. 3, issue 2, pp. 95-106.

4. Alvarez N., Terrados R., Ortolano G., et al. (2000) 'Genetic variation in the renin-angiotensin system and athletic performance', *EJAP*, 82, pp. 117-120. doi:10.1007/s004210050660

5. Rodas G., Osaba L., Arteta D., et al. (2020) 'Genomic prediction of tendinopathy risk in elite team sports', *IJSPP*, 15(2), pp. 257-263. doi: 10.1123/ijspp.2019-0431.

6. Ahmetov I.I., Fedotovskaya O.N. (2015) 'Current progress in sports genomics', in Makowski G.S. (ed.) *Advances in Clinical Chemistry*, 70, pp. 247-314. doi: 10.1016/bs.acc.2015.03.003.

7. Ahmetov I.I., Popov, D.V., Astratenkova I.V., et al. (2008) 'The use of molecular genetic methods for prognosis of aerobic and anaerobic performance in athletes', *Human Physiology*, 34(3), pp. 338-342. PMID: 18677952.

8. Dennison C.A., Legge, S.E., Pardiñas A.F., et al. (2020) 'Genome-wide association studies in schizophrenia: Recent advances, challenges, and future perspective', *Schizophrenia Research*, 217, pp. 4-12.

9. Weyerstraß J., Bryk A., Nikolaidis P.T., et al. (2018) Nine genetic polymorphisms associated with power athlete status – a meta-analysis, *Journal of Science and Medicine in Sport*, 21(2), pp. 213–220. doi: 10.1016/j.jsams.2017.06.012.

10. Ahmetov I.I., Hall E.C.R., Semenova E.A., et al. (2022) Advances in sports genomics, in Makowski G.S. (ed.) *Advances in Clinical Chemistry*, 107, pp. 215-263. doi: 10.1016/bs.acc.2021.07.004.

11 Guth L.M., Roth S.M. (2013) Genetic influence on athletic performance, *Current Opinion in Pediatrics*, 25(6), pp. 653-658. doi: 10.1097/MOP.0b013e3283659087.

12. Semenova E.A., Fuku N., Ahmetov I.I. (2019) Genetic profile of elite endurance athletes, in Barh D., Ahmetov I. (eds) Sports, exercise, and nutritional genomics: current status and future directions. London: Academic Press, pp. 73-104. doi:10.1016/b978-0-12-816193-7.00004-x

13. Murtagh C.F., Hall E.C.R., Brownlee T.E., Drust B., Williams A.G., Erskine R.M. (2023) The genetic association with athlete status, physical performance, and injury risk in soccer. *Int J Sports Med.*, 44(13), pp. 941-960. doi: 10.1055/a-2103-0165.

14. Varillas-Delgado D., Del Coso J., Gutiérrez-Hellín J., et al. (2022) Genetics and sports performance: the present and future in the identification of talent for sports based on DNA testing, *EJAP*, 122, pp. 1811-1830. doi: 10.1007/s00421-022-04945-z.

15. Mattson C.M., Wheeler M.T., Waggott D., et al. (2016) Sports genetics moving forward: lessons learned from medical research, *Physiological Genomics*, 48 (3), pp. 175-182.

16. Maciejewska-Skrendo A., Sawczuk M., Cieśnik P., et al. (2019) 'Genes and strength athlete status', in: Sport, physical exercises and food genomics, Cambridge, MA, USA: Academic Press, pp. 41-72.

17. Puthucheary Z., Skipworth J.R., Rawal, J., et al. (2011) The ACE gene and human performance: 12 years on, *Sports Medicine*, 41(6), pp. 433-448. doi: 10.2165/11588720-000000000-00000.

18 Silva R.C., Ayres F.M., Gigonzac T.C.V., Cruz A.S., Rodrigues F.M. (2024). Genetic polymorphisms of the *ACE* gene associated with elite athletes: an integrative systematic review. *Genet. Mol. Res.,* 23(1), GMR19149. https://doi.org/10.4238/gmr19149

19. Yang R.-Y., Wang Y.-B., Shen X.-Z., et al. (2014) Association of elite athlete performance and gene polymorphisms, *CJTER*, 18, pp. 1121-1128. doi: 10.3969/j.issn.2095-4344.2014.07.023.

20. Ma F., Yang Y., Li X., Zhou F., Gao C., et al. (2013) The association of sport performance with ACE and ACTN3 genetic polymorphisms: a systematic review and meta-analysis. PLoS ONE, 8(1), e54685. doi:10.1371/journal.pone.0054685.

21 Diet F., Graf C., Mahnke N., et al. (2001) ACE and angiotensinogen gene genotypes and left ventricular mass in athletes, *EJCI*, 31(10), pp. 836-842. doi: 10.1046/j.1365-2362.2001.00886.x.

22. Rizzo M., Gensini F., Fatini C., et al. (2003) ACE I/D polymorphism and cardiac adaptations in adolescent athletes, MSSE, 35(12), pp. 1986-1990. doi: 10.1249/01.MSS.0000098993.51693.0B.

23. Kasikcioglu E., Kayserilioglu A., Ciloglu, F., et al. (2004) Angiotensin-converting enzyme gene polymorphism, left ventricular remodeling, and exercise capacity in strength-trained athletes, *Heart and Vessels*, 19(6), pp. 287-293. doi: 10.1007/s00380-004-0783-7.

24. Ahmetov I., Mozhayskaya I., Astratenkova I., et al. (2005) PPAR-δ +294T/C polymorphism and endurance performance, in: Proceedings of the 10th Annual Congress of the European College of Sport Science, Belgrade, Serbia, p. 54.

25. Scott R.A., Irving R., Irwin L., et al. (2010) ACTN3 and ACE genotypes in elite Jamaican and US sprinters, *Medicine & Science in Sports & Exercise*, 42(1), pp. 107-112. doi: 10.1249/MSS.0b013e3181ae2bc0.

26. Zarębska A., Jastrzębski Z., Moska W., et al. (2016) The *AGT* gene M235T polymorphism and response of power-related variables to aerobic training, *JSSM*, 15(4), pp. 616-624.

27. Miyamoto-Mikami E., Murakami H., Tsuchie, H., et al. (2017) Lack of association between genotype score and sprint/power performance in the Japanese population, *JSAMS*, 20(1), pp. 98-103. doi: 10.1016/j.jsams.2016.06.005.

28. Pickering C., Suraci B., Semenova E.A., et al. (2019) A genome-wide association study of sprint performance in elite youth football players, *JSCR*, 33(9), pp. 2344-2351. doi: 10.1519/JSC.0000000000003259.

29. Zmijewski P., Trybek G., Czarny W., et al. (2021) GALNTL6 Rs558129: a novel polymorphism for swimming performance?, *Journal of Human Kinetics*, 80, pp. 199205. doi: 10.2478/hukin-2021-0098.

30. Rankinen T., et al. (2016) No evidence of a common DNA variant profile specific to world class endurance athletes, *PLoS ONE*, 11(1), e0147330. doi: 10.1371/journal.pone.0147330.

31. Díaz Ramírez J., et al. (2020) The *GALNTL6* gene rs558129 polymorphism is associated with power performance, *JSCR*, 34(11), pp. 3031-3036. doi: 10.1519/JSC.0000000000003814.

32. Ahmetov I., Kulemin N., Popov D., et al. (2015) Genome-wide association study identifies three novel genetic markers associated with elite endurance performance, *Biology of Sport*, 32(1), pp. 3-9. doi: 10.5604/20831862.1124568.

33. Repa J.J., Berge K.E., Pomajzl C., et al. (2002) Regulation of ATP-binding cassette sterol transporters ABCG5 and ABCG8 by the liver X receptors alpha and beta, *JBC*, 277(21), pp. 18793-18800. doi: 10.1074/jbc.M109927200.

34. Handa R.J., Sharma D., Uht R. (2011) A role for the androgen metabolite, 5α-androstane-3β,17β-diol (3β-diol) in the regulation of the hypothalamo-pituitary-adrenal axis, *Frontiers in Endocrinology*, 2, p. 65.

35. Al-Khelaifi F., Yousri N.A., Diboun I., et al. (2020) Genome-wide association study reveals a novel association between MYBPC3 gene polymorphism, endurance athlete status, aerobic capacity and steroid metabolism, *Frontiers in Genetics*, 11, 595. doi: 10.3389/fgene.2020.00595.

36. Ahmetov I.I., Fedotovskaya O.N. (2015) Current progress in sports genomics, *Advances in Clinical Chemistry*, 70, pp. 247-314. doi: 10.1016/bs.acc.2015.03.003.

37. Rogozkin V.A., Nazarov I.B., Kazakov V.I. (2000) Geneticheskie markery fizicheskoi rabotosposobnosti cheloveka [Genetic markers of human physical performance], Teorija i praktika fizicheskoy kul'tury [Theory and Practice of Physical Culture], 12, pp. 34-36.

38. Vostrikova A., Borisova T.N., Semenov A.E., et al. (2022) Gene polymorphism and total genetic score in martial arts athletes with different athletic qualifications, *Genes*, 13(9), 1677. doi: 10.3390/genes13091677.

39. Sorokina A.V., Boronnikova S.V. (2023) Molekulyarno-geneticheskii analiz genov ADRB2, NOS3 i PPARGC1A u edinobortsev goroda Permi [Molecular-genetic analysis of the ADRB2, NOS3, and PPARGC1A genes in martial artists from the city of Perm], Vestnik Permskogo universiteta. Serija Biologija [Perm University Herald. Series Biology], (4), pp. 385-393.

40. Gonzalez D., Quintero-Moreno A., Palomares R., et al. (2003) Use of Gliricidia sepium in feed supplementation of crossbred heifers and its effect on growth and the onset of puberty, *Revista Científica*, 13(1), pp. 45-52.

41. Ahmetov I.I. (2009) Molekulyarnaya genetika sporta: monografiya [Molecular genetics of sport: monograph], M.: Sovetskii sport [Soviet Sport], p. 248.

42. Guilherme J.P.L.F., Souza-Junior T.P., Lancha Junior A.H. (2021) Association study of performance-related polymorphisms in Brazilian combat-sport athletes highlights variants in the *GABPB1* gene, Physiological Genomics, 53(2), pp. 47-50. doi: 10.1152/physiolgenomics.00118.2020.

43. Maciejewska-Karłowska A., et al. (2012) The *GABPB1* gene A/G polymorphism in Polish rowers, *Journal of Human Kinetics*, 31, pp. 115-120. doi: 10.2478/v10078-012-0012.

44. Bosnyák E., Trájer E., Alszászi G., et al. (2020) Lack of association between the GNB3 rs5443, HIF1A rs11549465 polymorphisms, physiological and functional characteristics, *Annals of Human Genetics*, 84(5), pp. 393-399. doi: 10.1111/ahg.12387.

45. Tsianos G.I., et al. (2010) Associations of polymorphisms of eight muscle- or metabolism-related genes with performance in Mount Olympus marathon runners, *Journal of Applied Physiology*, 108(3), pp. 567-574. doi: 10.1152/japplphysiol.00780.2009.

46. Peake J.M., Della Gatta P., Suzuki K., et al. (2015) Cytokine expression and secretion by skeletal muscle cells: regulatory mechanisms and exercise effects, *Exercise Immunology Review*, 21, pp. 8-25.

47. Kazancı D., Polat T., Sercan Doğan C., et al. (2021) The determination of IL-6 rs1800795 polymorphism distribution in Turkish national cross-country skiing athletes sub-groups created referring to the 1km CCSTAs, *Clinical and Experimental Health Sciences*, 11(4), pp. 782-786. doi: 10.33808/clinexphealthsci.904524.

48. Potocka N., Skrzypa M., Zadarko-Domaradzka M., et al. (2023) Effects of the Trp64Arg polymorphism in the *ADRB3* gene on body composition, cardiorespiratory fitness, and physical activity in healthy adults, *Genes*, 14(8), p. 1541. doi: 10.3390/genes14081541.

49. Santiago C., Ruiz J.R., Buxens A., et al. (2011) Trp64Arg polymorphism in *ADRB3* gene is associated with elite endurance performance, *BJSM*, 45(2), pp. 147-149. doi: 10.1136/bjsm.2009.061366.

50. Pickering C., Kiely J. (2017) *ACTN3*: more than just a gene for speed, *Frontiers in Physiology*, 8, p. 1080. doi: 10.3389/fphys.2017.01080.

51. Yang N., et al. (2003) ACTN3 genotype is associated with human elite athletic performance, *American Journal of Human Genetics*, 73(3), pp. 627-631. doi: 10.1086/377590.

52. Fedotovskaya O.N., Danilova A.A., Akhmetov I.I. (2013) Effect of *AMPD1* gene polymorphism on muscle activity in humans, *Bulletin of Experimental Biology and Medicine*, 154(4), pp. 489-491. doi: 10.1007/s10517-013-1984-9.

53. Ginevičienė V., et al. (2014) AMPD1 rs17602729 is associated with physical performance of sprint and power in elite Lithuanian athletes, *BMC Genetics*, 15, p. 58. doi: 10.1186/1471-2156-15-58.

54. Rivera M.A., Fahey T.D. (2019) Association between aquaporin-1 and endurance performance: a systematic review, Sports Medicine – Open, 5, 40. doi: 10.1186/s40798-019-0213-0.

55. Taghvaei S., et al. (2021) Computational analysis of Gly482Ser single-nucleotide polymorphism in *PPARGC1A* gene associated with CAD, NAFLD, T2DM, obesity, hypertension, and metabolic diseases, PPAR Research, 2021, article 5544233. doi: 10.1155/2021/5544233.

56. Hsiao T.-J., Lin, E. (2015) The Pro12Ala polymorphism in the peroxisome proliferator-activated receptor gamma (*PPARG*) gene in relation to obesity and metabolic phenotypes in a Taiwanese population, *Endocrine*, 48 (3), pp. 786-793. doi: 10.1007/s12020-014-0407-7.

57. Kazancı D., et al. (2023) PPARA and IL6: exploring associations with athletic performance and genotype polymorphism, *CMB*, 69(11), pp. 69-75. doi: 10.14715/cmb/2023.69.11.12.

58. Ahmetov I.I., et al. (2022) Advances in sports genomics, *Advances in Clinical Chemistry*, 107, pp. 215-263. doi: 10.1016/bs.acc.2021.07.004.

59. Leońska-Duniec A., Borczyk M., Piechota M., et al. (2022) TTN variants are associated with physical performance and provide potential markers for sport-related, *International Journal of Environmental Research and Public Health*, 19, 10173. doi: 10.3390/ijerph191610173.

60. Stebbings G.K., et al. (2018) TTN genotype is associated with fascicle length and marathon running performance, *Scandinavian Journal of Medicine & Science in Sports*, 28(2), pp. 400-406. doi: 10.1111/sms.12927.

61. Roth S.M., Rankinen T., HagbergJ.M., et al. (2012) Advances in exercise, fitness, and performance genomics in 2011, *Medicine & Science in Sports & Exercise*, 44(5), pp. 809-817. doi: 10.1249/MSS.0b013e31824f28b6.

62. Voisin S., Guilherme J.P., Yan X., et al. (2016) ACVR1B rs2854464 is associated with sprint/power athletic status in a large cohort of Europeans but not Brazilians, *PLoS ONE*, 11(6), e0156316. doi: 10.1371/journal.pone.0156316.

63. Ali A.H.A.H., Shkurat T., Abbas A.H. (2021) Association analysis of FTO gene polymorphisms rs9939609 and obesity risk among adults: a systematic review and meta-analysis, *Meta Gene*, 27, 100832. doi: 10.1016/j.mgene.2020.100832.

64. Loos R., Yeo G. (2014) The bigger picture of FTO – the first GWAS-identified obesity gene, *Nature Reviews Endocrinology*, 10, pp. 51-61. doi: 10.1038/nrendo.2013.227.

65. Lysiak J.J., Kirby J.L., Tremblay J.J., et al. (2009) Hypoxia-inducible factor-1α is constitutively expressed in murine Leydig cells and regulates 3β-hydroxysteroid dehydrogenase type 1 promoter activity, *Journal of Andrology*, 30(2), pp. 146-156.

66. Ahmetov I.I., et al. (2008) Effect of HIF1A gene polymorphism on human muscle performance, *Bulletin of Experimental Biology and Medicine*, 146 (3), pp. 351-353. doi: 10.1007/s10517-008-0291-3.

67. Pickering C., et al. (2019) A genome-wide association study of sprint performance in elite youth football players, *JSCR*, 33(9), pp. 2344-2351. doi: 10.1519/JSC.0000000000003259.

68. Eynon N., Ruiz J.R., Yvert T., et al. (2012) The C allele in NOS3-786 T/C polymorphism is associated with elite soccer player's status, *International Journal of Sports Medicine*, 33 (7), pp. 521-524.

69. Henderson J., Withford-Cave J.M., Duffy, D.L., et al. (2005) The EPAS1 gene influences the aerobic-anaerobic contribution in elite endurance athletes, *Human Genetics*, 118(3-4), pp. 416-423. doi: 10.1007/s00439-005-0066-0.

70. Kozyrev A.V. (2011) Rol genov NOS, UCP2 i UCP3 v predraspolojennosti k zanyatiyu greblei [The role of the NOS, UCP2, and UCP3 genes in predisposition to rowing engagement]', *The Russian Journal of Physical Education and Sport*, 1(18), pp. 1-6.

71. Mosse I.B., Kil'chevskiy A.V., Kundas L.A., et al. (2017) Nekotorye aspekty svyazi genov s vysokimi sportivnymi dostijeniyami [Some aspects of gene association with high sport achievements], Vavilovskii jurnal genetiki i selektsii [Vavilov Journal of Genetics and Breeding], 21(3), pp. 296-303.

72. Petr M., Thiel D.V., KábelováK., et al. (2022) Speed and power-related gene polymorphisms associated with playing position in elite soccer players, *Biology of Sport*, 39(2), pp. 355-366. doi: 10.5114/biolsport.2022.105333.

73. Zarebska A., et al. (2017) GSTP1 c.313A>G polymorphism in Russian and Polish athletes, *Physiological Genomics*, 49(3), pp. 127-131. doi: 10.1152/physiolgenomics.00014.2016.

74. Thakkar D., et al. (2021) HFE genotype and endurance performance in competitive male athletes, *Medicine & Science in Sports & Exercise*, 53(7), pp. 1385-1390. doi: 10.1249/MSS.0000000000002595.

75. Gunel T., Gumusoglu E., Hosseini M.K., et al. (2014) Effect of angiotensin I-converting enzyme and α-actinin-3 gene polymorphisms on sport performance, *Molecular Medicine Reports*, 9(4), pp. 1422-1426. doi: 10.3892/mmr.2014.1974.

76. Boidin M., Dawson E.A., Thijssen D.H.J., et al. (2023) VEGFA rs2010963 GG genotype is associated with superior adaptations to resistance versus endurance training in the same group of healthy, young men, *MGG*, 298(1), pp. 119-129. doi: 10.1007/s00438-022-01965-4.

77. Ahmetov I.I., et al. (2009) Association of the *VEGFR2* gene His472Gln polymorphism with endurance-related phenotypes, *EJAP*, 107(1), pp. 95-103. doi: 10.1007/s00421-009-1105-7.

78. Chmielowiec K., Michałowska-Sawczyn M., Masiak J., et al. (2021) Analysis of *DRD2* gene polymorphism in the context of personality traits in a group of athletes, *Genes*, 12(8), 1219. doi: 10.3390/genes12081219.

79. Pietrzak R.H., et al. (2015) Association of the rs2242446 polymorphism in the norepinephrine transporter gene *SLC6A2* and anxious arousal symptoms of posttraumatic stress disorder, *JCP*, 76(4), pp. e537-e538. doi: 10.4088/JCP.14l09346.

80. Peplonska B., et al. (2019) Association of serotoninergic pathway gene variants with elite athletic status in the Polish population, *Journal of Sports Sciences*, 37(14), pp. 1655-1662. doi: 10.1080/02640414.2019.1583156.

81. Kuc K., BieleckiM., Racicka-Pawlukiewicz E., et al. (2020) The *SLC6A3* gene polymorphism is related to the development of attentional functions but not to ADHD, Scientific Reports, 10, 6176. doi: 10.1038/s41598-020-63296-x.
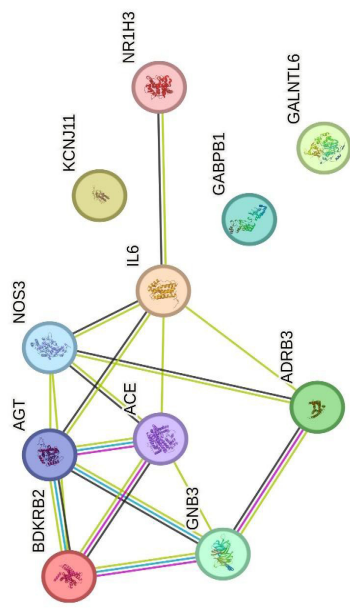
82. Purvis D., Gonsalves S., Deuster P.A. (2010) Physiological and psychological fatigue in extreme conditions: overtraining and elite athletes, *PM&R*, 2, pp. 442-450.

83. Mackinnon L.T. (2000) Overtraining effects on immunity and performance in athletes, *ICB*, 78(5), pp. 502-509. doi: 10.1111/j.1440-1711. 2000.t01-7-.x

84. McKinney J., Knappskog P.M., Haavik J. (2005) Different properties of the central and peripheral forms of human tryptophan hydroxylase, *Journal of Neurochemistry*, 92(2), pp. 311-320. doi: 10.1111/j.1471-4159.2004.02850. x.

85. van Dijk E.H.C., Tsonaka, R., Klar-Mohamad, N., et al. (2017) Systemic complement activation in central serous chorioretinopathy, *PLoS ONE*, 12(7), e0180312. doi: 10.1371/journal.pone.0180312.

86. Zagórska A., Partyka A., Jastrzębska-Więsek M., et al. (2023) Synthesis, computational simulations and biological evaluation of new dual 5HT1A/5HT7 receptor ligands based on purine-2,6-dione scaffold, *Bioorganic Chemistry*, 139, 106737. doi: 10.1016/j.bioorg.2023.106737.

87. Haslacher H., Michlmayr M., Batmyagmar D., et al. (2015) rs6295 [C]-allele protects against depressive mood in elderly endurance athletes, *JSEP*, 37(6), pp. 637-645. doi: 10.1123/jsep.2015-0111.

88. O'Connell K., et al. (2011) *COL6A1* gene and ironman triathlon performance, *International Journal of Sports Medicine*, 32(11), pp. 896-901. doi: 10.1055/s-0031-1277181.

89. O'Connell K., Posthumus M., Schwellnus M.P., et al. (2013) Collagen genes and exercise-associated muscle cramping, *CJSM*, 23(1), pp. 64-69. doi: 10.1097/JSM.0b013e3182686aa7.
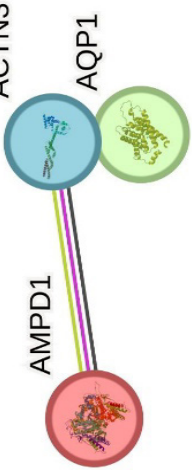
Appendix

Table 1 – Characteristics of markers of sporting qualities

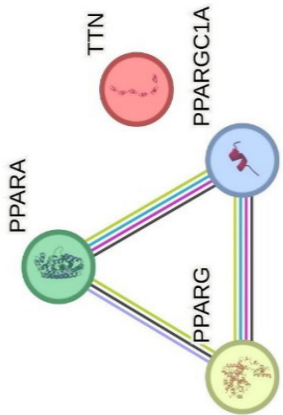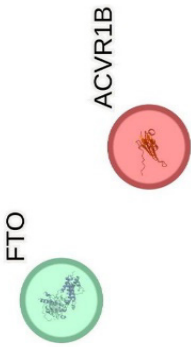| #	Gene	Chromosome	Genotype	SNP	Sporting qualities Markers of strength and endurance Name/Function	Studies with positive results
	ACE	17	G>A,C	rs4363	Angiotensin-converting enzyme. A proteolytic enzyme that converts angiotensin I to angiotensin II. Regulates blood pressure and water-salt balance.	[17-20]
	AGT	1	A>G	rs699	Angiotensinogen A peptide hormone that causes vasoconstriction, increased blood pressure, and the release of aldosterone from the adrenal cortex into the bloodstream.	[26-28]
	GALNTL6	4	G>A	rs558129	Polypeptide N-acetylgalactose-minyltransferase type 6 Promotes the biosynthesis of mucin-type o-glycans, mainly in the cells of the gastrointestinal tract, testes, brain, and muscles.	[29-32]
	NR1H3	11	T>A,C,G	rs7120118	Nuclear receptor Regulates macrophage functions, lipid metabolism, and inflammatory response. It is expressed in internal organs, including the liver, kidneys, and intestines.	[34-35]
	NF1A-AS2	1	G>T	rs1572312	Transcription factors NF1 (nuclear factor 1). Induces erythropoiesis.	[32], [36]
	NOS3	7	T>A, G	rs1799983	Endothelial nitric oxide synthase Synthesizes nitric oxide in endothelial cells and cardiomyocytes in response to neurohumoral effects and is responsible for relaxing smooth muscles and increasing the lumen of blood vessels.	[37-39]
	KCNJ11	11	T>A,C,G	rs5219	Inward rectifying potassium channel Restores the resting membrane potential during hyperpolarization by conducting potassium ions into the cell	[40-41]
	GABPB1	15	A>G	rs7181866	GA-binding protein transcription factor Plays a vital role in developing red blood cells and megakaryocytes, from which platelets are subsequently formed.	[42-43]
	GNB3	12	C>T	rs5443	Guanine binding protein beta 3 It is a transmembrane protein involved in cell differentiation, hormone secretion, and metabolism.	[44]
	BDKRB2	14	C>G,T	rs1799722	Bradykinin receptor type 2 Responsible for the relaxation of smooth muscles, increases the permeability of the vascular wall, regulates the energy consumption of skeletal muscles, and forms increased resistance to physical stress.	[45]

Continuation of the table

Sporting qualities

Markers of strength and endurance

#	Gene	Chromosome	Genotype	SNP	Name/Function	Studies with positive results
	IL6	6	C>G,T	rs1800795	Interleukin-6. It is an anti-inflammatory cytokine. Macrophages and T cells synthesize it and stimulate the immune response during traumatic tissue damage.	[46–47]
	ADRB3	8	A>G	rs4994	Beta-3 adrenergic receptor. Mediates lipolysis in adipocytes and affects fatty acid metabolism and obesity.	[48–49]

number of nodes: 11
number of ribs: 16
average node degree: 2.91
avg. local clustering coefficient: 0.461
expected number of ribs: 3
PPI enrichment value: 2.79e-07
This means that proteins interact more with each other than expected for a random set of proteins of the same size and degree of distribution taken from the genome. This enrichment indicates that the proteins are at least partially biologically related.

Evidence indicating a functional connection:

Experimental/biochemical evidence: none, but putative homologs interacting with other organisms have been found (score 0.129)
Association in curated databases: yes (score 0.500-0.900.
Co-citation in Pubmed Abstracts: yes (score 0.416-0.900).
Cooperative expression: yes (score 0.042).
Combined score: 0.416-0.917.

Markers of speed-strength abilities and muscle mass gain

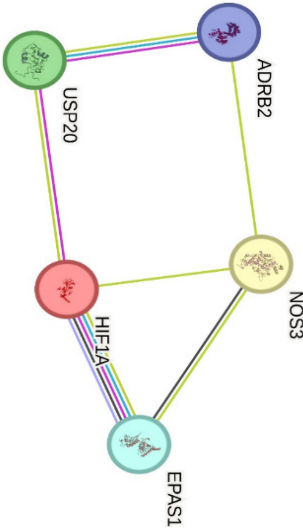| #	Gene	Chromosome	Genotype	SNP	Name/Function	Studies with positive results
	ACTN3	11	C>A,T	rs1815739	Alpha actinin-3. Stabilizes the contractile apparatus of skeletal muscles.	[9], [50–51]
	AMPD1	1	G>A,T	rs17602729	AMP deaminase. Participates in energy metabolism processes and characterizes the ability to perform high physical activity.	[52–53]
	AQP1	7	G>A,C	rs1049305	Aquaporin-1. It is a transmembrane protein that forms pores in the cell membrane necessary for water transport.	[54]

Continuation of the table

Sporting qualities

Markers of strength and endurance

#	Gene	Chromosome	Genotype	SNP	Name/Function	Studies with positive results
					number of nodes: 3 number of ribs: 1 average node degree: 0.667 avg. local clustering coefficient: 0.667 expected number of edges: 0 Enrichment PPI value: 0.0193 This means that proteins interact more with each other than expected for a random set of proteins of the same size and degree of distribution taken from the genome. This enrichment indicates that the proteins are at least partially biologically related. **Evidence indicating a functional connection:** Cooperative expression: yes (score 0.083). Additionally, putative homologs are coexpressed in other organisms (score 0.299) Experimental/biochemical evidence: no putative homologs interacting with other organisms have been found (score 0.087). Co-citation in Pubmed Abstracts: yes (score 0.592). Combined score:0.736	

Muscle fiber type and endurance

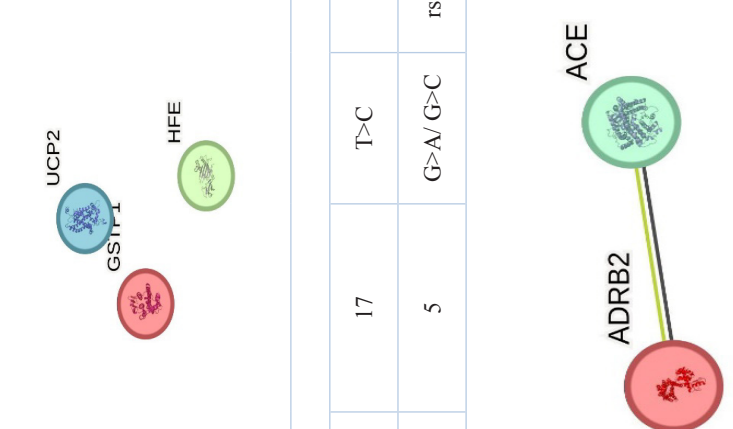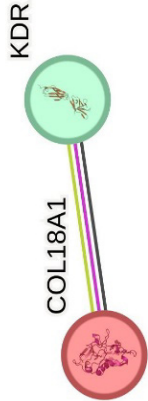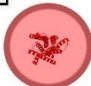| #	Gene	Chromosome	Genotype	SNP	Name/Function	Studies with positive results
	PPARGC1A	4	C>T	rs8192678	Coactivator 1-alpha receptor Plays a key role in energy metabolism in cardiac muscle cells.	[55]
	PPARG	3	C>G,T	rs1801282	Peroxisome proliferator-activated receptor gamma Plays an essential role in regulating the processes of cell differentiation and metabolism.	[56]
	PPARA	22	G>C,T чаще 7G>C	rs4253778	Peroxisome proliferator-activated receptor alpha Plays a vital role in regulating the processes of cell differentiation and metabolism.	[57-58]
	TTN	2	T>A,C	rs10497520	Connectin The largest of the single polypeptides. Plays a vital role in the process of contraction of striated muscles.	[59-60]

ACTN3   AQP1   AMPD1

Continuation of the table

#	Gene	Chromosome	Genotype	SNP	Name/Function	Studies with positive results
					Sporting qualities	
					Markers of strength and endurance	
		PPARA, TTN, PPARGC1A, PPARG			number of nodes: 4 number of ribs: 3 average node degree: 1.5 avg. local clustering coefficient: 0.75 expected number of edges: 1 Enrichment PPI value: 0.0673	
					Evidence indicating a functional connection: Co-expression: yes (score 0.043). In addition, putative homologs are coexpressed in other organisms (score 0.063). Association in curated databases: yes (score 0.500-0.900). Co-citation in Pubmed Abstracts: yes (score 0.999). In addition, putative homologs are mentioned together in other organisms (score 0.079). Combined score:0.999	
					Muscular strength	
	ACVR1B	12	A>C,G	rs2854464	Activin 1B receptor Transduces signals from activin or activin-like ligands (e.g., inhibin) Transmits the activin signal from the cell surface to the cytoplasm, regulates many physiological and pathological processes	[61-62]
	FTO	16	T>A G>A,C	rs9939609 rs1121980	Alpha-ketoglutarate-dependent dioxygenase Regulates the metabolism of fats and carbohydrates	[63-64]
		FTO, ACVR1B			number of nodes: 2 number of ribs: 0 average node degree: 0 avg. local clustering coefficient:0 expected number of edges: 0 Enrichment PPI value: 1	

Continuation of the table

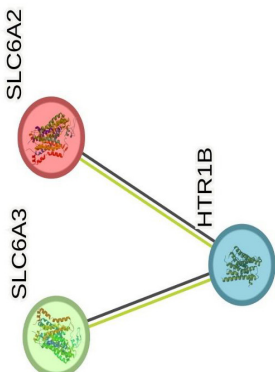| #	Gene	Chromosome	Genotype	SNP	Name/Function	Studies with positive results
					Sporting qualities	
					Markers of strength and endurance	
					Endurance in the absence of oxygen	
	HIF1A	14	C>T	rs11549465	Hypoxia factor HIF1-A Ensures normal cell functioning in conditions of lack of oxygen.	[65,66]
	ADRB2	5	G>A,C	rs1042713	Beta 2 adrenergic receptor Provides relaxation of smooth muscles, incl. the respiratory tract.	[67]
	NOS3	7	c.-51-762C>T	rs2070744	Endothelial nitric oxide synthase Synthesizes nitric oxide in endothelial cells and cardiomyocytes in response to neurohumoral effects and is responsible for relaxing smooth muscles and increasing the lumen of blood vessels.	[68]
	EPAS1	2	G>A	rs1867785	Endothelial protein Responsible for the synthesis of hypoxia-inducible factor 2 alpha	[69]
					number of nodes: 5 number of ribs: 6 average node degree: 2.4 avg. local clustering coefficient: 0.333 expected number of edges: 1 PPI enrichment value: 0.000103 This means that proteins interact more with each other than expected for a random set of proteins of the same size and degree of distribution taken from the genome. This enrichment indicates that the proteins are at least partially biologically related.	
					Evidence indicating a functional connection: Experimental/biochemical data: yes (score 0.510). Association in curated databases: yes (score 0.700).	
					Joint expression: estimate 0.056). In addition, putative homologs are coexpressed in other organisms (score 0.087). Co-mention in Pubmed Abstracts: score 0.369.	
					Endurance during aerobic training	
	UCP2	11	G>A	rs660339	Mitochondrial uncoupling protein 2 Regulates oxidative stress and energy production in mitochondria.	[70, 71]
	GSTP1	11	A>G,T	rs1695	Enzyme lutathione-S-transferase Participates in the detoxification process of a wide range of xenobiotics.	[73]

Continuation of the table

Sporting qualities

Markers of strength and endurance

#	Gene	Chromosome	Genotype	SNP	Name/Function	Studies with positive results
	HFE	6	C>G,T G>A	rs1799945 rs1800562	Homeostatic iron regulator They regulate the synthesis of the protein hepcidin, which is responsible for the absorption of iron ions from food.	[74]

number of nodes: 3
number of ribs: 0
average node degree: 0
average local clustering coefficient: 0
expected number of edges: 0
Enrichment PPI value: 1
This means that your current set of proteins is either relatively small (i.e., less than five proteins) or is essentially a random collection of poorly connected proteins.
Note: This does not necessarily mean that this is not a biologically significant choice of proteins – it is possible that these proteins have not yet been sufficiently studied, and their interactions are not yet known.

Strength and endurance for aerobic sports

#	Gene	Chromosome	Genotype	SNP	Name/Function	Studies with positive results
	ACE	17	T>C	rs4311	Angiotensin-converting enzyme. A proteolytic enzyme that converts angiotensin I to angiotensin II. Regulates blood pressure and water-salt balance.	[9], [75]
	ADRB2	5	G>A/ G>C	rs1042713	Beta 2 adrenergic receptor Provides relaxation of smooth muscles, incl. the respiratory tract.	[67]

number of nodes: 2
number of ribs: 1
average node degree: 1
average local clustering coefficient: 1
expected number of edges: 0
PPI enrichment value: 0.0503
This means that your current set of proteins is either relatively small (i.e., less than five proteins) or is essentially a random collection of poorly connected proteins.
Note: This does not necessarily mean that this is not a biologically significant selection of proteins–it is possible that these proteins have not yet been sufficiently studied and that STRING does not yet know about their interactions.

Evidence indicating a functional connection:
Co-mention in Pubmed Abstracts: score 0.052
Co-expression: Putative homologs are co-expressed in other organisms (score 0.045)
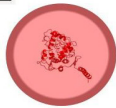
Endurance and features of the vascular system

Continuation of the table

Sporting qualities

Markers of strength and endurance

#	Gene	Chromosome	Genotype	SNP	Name/Function	Studies with positive results
	VEGFA	6	C>G,T	rs2010963	Vascular endothelial growth factor A Induces the proliferation of endothelial cells, promotes cell migration, and inhibits apoptosis.	[41], [76]
	VEGFR2	4	T>A	rs1870377	Vascular endothelial growth factor receptor type 2 Participates in angiogenesis.	[77]

Evidence indicating a functional connection:
Joint expression: 0.080
Experimental/biochemical data: yes (score 0.292).
Co-citation in Pubmed Abstracts: yes (score 0.944). In addition, putative homologs are mentioned together in other organisms (score 0.052).
Combined score: 0.960

number of nodes: 2
number of ribs: 1
average node degree: 1
avg. local clustering coefficient:1
expected number of edges: 0
Enrichment PPI value: 0.0592

KDR
COL18A1

Predisposition to combat sports

#	Gene	Chromosome	Genotype	SNP	Name/Function	Studies with positive results
	DRD2	11	C>T	rs1079597	Dopamine receptor type 2, whose activity is mediated by G proteins that inhibit adenylate cyclase. Blocks postsynaptic dopamine receptors and reduces the level of dopamine in the synaptic cleft.	[78]

number of nodes: 1
number of ribs: 0
average node degree: 0
average local clustering coefficient: 0
expected number of edges: 0
Enrichment PPI value: 1

DRD2

Fighting characteristics and qualities of a strength athlete

#	Gene	Chromosome	Genotype	SNP	Name/Function	Studies with positive results
	HTR1B	6	C>T	rs11568817	Serotonin 1B receptor Participates in the launch of intracellular processes that affect the activity of other neurotransmitter systems.	[80]
	SLC6A2	16	A>C	rs2242446	Dopamine transporter Responsible for the removal of norepinephrine from the synaptic cleft back into the cytosol of the presynaptic terminal.	[79]

Continuation of the table

Sporting qualities

Markers of strength and endurance

#	Gene	Chromosome	Genotype	SNP	Name/Function	Studies with positive results
	SLC6A3	5	T>C	rs6347	Dopamine transporter. Responsible for removing dopamine from the synaptic cleft and transferring it back into the cytosol of the presynaptic terminal.	[**80, 81**]

number of nodes: 3
number of ribs: 2
average node degree: 1.33
average local clustering coefficient: 0.667
expected number of edges: 0
Enrichment PPI value: 0.000317
Proteins have more interactions among themselves than would be expected for a random set of proteins of the same size and degree of distribution taken from the genome. This enrichment indicates that the proteins are at least partially biologically related.

Evidence indicating a functional connection:
Co-expression: none, but putative homologs are co-expressed in other organisms (score 0.054).
Co-citation in Pubmed Abstracts: yes (score 0.731). In addition, putative homologs are mentioned together in other organisms (score 0.090).
Combined score:0.748

Endurance of an athlete fighter

#	Gene	Chromosome	Genotype	SNP	Name/Function	Studies with positive results
	TPH2	12	A>C, G, T	rs7305115	Tryptophan hydroxylase enzyme. Participates in the synthesis of the neurotransmitters serotonin and melatonin	[**82-84**]
	NR3C2	4	G>A,C,T	rs2070951	Mineralocorticoid receptor; Receptor for both mineralocorticoids, such as aldosterone, and glucocorticoids, such as corticosterone or cortisol. It is part of the renin-angiotensin system and regulates water-salt balance and blood pressure.	[85]

Continuation of the table

#	Gene	Chromosome	Genotype	SNP	Name/Function	Studies with positive results
					Sporting qualities	
					Markers of strength and endurance	
		TPH2	NR3C2		number of nodes: 2 number of ribs: 0 average node degree: 0 avg. local clustering coefficient:0 expected number of edges: 0 Enrichment PPI value: 1 This means that your current set of proteins is either relatively small (i.e., less than five proteins) or is essentially a random collection of poorly connected proteins. Note: This does not necessarily mean that this is not a biologically significant choice of proteins – it is possible that these proteins have not yet been sufficiently studied, and their interactions are not yet known.	
					Marathon endurance	
	5HT1A	5	C>A,G	rs6295	Serotonin receptor gene It is the primary excitatory receptor for serotonin and is involved in memory formation and learning.	[87]
					Speed indicators	
	COL6A1	21	C>G,T	rs35796750	Alpha 1 chain of type VI collagen Plays an essential role in maintaining the structure and function of the extracellular matrix.	[88]

Information about authors:

Altynova Nazym Kalikhanovna – (corresponding author) – PhD, Head of the Laboratory of Population Genetics, Institute of Genetics and Physiology, Almaty, Kazakhstan, email: naz10.79@mail.ru

Tokmurzina Saida Sakenovna – master's student, senior laboratory assistant, Institute of Genetics and Physiology, Almaty, Kazakhstan, email:its2saida@gmail.com

Kassymbekova Aigerim Muratbekovna – senior laboratory assistant Institute of Genetics and Physiology, Almaty, Kazakhstan, email:kassymbekova01@gmail.com

Kereyev Tamerlan Nurlanovich – master's student, senior laboratory assistant, Institute of Genetics and Physiology, Al-Farabi Kazakh National University, Almaty, Kazakhstan, email: kalaysindos@gmail.com

Musralina Lyazzat Zenurainovna – Ph.D, senior researcher, Institute of Genetics and Physiology, Al-Farabi Kazakh National University, Almaty, Kazakhstan, email:musralinal@gmail.com

Lebedeva Lina Pavlovna – researcher, Institute of Genetics and Physiology, Almaty, Kazakhstan, email:lebedevaleena@gmail.com

Djansugurova Leyla Bulatovna – Candidate of Biological Sciences, Head of the Center for Paleogenetics and Ethnogenomics, Professor, Academician of MAIN, Institute of Genetics and Physiology, Al-Farabi Kazakh National University, Almaty, Kazakhstan, email: leylad@mail.ru

A.N. Aralbaeva*[1] ![iD], G.A. Yeszhanova[1] ![iD], A.N. Aralbayev[2] ![iD],

G.T. Zhamanbayeva[1] ![iD], N.I. Zhaparkulova[1] ![iD], A.I. Zhussupova[1] ![iD],

M.K. Murzakhmetova[1] ![iD]

[1]Al-Farabi Kazakh National University, Almaty, Kazakhstan
[2]Seifullin Kazakh Agro-Technical Research University, Astana, Kazakhstan
*e-mail: a_aralbaeva83@bk.ru
(Received 27 April 2023; received in revised form 18 May 2024; accepted 13 June 2024)

Overview on the heavy metal toxicity mechanisms and the role of alimentary factors in detoxification

Abstract. People are continuously subject to various environmental and chemical pollutants originating from industrial and agricultural activities. Heavy metals can be identified as a separate group of xenobiotics that pose a danger to human health. They affect almost all body systems, exerting toxic, allergic, carcinogenic, and gonadotropic effects. The toxicity of heavy metals to the body, their neutralization and elimination from the body depends on several factors, including nutritional status, as there are detoxification mechanisms in the human body, which require the intake of certain nutritional compounds. The quality of nutrition directly affects the state of the body since the essential compounds are mostly obtained from the food. Consumption of nutritional compounds is a significant factor that determines human health, growth, development, physical and mental activities and promotes more effective recovery during illness. The use of knowledge on the intoxication mechanisms and the role of alimentary factors in the body detox contribute to a deeper understanding of the processes in the development of the ways to neutralize the negative effects of various toxic compounds. At the same time, a large number of articles and reviews are devoted to the study and analysis of the manifestation of toxic effects of heavy metal compounds, mechanisms of their transformation in the environment, as well as damaging effects on the body systems; articles devoted to the study of the neutralization of the poisoning effect of various xenobiotics are aimed at investigating the detoxification effect of finished dosage forms. The importance of examining how nutritional factors like proteins, probiotics, vitamins, and dietary fiber contribute to the body detoxification processes is significant. This review analyses literature data of scientists from Kazakhstan, far and near abroad on the mechanisms of toxicity of a wide range of heavy metals, as well as the role of key nutrients in the process of their detoxification.

Key words: heavy metals, nutritional status, biotransformation, detoxification, alimentary factors.

Introduction

Nutrition is an individual's most significant physiological need and one of the crucial exposome factors, which directly affects human health, growth, development, physical and mental activities as well as tolerance to injurious factors [1].

Food items consist of intricate, multi-component combinations of chemical compounds, including nutrients such as proteins (valuable facts of which are presented on Figure 1), fats, carbohydrates, vitamins, and dietary fiber, which possess energetical, structural, and regulatory significance, as well as biologically active compounds such as organic acids, saponins, alkaloids, and polyphenols that take part in regulation of metabolic processes [2].

Importantly nutritional status of an individuum is defined as the state of food supply with major macro- and micronutrients, influenced not only by the quantity, but also by the quality of ingested food [4]. Epidemiological studies conducted in the past twenty years indicate a continuous rise in illnesses and disorders related to changes in the structure and quality of nutrients [5].
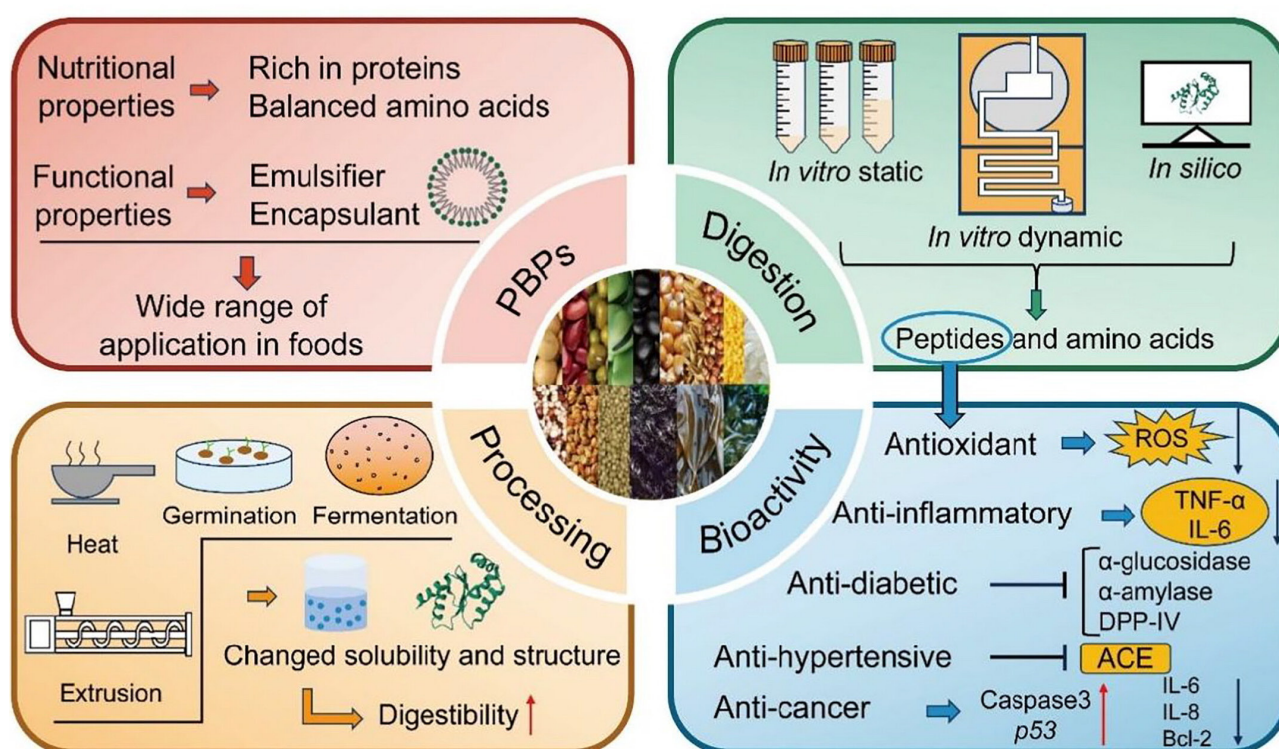
Figure 1 – Plant-based proteins (PBPs): advances in their sources,
digestive profiles *in vitro* and potential health benefits [3]

An unbalanced diet can cause disorders of the digestive and respiratory systems, dermatological, musculoskeletal disorders and a number of nervous ailments, poor health and even death [6].

The problem of nutrition shortage, or "hidden hunger," characterized as lacking or deficiency of nutrients associated with food deficiency for vital functions of the body, is an issue in a range of African and Southeast Asian countries [7]. Unbalanced nutrition and consumption of nutrients in quantities exceeding the body's needs is the other side of the coin. Undernutrition and obesity can lead to effects across generations as both maternal undernutrition and obesity are associated with poor health in offspring [8].

Nutrition is an integral component of a person's lifestyle and may contribute to the development of many chronic diseases such as obesity, cardiovascular disease, hypertension, stroke, type 2 diabetes, metabolic syndrome, cancer, and presumably some

neurological disorders. In addition, impairment of one of the body functions may entail the development of other pathological conditions. For example, obesity appears as a risk factor for type 2 diabetes, hypertension and metabolic syndrome, among others [9]. Therefore, maintaining good health and preventing diseases heavily relies on proper nutrition and equivalent physical exertion, as the nutritional component is a fundamental aspect of nearly every disease [10].

Additionally, food may contain anti-nutritional elements (e.g. phytic acid, saponins, alkaloids, certain oligosaccharides, protease inhibitors, glucosinolates, tannins, and cyanogenic glycosides) displaying varying biological activities (Figure 2).

However, there exist certain chemical compounds (including non-essential and essential heavy metals) whose metabolic byproducts can directly induce toxicity.
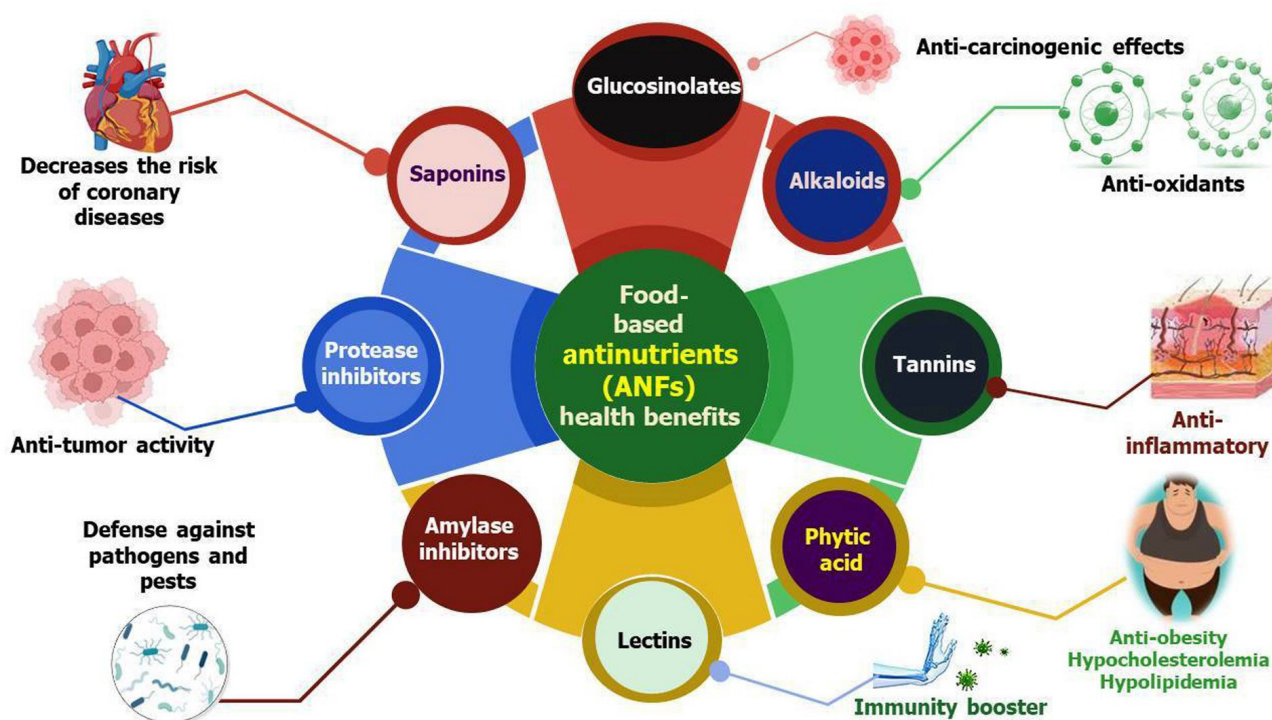
Figure 2 – Schematic representation of ANFs role in human life [11]

Toxic effects of non-essential heavy metals

The current pace of life involves considerable physical and emotional strain, compounded by unfavorable environmental circumstances, the infiltration of toxic compounds into the body, inadequate nutrition, and a decline in the quality of the food we consume. The cumulative effect of all these factors leads to chronic intoxication caused by the buildup of substances with varying degrees of toxicity. According to the World Health Organization (WHO), unsatisfactory environmental circumstances result in the demise of over 13 million individuals annually [12]. Toxic substances can accumulate in the body either by external exposure from the environment (e.g. chemicals at the workplace, Figure 3) or by being synthesized within the body itself. All toxins have the potential to generate free radicals, which can trigger oxidative stress and initiate pathological alterations within the body [13].

Heavy metals (HM) can be identified as a distinct category of xenobiotics that pose a threat to human health. Today, from a biological point of view the term heavy metals refers to metals with a relatively high atomic mass that can have a harmful impact on living organisms [9]. The ingress of HMs, and their salts into the human body occurs with the inhalation of air, the use of water from the water supply system, and some food products.

Forty chemical elements of the Mendeleev periodical system belong to the group of heavy metals. The heavy metals arsenic (As), cadmium (Cd), chromium (Cr) (VI), mercury (Hg), and lead (Pb) can have poisonous effects at extremely low concentrations. These heavy metals are known as the most toxic. Pollution of the environment with these toxins occurs due to the activities of a number of industries and some natural processes. High concentrations of heavy metals are found everywhere, including the atmosphere, hydrosphere, and lithosphere. The resulting heavy metal poisoning of ecosystems has devastating effects on all living organisms [15].

Toxic metal pollution in the environment has a greater impact on children due to the high accumulation of various toxic elements, including in the placenta. This can result in congenital malformations, weakened immunity, and the development of chronic diseases, as well as delays in mental and physical development [16-19].
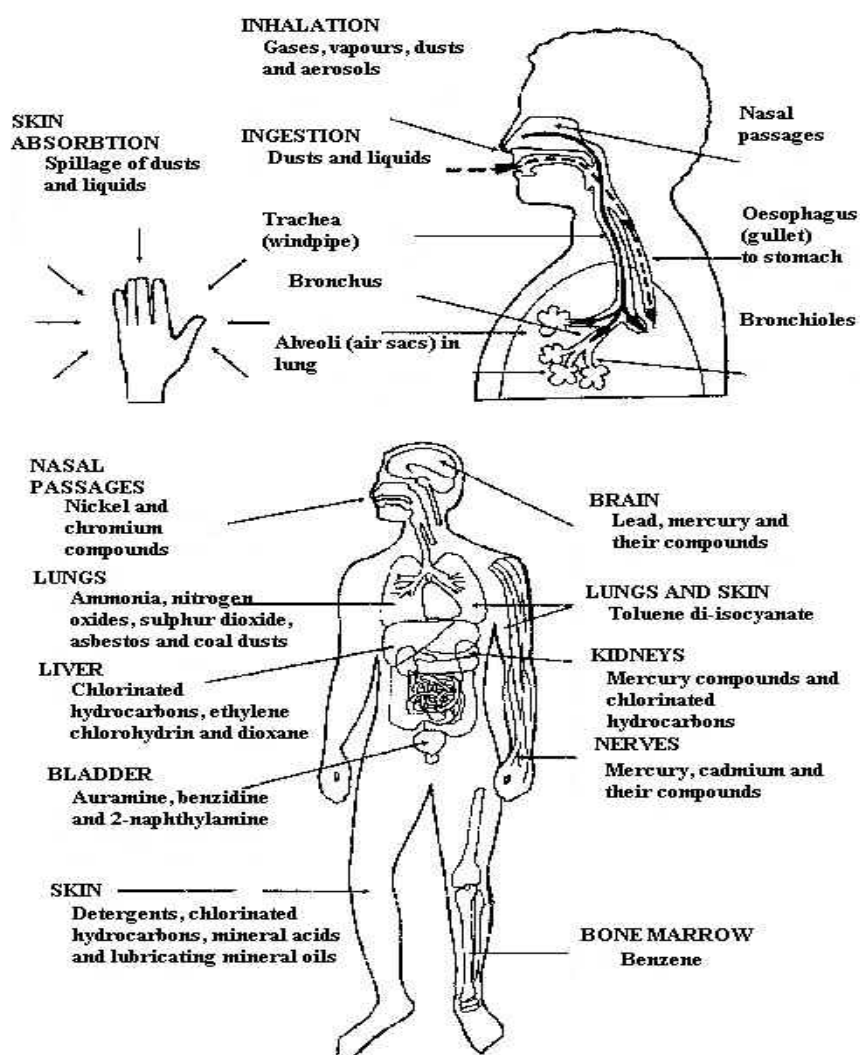
Figure 3 – Different organs and tissues that can be affected
by certain toxic industrial chemicals [14]

Lead is a noxious element that has detrimental effects on the human body. Lead is classified as a highly hazardous substance, along with other elements such as arsenic, cadmium, mercury, selenium, zinc, fluorine, and benzo(a)pyrene, based on its adverse effects on living organisms. The danger of lead to humans is determined by its significant toxicity and ability to accumulate in the body. Lead enters the human body from various sources such as food (accounting for 40-70% of intake in different countries and age groups), drinking water, the air we breathe, smoking, and accidental ingestion of lead-containing paint or soil. The main sources of environmental pollution with lead are vehicles using lead-containing gasoline, and stationary sources of non-ferrous metallurgy enterprises [20].

The first signs of lead's harmful effects typically manifest as central nervous system disorders. Asthenic syndrome tends to occur frequently and can be characterized by symptoms such as headaches, heightened fatigue, memory problems, and signs of autonomic dysfunction, where the parasympathetic tone is dominant. It is crucial, particularly for children, to lower their IQ levels and modify their visual, auditory-motor reaction times, and physical activity. Once lead enters the body, it typically moves into the bloodstream within a matter of minutes and readily attaches to red blood cells. This can lead to disruptions in porphyrin metabolism, heme synthesis, and an increase in anaerobic glycolysis, which may intensify platelet aggregation. Lead can bring about hypochromic anemia by impeding heme

synthesis enzymes. Continued exposure to lead can trigger the production of endogenous oxalic acid, leading to alterations in the renal tubules. Prolonged ingestion of lead can also result in chronic and irreversible nephropathy, ultimately progressing to renal failure. Lead does not have an affinity for the heart muscle. However, prolonged exposure to lead can lead to the development of bradycardia and an increase in blood pressure [21, 22]. Lead compounds affect membrane permeability and lipid peroxidation processes in many organs. Cells of the brain and liver are most sensitive to the influence of solutions of lead salts. Studies have also shown a higher incidence of primary infertility and miscarriage due to lead's ability to easily pass through the placental barrier, accumulate in fetal tissues, and potentially harm both mother and child. Women at risk of giving birth to babies with congenital malformations had a frequency of 4.6 births per 100 newborns. Non-specific gastrointestinal reactions may also be observed [23, 24].

The manifestation of heavy metal toxicity in cells of various organs occurs as a consequence of oxidative stress due to the intense formation of reactive oxygen species (ROS). ROS can cause damage to the liver, kidney, and cardiovascular system and cause diseases associated with inflammation. The damaging effects of ROS are usually neutralized by internal and external antioxidants, which helps to reduce the toxic load; however, in some cases, the toxic effects of heavy metals can damage antioxidant defense mechanisms [25, 26]. Lead's impact on mitochondria may be attributed to its transport into subcellular structures through a calcium transmembrane transport system. Pb has a high affinity for processes involving divalent metals. Thus, the mechanisms of lead toxicity have the property to modulate a number of processes in mitochondria, which leads to disruption of oxidative metabolism. Lead is potentially hazardous for human health, even in small amounts. There are a lot of molecules that could be targeted at Pb poisoning in the body. Disruption of bioenergetic homeostasis in cells exposed to Pb leads to a loss of cell ability to synthesize ATP. In addition, lead disrupts processes of homeostasis maintenance, such as apoptosis, mitophagy, and mitochondrial dynamics [27, 28].

Cadmium is toxic non-essential HM that precipitates adverse health effects in humans and animals. The detrimental effects of this HM are more widely recognized. Cadmium and its compounds are classified as Class I hazards [29]. Cadmium oxide is considered the most hazardous form of cadmium, as inhalation of its vapors can lead to acute poisoning and even death. A significant amount of cadmium enters the human body through smoking. Cadmium can be ingested through food when using ceramic dishes as it is present in the paints and glazes used to coat the surface of ceramics. The initial signs of cadmium poisoning include renal impairment (presence of protein in urine), heart muscle damage, nervous system dysfunction, and dysfunction of the reproductive system and lungs [30]. Later, individuals may experience severe bone pain in their legs and back. Cadmium salts, as well as such of many other HMs, causes peroxidation in membrane lipids [31, 23]. Cadmium induces the formation of free oxygen radical species and the inactivation of the cellular antioxidant system, leading to damage to various biomolecules [32]. Moreover, some studies have shown that cadmium may act as a carcinogen [30]. Oxidative stress is one of the mechanisms of cadmium-induced carcinogenesis [33-36]. The latter can easily occur because cadmium is excreted from the human body very slowly, even after a certain amount has been absorbed. Individuals with diabetes, pregnant and lactating women, children, and smokers are at higher risk of exposure to metals [37-39]. The metabolism of cadmium is strongly interrelated with many microelements, whereby the deficiency of calcium and copper significantly enhances the absorption and accumulation of HM in the human body. Conversely, with the adequate intake of zinc and selenium, the deposition of cadmium by internal organs markedly reduces [40]. Moreover, iron acts as an antagonist to cadmium [41].

Arsenic is considered a potentially vital and immunotoxic element for humans [42]. Acute and chronic poisoning can be caused by a wide range of toxic compounds, including arsenic. Arsenic compounds can enter the human body through various sources such as drinking and mineral water, grape wines and juices, seafood, medicines, pesticides, and herbicides [43].

Continuous intoxication by arsenic salts results in various pathologies like skin damage, neuropathies, and cancer [44, 45]. The gastrointestinal tract absorbs approximately 80% of arsenic, while 10% enters the body through the lungs and about 1% through the skin. Inorganic arsenic compounds, which make up more than 90% of arsenic, are soluble and therefore easily absorbed. Afterwards, inorganic arsenic is transported to the liver, where it undergoes methylation. The accumulation of arsenic occurs in several organs including the lungs, liver, skin, and small in-

testine. Arsenic primarily deposits in the reticuloendothelial system, possibly due to the binding of arsenite with SH-groups of proteins that are abundant in these tissues [46, 47]. Arsenic has a long retention time in the body, and its toxicity targets various organs such as the bone marrow, gastrointestinal tract, skin, lungs, and kidneys. There is abundant evidence supporting the carcinogenic effects of inorganic arsenic compounds [48]. Workers in pesticide production, gold mining, and smelting of arsenic alloys with other metals, as well as non-ferrous metals (particularly copper), have reported high mortality rates from lung cancer. Extended exposure to arsenic-contaminated water or drugs has been linked to the development of poorly differentiated skin cancer, known as Bowen's cancer. Additionally, liver hemangioendothelioma may also be a tumor that is dependent on arsenic exposure [49, 50].

The inhibition of dehydrolipoic acid and coenzyme A by arsenites disrupts the tricarboxylic acid cycle. The inactivation of ketoglutarate dehydrogenase disrupts the synthesis of citric and oxaloacetic acids, while the blockage of DNA polymerase results in the disruption of DNA synthesis and decoupling. The inhibitory effects of arsenic compounds on enzymes such as monoamine oxidase, urease, pyruvate oxidase, alanine aminotransferase, aspartate aminotransferase, and fumarase are also associated with their toxic effects. In the process of oxidative phosphorylation, arsenic comes into contact with phosphates, disrupting the formation of ATP from ADP. This action makes it an uncoupler of phosphorylation and oxidation [51, 26].

Mercury is an exceptional chemical element, as it is the sole metal that exists in a liquid state on Earth. Mercury is highly toxic and ubiquitous in the environment, with a tendency to bioaccumulate and transfer through food webs [52]. Mercury is introduced into the environment through various sources, such as the mining and smelting of mercury-containing ores, non-ferrous metal smelting from sulfide ores, gold extraction from ores, cellulose bleaching, chlorine and caustic production, vinyl chloride and electrical equipment manufacturing, production of measuring and control instruments (e.g. thermometers, pressure gauges), use of mercury-containing medical products and pesticides, cement production, and combustion of coal and fuel oil. Waste incineration is a significant source of mercury release into the environment [53]. Mercury primarily enters the human body through inhalation of air, consumption of food products, and drinking water. From the point of view of human pathology, mercury has a broad spectrum of toxic effects on human health, which vary depending on the form in which it enters the body (metallic mercury vapor, inorganic or organic compounds), the route of exposure, and the dose [23]. Mercury exposure can result in acute poisoning (occurring quickly and abruptly, usually at high doses) or chronic poisoning (resulting from low doses of mercury exposure over a prolonged period of time). Inorganic mercury compounds and fumes can lead to the development of contact dermatitis [54]. Mercury vapor is absorbed upon inhalation and accumulates in the brain and kidneys. Around 80% of mercury vapor that is inhaled is retained by the human body. Methylmercury is absorbed almost entirely in the gastrointestinal tract. It has been reported that various forms of mercury can penetrate the human body through the skin [55]. Additionally, in pregnant women, mercury can cross the placental barrier and affect the developing fetus. Furthermore, methylmercury can be transferred to breast milk, leading to dangerous levels in the bloodstream of nursing infants [51].

Mercury is a neurotoxin, and its salts can induce glomerulonephritis, where the formation of autoimmune complexes plays a significant role in its development mechanism [56]. Mercury compounds can decrease the function of T-cells, as well as the T-dependent humoral immune response of macrophages. The toxic mechanisms of mercury are related to the deactivation of enzymes containing thiol groups and the disruption of the transport of sodium and potassium across cell membranes [57]. Mercury compounds of inducing lipid peroxidation processes, altering the properties of cell membranes, disrupting their integrity, and leading to cell death and tissue damage at the organ level. It has been established that when mercury enters the body, the activity of the antioxidant defense system is significantly reduced [58].

Toxic effects of some essential heavy metals

Some metals are elements that are present in the environment and in small amounts in human bodies as essential components. Cobalt, chromium, copper, magnesium, iron, molybdenum, manganese, selenium, nickel and zinc are involved in physiological and biochemical processes, and their deficiency can lead to various disorders, but excessive exposure can also be hazardous to health [59].

Iron toxicity. The liver plays a key role in iron metabolism. Experiments *in vivo* prove that iron exposure leads to the growth of oxidative damage in this organ [36]. The mechanisms underlying iron toxicity are linked to the conversion of ferrous iron in the blood to ferric iron through oxidation. Ions of the latter form complexes with plasma proteins such as transferrin and gamma-globulin [60]. Acute iron poisoning can impair the function of cytotoxic T-lymphocytes, while chronic overdose can disrupt immunoregulation. These effects could be causally relevant to the development of cancer and infections that are linked to excessive iron in the body [61]. Individuals with excessive iron may experience a reduction in the phagocytic activity of macrophages, as well as T-helpers and natural killer cells in some cases. T-lymphocyte response can also be suppressed in mixed cultures, and the number of circulating T-suppressor cells may increase. Excess iron deposition in numerous brain regions has been seen in many neurodegenerative disorders, including Alzheimer's and Parkinson's disease, with possible toxicity. Due to its role as the primary biological catalyst of free radical reactions and the Fenton reaction, iron has been linked to all diseases associated with free radical pathology and tissue damage [41].

Cobalt toxicity is linked to the inhibition of iron absorption, which leads to the blocking of hemoglobin synthesis, impaired tissue respiration, inactivation of various oxidases including α-ketoglutarate dehydrogenase and pyruvate dehydrogenase, and interaction with thiol groups of lipoic acid [62]. In addition, insoluble cobalt compounds can be phagocytosed by macrophages when administered intravenously. Exposure to high doses of cobalt can lead to polycythemia, while a concentration of 35 mm cobalt chloride can inhibit the immune response of human thymocytes. Cobalt salts exhibit strong sensitizing properties and are known contact allergens. Contact with cobalt may even trigger asthma attacks [63, 64].

Magnesium toxicity is usually caused by overuse of magnesium-containing medications or insufficient renal excretion of magnesium [65]. At high doses, magnesium acts as a calcium antagonist and suppresses the activity of the central nervous system and neuromuscular synapses by reducing the release of acetylcholine from the postsynaptic membrane of the nerve fibers that innervate the muscles, as well as in the synapses of the autonomic ganglia [66].

When administered intravenously, it acts as a general anesthetic. Deficiency of magnesium in food can lead to impaired humoral immune response [67].

Manganese toxicity mechanisms are linked to the displacement of calcium and reduced iron absorption and metabolism due to manganese's iron antagonistic nature. These effects can lead to a decline in hemoglobin synthesis. At high doses, manganese affects glucose metabolism by altering the activity of enzymes involved in glycolysis. Low concentrations of manganese activate these enzymes, while high concentrations inhibit them. Manganese has both essential and neurotoxic properties and causes the development of neurotoxic and neurodegenerative diseases in humans [68]. Manganese also inhibits respiratory enzymes found in mitochondria [69].

Copper toxicity is linked to various mechanisms. Excess copper induces not only oxidative stress but also DNA damage and reduced cell proliferation [70]. The interaction of copper with sulfhydryl groups of erythrocytes leads to increase cellular permeability, inhibition of glutathione reductase and a subsequent decrease in reduced glutathione, agglutination of erythrocytes, and excessive stimulation of the hexose monophosphate shunt. In high doses, copper exhibits selenium-antagonistic properties, leading to selenium deficiency. Copper plays a role in maintaining immune homeostasis, but excessive amounts can suppress the T-dependent immune response and reduce the synthesis of IL-1B and IL-2, as well as leukocyte chemotaxis [71].

Nickel toxicity is caused by the variable oxidation state of the element, which inhibits oxidative enzymes [23]. High doses of nickel salts decrease the function of T-cells, natural killers, and T-dependent antibody production. Furthermore, the metal is known to cause allergic reactions such as contact dermatitis and has a carcinogenic effect [72].

Selenium toxicity mechanisms are linked to the induction of oxidative stress and the disruption of sulfur metabolism in the body. The replacement of sulfhydryl groups with selenol groups (SeH) in various enzymes leads to the inhibition of cellular respiration, a reduction in the activity of dehydrogenases, blockage of the tricarboxylic acid cycle, and glutathione metabolism. The functioning of enzymes can be disrupted due to a change in their tertiary structure caused by the formation of

selenium trisulfide complexes. Selenium as well as zinc, iron, copper, and germanium are classified as immunomodulatory elements [73].

Chromium is the second element that induces contact hypersensitivity after nickel [74]. In this case, the mechanisms involved are associated with both the action of chromium itself and its conjugation with proteins. Chromium exhibits significant allergic and autoimmune effects, enhances the functional activity of B-lymphocytes, and decreases the T-dependent humoral immune response. Chromium plays a crucial role in insulin-mediated carbohydrate metabolism [75].

The toxicity of Cr(VI) is strongly linked to the generation of ROS during its reduction process. The latter cause oxidation of cellular macromolecules, such as proteins, lipids, and DNA, thereby altering their functions. A major genotoxic effect of Cr(VI) that contributes to carcinogenesis is the formation of DNA adducts, which can lead to DNA damage [46]. Modulations of cellular signaling pathways, as evidenced by the modulation in p53 signaling pathway, and epigenetics may also contribute to the carcinogenic effects of Cr(VI). Several studies demonstrated that Cr(VI) induces cellular death through apoptosis and autophagy, genotoxicity, functional alteration of mitochondria, endocrine and reproductive impairments [76]. Cr(VI) has a major impact on many aspects of mitochondrial biology, including oxidative phosphorylation, mitophagy, and mitochondrial biogenesis [77]. It was concluded that occupational exposure to Cr(VI) can cause lung cancer, nose and nasal sinus cancer in humans. Cr(VI) is suspected to cause stomach cancer and laryngeal cancer in humans. It is currently insufficiently clear if Cr(VI) can cause cancer of the small intestine, oral cavity, pancreas, prostate or bladder in humans [78, 79].

Mammals, including humans, are exposed to Cr, including Cr (VI), frequently through inhalation, drinking water, and food.

Zinc is an element commonly found in the Earth's crust. It is released to the environment from both natural and anthropogenic sources. The primary anthropogenic sources of zinc in the environment (air, water, soil) are related to mining and metallurgic operations involving zinc and use of commercial products containing zinc. Although zinc has a rather low toxicity, and a severe impact on human health by intoxication with zinc is a relatively rare event people living near smelters or industries using zinc could be exposed to higher levels of zinc by drinking water, breathing air and touching soil that contains the metal [80].

Ingestion of zinc and zinc-containing compounds can result in a variety of chronic effects in the gastrointestinal, hematological and respiratory systems along with alterations in the cardiovascular and neurological systems of humans. Prolonged zinc exposure via these routes has been shown to result in copper deficiency characterized by hypocupremia, anemia, leucopenia and neutropenia; some subjects additionally report headache, abdominal cramps and nausea. The antioxidant enzyme Cu, Zn-superoxide dismutase (SOD) is said to be very sensitive to changes in plasma Zn/Cu ratio and alterations in SOD activity with zinc supplementation may result in excess free radicals that are damaging to the cell membrane. Studies have also noted some competitive interaction between zinc and iron that can result in decreased serum ferritin and hematocrit concentrations especially in women [81, 82].

Table 1 – Summary of toxic effects of essential and non-essential heavy metals

Heavy metal	Sources	Effects on human body	Symptoms of poisoning	Chronic exposure risks	References
Lead (Pb)	Lead-based paints, plumbing, contaminated water, soil, industrial processes	Affects nervous system, kidneys, blood, and bones	Fatigue, abdominal pain, headaches, irritability, anemia	Cognitive decline, developmental delays in children, kidney damage, hypertension	[83]
Mercury (Hg)	Fish (especially large fish), industrial emissions, dental fillings (amalgam), thermometers	Affects the nervous system, kidneys, and immune system	Tremors, vision/ hearing problems, memory loss, fatigue	Neurological damage, immune system dysfunction, developmental delays in children	[84]

Continuation of the table

Heavy metal	Sources	Effects on human body	Symptoms of poisoning	Chronic exposure risks	References
Arsenic (As)	Contaminated water, pesticides, industrial emissions, contaminated food (especially rice)	Affects skin, lungs, liver, kidneys, and nervous system	Nausea, vomiting, abdominal pain, skin lesions, diarrhea	Cancer (skin, lung, liver), cardiovascular disease, peripheral neuropathy	[85]
Chromium (Cr)	Industrial processes, contaminated water, air pollution	Affects liver, kidneys, and nervous system	Abdominal pain, nausea, vomiting, skin irritation	Cancer (lung, stomach), kidney damage, respiratory issues	[86]
Nickel (Ni)	Industrial processes, contaminated water, certain alloys, jewelry	Affects lungs, skin, kidneys, and cardiovascular system	Skin rashes, respiratory issues, fatigue, headache	Lung cancer, respiratory diseases, kidney damage	[87]
Cadmium (Cd)	Cigarette smoke, industrial emissions, contaminated food (especially shellfish, rice)	Affects kidneys, lungs, bones, and liver	Shortness of breath, kidney dysfunction, abdominal pain, weakness	Kidney failure, osteoporosis, lung cancer, cardiovascular disease	[88]
Iron (Fe)	Meat, fish, beans, fortified cereals, supplements	Essential for oxygen transport, but excessive iron can damage organs	Nausea, vomiting, abdominal pain, liver damage, fatigue	Organ damage (liver, heart), diabetes, arthritis, neurological damage	[88]
Cobalt (Co)	Seafood, meat, industrial exposure (e.g., batteries, alloys)	Essential in small amounts (vitamin B12), but excessive exposure can damage heart, liver, and kidneys	Vomiting, diarrhea, heart failure, skin rashes	Heart damage, lung disease, neurological issues, cancer	[37]
Magnesium (Mg)	Nuts, seeds, whole grains, leafy greens, supplements	Essential for muscle function, bone health, and metabolism	Diarrhea, nausea, lethargy, difficulty breathing	Hypotension, heart arrhythmias, kidney damage (in excessive amounts)	[89]
Manganese (Mn)	Nuts, seeds, whole grains, industrial exposure (e.g., welding, mining)	Essential in trace amounts for bone health and metabolism	Fatigue, dizziness, tremors, difficulty walking, facial muscle spasms	Manganism (Parkinson-like syndrome), liver damage, reproductive toxicity	[65]
Copper (Cu)	Seafood, meat, nuts, seeds, water (in copper pipes), supplements	Essential for enzymes, but too much can lead to toxicity	Nausea, vomiting, abdominal pain, diarrhea, jaundice	Liver damage, kidney damage, gastrointestinal bleeding, neurological issues	[90]
Selenium (Se)	Brazil nuts, seafood, meat, grains	Essential antioxidant for cellular function, but toxicity can occur	Nausea, vomiting, hair loss, fatigue, garlic-like odor on breath	Liver and kidney damage, brittle nails, hair loss, neurological damage	[91]
Zinc (Zn)	Meat, shellfish, legumes, seeds, dairy products	Essential for immune function, protein synthesis, and wound healing	Nausea, vomiting, loss of appetite, stomach cramps, diarrhea	Immune system suppression, reduced copper absorption, gastrointestinal issues	[82]

General mechanisms of heavy metal toxicity

HMs have an impact on nearly all body systems, causing toxic, allergic, carcinogenic, and gonadotropic effects. Some HMs selectively accumulate in certain organs and tissues, which can lead to structural and functional disruptions [92]. They have been seen to have an embryotoxic effect through the fetoplacental system and a mutagenic effect (Figure 4).
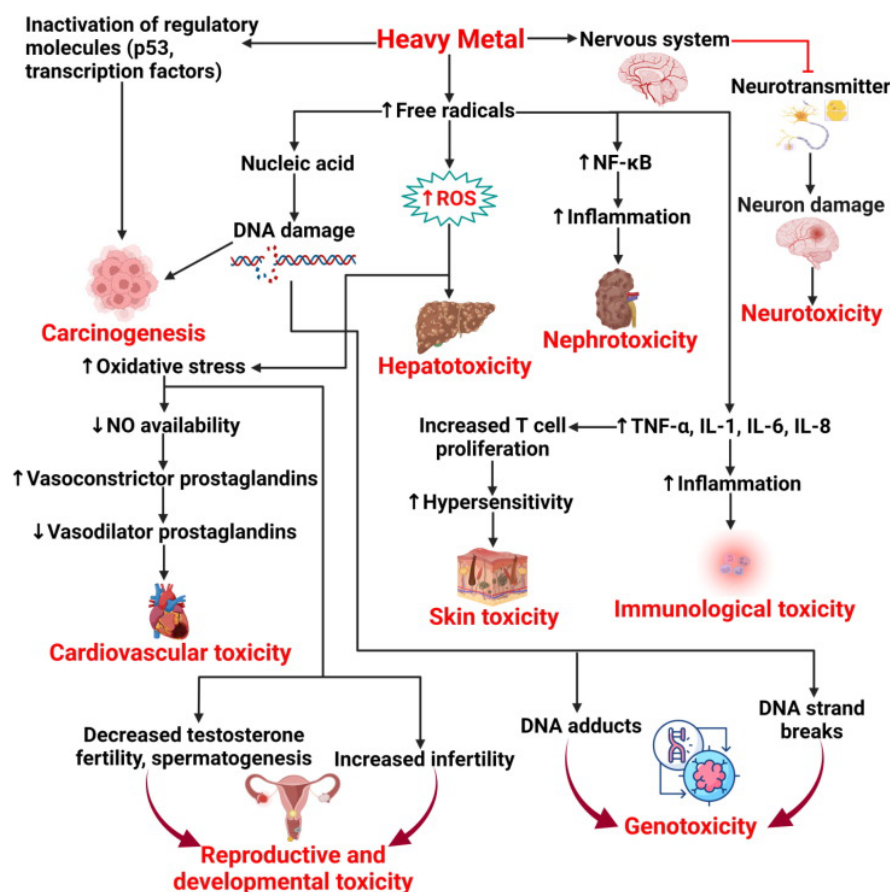

Figure 4 – Various toxicity effects of heavy metal accumulation in human body [93]

HMs toxicity is strongly associated with the extent of protein synthesis inhibition. Metals cause oxidative stress, DNA damage, mitochondrial malfunction, and apoptosis by disrupting molecular processes. HMs effect on specific organs can also depend on the dose and route of their entry into the body [16, 17].

The formation of metalloprotein complexes by HMs is a crucial factor in their distribution throughout the body [94]. This leads to the following model of how HMs behave in the body: binding with organic substances, breakdown of organometallic compounds, and alteration of the metal's oxidation state within the biological system (Figure 5).

The process of biotransformation usually results in detoxification. The amount and duration of metal accumulation are determined by their type and involved organ. Individual metals are distributed in various ways in the body: usually, muscles accumulate nickel, copper, and zinc in the smallest amounts, whereas copper accumulates to a greater extent in the liver and nickel in the kidneys [96].

The metabolism of metals has a considerable influence on their accumulation in the body, their distribution within tissues, and their toxic effects [97].

HMs exert their effects by forming coordinate covalent bonds with various molecules (ligands), which is the underlying mechanism of their action. Metals interact with ligands of biological significance, such as proteins and nucleic acids, which contain electron-donor groups such as oxygen, nitrogen, and sulfur in their molecule [98].
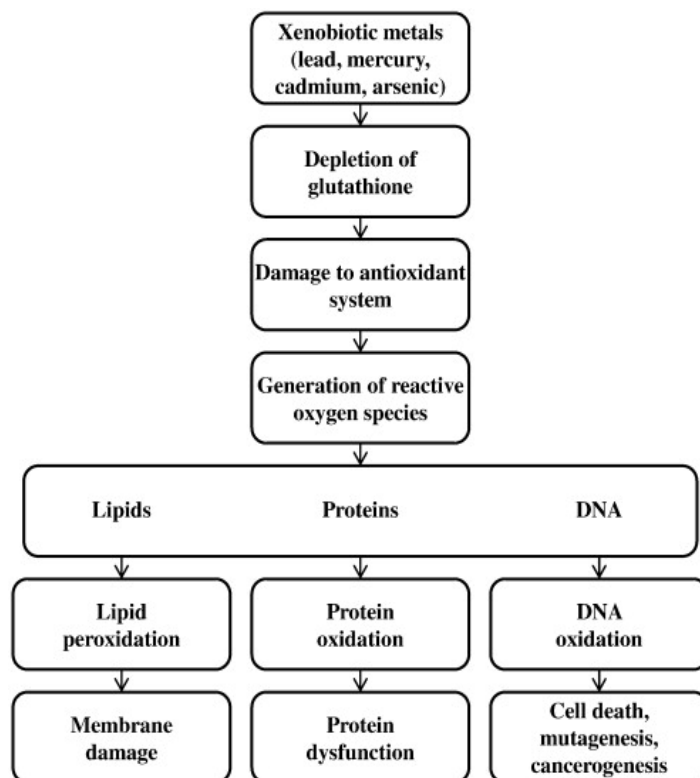
Figure 5 – Hypothetical mechanisms of metal toxicity [95]

There are various outcomes of the interaction between metals and ligands. The primary effects of this interaction include the disruption of hydrogen bonds within the macromolecule, the displacement of other metals bound to the ligands, and consequently, alterations in the tertiary structure of the complex. This leads to changes in their biological properties such as enzyme activity inhibition, alteration of transport properties, and others. The binding of metals to membrane structure ligands primarily results in the disruption of active or passive transmembrane transport processes. The inhibition of enzymes that participate in the DNA repair process may also have a role in the onset of mutagenesis and carcinogenesis [99].

Each metal exhibits a distinct pattern of affinity constants for different ligands across various tissues. Metals with an increased affinity for SH- groups are among the so-called thiol poisons (mercury, arsenic, etc.). The non-competitive inhibition of enzymes happens when metals interact with the structural components of the enzyme molecule and alter its conformation, even if the active center remains intact. Interacting with nucleic acids, metal cations can disrupt hydrogen bonds and create coordination-covalent bonds with phosphate groups and nitrogen atoms of nitrogen bases, they may destabilize DNA structure, what results in the disturbance of both transcription and translation processes [100].

At times, metals can serve as enzyme activators and participate in nucleic acid synthesis and repair. For instance, thymidine kinase activity requires zinc. However, when other metals, such as cadmium, replace zinc during intoxication, the enzyme activity is disrupted, and DNA synthesis is impeded. The inhibition of DNA repair enzymes is partly linked to the mutagenic activity of arsenic compounds. In this regard, investigation of how toxicants interact with ligands that are bound to membranes is crucial. The ability of metals to interact precisely with these structures is determined not only by their specific properties but also by their position [101].

Metals primarily interact with the outer surface of the cell membrane. Slowly penetrating substances can bind strongly to ligands and consequently alter the properties of the membrane. For instance, the organomercury compound chlormerodrin inhibits the transport of sugars through the membrane by interacting with the -SH groups of erythrocytes. Thereby metals can interact with any organelles that are enclosed by a membrane, including mitochondria, endoplasmic reticulum, and lysosomes. However, the

substances that can easily cross the membrane, such as methylmercury, are unlikely to have a significant effect on its properties [102, 103].

Certain metals may have a harmful impact because they compete with crucial elements necessary for proper functioning. Thus, tungsten acts as a competitor to molybdenum and inhibits xanthine oxidase, while lead hinders the utilization of iron in heme synthesis and therefore inhibits ferrochelatase activity. There is evidence that cadmium inhibits the transfer of zinc from the mother to the fetus through the placenta, leading to teratogenic effects [104].

Body detoxification mechanisms

Under normal circumstances, a healthy organism is a comprehensive and integrated system, capable of eliminating various toxins by converting them into water-soluble molecules. Detoxification is a metabolic process aimed at inactivating and removing toxic substances from the body. The process of metabolic detoxification includes a series of enzymatic reactions that neutralize and dissolve toxins, eventually transporting them to secretory organs (such as the liver and kidneys) for complete elimination from the body, what enables the converted toxins to be excreted directly through the renal tubules or gallbladder [105].

The enzymatic system that transforms xenobiotics is a mechanism that helps the body adapt to the impact of both exogenous and endogenous toxins Metabolic detoxification reactions are crucial not only for shielding the body from unfavorable environmental conditions, but also for sustaining homeostatic equilibrium within the body [106].

The detoxification or biotransformation system includes 3 steps: bioactivation, conjugation and evacuation (Figure 6).
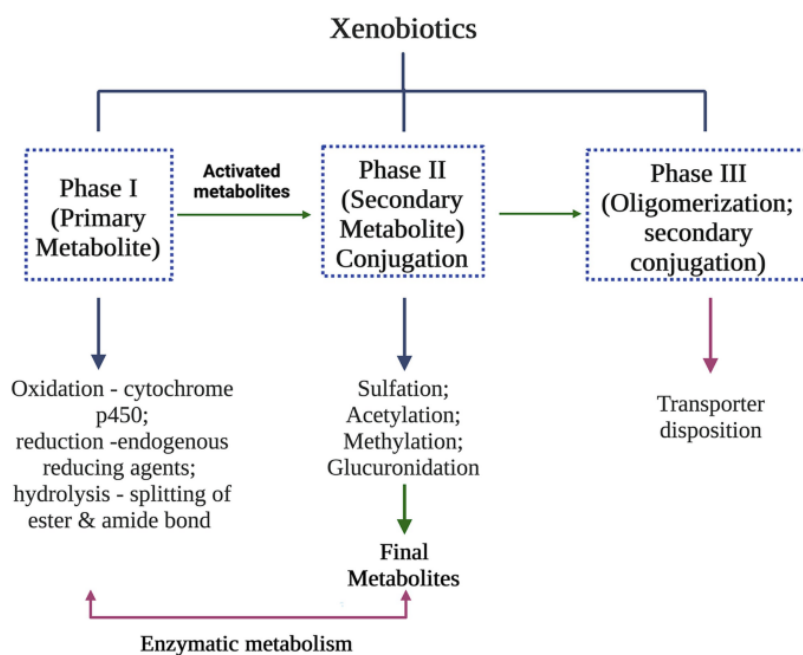
Figure 6 – Simple scheme of xenobiotics detoxification [107]

During the initial stage of metabolism, biotransformation reactions take place to convert fat-soluble toxins into water-soluble molecules prior to their entry into the circulation system. In some cases, toxins can even be detoxified before reaching the liver through the same biotransformation reactions that occur in the intestinal tract [108, 109]. A number of chemicals, such as 3-MC, benzpyrene, and DDT, once in the body, spread through the lymph stream to cells and tissues of various systems and organs, bypassing the inactivation process in the liver. which exacerbate their toxicity. The enzymes that metabolize xenobiotics, located in the endoplasmic reticulum of the intestine, have biochemical characteristics similar to those of the liver. In general, the rate of xenobiotic metabolism

by the intestinal enzymes is lower than that of similar hepatic enzymes. [110].

Enzymes such cytochromes P450, dihydropyrimidine dehydrogenase, butyrylcholinesterase, paraxonase, alcohol hydrogenase, aldehyde dehydrogenase, etc., offer the first stage of the biotransformation process. Microsomal oxidation is caused by the cytochrome P-450 superfamily (CYP-450), a collection of enzymes with over 1000 different isoforms that not only metabolize medicines but also take part in the creation of cholesterol, steroid hormones, and other chemicals. Hepatocytes, as well as organs like the intestines, kidneys, lungs, brain, and heart, contain the greatest number of cytochromes [111].

The intestinal mucosa is responsible for approximately 25% of biotransformation processes in the body, making it the second most actively involved tissue in the detoxification process. All cells in the intestinal lining possess the ability to detoxify [112, 113]. Numerous transferases involved in the metabolism of bilirubin, other hormones (thyroxine, triiodothyronine), morphine, chloramphenicol, paracetamol, and other substances cause further alterations to toxic chemicals created during biotransformation [108].

Currently, the third phase of biotransformation is distinguished: the so-called evacuation phase, in which the main role is assigned to specific transport systems – proteins (P-glycoproteins – P-gp), involved in the regulation of absorption, distribution, and excretion of xenobiotics (into bile, blood). P-gps remove xenobiotics from cell membrane and cytoplasm, preventing the absorption of xenobiotics in the intestine. The activation of transporters may result in diverse alterations (primarily an elevation) in the levels of a substance in the bloodstream, based on the role of that particular transporter. Transporters that carry organic anions and cations are responsible for excreting hydrophilic xenobiotics and their metabolites into bile by the liver and urine by the kidneys [114, 115].

Role of nutrients in detoxification processes

The process of detoxification can be significantly influenced by normal digestion. The ingestion of food is recognized to influence the absorption of chemicals by affecting gastric emptying, intestinal transit, pH, and bile production. Metabolites of toxins and drugs that undergo conjugation in the intestinal tract are primarily excreted through bile and eventually eliminated in feces [116].

Nutrients play a crucial role in supporting biotransformation, beyond just aiding in excretion.

An adequate supply of nutrients is essential not only for energy production but also for the formation of new enzymes and protein synthesis, which are critical for the detoxification process. Hence, it is necessary to have sufficient intake of carbohydrates, energy-supporting fats, and high-quality proteins to maintain the body's defense mechanisms against toxic damage [117].

The mechanisms of detoxification related to metal ions are not well understood at present. HMs can be harmful as they are not efficiently eliminated from the body. However, some of the metals can be transformed into less hazardous forms through several ways, including the formation of insoluble complexes in the intestinal tract, transportation of metal via the blood to other tissues where it can be immobilized (such as Pb^{2+} in bones), and conversion into less toxic forms by the liver and kidneys [81, 113].

Detoxification can be facilitated by the binding of toxins to protein molecules. The breakdown of poisons or conversion into a soluble form by liver enzymes is especially crucial for detoxification in humans, as it leads to their quick elimination [108].

Maintaining a balanced, normal, and complete detox requires the preservation of numerous conjugation processes. The conjugation pathway with glutathione has received more research attention compared to other pathways. Glutathione, a tripeptide composed of glutamic acid, cysteine, and glycine, participates in the conjugation reaction of over 40 various compounds of both exogenous and endogenous origin. The conjugation reaction involving glutathione proceeds through three or four stages, with the resulting conjugates being successively cleaved of glutamic acid and glycine. The remaining complex containing xenobiotics and cysteine can be excreted from the body in this form. However, the fourth stage is more commonly observed where the amino group of cysteine is acetylated, resulting in the formation of mercapturic acid, which is then excreted through the bile [118].

Another significant role of glutathione is in neutralizing endogenously formed peroxides that can cause toxicity. Amino acid conjugation in humans usually involves glycine, glutamine, and taurine, although other amino acids can also be utilized. The last two types of conjugation reactions involve the transfer of either a methyl or acetyl radical to the xenobiotic compound. These reactions are catalyzed by methyl or acetyltransferases found in various organs such as the liver, lungs, spleen, and adrenal glands [119].

Proteins involved in the ABC transporter superfamily are among the many transport proteins that can participate in safeguarding cells against harmful substances. These proteins, present in all living organisms, transport various substances (lipids, many xenobiotics, etc.) through the cell membrane. The functioning of P-glycoprotein (a transport ATPase) is a crucial mechanism for removing hydrophobic xenobiotics from cells. Present in the plasma membrane of various tissues, particularly the kidneys and intestines, P-glycoprotein is a phosphoglycoprotein with a molecular weight of 170 kDa. Its primary role is to remove chloride ions and hydrophobic toxic compounds from cells. Have been shown that utilization of biogen amins like serotonin and hydroxitriptophane provides defense of the body from damaging effect of non-symmetrical dimethylhydrozine and cadmium salts. Results of experiments allow us to predict their correcting action on the cell membrane state and reducing the organism's inner medium's hazards from chemical agents [120].

Metallothioneins play a crucial role in binding HMs, forming mercaptides that can bind up to seven HM ions per molecule. They are also capable of replacing glutathione in the glutathione peroxidase system [121]. As these molecules contain up to 30% cysteine, it is important to consume dietary proteins that are balanced in their amino acid composition. Therefore, a balanced diet is essential for neutralizing any chemical compounds [122].

Various reactions in the body, including detoxification processes, require many vitamins and minerals as essential components for the production of enzymes. Vitamins are involved in various mechanisms in the metabolism of foreign chemicals and drugs [123].

Xenobiotics undergo various changes during their metabolism, including the formation of new functional groups in functionalization reactions. These reactions take place in the liver's endoplasmic reticulum, with the cytochrome P450 system, which is part of the NADPH-dependent monooxygenase system, being the most important enzyme involved. Conjugation reactions, the formation of paired compounds with glutathione, sulfuric, and glucuronic acids, represent the second crucial step in the transformation of foreign substances [106]. Vitamins play a direct role in these processes, acting as coenzymes in detoxification reactions, as well as an indirect role through the synthesis of components of the microsomal oxidation chain and other detoxification reactions. Fat-soluble vitamins also play a critical role in the biotransformation of xenobiotics by regulating the structural integrity of membranes, including microsomes, to ensure their normal functioning [124].

Among the vitamins associated with the metabolism of foreign substances, the most important can be considered ascorbic acid, vitamins PP, A, E, B12, folic acid, and other coenzymatic B vitamins. Studies have shown that the presence of foreign compounds in the body can lead to a decrease in the levels of ascorbic acid, which is stored in the liver and adrenal glands. Additionally, there is a direct correlation between the concentration of ascorbic acid and the levels of cytochrome P450, a crucial component in the system responsible for transforming foreign substances [117].

The role of vitamin A in the biotransformation of xenobiotics has been under study in recent years due to interesting reports on the anticarcinogenic properties of retinol and carotenes, specifically their effect on chemically induced tumors. It has been found that there is a strong correlation between the concentration of vitamin A and cytochrome P450 levels in the liver of rats fed with varying levels of vitamin A [125, 126].

Similar results were observed for vitamins B12 and B6 when their effect on the microsomal oxidation system was studied. These vitamins act as transmethylation coenzymes along with folic acid and methionine, which donate methyl groups, and affect the metabolism of xenobiotics. The deficiency of these three nutrients in the diet resulted in a significant reduction in cytochrome P450 concentration in the liver microsomes of experimental animals [117].

Tocopherol is undoubtedly also involved in the detoxification of foreign substances. During the biotransformation of drugs, toxic free-radical compounds can be formed, which require antioxidants, in particular vitamin E, to "extinguish" them. Studies have demonstrated the function of vitamin E in mitigating the harmful impact of the foreign toxic substance heptachlor on liver microsomes. It has been established that the metabolization of this poison in liver microsomes is accompanied by the active formation of free radical products, which are the main cell-damaging factor. At the same time, the leading role in the activation of LPO is played by microsomal enzymes – cytochromes P450 and P448. Vitamin E has been found to have a significant positive effect by reducing the intensity of lipid peroxidation and activating antioxidant defense mechanisms in cases of liver damage caused by chemical agents. This leads to the preservation of cell membrane structure and function [127].

Thereby vitamins and minerals needed to support detoxification processes include vitamins A, B2, B3, B5, B6, folic acid (B9), B12, C, and E, iron, calcium, copper, zinc, magnesium, and selenium. It was established that vitamins C and E, sodium selenite protect erythrocytes from disruption by action of 1,1-dimetylhydrazine *in vitro* and *in vivo*. The protective effect of these biologically active compounds is more pronounced when combined [128, 129].

It is known that a small number of ions of such metals as cobalt, lead, cadmium, copper, has a catalytic effect on the oxidative destruction of many vitamins. Metals can affect the activity of retinol, riboflavin, pantothenic acid, ascorbic acid, cholecalciferol, and ergocalciferol. It has been established that during the absorption process in the intestine, many mineral substances compete with each other, such as calcium with iron, copper, magnesium, and lead; copper with zinc, calcium, and magnesium; and iron with calcium, lead, cadmium, and zinc. Cadmium acts as an antagonist to almost all macro- and microelements. Zinc, copper, selenium, and calcium can prevent the absorption of cadmium [130].

Regular bowel movements are essential for their complete removal. Consuming an adequate amount of dietary fiber is crucial for regular bowel movements and the removal of biologically transformed toxins from the body. It helps by binding certain toxins, providing an excretory route. Plant foods are the main source of dietary fiber and various vitamins in the human body. Unlike other nutrients, dietary fiber is not a source of energy. Once consumed, they undergo partial breakdown by microorganisms in the large intestine. The breakdown of cellulose is around 30-40%, while hemicellulose and pectin substances break down by 60-84% and 35%, respectively. The energy released during this process is mostly utilized by intestinal bacteria for their own metabolic processes. The majority of monosaccharides that result from the breakdown of dietary fiber are transformed into volatile fatty acids such as acetic, propionic, and butyric acid, as well as gases such as methane and hydrogen that are essential for regulating the functioning of the large intestine. These substances can be partially absorbed through the intestinal walls, but only about 1% of the nutrients formed during the breakdown of dietary fiber enter the human body [131].

The presence of insoluble dietary fiber in food products can speed up the elimination of different foreign substances from the body. These substances may include carcinogens, endotoxins, exotoxins, and incompletely digested nutrient products. Ballast substances possess a fibrous-capillary structure that makes them effective natural enterosorbents. This structure enables dietary fibers to absorb or dissolve toxins, which decreases the likelihood of toxins coming into contact with the intestinal mucosa. As a result, there is a reduction in the severity of the intoxication syndrome and inflammatory-dystrophic changes in the mucous membrane [132].

The presence of dietary fiber in food products can lower the levels of free ammonia and other carcinogens that are generated during putrefaction, fermentation, or are present in the food. As plant fibers are not absorbed in the intestines, they are promptly eliminated from the body through feces, along with the compounds they have absorbed. Moreover, dietary fibers possess ion-exchange properties that allow them to eliminate HM ions like lead and strontium from the body. In addition, dietary fibers impact the electrolyte metabolism in the body and the electrolyte composition of feces. As a natural product, dietary fibers demonstrate anti-inflammatory activity [133].

Dietary fiber is the substrate on which bacteria of the intestinal microflora develop, and pectins are also nutrients for these bacteria. The regular microbial population in the intestines comprises numerous bacterial species, amounting to several hundred. Beneficial intestinal bacteria rely on dietary fiber to carry out their essential functions. Consequently, the number of bacteria required by the body increases, which has a positive effect on the formation of fecal matter. Additionally, these beneficial bacteria generate substances that are necessary for the human body, such as vitamins, amino acids, and specific fatty acids that are utilized by intestinal cells. Moreover, dietary fiber enhances the production of vitamins B1, B2, B6, PP, and folic acid by the intestinal bacteria [134]. Studies of the intensity level of lipid peroxidation processes in the cells of vital organs during intoxication with lead compounds have shown that the use of dietary fiber from rice husks can reduce the number of peroxide radicals, which is explained by the process of ion absorption [135]. The regular microbial population in the intestines acts as a metabolic organ that participates in the metabolism of both endogenous and exogenous compounds. This structure serves as the primary site for absorption and is responsible for the translocation of all agents. The fact of existence of a biofilm lining the mucous membranes and including numerous microcolonies of various bacteria is not denied [136, 137].

Soluble fibers have been found to be more effective in removing HMs, toxic substances, radioisotopes, and cholesterol from the body. Soluble dietary fibers, such as pectins, gums, alginates, etc., are often utilized in the food industry as processing aids to enhance the structure, taste, texture, and other characteristics of the final product. These fibers are also beneficial for therapeutic and preventive nutrition, as they satisfy two important principles: slowing down the absorption of harmful substances from the gastrointestinal tract and accelerating their removal from the body [138].

Carrageenans are sulfated polysaccharides from red seaweeds. Medical and biological tests have demonstrated that carrageenans aid in the removal of HMs, radioactive isotopes, and excess cholesterol from the body. They cannot be broken down by human gastrointestinal enzymes. Moreover, carrageenans, which are present in food products, play significant physiological roles as dietary fiber: they regulate the function of the gastrointestinal tract and have a beneficial impact on the intestinal bacterial habitat [139].

Clinical and biological tests have shown that alginates have the ability to absorb HMs and their radioisotopes without affecting calcium metabolism in the human body. Food products containing alginates exhibit similar characteristics. Alginates obtained through chemical hydrolysis with low and medium molecular weights have the ability to strongly and effectively bind lead and cadmium ions. The binding efficiency of alginates is dependent on their molecular weight, with low molecular weight calcium alginate exhibiting higher sorption capacity than high and medium molecular weight samples [140].

A significant amount of information has been gathered, suggesting that the gastrointestinal tract's microflora plays a crucial role in the detoxification of specific endogenous and exogenous substances [141]. It also regulates the absorption and excretion of elements such as Na, K, Ca, Mg, Zn, Fe, Cu, Mn, Mo, among others. The study of microorganisms present in probiotic formulations and their ability to absorb HM ions is an area of significant interest. Moreover, research conducted on livestock has demonstrated that the use of probiotic preparations resulted in a substantial reduction in the accumulation of toxic metals [142].

There is evidence that different strains of lactobacilli, propionic acid bacteria, and bifidobacteria can effectively absorb cadmium and lead ions on their surface. Lactobacillus plantarum culture, for instance, was demonstrated to dramatically lower the hazardous burden of cadmium in fish trials by lowering the degree of bioaccumulation, reestablishing intestinal microbiota, and boosting the body's antioxidant reserve. Similarly, studies on mice have demonstrated that the BT36 strain of *Pediococcus acidilactici* efficiently lowers oxidative stress and chromium compound buildup, minimizing liver tissue damage [143, 144]. Thus, the presence of probiotics and alimentary fibers in diet has a beneficial effect on the detoxification of harmful agents in the body.

Conclusion

Despite the extensive research conducted on HMs intoxication over the past few decades, several aspects still require the attention of researchers. One such area is the detoxification of HMs in the body and minimization of the consequences of acute or chronic poisoning. HMs have diverse mechanisms of toxicity, depending on their chemical properties and their affinity for components in the living cells. Some metals are essential for the normal functioning of cells in moderate amounts, but excess amounts can have a damaging effect. Most HMs tend to accumulate in the body tissues. In natural conditions, excess toxins are neutralized through various detoxification mechanisms, including binding, biotransformation, and excretion. These mechanisms involve the participation of different proteins, vitamins, vitamin-like substances, and sorption-active compounds that are present in food products. Despite the numerous studies that have evaluated the detoxification properties of individual components in food raw materials, these investigations remain relevant. The identification of the mechanisms by which dietary factors interact with toxic compounds can facilitate the creation of functional food products with enhanced detoxification capabilities. This review allows us to systematize some scattered data on the data on detoxifying characteristics of various food components and to define a field for future scientific research on the interaction of nutritional factors and xenobiotics, HMs in particular, in the body.

Conflict of interest

All authors are aware of the article's content and declare no conflict of interest.

References

1. Peña-Romero A.C., Navas-Carrillo D., Marín F., Orenes-Piñero E. (2018). The future of nutrition: Nutrigenomics and nutrigenetics in obesity and cardiovascular diseases. *Crit Rev Food Sci Nutr.,* 58(17), pp. 3030-3041. https://doi.org/10.1080/104083 98.2017.1349731.

2. Cline J.C. (2015). Nutritional aspects of detoxification in clinical practice. *Altern Ther Health Med.,* 21(3), pp. 54-62.

3. Li M., Zou L., Zhang L., Ren G., Liu Y., Zhao X., Qin P. (2024). Plant-based proteins: advances in their sources, digestive profiles in vitro and potential health benefits. *Crit Rev Food Sci Nutr*, pp. 1-21. https://doi.org/10.1080/10408398.2024.2315448.

4. Zinchuk V.V. (2014). Physiological foundations of nutrition [Fiziologicheskiye osnovy pitaniya]. *Journal of the Grodno State Medical University*, 3, pp. 140-143.

5. Santosa A., Wall S., Fottrell E., Högberg U., Byass P. (2014). The development and experience of epidemiological transition theory over four decades: a systematic review. *Global health action*, 7. https://doi.org/10.3402/gha.v7.23574.

6. Kunzul K., Dua N., Rameesha A., Rabia A., Momina A., et al. (2023). Nutritional deficiency disorders and supplements. Nutrition and dietetics in fundamental and practical concepts, USA: SciKnowPub, 50 p., ISBN 978-1-960740-14-4.

7. Li H., Ren H., Guo X., Chen Z. (2023). Nutritional deficiencies in low-sociodemographic-index countries: a population-based study. Front Nutr., 10. doi: 10.3389/fnut.2023.985221.

8. Parlee S.D., MacDougald O.A. (2014). Maternal nutrition and risk of obesity in offspring: the Trojan horse of developmental plasticity *Biochim Biophys Acta*., 1842(3), pp. 495-506. doi: 10.1016/j.bbadis.2013.07.007.

9. Gropper S.S. (2023). The role of nutrition in chronic disease. *Nutrients*, 15(3), doi: 10.3390/nu15030664

10. Chen Y., Michalak M., Agellon L.B. (2018). Importance of nutrients and nutrient metabolism on human health. *Yale J Biol Med.,* 91(2), pp. 95-103.

11. Salim R., Nehvi I.B., Mir R.A., Tyagi A., Ali S., Bhat O.M. (2023). A review on anti-nutritional factors: unraveling the natural gateways to human health. *Front. Nutr.* 10:1215873. doi: 10.3389/fnut.2023.1215873

12. Fuller R, Landrigan PJ, Balakrishnan K., et al (2022). Pollution and health: a progress update. *Lancet Planet Health no* 6, pp.535-547. doi: 10.1016/S2542-5196(22)00090-0

13. Kovacic P., Pozos R.S., Somanathan R., Shangari N., O'Brien P.J. (2005). Mechanism of mitochondrial uncouplers, inhibitors, and toxins: focus on electron transfer, free radicals, and structure-activity relationships. *Curr. Med. Chem.,* 12(22), pp. 2601-2623. https://doi.org/10.2174/092986705774370646

14. Your health and safety at work: chemicals in the workplace (1993), Geneve: ILO, 50p., ISBN 92-2-108006-4. https://training. itcilo.org/actrav_cdrom2/en/osh/kemi/ciwmain.htm

15. Rahman Z., Singh V.P. (2019). The relative impact of toxic heavy metals (THMs) (arsenic (As), cadmium (Cd), chromium (Cr)(VI), mercury (Hg), and lead (Pb) on the total environment: an overview. *Environ Monit Assess*., 19(7), pp. 419. doi: 10.1007/s10661-019-7528-7

16. Fu Z., Xi S. (2020). The effects of heavy metals on human metabolism. *Toxicol Mech Methods*., 30(3), pp. 167-176. doi: 10.1080/15376516.2019.1701594

17. Rebelo F.M., Caldas E.D. (2016). Arsenic, lead, mercury and cadmium: toxicity, levels in breast milk and the risks for breastfed infants. *Environ Res.*, 151. pp. 671-688. doi: 10.1016/j.envres.2016.08.027

18. Charkiewicz A.E., Backstrand J.R. (2020). Lead toxicity and pollution in Poland. *Int J Environ Res Public Health.,* Vol. 17, no 12, pp. 4385. doi: 10.3390/ijerph17124385

19. Murzahmetova M.K., Turmuhambetova V.K., Utegalieva. R.S. (2002) The effect of intoxication of rats with salts of heavy metals and pesticides on the condition of cell membranes [Vliyanie intoksikacii krys solyami tyazhelyh metallov i pesticidami na sostoyanie kletochnyh membrane] *Izvestiya MON RK, NAN RK. Ser.biol. i med*., 3, pp. 55-62.

20. Aralbaeva A.N., Mamataeva A.T., Utegalieva R.S., Murzahmetova M.K. (2019). Comparative study of the effect of heavy metals on the resistance of erythrocyte membranes *in vitro* [Sravnitel'noe izuchenie vliyaniya tyazhelyh metallov na rezistentnost' membran eritrocitov v usloviyah *in vitro*], *KazNU Bulletin, biology series* [*Vestnik KazNU (seriya biol.)*], 80(3), pp. 182-191. https://doi.org/10.26577/eb-2019-3-b16.

21. Genchi G., Sinicropi M. S., Lauria G., Carocci A, Catalano A. (2020). The effects of cadmium toxicity *Int. J. Environ. Res. Public Health*. 17(11), p. 3782. doi:10.3390/ijerph17113782.

22. Tan Q., Ma J., Zhou M., et al. (2020). Heavy metals exposure, lipid peroxidation and heart rate variability alteration: association and mediation analyses in urban adults. *Ecotoxicol Environ Saf.*, 205: 111149. doi: 10.1016/j.ecoenv.2020.111149.

23. Shafiq-ur-Rehman (2013). Effect of lead on lipid peroxidation, phospholipids composition, and methylation in erythrocyte of human. *Biol Trace Elem Res.*, 154(3), pp.433-439. doi: 10.1007/s12011-013-9745-1.

24. Renu K., Chakraborty R., Myakala H., et al. (2021). Molecular mechanism of heavy metals (lead, chromium, arsenic, mercury, nickel and cadmium) – induced hepatotoxicity – a review. *Chemosphere*, 271: 129735. doi: 10.1016/j.chemosphere.2021.129735

25. Chlubek M., Baranowska-Bosiacka I. (2024). Selected functions and disorders of mitochondrial metabolism under lead exposure. *Cells*, 13(14), pp. 1182. doi: 10.3390/cells13141182.

26. Zhang J., Su P., Xue C., Wang D., Zhao F., Shen X., Luo W. (2022) Lead disrupts mitochondrial morphology and function through induction of ER stress in model of neurotoxicity. *Int J Mol Sci.,* 23(19), pp. 11435. doi: 10.3390/ijms231911435

27. Bhattacharya S. (2022). Protective role of the essential trace elements in the obviation of cadmium toxicity: glimpses of mechanisms. *Biol Trace Elem Res.*, 200(5), pp. 2239-2246. doi: 10.1007/s12011-021-02827-7

28. Charkiewicz A.E., Omeljaniuk W.J., Nowak K., Garley M., Nikliński J. (2023) Cadmium toxicity and health effects – a brief summary. *Molecules*. 28(18), p. 6620. doi: 10.3390/molecules28186620.

29. Murzahmetova M.K., Turmuhambetova V.K., Utegalieva R.S. (2002) The effect of intoxication of rats with salts of heavy metals and pesticides on the condition of cell membranes [Vliyanie intoksikacii krys solyami tyazhelyh metallov i pesticidami na sostoyanie kletochnyh membran]. *NSA Bulletim, biology and medicine series* [*Izvestiya MON RK, NAN RK. Ser.biol. i med.*], 3, pp. 55-62.

30. Unsal V., Dalkıran T., Çiçek M., Kölükçü E. (2020). The role of natural antioxidants against reactive oxygen species produced by cadmium toxicity: a review. *Adv Pharm Bull.* 10(2), pp. 184-202. doi: 10.34172/apb.2020.023.

31. Rani A., Kumar A., Lal A., Pant M. Cellular mechanisms of cadmium-induced toxicity: a review (2022) *Int. J. Environ. Health Res.,* 24, pp. 378-399. doi: 10.1080/09603123.2013.835032.

32. Huff J., Lunn R. M., Waalkes M.P., Tomatis L., Infante P.F. (2007). cadmium-induced cancers in animals and in humans. *Int J Occup Environ Health.* 13(2), pp. 202–212. doi: 10.1179/oeh.2007.13.2.202

33. Luevano J., Damodaran C.A (2014) Review of molecular events of cadmium-induced carcinogenesis. *J Environ Pathol Toxicol Oncol.*, 33(3), pp. 183-194. doi: 10.1615/jenvironpatholtoxicoloncol.2014011075.

34. Peana M., Pelucelli A., Chasapis C.T., Perlepes S.P., Bekiari V., Medici S., Zoroddu M.A. (2023) Biological effects of human exposure to environmental cadmium. *Biomol.*, 13(1), pp. 36. doi: 10.3390/biom13010036.

35. Mezynska M., Brzóska M.M. (2018) Environmental exposure to cadmium-a risk for health of the general population in industrialized countries and preventive strategies. *Environ Sci Pollut Res Int.*, 25(4), pp. 3211-3232. doi: 10.1007/s11356-017-0827-z.

36. Geng H.X., Wang L. (2019) Cadmium: toxic effects on placental and embryonic development. *Environ Toxicol Pharmacol.*, 67, pp. 102-107. doi: 10.1016/j.etap.2019.02.006.

37. Zhang X., Wei H., Guan Q., Yang X., Yu Q., Zhang M., Xia Y. (2023) Maternal exposure to trace elements, toxic metals, and longitudinal changes in infancy anthropometry and growth trajectories: a prospective cohort study. *Environ Sci Technol.*, 57(32), pp. 11779-11791. doi: 10.1021/acs.est.3c02535

38. Priante E., Pietropoli E., Piva E., Santovito G., Schumann S., Irato P. (2022) Cadmium-zinc interaction in *Mus musculus* fibroblasts. *Int J Mol Sci.*, 23(19), pp. 12001. doi: 10.3390/ijms231912001.

39. Kontoghiorghes G.J. (2023). Iron load toxicity in medicine: from molecular and cellular aspects to clinical implications. *Int. J. Mol. Sci.*, 24(16), pp.12928. doi.org/10.3390/ijms241612928

40. Dangleben N.L., Skibola C. F., Smith M.T. (2013) Arsenic immunotoxicity: a review. *Environ Health*, 12(73), doi: 10.1186/1476-069X-12-73.

41. Chung J.Y., Yu S.D, Hong Y.S. (2014) Environmental source of arsenic exposure. *J Prev Med Public Health*, 47(5), pp. 253-257. doi: 10.3961/jpmph.14.036.

42. Banerjee S., Dhar S., Sudarshan M., Chakraborty A., Bhattacharjee S., Bhattacharjee P. (2023). Investigating the synergistic role of heavy metals in arsenic-induced skin lesions in West Bengal, India. *J Trace Elem Med Biol.,* 75, pp. 127103. doi.org/10.1016/j.jtemb.2022.127103.

43. Karak P. (2022) Arsenic contamination and its impact on the human. *Curr World Environ.*, 17(1), pp.58-73. http://dx.doi.org/10.12944/CWE.17.1.6.

44. Straub A.C., Stolz D.B., Vin H., et al. (2007) Low level arsenic promotes progressive inflammatory angiogenesis and liver blood vessel remodeling in mice. *Toxicol Appl Pharmacol.*, 222(3), pp. 327-336. doi: 10.1016/j.taap.2006.10.011.

45. Sadiku O.O., Rodríguez-Seijo A. (2022) Metabolic and genetic derangement: a review of mechanisms involved in arsenic and lead toxicity and genotoxicity. *Arh Hig Rada Toksikol.*, 73(4), pp. 244-255. doi: 10.2478/aiht-2022-73-3669.

46. Muzaffar S., Khan J., Srivastava R. (2023) Mechanistic understanding of the toxic effects of arsenic and warfare arsenicals on human health and environment. *Cell Biol Toxicol.,* 39, pp. 85-110. doi.org/10.1007/s10565-022-09710-8.

47. Speer R.M., Zhou X., Volk L.B., Liu K.J., Hudson L.G. (2023) Arsenic and cancer: evidence and mechanisms. *Adv Pharmacol.*, l(96), pp. 151-202. doi: 10.1016/bs.apha.2022.08.001.

48. Lin M.-H., Li C.-Y., Cheng Y.-Y., Guo H.-R. (2022) Arsenic in drinking water and incidences of leukemia and lymphoma: implication for its dual effects in carcinogenicity. Front. Public Health., 10: 863882. doi: 10.3389/fpubh.2022.863882Fu Z., Xi S. (2020). The effects of heavy metals on human metabolism. *Toxicol. Mech. Methods.,* 30(3), pp. 67-176. doi.org/10.1080/15376516.2 019.1701594.

49. Clarkson T.W., Magos L. (2006) The toxicology of mercury and its chemical compounds. *Crit Rev Toxicol.*, 36(8), pp.609-62. doi: 10.1080/10408440600845619.

50. van Veizen D, Langenkamp H, Herb G. (2002) Review: mercury in waste incineration. *Waste Manag Res.* 20(6), pp.556-68. doi: 10.1177/0734242X0202000610. PMID: 12549668.

51. Shin J., Kim B.M., Ha M., et al. (2019) The association between mercury exposure and atopic dermatitis in early childhood: a mothers and children's environmental health study. *Epidemiol.*, 30(1), pp.3-8. doi: 10.1097/EDE.0000000000001002

52. Bastiansz A., Ewald J., Rodríguez Saldaña V., Santa-Rios A., Basu N. (2022) A systematic review of mercury exposures from skin-lightening products. *Environ Health Perspect.,* 130(11), pp.116002. doi: 10.1289/EHP10808

53. Carocci A., Rovito N., Sinicropi M.S., Genchi G. (2014) Mercury toxicity and neurodegenerative effects. *Rev Environ Contam Toxicol.*, 229, pp. 1-18. doi: 10.1007/978-3-319-03777-6_1.

54. Jan A.T., Ali A., Haq Q. (2011) Glutathione as an antioxidant in inorganic mercury induced nephrotoxicity. *J Postgrad Med.,* 57, pp. 72-77. doi: 10.4103/0022-3859.74298.

55. Murzahmetova M.K., Turmuhambetova V.K., Utegalieva R.S., Mamataeva A.T. (2007) The effect of mercury on the processes of peroxidation in microsomes of various organs of rats [Vliyanie rtuti na processy perekisnogo okisleniya v mikrosomah razlichnyh organov krys] *Vestnik KazNU. Seriya biol.*, 34(4), pp. 206-208.

56. Azeh E.G., Udoka F.P., Nweke N.F., Unachukwu N.M. (2019) Mechanism and health effects of heavy metal toxicity in humans. *IntechOpen*, doi: 10.5772/intechopen.82511.

57. Dutt S., Hamza I., Bartnikas T.B. (2022) Molecular mechanisms of iron and heme metabolism. *Annu Rev Nutr.*, 42, pp. 311-335. doi: 10.1146/annurev-nutr-062320-112625

58. Camaschella C., Nai A., Silvestri L. (2020) Iron metabolism and iron disorders revisited in the hepcidin era. *Haematol.*, 105(2), pp. 260-272. doi: 10.3324/haematol.2019.232124.

59. Leyssens L., Vinck B., Van Der Straeten C., Wuyts F., Maes L. (2017) Cobalt toxicity in humans-a review of the potential sources and systemic health. *Toxicol.*, 387, pp. 43-56. doi: 10.1016/j.tox.2017.05.015.

60. Alinaghi F., Havmose M., Thyssen J.P., Zachariae C., Johansen J.D. (2023) Contact allergy to metals in metalworkers: a systematic review and meta-analysis. *Contact Dermat.,* 88(1), pp. 1-9. doi: 10.1111/cod.14232.

61. Al-Abcha A., Wang L., Reilly M.J., Rosenman K.D. (2021) Work-related asthma in cobalt-exposed workers. *J Asthma*, 58(8), pp. 1032-1041. doi: 10.1080/02770903.2020.1759090

62. Al Alawi A.M., Majoni S.W., Falhammar H. (2018) Magnesium and human health: perspectives and research directions. *Int. J. Endocrinol.,* 9041694. doi: 10.1155/2018/9041694.

63. Aal-Hamad A.H, Al-Alawi A.M., Kashoub M.S., Falhammar H. (2023) hypermagnesemia in clinical practice. *Medicina (Kaunas)*, 59(7), pp.1190. doi: 10.3390/medicina59071190.

64. Baj J., Flieger W., Barbachowska A., Kowalska B., et al. (2023) Consequences of disturbing manganese homeostasis. *Int J Mol Sci.,* 24(19), pp.14959. doi: 10.3390/ijms241914959

65. Dorman D.C. (2023). The Role of Oxidative Stress in Manganese Neurotoxicity: A Literature Review Focused on Contributions Made by Professor Michael Aschner. *Biomolecules*, 13(8), pp. 1176. https://doi.org/10.3390/biom13081176

66. Smith M.R., Fernandes J., Go Y.M., Jones D.P. (2017) Redox dynamics of manganese as a mitochondrial life-death switch. *Biochem. Biophys. Res. Commun.,* 482(3), pp.388-398. doi: 10.1016/j.bbrc.2016.10.126.

67. Oe S., Miyagawa K., Honma Y., Harada M. (2016). Copper induces hepatocyte injury due to the endoplasmic reticulum stress in cultured cells and patients with Wilson disease. *Exp Cell Res.,* 347(1), pp. 192-200. doi: 10.1016/j.yexcr.2016.08.003.

68. Li Y., Liang J., Wang Y. (2023) The mechanism of copper homeostasis and its role in disease. *iLABMED,* 1(2), pp. 109-120. doi.org/10.1002/ila2.22.

69. Song X., Kenston S.S.F., Kong L., Zhao J. (2017) Molecular mechanisms of nickel induced neurotoxicity and chemoprevention. *Toxicol., 392, pp.* 47-54. doi: 10.1016/j.tox.2017.10.006.

70. Gombart A.F., Pierre A., Maggini S. (2020) A review of micronutrients and the immune system-working in harmony to reduce the risk of infection. *Nutrients*,12(1). doi: 10.3390/nu12010236.

71. Alinaghi F., Havmose M., Thyssen J.P., Zachariae C., Johansen J.D. (2023) Contact allergy to metals in metalworkers: a systematic review and meta-analysis. *Contact Dermatitis.*, 88(1), pp. 1-9. doi: 10.1111/cod.14232.

72. Mattos Pereira V, Nair S. (2024) Targeting Mitochondrial ATP-Synthase: Evolving Role of Chromium as a Regulator of Carbohydrate and Fat Metabolism. *Biol Trace Elem Res*. 202(4), pp.1318-1324. doi: 10.1007/s12011-023-04017-z.

73. Islam S., Kamila S., Chattopadhyay A. (2022) Toxic and carcinogenic effects of hexavalent chromium in mammalian cells *in vivo* and *in vitro*: a recent update. *J Environ Sci Health C Toxicol. Carcinog*., 40(3-4), pp. 282-315. doi: 10.1080/26896583.2022.2158675.

74. Alur A., Phillips J., Xu D. (2024) Effects of hexavalent chromium on mitochondria and their implications in carcinogenesis. *J Environ Sci Health C Toxicol Carcinog*., 42(2), pp. 109-125. doi: 10.1080/26896583.2024.2301899

75. den Braver-Sewradj S.P., van Benthem J., Staal Y.C.M., Ezendam J., Piersma A.H., Hessel E.V.S. (2021) Occupational exposure to hexavalent chromium. Part II. Hazard assessment of carcinogenic effects. *Regul Toxicol Pharmacol*., 126, pp. 105045. doi: 10.1016/j.yrtph.2021.105045.

76. Krawic C., Zhitkovich A. (2023) Chemical mechanisms of DNA damage by carcinogenic chromium(VI). *Adv Pharmacol*., 96, pp. 25-46. doi: 10.1016/bs.apha.2022.07.003.).

77. Rahimzadeh M.R., Rahimzadeh M.R., Kazemi S., Moghadamnia A.A. (2020) Zinc poisoning – symptoms, causes, treatments. *Mini Rev Med Chem.*, 20(15), pp. 1489-1498. doi: 10.2174/1389557520666200414161944

78. Fosmire G.J. (1990). Zinc toxicity. *Am J Clin Nutr.,* 51(2), pp. 225-227. doi.org/10.1093/ajcn/51.2.225.

79. Balali-Mood M., Naseri K., Tahergorabi Z., Khazdair M.R., Sadeghi M. (2021) Toxic mechanisms of five heavy metals: mercury, lead, chromium, cadmium, and arsenic. *Front Pharmacol.,* 12: 643972. doi: 10.3389/fphar.2021.643972.

80. Plum L.M., Rink L., Haase H. (2010) The essential toxin: impact of zinc on human health. *Int J Environ Res Public Health*., 7(4), pp. 1342-1365. doi: 10.3390/ijerph7041342.

81. Hussain S., Khan M., Sheikh T.M.M., et al. (2022) Zinc essentiality, toxicity, and its bacterial bioremediation: a comprehensive insight. *Front Microbiol.*, 13, doi: 10.3389/fmicb.2022.900740.

82. Gidlow DA. (2015) Lead toxicity. *Occup Med (Lond)*. 65(5), pp. 348-56. doi: 10.1093/occmed/kqv018.

83. Yang L., Zhang Y., Wang F., Luo Z., Guo S., Strähle U. (2020) Toxicity of mercury: Molecular evidence. *Chemosphere.* 245, pp.125586. doi: 10.1016/j.chemosphere.2019.125586.

84. Ratnaike R.N. (2003) Acute and chronic arsenic toxicity. *Postgrad Med J.* 79(933), pp. 391-396. doi: 10.1136/pmj.79.933.391.

85. Hossini H., Shafie B., Niri AD., et al. (2022) A comprehensive review on human health effects of chromium: insights on induced toxicity. *Environ Sci Pollut Res Int*. 29(47), pp.70686-70705. doi: 10.1007/s11356-022-22705-6.

86. Genchi G., Carocci A., Lauria G., Sinicropi M.S., Catalano A. (2020) Nickel: Human Health and Environmental Toxicology. *Int J Environ Res Public Health.* 17(3), pp. 679. doi: 10.3390/ijerph17030679.

87. Fine J.S. (2000) Iron poisoning. *Curr Probl Pediat*r.3, pp. 71-90. doi: 10.1067/mps.2000.104055..

88. Díaz Gómez C., López Amor L., García Prieto E., Escudero Augusto D. (2018) Magnesium poisoning, multi-organ failure and ischemic colitis secondary to chronic ingestion of a parapharmacy product. *Rev Esp Enferm Dig*. 110(6), pp. 404-406. doi: 10.17235/reed.2018.5355/2017. PMID: 29667416.

89. Kahlson M.A., Dixon S.J. (2022) Copper-induced cell death. *Science*, 375(6586), pp.1231-1232. doi: 10.1126/science.abo3959.

90. Hadrup N., Ravn-Haren G. Acute human toxicity and mortality after selenium ingestion: A review. *J Trace Elem Med Biol*. 2020, 58, pp.126435. doi: 10.1016/j.jtemb.2019.126435.

91. Perrelli M., Wu R., Liu D.J., et al. (2022) Heavy metals as risk factors for human diseases – a Bayesian network approach. *Eur Rev Med Pharmacol Sci*., 26(24), pp. 9275-9310. doi: 10.26355/eurrev_202212_30681

92. Mitra S., Chakraborty A.J., Tareq A.M., Emran T.B., Nainu F., Khusro A., et al. (2022) Impact of heavy metals on the environment and human health: Novel therapeutic insights to counter the toxicity, *Journal of King Saud University – Science*, 34(3), 101865, https://doi.org/10.1016/j.jksus.2022.101865.

93. Ashaolu J.T., Lee C.C., Opeolu A.J., Pourjafar H., Jafari S.M. (2023) Metal-binding peptides and their potential to enhance the absorption and bioavailability of minerals. *Food Chem*., 428, pp. 136678. doi: 10.1016/j.foodchem.2023.136678.

94. Solenkova N., Newman J.,Berger J., Hochman J.,Lamas G. (2014). Metal pollutants and cardiovascular disease: Mechanisms and consequences of exposure: Progress in Cardiology. *American Heart Journal*. 168(6), pp.812-822. doi: 10.1016/j.ahj.2014.07.007.

95. Briffa J., Sinagra E., Blundell R. (2020) Heavy metal pollution in the environment and their toxicological effects on humans. *Heliyon*, 6(9). doi: 10.1016/j.heliyon.2020.e04691

96. Rehman K., Fatima F., Waheed I., Akash M.S.H. (2018) Prevalence of exposure of heavy metals and their impact on health consequences. *J. Cell. Biochem.*, 119(1), pp. 157-184. https://doi.org/10.1002/jcb.26234.

97. Jan A.T., Azam M., Siddiqui K., Ali A., Choi I., Haq Q.M. (2015) Heavy metals and human health: mechanistic insight into toxicity and counter defense system of antioxidants. *Int J Mol Sci*., 16(12), pp. 29592-29630. doi: 10.3390/ijms161226183.

98. Chen Q.Y., DesMarais T., Costa M. (2019) Metals and mechanisms of carcinogenesis. *Annu Rev Pharmacol Toxicol*., 59, pp. 537-554. doi: 10.1146/annurev-pharmtox-010818-021031

99. Chafin, Braxton A. (2022) "The mutagenic and cytotoxic effects of exposure to heavy metals and other oxidative species from e-cigarettes on epithelial cells". Honors theses, 931. https://encompass.eku.edu/honors_theses/931

100. Kocadal K., Alkas F., Battal D., Saygi S..(2020) Cellular pathologies and genotoxic effects arising secondary to heavy metal exposure: A review. *Human & Experimental Toxicology*. 39(1), pp.3-13. doi:10.1177/0960327119874439

101. Elmorsy E., Al-Ghafari A., Al Doghaither H., Ghulam J. (2021) Effects of environmental metals on mitochondrial bioenergetics of the CD-1 mice pancreatic beta-cells. *Toxicol In Vitro*, 70, pp.105015. doi: 10.1016/j.tiv.2020.105015.

102. Oves M., Saghir M., Huda Q. (2016). Heavy Metals: Biological Importance and Detoxification Strategies. *Journal of Bioremediation & Biodegradation*, 7(2). DOI:10.4172/2155-6199.1000334

103. Witkowska D., Słowik J., Chilicka K. (2021) Heavy metals and human health: possible exposure pathways and the competition for protein binding sites. *Molecules*, 26(19). doi: 10.3390/molecules26196060.

104. van Vugt-Lussenburg B.M.A., Capinha L., Reinen J. et al/ (2022). "Commandeuring" xenobiotic metabolism: advances in understanding xenobiotic metabolism. *Chem. Res. Toxicol.*, 35(7), pp. 1184-1201. https://doi.org/10.1021/acs.chemrestox.2c00067.

105. Liska D., Lyon M., Jones D.S. (2006). Detoxification and biotransformational imbalances. *Explore (New York, N.Y.)*, 2(2), pp. 122-140. https://doi.org/10.1016/j.explore.2005.12.009.

106. Paul S., Ghosh U., Saha M. (2023). Transport and metabolism of xenobiotics in the urban ecosystem. In: Xenobiotics in urban ecosystems. Eds. Singh R., Singh P., Tripathi S., Chandra K.K., Bhadouria R. *Springer Nature*, pp 69-85. https://doi.org/10.1007/978-3-031-35775-6_4

107. Kostyuk S. Xenobiotics biotransformation system: detoxification genes [Sistema biotransformacii ksenobiotikov: geny detoksikacii] (2020). *Medical News* [Medicinskie novosti.] 11(314). URL: https://cyberleninka.ru/article/n/sistema-biotransformatsii-ksenobiotikov-geny-detoksikatsii/

108. Arana M., Arias A, Villanueva S, Mottino A. (2014) Hepatic and intestinal biotransformation and transport of xenobiotics during pregnancy and lactation. *Physiological Mini Reviews*, 7(2), pp. 14-27. DOI: 10.5772/64755.

109. Chhabra R.S. (1979) Intestinal absorption and metabolism of xenobiotics. *Environ Health Perspect.*, 33, pp. 61-69. doi: 10.1289/ehp.793361.

110. Zhao M., Ma J., Li M., et al. (2021) Cytochrome P450 Enzymes and Drug Metabolism in Humans. *Int J Mol Sci.*, 22(23), pp.12808. doi: 10.3390/ijms222312808.

111. Collins S.L., Patterson A.D. (2020) The gut microbiome: an orchestrator of xenobiotic metabolism. *Acta Pharm Sin B.*, 10(1), pp.19-32. doi: 10.1016/j.apsb.2019.12.001.

112. Saghir S.A., Ansari R.A, Munir S.T. (2024) Fate of chemicals following exposure III: Metabolism (biotransformation) in Encyclopedia of Toxicology, Editor(s): Philip Wexler, Fourth Edition, Academic Press, pp. 635-668, https://doi.org/10.1016/B978-0-12-824315-2.00050-6.

113. Rembovsky V.R., Mogilenkova L.A. (2015). The natural processes of detoxification of chemicals, pollutants of human habitat [Yestestvennyye protsessy detoksikatsii khimicheskikh veshchestv, zagryazniteley sredy obitaniya cheloveka]. *Russ. biomed j.[Rossiyskiy biomedicinskiy zhurnal]*, 16(1), pp. 216-239.

114. Järvinen E., Deng F., Kiander W., Sinokki A., Kidron H., Sjöstedt N. (2022) The Role of Uptake and Efflux Transporters in the Disposition of Glucuronide and Sulfate Conjugates. *Front Pharmacol.*, 12, pp. 802539. doi: 10.3389/fphar.2021.802539.

115. Flanagan R., Cuypers E., Hans M., Whelpton R. (2020). absorption, distribution, metabolism, and excretion of xenobiotics. In fundamentals of analytical toxicology: clinical and forensic, Eds. Flanagan R., Cuypers E., Hans M., Whelpton R. pp.345-378 John Wiley & Sons, Ltd, 9781119122340, 10.1002/9781119122357.ch15

116. Hodges R.E., Minich D.M. (2015) Modulation of Metabolic Detoxification Pathways Using Foods and Food-Derived Components: A Scientific Review with Clinical Application. *J Nutr Metab.,* 2015:760689. doi: 10.1155/2015/760689.

117. Georgiou-Siafis S.K., Tsiftsoglou A.S. (2023) The Key Role of GSH in Keeping the Redox Balance in Mammalian Cells: Mechanisms and Significance of GSH in Detoxification via Formation of Conjugates. *Antioxidants (Basel).*, 12(11), pp. 1953. doi: 10.3390/antiox12111953.

118. Mannervik B. (2023) Versatility of glutathione transferase proteins. *Biomolecules.* 6(13), doi: 10.3390/biom13121749.

119. Miroshina T.N., Murzahmetova M.K., Utegalieva R.S., Shajhynbekova R.M., Mihalkina N.I. (2002) Corrective effect of indolamines on the state of erythrocyte membranes under the influence of cadmium ions [Korrigiruyushchee vliyanie indolaminov na sostoyanie membran eritrocitov pri dejstvii ionov kadmiya]. *KazNU Bulletin, Biology series* [*Vestnik KazNU. Seriya biol.]*, 3, pp. 80-86.

120. Pavić M., Turčić P., Ljubojević M. (2019) Forgotten partners and function regulators of inducible metallothioneins. *Arh Hig Rada Toksikol.* 70(4), pp.256-264. doi: 10.2478/aiht-2019-70-3317.

121. Babula P., Masarik M., Adam V., et al (2012) Mammalian metallothioneins: properties and functions. *Metallomics,* 4(8), pp. 739-50. doi: 10.1039/c2mt20081c.

122. Scheinfeld N., Dahdah M.J., Scher R. (2007) Vitamins and minerals: their role in nail health and disease. *J Drugs Dermatol.* 6(8), pp. 782-787.

123. Sitek A., Kozłowska L. (2022) The role of well-known antioxidant vitamins in the prevention of cadmium-induced toxicity. *Int J Occup Med Environ Health,* 35(4), pp. 367-392. doi: 10.13075/ijomeh.1896.01912.

124. Wang K., Chen S., Xie W., Wan Y.J.Y. (2008) Retinoids induce cytochrome P450 3A4 through RXR/VDR-mediated pathway. *Biochemical Pharmacology,* 75(11), pp. 2204-2213. doi.org/10.1016/j.bcp.2008.02.030.

125. Shmarakov I.O. (2015) Retinoid-xenobiotic interactions: the Ying and the Yang. *Hepatobiliary Surgery and Nutrition*, 4(4), pp.243-267. https://hbsn.amegroups.org/article/view/6877

126. Murzakhmetova M.K. (1999) The mechanism of stabilization of sarcoplasmic reticulum membranes by α-tocopherol under the damaging effects of free fatty acids [Mekhanizm stabilizacii membran sarkoplazmaticheskogo retikuluma α-tokoferolom pri povrezhdayushchem dejstvii svobodnyh zhirnyh kislot]. *Bulletin of NSA, Boil. and Med. Line* [*Izvestiya MON RK, NAN RK. Ser. biol. i med.*], 2, pp. 64-75.

127. Peraza M.A., Ayala-Fierro F., Barber D.S., et al (1998). Effects of micronutrients on metal toxicity. *Environmental Health Perspectives, 106*, pp. 203 – 216.

128. Moldakarimov S.B., Miroshina T. (2006) Influence of vitamin C on state of human erythrocyte membrane. *Proceedings of the 31 FEBS Congress «Molecules in Health & Disease»,* Turkey, p. 13.

129. Hyman M., Bradley E. (2022). Food, medicine, and function: food is medicine. *Phys Med Rehabil Clin N Am.*, 33(3), pp. 571-586. doi.org/10.1016/j.pmr.2022.04.002.

130. Pérez-Jiménez J. (2024) Dietary fiber: Still alive. *Food Chem.* 439, pp. 138076. doi: 10.1016/j.foodchem.2023.138076.

131. Snauwaert E., Paglialonga F., Vande Walle J., et al. (2023) The benefits of dietary fiber: the gastrointestinal tract and beyond. *Pediatr Nephrol.*, 38(9), pp.2929-2938. doi: 10.1007/s00467-022-05837-2.

132. Yao M., Shao X., Wei Y., Zhang X., Wang H., Xu F. (2022). Dietary fiber ameliorates lead-induced gut microbiota disturbance and alleviates neuroinflammation. *J. Sci. Food Agric.,* 102(15), pp. 6795-6803. doi.org/10.1002/jsfa.12074).

133. Gill S.K., Rossi M., Bajka B., Whelan, K. (2021). Dietary fibre in gastrointestinal health and disease. *Nat. Rev. Gastroenterol. Hepatol.,* 18(2), pp. 101-116. doi.org/10.1038/s41575-020-00375-4.

134. Sinyavskij Y.A., Aralbaeva A.N., Tugunov D.N., Deripaskina E.A., Kucherbaeva M.M, Murzahmetova M.K. (2020) Assessment of the detoxification potential of sorbents based on rice husk [Ocenka detoksikacionnogo potenciala sorbentov na osnove risovoj sheluh]. *Exp. Biol.[Experimentalnaya biologia],* 4, pp. 116-127.

135. Rowland I., Gibson G., Heinken A., et al. (2018). Gut microbiota functions: metabolism of nutrients and other food components. *Eur. J. Nutr.,* 57(1), pp. 1-24. https://doi.org/10.1007/s00394-017-1445-8.

136. Monachese M., Burton J.P., Reid G. (2012). Bioremediation and tolerance of humans to heavy metals through microbial processes: a potential role for probiotics? *Appl. Environ. Microbiol.*, 78(18), pp. 6397-6404. doi.org/10.1128/AEM.01665-12.

137. Jandosov J., Alavijeh M., Sultakhan S., et al. (2022). Activated carbon/pectin composite enterosorbent for human protection from intoxication with xenobiotics Pb(II) and sodium diclofenac. *Molecules*, 27(7), pp.2296. doi.org/10.3390/molecules27072296

138. Pradhan B., Ki J.S. (2023) Biological activity of algal derived carrageenan: A comprehensive review in light of human health and disease. *Int J Biol Macromol.* 31(238), pp.124085. doi: 10.1016/j.ijbiomac.2023.124085.

139. Kondrashina V.V. (2017). Dietary fibers and their role in shaping human health [Pishchevye volokna ih rol□ v formirovanii zdorov□ya cheloveka]. *Mod. Sci. Res. Innov. [Sovremennye nauchnуe issledovatiф и innovacii],* 5, https://web.snauka.ru/issues/2017/05/82426

140. Zafar H., Saier M.H. Jr. (2021) Gut *Bacteroides* species in health and disease. *Gut Microbes,* 13(1), pp.1-20. doi: 10.1080/19490976.2020.1848158.

141. Baralić K., Živančević K., Bozic D., Đukić-Ćosić D. (2023) Probiotic cultures as a potential protective strategy against the toxicity of environmentally relevant chemicals: State-of-the-art knowledge. *Food Chem Toxicol.* 172, pp.113582. doi: 10.1016/j.fct.2022.113582.

142. Shang X., Xu W., Zhao Z., et al. (2022) Effects of exposure to cadmium (Cd) and selenium-enriched Lactobacillus plantarum in Luciobarbus capito: Bioaccumulation, antioxidant responses and intestinal microflora. *Comp Biochem Physiol C Toxicol Pharmacol.* 257, pp.109352. doi: 10.1016/j.cbpc.2022.109352.

143. Feng P., Ye Z., Han H., et al. (2020) Tibet plateau probiotic mitigates chromate toxicity in mice by alleviating oxidative stress in gut microbiota. *Commun Biol.* 3(1), pp. 242. doi: 10.1038/s42003-020-0968-3.

Information about authors:

Aralbaeva Arailym – (corresponding author) – candidate of biological sciences, Associate Professor, Department of Fundamental Medicine, Al-Farabi Kazakh National University, Almaty, Kazakhstan, e-mail: a_aralbaeva83@bk.ru

Yeszhanova Gaukhar – MS in biology, Department of Fundamental Medicine, Al-Farabi Kazakh National University, Almaty, Kazakhstan, e-mail: gauhar_eszhanova@mail.ru

Aralbayev Altai – MS in ecology, Department of Ecology, Seifullin Kazakh Agro-Technical Research University, Astana, Kazakhstan, e-mail: altai_an@mail.ru

Zhamanbayeva Gulzhan – candidate of biological sciences, Assistant Professor, Department of Biophysics, Biomedicine and Neurosciences, Al-Farabi Kazakh National University, Almaty, Kazakhstan, e-mail: gulzhan.zhamanbayeva@gmail.com

Zhaparkulova Nazgul – candidate of biological sciences, Associate Professor, Department of Biophysics, Biomedicine and Neurosciences, Al-Farabi Kazakh National University, Almaty, Kazakhstan, e-mail: jni777@mail.ru

Zhussupova Aizhan – PhD, Associate Professor, Department of Molecular Biology and Genetics, Al-Farabi Kazakh National University, Almaty, Kazakhstan, e-mail: aizhan.zhusupova@gmail.com

Murzakhmetova Maira – doctor of biological sciences, Professor, Department of Biophysics, Biomedicine and Neurosciences, Al-Farabi Kazakh National University, Almaty, Kazakhstan, e-mail: mairamur@mail.ru

F. Islamoğlu

Recep Tayyip Erdoğan University, Rize, Turkey
e-mail: fatih.islamoglu@erdogan.edu.tr

Theoretical determination of the biological activities of some benzimidazole derivative compounds with potential as active pharmaceutical agents

Abstract. The biological activities of twelve different benzimidazole derivative compounds synthesized and registered in the literature were theoretically calculated with Way2Drug PASS software. Seven different biological activities, including acute rat toxicity, adverse drug effects, antibacterial activity, antifungal activity, anti-HIV activity, antiviral activity, and cell line cytotoxicity, were calculated for each benzimidazole derivative compound examined here. Rat acute toxicity was calculated in four different ways. These are Rat IP (intraperitoneal administration route) LD_{50}, Rat IV (intravenous administration route) LD_{50}, Rat Oral (oral administration route) LD_{50}, and Rat SC (subcutaneous administration route) LD_{50}. According to the results, a classification was also made for each method. Adverse effects that the molecules may show were determined with the help of the calculated Pa (probability of activity) and Pi (probability of inactivity) values. The antibacterial effect of each molecule against which bacteria was determined, and the confidence value of this effect was calculated. Likewise, it was determined whether the molecules showed antifungal properties. It was determined against which fungus the molecules showing antifungal properties showed this effect, and the confidence value was calculated. The anti-HIV properties of the molecules were studied for five different targets (protease (HIV-1), reverse transcriptase (HIV-1), integrase (HIV-1), REV (regulator of virion) (HIV-1), and TAT (trans-activator of transcription) (HIV-1)) and the p function of the IC_{50} (half maximal inhibitory concentration) values obtained were analyzed. Antiviral effects of molecules examined. Here, the viruses against which they show this effect were determined, and the confidence value was calculated together with the target protein. Finally, cancer cell line and non-tumor cell line properties of the molecules were determined by Pa and Pi values as well as tissue and tumor type.

Key words: biological activities, benzimidazole derivatives, antibacterial, antifungal, anti-HIV, antiviral activity.

Introduction

A family of chemical compounds called benzimidazole derivatives is made up of molecules that have fused benzene and imidazole rings to form a benzimidazole moiety. These substances have been thoroughly researched and used in a variety of sectors, such as material science, medical chemistry, and agriculture, due to the wide range of biological activities [1]. Benzimidazole derivatives are known to have various biological activities. Many benzimidazole derivatives exhibit potent antibacterial and antifungal activities. They can inhibit the growth of a wide variety of pathogens by interfering with vital cellular processes [2]. Some benzimidazole derivatives are effective against parasites. For example, albendazole and mebendazole are used to treat parasitic worm infections by inhibiting

microtubule synthesis [3]. Some derivatives exhibit antiviral properties, including activity against HIV and hepatitis viruses. They may inhibit viral replication by targeting viral enzymes or proteins [4]. Benzimidazole derivatives have shown potential as anticancer agents. They can induce apoptosis in cancer cells, inhibit cell proliferation, and disrupt cancer cell signaling pathways [5]. Some derivatives have been found to have anti-inflammatory and analgesic properties, making them potential candidates for the treatment of inflammatory diseases and pain management [6]. Benzimidazole derivatives are used in various therapeutic applications [7]. Drugs such as albendazole, mebendazole, and thiabendazole are used to treat helminth infections by inhibiting tubulin polymerization in the parasites [8]. Compounds such as omeprazole, lansoprazole, and pantoprazole are benzimidazole derivatives used

to treat gastroesophageal reflux disease (GERD) by inhibiting the gastric H^+/K^+ ATPase enzyme [9]. Various benzimidazole derivatives are being investigated as potential anticancer agents due to their ability to inhibit cell proliferation and induce apoptosis in cancer cells [10]. Some derivatives are used as antifungal agents in agriculture and medicine to control fungal infections [11]. Continuous research is being conducted to develop new benzimidazole derivatives with increased efficacy, reduced toxicity, and a broader spectrum of activity [12]. The studies aim to understand the molecular mechanisms by which benzimidazole derivatives exert their biological effects, which may aid in the design of more potent and selective compounds. The biological actions of benzoimidazole derivatives are diverse and include antibacterial, antiparasitic, antiviral, anticancer, anti-inflammatory, and analgesic properties. They continue to be the subject of study for the creation of novel medications and treatments. They are utilized in a variety of therapeutic applications, including anthelmintics and proton pump inhibitors [13-15].

Way2Drug PASS is a powerful computational tool for predicting the biological activity spectra of chemical compounds. Based on the structural formula of compounds, it provides predictions of therapeutic effects, modes of action, toxicities, and other features by utilizing a large database of known activities [16]. PASS facilitates the early stages of drug development by directing the validation of experiments and identifying promising activities. Notwithstanding its drawbacks, PASS is an invaluable tool for scientists studying chemical biology, pharmaceutical development, and related subjects [17].

Studied molecules. In this study, twelve different benzimidazole derivatives synthesized and registered [18] in the literature were studied. These benzimidazole derivatives are 1,3-Bis((5-(ethylamino)-1,3,4-thiadiazol-2-yl) methyl)-1,3-dihydro-2H-benzimidazol-2-one (1), 1,3-Bis((5-(phenylamino)-1,3,4-thiadiazol-2-yl) methyl)-1,3-dihydro-2H-benzimidazol-2-one (2), 1,3-Bis((5-((4-nitro phenyl) amino)-1,3,4-thiadiazol-2-yl)methyl)-1,3-dihydro-2H-benzimidazol-2-one (3), 1,3-Bis((5-((4-fluoro phenyl) amino)-1,3,4-thiadiazol-2-yl)methyl)-1,3-dihydro-2H-benzimidazol-2-one (4), 1,3-Bis((5-(ethylamino)-1,3,4-thiadiazol-2-yl)methyl)-5-methyl-1,3-dihydro-2H-benzimidazol-2-one (5), 5-methyl-1,3-bis((5-(phenylamino)-1,3,4-thiadiazol-2-yl)methyl)-1,3-dihydro-2H-benzimidazol-2-one (6), 5-methyl-1,3-bis((5-((4-nitrophenyl) amino)-1,3,4-thia diazol-2-yl)methyl)-1,3-dihydro-

2H-benzimidazol-2-one (7), 1,3-Bis((5-((4-fluorophenyl)amino)-1,3,4-thiadiazol-2-yl) methyl)-5-methyl-1,3-dihydro-2H-benzimidazol-2-one (8), 1,3 -Bis((5-(ethylamino)-1,3,4-thiadiazol -2-yl) methyl)-5-nitro-1,3-dihydro-2H-benzimidazol-2-one (9), 5-nitro-1,3-bis((5-(phenylamino)-1, 3,4-thiadiazol-2-yl)methyl)-1,3-dihydro-2H-benzimidazol-2-one (10), 5-nitro-1,3-bis((5-((4-nitro phenyl)amino)-1,3,4-thiadiazol-2-yl) methyl)-1,3-dihydro-2H-benzimidazol-2-one (11), and 1,3-Bis ((5-((4-fluorophenyl)amino)-1,3,4-thiadiazol-2-yl) methyl)-5-nitro-1,3-dihydro-2H-benzimidazol-2-one (12) The open structures of these molecules are given in Figure 1.
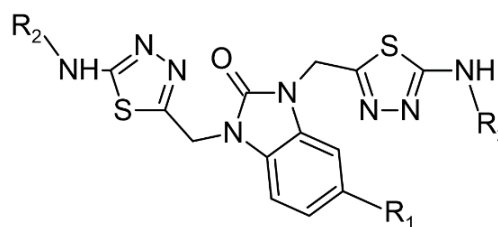
Mol.	R_1	R_2	Mol.	R_1	R_2
1	-H	$-C_2H_5$	7	$-CH_3$	$-(4)NO_2-C_6H_4$
2	-H	$-C_6H_5$	8	$-CH_3$	$-(4)F-C_6H_4$
3	-H	$-(4)NO_2-C_6H_4$	9	$-NO_2$	$-C_2H_5$
4	-H	$-(4)F-C_6H_4$	10	$-NO_2$	$-C_6H_5$
5	$-CH_3$	$-C_2H_5$	11	$-NO_2$	$-(4)NO_2-C_6H_4$
6	$-CH_3$	$-C_6H_5$	12	$-NO_2$	$-(4)F-C_6H_4$

Figure 1 – Molecular formulas of studied benzimidazole derivatives

Determination of acute rat toxicity. The term "acute rat toxicity" describes the harmful consequences that occur in rats following a single or brief exposure to a chemical. Toxicology uses this kind of testing frequently to assess the possible health risks associated with chemicals, medications, and other substances. For humans and other animals, the outcomes of acute toxicity testing are utilized to establish safe dosage ranges [19,20]. There are numerous recorded instances of using the GUSAR online application to forecast acute rat toxicity [21-23]. We calculated acute rat toxicity for all molecules as four administration methods using Way2Drug PASS software. The methods we calculated here are Rat IP LD_{50} (intraperitoneal administration toxicity measure), Rat IV LD_{50} (intravenous administration toxicity measure), Rat Oral LD_{50} (oral administration toxicity measure), and Rat SC LD_{50} (subcutaneous

administration toxicity measure). Calculations for each method were made as LD_{50} log10 (mmol/kg), LD_{50} (mg/kg), and LD_{50} Classification, and the obtained data were tabulated in this form. The classification recorded in the literature [24] is given in Table 1, and the data obtained is provided in Table 2.

Table 1 – Oral toxicity, dermal toxicity, and inhalation toxicity (for gases, vapors, and dusts/mists) classification and values recorded in the literatüre [24]

Category	Oral Toxicity	Dermal Toxicity	Inhalation Toxicity (for gases, vapors, and dusts/mists)
1	$LD_{50} \leq 5$ mg/kg	$LD_{50} \leq 50$ mg/kg	Gases: ≤ 100 ppm Vapors: ≤ 0.5 mg/L Dusts/Mists: ≤ 0.05 mg/L
2	5 mg/kg $< LD_{50}$ ≤ 50 mg/kg	50 mg/kg $< LD_{50}$ ≤ 200 mg/kg	Gases: 100 ppm $< LC_{50} \leq 500$ ppm Vapors: 0.5 mg/L $< LC_{50} \leq 2$ mg/L Dusts/Mists: 0.05 mg/L $< LC_{50} \leq 0.5$ mg/L
3	50 mg/kg $< LD_{50}$ ≤ 300 mg/kg	200 mg/kg $< LD_{50}$ ≤ 1000 mg/kg	Gases: 500 ppm $< LC_{50} \leq 2500$ ppm Vapors: 2 mg/L $< LC_{50} \leq 10$ mg/L Dusts/Mists: 0.5 mg/L $< LC_{50} \leq 1$ mg/L
4	300 mg/kg $< LD_{50}$ ≤ 2000 mg/kg	1000 mg/kg $< LD_{50}$ ≤ 2000 mg/kg	Gases: 2500 ppm $< LC_{50} \leq 5000$ ppm Vapors: 10 mg/L $< LC_{50} \leq 20$ mg/L Dusts/Mists: 1 mg/L $< LC_{50} \leq 5$ mg/L
5	2000 mg/kg $< LD_{50}$ ≤ 5000 mg/kg	2000 mg/kg $< LD_{50}$ ≤ 5000 mg/kg	Gases: 5000 ppm $< LC_{50} \leq 20000$ ppm Vapors: 20 mg/L $< LC_{50} \leq 50$ mg/L Dusts/Mists: 5 mg/L $< LC_{50} \leq 10$ mg/L

Determination of adverse effect. The Way2Drug platform offers a tool called adverse effect that is intended to help predict the possible negative effects of chemical compounds. This tool provides information about potential toxicological and pharmacological side effects that a substance may show using cheminformatics techniques [25].

Adverse effect forecasts a broad spectrum of unfavorable outcomes that may result from coming into contact with a chemical substance. Numerous pharmacological and toxicological outcomes may be among these consequences [26]. The adverse effect values (Pa and Pi) calculated for all molecules and the side effect made by the adverse effect values are given in Table 3.

Determination of antibacterial activity. The term "antibacterial activity" describes a substance's capacity to either stop or eradicate bacterial growth. This quality is essential in many industries, including food safety, agriculture, and healthcare [27]. In microbiology, biochemistry, and medicine, antibacterial activity is a major field of study that focuses on the identification of novel antibacterial agents, comprehension of their modes of action, and development of strategies to counter antibiotic resistance [28]. The antibacterial properties of the molecules we studied against which bacteria and their confidence values (high confidence (> 0.7, there's a good chance the substance will have antibacterial properties. These substances are typically given priority for additional experimental investigation and advancement), medium confidence, (0.5-0.7, the chemical may have antibacterial activity, but more research is needed to confirm this claim), low confidence (<0.5, there is little chance that the substance will exhibit antibacterial activity. These kinds of chemicals are typically regarded as less important)) and MIC(µg/mL) values are given in Table 4.

Table 2 – Acute rat toxicity values and classification of molecules

Molecule	Rat Acute Toxicity											
	Rat IP LD$_{50}$ log10 (mmol/kg)	Rat IP LD$_{50}$ (mg/kg)	Rat IP LD$_{50}$ Classification	Rat IV LD$_{50}$ log10 (mmol/kg)	Rat IV LD$_{50}$ (mg/kg)	Rat IV LD$_{50}$ Classification	Rat Oral LD$_{50}$ log10 (mmol/kg)	Rat Oral LD$_{50}$ (mg/kg)	Rat Oral LD$_{50}$ Classification	Rat SC LD$_{50}$ log10 (mmol/kg)	Rat SC LD$_{50}$ (mg/kg)	Rat SC LD$_{50}$ Classification
1	0.341 out of AD	913.000 out of AD	Class 5 out of AD	-0.192 in AD	267.900 in AD	Class 4 in AD	0.665 in AD	1928.000 in AD	Class 4 in AD	0.533 in AD	1421.000 in AD	Class 5 in AD
2	-0.006 in AD	505.100 in AD	Class 5 in AD	-0.139 in AD	371.900 in AD	Class 5 in AD	0.538 in AD	1769.000 in AD	Class 4 in AD	0.542 in AD	1786.000 in AD	Class 5 in AD
3	0.573 out of AD	2255.000 out of AD	Non Toxic out of AD	-0.473 in AD	202.700 in AD	Class 4 in AD	0.484 in AD	1838.000 in AD	Class 4 in AD	0.548 out of AD	2130.000 out of AD	Class 5 out of AD
4	0.324 out of AD	1157.000 out of AD	Class 5 out of AD	-0.288 in AD	282.600 in AD	Class 4 in AD	0.701 in AD	2757.000 in AD	Class 5 in AD	0.520 out of AD	1819.000 out of AD	Class 5 out of AD
5	0.085 in AD	523.900 in AD	Class 5 in AD	-0.436 in AD	157.600 in AD	Class 4 in AD	0.699 in AD	2153.000 in AD	Class 5 in AD	0.563 out of AD	1574.000 out of AD	Class 5 out of AD
6	0.156 in AD	754.000 in AD	Class 5 in AD	-0.379 in AD	219.900 in AD	Class 4 in AD	0.613 out of AD	2159.000 out of AD	Class 5 out of AD	0.959 in AD	4788.000 in AD	Non Toxic in AD
7	0.174 in AD	921.000 in AD	Class 5 in AD	-0.481 in AD	203.800 in AD	Class 4 in AD	-0.160 out of AD	426.200 out of AD	Class 4 out of AD	0.419 out of AD	1617.000 out of AD	Class 5 out of AD
8	0.187 out of AD	865.800 out of AD	Class 5 out of AD	-0.483 in AD	185.000 in AD	Class 4 in AD	0.637 out of AD	2438.000 out of AD	Class 5 out of AD	0.425 out of AD	1497.000 out of AD	Class 5 out of AD
9	0.414 out of AD	1197.000 out of AD	Class 5 out of AD	-0.348 in AD	207.200 in AD	Class 4 in AD	0.625 in AD	1947.000 in AD	Class 4 in AD	0.422 out of AD	1219.000 out of AD	Class 5 out of AD
10	0.261 in AD	1016.000 in AD	Class 5 in AD	-0.464 in AD	191.400 in AD	Class 4 in AD	0.809 in AD	3592.000 in AD	Class 5 in AD	0.389 in AD	1365.000 in AD	Class 5 in AD
11	0.158 in AD	932.100 in AD	Class 5 in AD	-0.330 in AD	302.800 in AD	Class 5 in AD	0.493 in AD	2013.000 in AD	Class 5 in AD	0.074 in AD	767.800 in AD	Class 4 in AD
12	0.223 in AD	991.700 in AD	Class 5 in AD	-0.385 in AD	244.600 in AD	Class 4 in AD	-0.043 out of AD	537.400 out of AD	Class 4 out of AD	0.198 out of AD	937.500 out of AD	Class 4 out of AD

*: In AD (Inside Applicability Domain), Out of AD (Outside Applicability Domain)

Table 3 – Adverse effect properties realized by molecules

Molecule	Pa	Pi	Side Effect
1	-	-	-
2	0.273	0.187	Nephrotoxicity
3	0.419	0.245	Hepatotoxicity
4	0.410 0.357 0.324	0.252 0.110 0.266	Hepatotoxicity Nephrotoxicity Arrhythmia
5	-	-	-
6	-	-	-
7	0.403	0.257	Hepatotoxicity
8	0.394 0.306	0.263 0.150	Hepatotoxicity Nephrotoxicity
9	-	-	-
10	0.422	0.243	Hepatotoxicity
11	0.422	0.243	Hepatotoxicity
12	0.641	0.124	Hepatotoxicity

Table 4 – Antibacterial activity properties of molecules

Molecule	Name	Confidence	MIC(μg/mL)
1	Shigella sp.	0.2737	0.73073
1	Pseudomonas sp.	0.0280	7.14286
1	Providencia rettgeri	0.1150	1.73913
1	Morganella morganii	0.0069	28.98551
1	Haemophilus parainfluenzae	0.0280	7.14286
1	Citrobacter koseri	0.0280	7.14286
1	Acinetobacter calcoaceticus	0.1521	1.31492
2	Shigella sp.	0.2067	0.96759
3	Shigella sp.	0.0801	2.49688
3	Clostridium difficile	0.0655	3.05344
3	Bacillus cereus	0.0315	6.34921
3	Bacteroides stercoris	0.0010	200.00000
4	Shigella sp.	0.1973	1.01368
4	Bacillus sphaericus	0.0099	20.20202
4	Yersinia pseudotuberculosis	0.0087	22.98851
5	Shigella sp.	0.2288	0.87413
5	Acinetobacter calcoaceticus	0.1059	1.88857
5	Providencia rettgeri	0.0940	2.12766
5	Bacteroides stercoris	0.0441	4.53515
5	Citrobacter koseri	0.0133	15.03759
5	Haemophilus parainfluenzae	0.0133	15.03759
5	Pseudomonas sp.	0.0133	15.03759
6	Shigella sp.	0.1730	1.15607
6	Yersinia pseudotuberculosis	0.0062	32.25806

Continuation of the table

Molecule	Name	Confidence	MIC(μg/mL)
7	Bacteroides stercoris	0.1473	1.35777
	Shigella sp.	0.0590	3.38983
	Bacillus cereus	0.0384	5.20833
	Clostridium difficile	0.0198	10.10101
8	Shigella sp.	0.1696	1.17925
	Yersinia pseudotuberculosis	0.0345	5.79710
	Bacillus sphaericus	0.0246	8.13008
9	Bacteroides stercoris	0.1355	1.47601
	Shigella sp.	0.1327	1.50716
	Dialister invisus	0.0895	2.23464
	Providencia rettgeri	0.0812	2.46305
	Clostridium difficile	0.0717	2.78940
	Acinetobacter calcoaceticus	0.0250	8.00000
	Actinomyces meyeri	0.0070	28.57143
	Helicobacter pylori	0.0004	500.00000
	Citrobacter koseri	0.0001	2000.00000
	Haemophilus parainfluenzae	0.0001	2000.00000
	Pseudomonas sp.	0.0001	2000.00000
10	Shigella sp.	0.0516	3.87597
	Clostridium difficile	0.0457	4.37637
	Mycobacterium tuberculosis H37Rv	0.0441	4.53515
	Bacillus cereus	0.0038	52.63158
11	Shigella sp.	0.0496	4.03226
	Mycobacterium tuberculosis H37Rv	0.0469	4.26439
	Clostridium difficile	0.0427	4.68384
	Bacillus cereus	0.0048	41.66667
12	Mycobacterium tuberculosis H37Rv	0.0755	2.64901
	Shigella sp.	0.0608	3.28947
	Clostridium difficile	0.0453	4.41501
	Bacillus sphaericus	0.0403	4.96278

Determination of antifungal activity. Antifungal activity refers to the ability of a substance to inhibit the growth of or kill fungi. Treating fungal infections in people, animals, and plants requires this characteristic. Research on antifungal action is essential in the fields of pharmacy, agriculture, and medical mycology [29]. Research is still being done to find new antifungal medicines, comprehend how they work, and deal with the problem of antifungal resistance [30]. Antifungal activity is divided into four classes according to the MIC (μg/mL) value. These are; highly active (MIC ≤ 1 μg/mL, indicates strong antifungal activity and the agent is effective at very low concentrations), moderately active (MIC 1-10 μg/mL, shows good antifungal activity at moderate concentrations), weakly active (MIC 10-50 μg/mL, exhibits some antifungal activity but requires higher concentrations to be effective), and inactive (MIC > 50 μg/mL, indicates little to no antifungal activity, even at high concentrations). The fungi for which the molecules show antifungal effect, and the confidence and MIC(μg/mL) values of this effect are given in Table 5.

Table 5 – Antifungal activity properties of molecules

Molecule	Name	Confidence	MIC (µg/mL)
1	Cryptococcus bacillisporus	0.0050	20.00000
2	-	-	-
3	-	-	-
4	Cryptococcus bacillisporus	0.1019	0.98135
	Cryptococcus albidus	0.0574	1.74216
5	-	-	-
6	-	-	-
7	-	-	-
8	Cryptococcus bacillisporus	0.0582	1.71821
	Cryptococcus albidus	0.0217	4.60829
9	-	-	-
10	-	-	-
11	-	-	-
12	-	-	-

Determination of HIV targets. The term "HIV targets" refers to the process of locating and forecasting possible biological targets that may be utilized in the development or improvement of HIV-related medications and treatments [31]. This is essential for creating successful therapies that can change the host's immune response, stop the virus from replicating, or stop it from infecting new cells. All things considered, HIV targets prediction is an important field of study in the continuous endeavor to manage and ultimately eradicate HIV/AIDS [32]. When it comes to predicting HIV targets, pIC_{50} (pIC_{50} = -log (IC_{50}, half maximal inhibitory concentration)) is a metric that expresses how well a substance inhibits a particular biological target-like an enzyme or receptor-that is essential to the HIV life cycle. The potency of various compounds in blocking important targets implicated in the HIV life cycle may be evaluated and compared in a straightforward and scalable manner using pIC_{50}, a crucial parameter in the prediction of HIV targets [33]. HIV targets and pIC_{50} values determined for the molecules are given in Table 6.

Table 6 – HIV targets and prediction pIC_{50} value of molecules

Molecule	Target	pIC_{50}	IC_{50} (µM)
1	Protease (HIV-1)	5.014	9.68278E-06
	Reverse transcriptase (HIV-1)	5.163	6.87068E-06
	Integrase (HIV-1)	4.776	1.67494E-05
	REV (regulator of expression of virion proteins) (HIV-1)	4.697	2.00909E-05
	TAT (trans-activator of transcription) (HIV-1)	inactive	inactive
2	Protease (HIV-1)	5.510	3.09030E-06
	Reverse transcriptase (HIV-1)	4.615	2.42661E-05
	Integrase (HIV-1)	4.551	2.81190E-05
	REV (HIV-1)	4.731	1.85780E-05
	TAT (HIV-1)	inactive	inactive

Continuation of the table

Molecule	Target	pIC$_{50}$	IC$_{50}$ (µM)
3	Protease (HIV-1)	5.835	1.46218E-06
	Reverse transcriptase (HIV-1)	4.815	1.53109E-05
	Integrase (HIV-1)	4.677	2.10378E-05
	REV (HIV-1)	4.895	1.27350E-05
	TAT (HIV-1)	active	active
4	Protease (HIV-1)	6.259	5.50808E-07
	Reverse transcriptase (HIV-1)	5.143	7.19449E-06
	Integrase (HIV-1)	4.889	1.29122E-05
	REV (HIV-1)	4.464	3.43558E-05
	TAT (HIV-1)	inactive	inactive
5	Protease (HIV-1)	5.471	3.38065E-06
	Reverse transcriptase (HIV-1)	5.373	4.23643E-06
	Integrase (HIV-1)	4.894	1.27644E-05
	REV (HIV-1)	4.577	2.64850E-05
	TAT (HIV-1)	inactive	inactive
6	Protease (HIV-1)	6.190	6.45654E-07
	Reverse transcriptase (HIV-1)	4.829	1.48252E-05
	Integrase (HIV-1)	4.415	3.84592E-05
	REV (HIV-1)	4.616	2.42103E-05
	TAT (HIV-1)	inactive	inactive
7	Protease (HIV-1)	6.125	7.49894E-07
	Reverse transcriptase (HIV-1)	5.084	8.24138E-06
	Integrase (HIV-1)	4.666	2.15774E-05
	REV (HIV-1)	4.775	1.67880E-05
	TAT (HIV-1)	active	active
8	Protease (HIV-1)	6.662	2.17771E-07
	Reverse transcriptase (HIV-1)	5.337	4.60257E-06
	Integrase (HIV-1)	4.817	1.52405E-05
	REV (HIV-1)	4.400	3.98107E-05
	TAT (HIV-1)	inactive	inactive
9	Protease (HIV-1)	5.038	9.16220E-06
	Reverse transcriptase (HIV-1)	5.470	3.38844E-06
	Integrase (HIV-1)	5.135	7.32825E-06
	REV (HIV-1)	4.935	1.16145E-05
	TAT (HIV-1)	inactive	inactive
10	Protease (HIV-1)	5.776	1.67494E-06
	Reverse transcriptase (HIV-1)	4.840	1.44544E-05
	Integrase (HIV-1)	4.649	2.24388E-05
	REV (HIV-1)	4.932	1.16950E-05
	TAT (HIV-1)	inactive	inactive

Continuation of the table

Molecule	Target	pIC$_{50}$	IC$_{50}$ (µM)
11	Protease (HIV-1)	6.120	7.58578E-07
	Reverse transcriptase (HIV-1)	4.866	1.36144E-05
	Integrase (HIV-1)	4.687	2.05589E-05
	REV (HIV-1)	4.970	1.07152E-05
	TAT (HIV-1)	active	active
12	Protease (HIV-1)	6.224	5.97035E-07
	Reverse transcriptase (HIV-1)	5.355	4.41570E-06
	Integrase (HIV-1)	4.972	1.06660E-05
	REV (HIV-1)	4.677	2.10378E-05
	TAT (HIV-1)	inactive	inactive

Determination of antiviral properties. The ability of a material or molecule to prevent or treat viral infections by blocking the replication or activity of viruses is known as its antiviral capabilities. These characteristics are crucial for the creation of antiviral medications, which fight viral illnesses as COVID-19, hepatitis, HIV, and influenza [34]. A substance's ability to impede a virus at any point in its life cycle-from entry through replication, assembly, and release is referred to as its antiviral property [35]. Effective antiviral therapy depends on these qualities, with selectivity, resistance, and clinical use being key factors in the development and use of antiviral medications that can cure or prevent viral infections [36]. Confidence values closer to 1 indicate a higher probability that the compound has the predicted antiviral activity. The viruses, target proteins and confidence values calculated for the antiviral effect of the molecules are given in Table 7.

Determination of cancer line cell. In general, the phrase "cancer cell line value" describes how active a substance is in relation to a particular cancer cell line. A population of cells that can be cultivated and maintained in a laboratory environment that are derived from a specific cancer is known as a cancer cell line. A549 (lung cancer), MCF-7 (breast cancer), and the HeLa cell line (cervical cancer) are a few examples [37]. These cell lines are used by researchers to examine how substances affect cancer cells, evaluate possible anticancer medications, and comprehend the biology of cancer [38]. Pa and Pi values are crucial in drug discovery and development, as they provide a quantitative measure of a compound's efficacy against specific cancer types [39]. To determine which substances are the most effective anticancer medicines, researchers evaluate the Pa and Pi values of various chemicals and cell lines, and these values are used in predictive models to estimate the potential clinical effectiveness of new compounds [40]. The cell-line, non-tumor cell line, cell-line full name, tissue, and tumor type we determined for the molecules and the Pa and Pi values we calculated based on these are given in Table 8.

Table 7 – Antiviral activity properties of molecules

Molecule	Virus	Protein target	Confidence
1	Dengue virus 2	Genome polyprotein	0.5092
	Vaccinia virus (strain Western Reserve) (VACV) (Vaccinia virus (strainWR))	DNA polymerase	0.1266
	Varicella-zoster virus (strain Dumas) (HHV-3) (Human herpesvirus 3)	DNA polymerase	0.1015
	Herpes simplex virus (type 1 / strain 17)	Human herpesvirus 1 DNA polymerase	0.1015
	Severe acute respiratory syndrome coronavirus 2	Replicase polyprotein 1ab	0.0846
	Middle East respiratory syndrome-related coronavirus (isolate UnitedKingdom/ H123990006/2012) (Betacoronavirus England 1) (Humancoronavirus EMC)	Replicase polyprotein 1ab	0.0475
	Human herpesvirus 6A (strain Uganda-1102) (HHV-6 variant A) (Human Blymphotropic virus)	Human herpesvirus 6 DNA polymerase	0.0263

Continuation of the table

Molecule	Virus	Protein target	Confidence
2	Dengue virus 2	Genome polyprotein	0.3627
	Severe acute respiratory syndrome coronavirus 2	Replicase polyprotein 1ab	0.3075
	Varicella-zoster virus (strain Dumas) (HHV-3) (Human herpesvirus 3)	DNA polymerase	0.1398
	Herpes simplex virus (type 1 / strain 17)	Human herpesvirus 1 DNA polymerase	0.1398
	Dengue virus type 2	Genome polyprotein	0.1253
	Vaccinia virus (strain Western Reserve) (VACV) (Vaccinia virus (strainWR))	DNA polymerase	0.1083
	Macacine herpesvirus 1	Thymidine kinase	0.0362
	Human herpesvirus 6A (strain Uganda-1102) (HHV-6 variant A) (Human Blymphotropic virus)	Human herpesvirus 6 DNA polymerase	0.0240
	Middle East respiratory syndrome-related coronavirus (isolate UnitedKingdom/H123990006/2012) (Betacoronavirus England 1) (Humancoronavirus EMC)	Replicase polyprotein 1ab	0.0177
3	Severe acute respiratory syndrome coronavirus 2	Replicase polyprotein 1ab	0.3104
	Dengue virus 2	Genome polyprotein	0.3050
	Human herpesvirus 6A (strain Uganda-1102) (HHV-6 variant A) (Human Blymphotropic virus)	Human herpesvirus 6 DNA polymerase	0.0700
	Infectious bronchitis virus	3C-like protease	0.0242
	SARS coronavirus	SARS coronavirus 3C-like proteinase	0.0060
4	Dengue virus 2	Genome polyprotein	0.3262
	Severe acute respiratory syndrome coronavirus 2	Replicase polyprotein 1ab	0.1594
5	Dengue virus 2	Genome polyprotein	0.4442
	Vaccinia virus (strain Western Reserve) (VACV) (Vaccinia virus (strainWR))	DNA polymerase	0.0899
	Severe acute respiratory syndrome coronavirus 2	Replicase polyprotein 1ab	0.0729
	Varicella-zoster virus (strain Dumas) (HHV-3) (Human herpesvirus 3)	DNA polymerase	0.0642
	Herpes simplex virus (type 1 / strain 17)	Human herpesvirus 1 DNA polymerase	0.0642
6	Dengue virus 2	Genome polyprotein	0.3082
	Severe acute respiratory syndrome coronavirus 2	Replicase polyprotein 1ab	0.2992
	Dengue virus type 2	Genome polyprotein	0.1655
	Vaccinia virus (strain Western Reserve) (VACV) (Vaccinia virus (strainWR))	DNA polymerase	0.0842
	Varicella-zoster virus (strain Dumas) (HHV-3) (Human herpesvirus 3)	DNA polymerase	0.0642
	Herpes simplex virus (type 1 / strain 17)	Human herpesvirus 1 DNA polymerase	0.0642
7	Severe acute respiratory syndrome coronavirus 2	Replicase polyprotein 1ab	0.2983
	Dengue virus 2	Genome polyprotein	0.2671
	Infectious bronchitis virus	3C-like protease	0.0304
	Human herpesvirus 6A (strain Uganda-1102) (HHV-6 variant A) (Human Blymphotropic virus)	Human herpesvirus 6 DNA polymerase	0.0284
8	Dengue virus 2	Genome polyprotein	0.2862
	Severe acute respiratory syndrome coronavirus 2	Replicase polyprotein 1ab	0.1463

Continuation of the table

Molecule	Virus	Protein target	Confidence
9	Dengue virus 2	Genome polyprotein	0.4178
	Severe acute respiratory syndrome coronavirus 2	Replicase polyprotein 1ab	0.1287
	Human herpesvirus 6A (strain Uganda-1102) (HHV-6 variant A) (Human Blymphotropic virus)	Human herpesvirus 6 DNA polymerase	0.0668
	Infectious bronchitis virus	3C-like protease	0.0526
10	Severe acute respiratory syndrome coronavirus 2	Replicase polyprotein 1ab	0.3533
	Dengue virus 2	Genome polyprotein	0.2952
	Human herpesvirus 6A (strain Uganda-1102) (HHV-6 variant A) (Human Blymphotropic virus)	Human herpesvirus 6 DNA polymerase	0.0598
	Infectious bronchitis virus	3C-like protease	0.0482
11	Severe acute respiratory syndrome coronavirus 2	Replicase polyprotein 1ab	0.3489
	Dengue virus 2	Genome polyprotein	0.2982
	Human herpesvirus 6A (strain Uganda-1102) (HHV-6 variant A) (Human Blymphotropic virus)	Human herpesvirus 6 DNA polymerase	0.0608
	Infectious bronchitis virus	3C-like protease	0.0437
12	Dengue virus 2	Genome polyprotein	0.2735
	Severe acute respiratory syndrome coronavirus 2	Replicase polyprotein 1ab	0.1983
	Human herpesvirus 6A (strain Uganda-1102) (HHV-6 variant A) (Human Blymphotropic virus)	Human herpesvirus 6 DNA polymerase	0.0009

Table 8 – Cancer cell line and non-tumor cell line types of molecules and calculated Pa/Pi values

Molecule	Pa	Pi	Cell-line	Cell-line full name	Tissue	Tumor type
1	*Cancer cell line prediction*					
	0.145	0.063	HOS-TE85	Osteosarcoma	Bone	Sarcoma
	0.116	0.104	Melanoma cells	Melanoma	Skin	Melanoma
	0.354	0.003	SK-MEL	Melanoma	Skin	Melanoma
	0.070	0.048	MV4-11	Myeloid leukemia	Haematopoietic and lymphoid tissue	Leukemia
	0.171	0.079	Ramos	Burkitts lymhoma B-cells	Blood	Leukemia
	0.093	0.087	RT-4	Bladder carcinoma	Urinary tract	Carcinoma
	0.142	0.046	LNCaP	Prostate carcinoma	Prostate	Carcinoma
	0.160	0.148	MIA PaCa-2	Pancreatic carcinoma	Pancreas	Carcinoma
	0.372	0.041	SK-MES-1	Squamous cell lung carcinoma	Lung	Carcinoma
	0.377	0.134	YAPC	Pancreatic carcinoma	Pancreas	Carcinoma
	0.072	0.038	SISO	Uterine cervical adenocarcinoma	Cervix	Adenocarcinoma
	0.265	0.097	AGS	Gastric adenocarcinoma	Stomach	Adenocarcinoma
	0.347	0.045	OVCAR-3	Ovarian adenocarcinoma	Ovarium	Adenocarcinoma
	0.420	0.045	MDA-MB-231	Breast adenocarcinoma	Breast	Adenocarcinoma
	0.421	0.031	PC-9	Lung adenocarcinoma	Lung	Adenocarcinoma
	Non-tumor cell line prediction					
	0.364	0.040	HEK293	Embryonic kidney fibroblast	Kidney	-
	0.086	0.049	PBMC	Peripheral blood mononuclear cell	Blood	-

Continuation of the table

Molecule	Pa	Pi	Cell-line	Cell-line full name	Tissue	Tumor type
2	*Cancer cell line prediction*					
	0.731	0.005	MDA-MB-231	Breast adenocarcinoma	Breast	Adenocarcinoma
	0.590	0.013	OVCAR-3	Ovarian adenocarcinoma	Ovarium	Adenocarcinoma
	0.420	0.014	SK-MES-1	Squamous cell lung carcinoma	Lung	Carcinoma
	0.410	0.034	PC-9	Lung adenocarcinoma	Lung	Adenocarcinoma
	0.394	0.108	YAPC	Pancreatic carcinoma	Pancreas	Carcinoma
	0.309	0.033	AGS	Gastric adenocarcinoma	Stomach	Adenocarcinoma
	0.258	0.005	SK-MEL	Melanoma	Skin	Melanoma
	0.259	0.010	LNCaP	Prostate carcinoma	Prostate	Carcinoma
	0.180	0.019	HOS-TE85	Osteosarcoma	Bone	Sarcoma
	0.201	0.118	J82	Bladder carcinoma	Urinary tract	Carcinoma
	0.085	0.018	SISO	Uterine cervical adenocarcinoma	Cervix	Adenocarcinoma
	0.100	0.039	DAN-G	Human pancreas adenocarcinoma cell line	Pancreas	Adenocarcinoma
	0.072	0.030	SK-ES1	Ewing sarcoma	Bone	Sarcoma
	0.100	0.059	RT-4	Bladder carcinoma	Urinary tract	Carcinoma
	0.165	0.135	MIA PaCa-2	Pancreatic carcinoma	Pancreas	Carcinoma
	0.197	0.174	PC-3	Prostate carcinoma	Prostate	Carcinoma
	0.154	0.144	Ramos	Burkitts lymhoma B-cells	Blood	Leukemia
	0.114	0.110	Melanoma cells	Melanoma	Skin	Melanoma
	Non-tumor cell line prediction					
	0.346	*0.044*	*HEK293*	*Embryonic kidney fibroblast*	*Kidney*	*-*
3	*Cancer cell line prediction*					
	0.631	0.011	MDA-MB-231	Breast adenocarcinoma	Breast	Adenocarcinoma
	0.568	0.015	OVCAR-3	Ovarian adenocarcinoma	Ovarium	Adenocarcinoma
	0.454	0.029	YAPC	Pancreatic carcinoma	Pancreas	Carcinoma
	0.400	0.021	SK-MES-1	Squamous cell lung carcinoma	Lung	Carcinoma
	0.313	0.031	AGS	Gastric adenocarcinoma	Stomach	Adenocarcinoma
	0.338	0.068	PC-9	Lung adenocarcinoma	Lung	Adenocarcinoma
	0.219	0.015	LNCaP	Prostate carcinoma	Prostate	Carcinoma
	0.291	0.091	5637	Urothelial bladder carcinoma	Urinary tract	Carcinoma
	0.178	0.020	HOS-TE85	Osteosarcoma	Bone	Sarcoma
	0.158	0.009	SK-MEL	Melanoma	Skin	Melanoma
	0.142	0.013	DAN-G	Human pancreas adenocarcinoma cell line	Pancreas	Adenocarcinoma
	0.133	0.013	RT-4	Bladder carcinoma	Urinary tract	Carcinoma
	0.106	0.005	SISO	Uterine cervical adenocarcinoma	Cervix	Adenocarcinoma
	0.204	0.108	J82	Bladder carcinoma	Urinary tract	Carcinoma
	0.275	0.190	U-266	Plasma cell myeloma	Blood	Myeloma
	0.268	0.207	RKO	Colon carcinoma	Colon	Carcinoma
	0.270	0.210	T98G	Glioblastoma	Brain	Carcinoma
	0.079	0.020	SK-ES1	Ewing sarcoma	Bone	Sarcoma
	0.166	0.132	MIA PaCa-2	Pancreatic carcinoma	Pancreas	Carcinoma
	0.109	0.102	NSCLC	Non-small cell lung carcinoma	Lung	Carcinoma
	Non-tumor cell line prediction					
	0.416	0.033	HEK293	Embryonic kidney fibroblast	Kidney	-

Continuation of the table

Molecule	Pa	Pi	Cell-line	Cell-line full name	Tissue	Tumor type
4	*Cancer cell line prediction*					
	0.650	0.009	MDA-MB-231	Breast adenocarcinoma	Breast	Adenocarcinoma
	0.522	0.019	OVCAR-3	Ovarian adenocarcinoma	Ovarium	Adenocarcinoma
	0.413	0.016	SK-MES-1	Squamous cell lung carcinoma	Lung	Carcinoma
	0.387	0.043	PC-9	Lung adenocarcinoma	Lung	Adenocarcinoma
	0.298	0.042	AGS	Gastric adenocarcinoma	Stomach	Adenocarcinoma
	0.374	0.139	YAPC	Pancreatic carcinoma	Pancreas	Carcinoma
	0.240	0.012	LNCaP	Prostate carcinoma	Prostate	Carcinoma
	0.205	0.007	SK-MEL	Melanoma	Skin	Melanoma
	0.181	0.019	HOS-TE85	Osteosarcoma	Bone	Sarcoma
	0.179	0.067	NCI-N87	gastric carcinoma	Stomach	Carcinoma
	0.282	0.184	RKO	Colon carcinoma	Colon	Carcinoma
	0.212	0.129	MDA-MB-468	Breast adenocarcinoma	Breast	Adenocarcinoma
	0.081	0.017	SK-ES1	Ewing sarcoma	Bone	Sarcoma
	0.195	0.141	J82	Bladder carcinoma	Urinary tract	Carcinoma
	0.235	0.204	HuP-T3	Pancreatic adenocarcinoma	Pancreas	Adenocarcinoma
	0.164	0.137	MIA PaCa-2	Pancreatic carcinoma	Pancreas	Carcinoma
	0.272	0.253	Hs 683	Oligodendroglioma	Brain	Glioma
	Non-tumor cell line prediction					
	0.260	0.075	HEK293	Embryonic kidney fibroblast	Kidney	-
5	*Cancer cell line prediction*					
	0.391	0.041	PC-9	Lung adenocarcinoma	Lung	Adenocarcinoma
	0.393	0.052	MDA-MB-231	Breast adenocarcinoma	Breast	Adenocarcinoma
	0.327	0.004	SK-MEL	Melanoma	Skin	Melanoma
	0.366	0.047	SK-MES-1	Squamous cell lung carcinoma	Lung	Carcinoma
	0.314	0.056	OVCAR-3	Ovarian adenocarcinoma	Ovarium	Adenocarcinoma
	0.366	0.153	YAPC	Pancreatic carcinoma	Pancreas	Carcinoma
	0.172	0.075	Ramos	Burkitts lymhoma B-cells	Blood	Leukemia
	0.138	0.050	LNCaP	Prostate carcinoma	Prostate	Carcinoma
	0.237	0.154	AGS	Gastric adenocarcinoma	Stomach	Adenocarcinoma
	0.132	0.108	HOS-TE85	Osteosarcoma	Bone	Sarcoma
	0.163	0.140	MIA PaCa-2	Pancreatic carcinoma	Pancreas	Carcinoma
	0.244	0.227	C8166	Leukemic T-cells	Blood	Leukemia
	0.065	0.064	SISO	Uterine cervical adenocarcinoma	Cervix	Adenocarcinoma
	Non-tumor cell line prediction					
	0.337	0.046	HEK293	Embryonic kidney fibroblast	Kidney	-
	0.090	0.045	PBMC	Peripheral blood mononuclear cell	Blood	-

Molecule	Pa	Pi	Cell-line	Cell-line full name	Tissue	Tumor type
6	*Cancer cell line prediction*					
	0.650	0.009	MDA-MB-231	Breast adenocarcinoma	Breast	Adenocarcinoma
	0.515	0.020	OVCAR-3	Ovarian adenocarcinoma	Ovarium	Adenocarcinoma
	0.405	0.019	SK-MES-1	Squamous cell lung carcinoma	Lung	Carcinoma
	0.364	0.053	PC-9	Lung adenocarcinoma	Lung	Adenocarcinoma
	0.386	0.120	YAPC	Pancreatic carcinoma	Pancreas	Carcinoma
	0.227	0.014	LNCaP	Prostate carcinoma	Prostate	Carcinoma
	0.279	0.068	AGS	Gastric adenocarcinoma	Stomach	Adenocarcinoma
	0.197	0.007	SK-MEL	Melanoma	Skin	Melanoma
	0.162	0.033	HOS-TE85	Osteosarcoma	Bone	Sarcoma
	0.257	0.184	C8166	Leukemic T-cells	Blood	Leukemia
	0.160	0.115	Ramos	Burkitts lymhoma B-cells	Blood	Leukemia
	0.075	0.032	SISO	Uterine cervical adenocarcinoma	Cervix	Adenocarcinoma
	0.191	0.155	MDA-MB-468	Breast adenocarcinoma	Breast	Adenocarcinoma
	0.248	0.214	5637	Urothelial bladder carcinoma	Urinary tract	Carcinoma
	0.166	0.132	MIA PaCa-2	Pancreatic carcinoma	Pancreas	Carcinoma
	0.098	0.065	RT-4	Bladder carcinoma	Urinary tract	Carcinoma
	0.085	0.064	DAN-G	Human pancreas adenocarcinoma cell line	Pancreas	Adenocarcinoma
	0.186	0.182	J82	Bladder carcinoma	Urinary tract	Carcinoma
	0.187	0.183	PC-3	Prostate carcinoma	Prostate	Carcinoma
	Non-tumor cell line prediction					
	0.316	0.053	HEK293	Embryonic kidney fibroblast	Kidney	-
7	*Cancer cell line prediction*					
	0.584	0.016	MDA-MB-231	Breast adenocarcinoma	Breast	Adenocarcinoma
	0.505	0.021	OVCAR-3	Ovarian adenocarcinoma	Ovarium	Adenocarcinoma
	0.443	0.039	YAPC	Pancreatic carcinoma	Pancreas	Carcinoma
	0.391	0.026	SK-MES-1	Squamous cell lung carcinoma	Lung	Carcinoma
	0.285	0.058	AGS	Gastric adenocarcinoma	Stomach	Adenocarcinoma
	0.307	0.089	PC-9	Lung adenocarcinoma	Lung	Adenocarcinoma
	0.295	0.081	5637	Urothelial bladder carcinoma	Urinary tract	Carcinoma
	0.208	0.018	LNCaP	Prostate carcinoma	Prostate	Carcinoma
	0.272	0.141	C8166	Leukemic T-cells	Blood	Leukemia
	0.162	0.032	HOS-TE85	Osteosarcoma	Bone	Sarcoma
	0.137	0.010	SK-MEL	Melanoma	Skin	Melanoma
	0.126	0.017	RT-4	Bladder carcinoma	Urinary tract	Carcinoma
	0.114	0.026	DAN-G	Human pancreas adenocarcinoma cell line	Pancreas	Adenocarcinoma
	0.092	0.011	SISO	Uterine cervical adenocarcinoma	Cervix	Adenocarcinoma
	0.266	0.212	RKO	Colon carcinoma	Colon	Carcinoma
	0.168	0.129	MIA PaCa-2	Pancreatic carcinoma	Pancreas	Carcinoma
	0.258	0.227	U-266	Plasma cell myeloma	Blood	Myeloma
	0.190	0.162	J82	Bladder carcinoma	Urinary tract	Carcinoma
	0.262	0.236	T98G	Glioblastoma	Brain	Carcinoma
	0.066	0.051	CCRF-SB	Childhood T acute lymphoblastic leukemia	Blood	Leukemia
	0.061	0.057	SK-ES1	Ewing sarcoma	Bone	Sarcoma
	Non-tumor cell line prediction					
	0.373	0.039	HEK293	Embryonic kidney fibroblast	Kidney	-

Continuation of the table

Molecule	Pa	Pi	Cell-line	Cell-line full name	Tissue	Tumor type
8	*Cancer cell line prediction*					
	0.602	0.014	MDA-MB-231	Breast adenocarcinoma	Breast	Adenocarcinoma
	0.456	0.025	OVCAR-3	Ovarian adenocarcinoma	Ovarium	Adenocarcinoma
	0.402	0.020	SK-MES-1	Squamous cell lung carcinoma	Lung	Carcinoma
	0.353	0.059	PC-9	Lung adenocarcinoma	Lung	Adenocarcinoma
	0.222	0.015	LNCaP	Prostate carcinoma	Prostate	Carcinoma
	0.364	0.157	YAPC	Pancreatic carcinoma	Pancreas	Carcinoma
	0.274	0.078	AGS	Gastric adenocarcinoma	Stomach	Adenocarcinoma
	0.166	0.008	SK-MEL	Melanoma	Skin	Melanoma
	0.165	0.029	HOS-TE85	Osteosarcoma	Bone	Sarcoma
	0.230	0.109	MDA-MB-468	Breast adenocarcinoma	Breast	Adenocarcinoma
	0.278	0.191	RKO	Colon carcinoma	Colon	Carcinoma
	0.167	0.095	NCI-N87	gastric carcinoma	Stomach	Carcinoma
	0.166	0.134	MIA PaCa-2	Pancreatic carcinoma	Pancreas	Carcinoma
	0.244	0.227	C8166	Leukemic T-cells	Blood	Leukemia
	0.063	0.050	SK-ES1	Ewing sarcoma	Bone	Sarcoma
	0.242	0.230	5637	Urothelial bladder carcinoma	Urinary tract	Carcinoma
	Non-tumor cell line prediction					
	0.250	0.079	HEK293	Embryonic kidney fibroblast	Kidney	-
9	*Cancer cell line prediction*					
	0.436	0.046	YAPC	Pancreatic carcinoma	Pancreas	Carcinoma
	0.354	0.043	OVCAR-3	Ovarian adenocarcinoma	Ovarium	Adenocarcinoma
	0.355	0.058	SK-MES-1	Squamous cell lung carcinoma	Lung	Carcinoma
	0.298	0.004	SK-MEL	Melanoma	Skin	Melanoma
	0.351	0.060	PC-9	Lung adenocarcinoma	Lung	Adenocarcinoma
	0.310	0.081	MDA-MB-231	Breast adenocarcinoma	Breast	Adenocarcinoma
	0.278	0.071	AGS	Gastric adenocarcinoma	Stomach	Adenocarcinoma
	0.165	0.030	HOS-TE85	Osteosarcoma	Bone	Sarcoma
	0.265	0.166	5637	Urothelial bladder carcinoma	Urinary tract	Carcinoma
	0.120	0.022	RT-4	Bladder carcinoma	Urinary tract	Carcinoma
	0.083	0.019	SISO	Uterine cervical adenocarcinoma	Cervix	Adenocarcinoma
	0.123	0.076	LNCaP	Prostate carcinoma	Prostate	Carcinoma
	0.093	0.048	DAN-G	Human pancreas adenocarcinoma cell line	Pancreas	Adenocarcinoma
	0.165	0.135	MIA PaCa-2	Pancreatic carcinoma	Pancreas	Carcinoma
	0.070	0.049	MV4-11	Myeloid leukemia	Haematopoietic and lymphoid tissue	Leukemia
	Non-tumor cell line prediction					
	0.402	0.035	HEK293	Embryonic kidney fibroblast	Kidney	-
	0.099	0.085	WI-38	Embryonic lung fibroblast	Lung	-

Molecule	Pa	Pi	Cell-line	Cell-line full name	Tissue	Tumor type
	Cancer cell line prediction					
	0.615	0.013	MDA-MB-231	Breast adenocarcinoma	Breast	Adenocarcinoma
	0.566	0.015	OVCAR-3	Ovarian adenocarcinoma	Ovarium	Adenocarcinoma
	0.448	0.034	YAPC	Pancreatic carcinoma	Pancreas	Carcinoma
	0.396	0.023	SK-MES-1	Squamous cell lung carcinoma	Lung	Carcinoma
	0.314	0.030	AGS	Gastric adenocarcinoma	Stomach	Adenocarcinoma
	0.324	0.077	PC-9	Lung adenocarcinoma	Lung	Adenocarcinoma
	0.213	0.017	LNCaP	Prostate carcinoma	Prostate	Carcinoma
	0.290	0.095	5637	Urothelial bladder carcinoma	Urinary tract	Carcinoma
	0.192	0.015	HOS-TE85	Osteosarcoma	Bone	Sarcoma
	0.160	0.009	SK-MEL	Melanoma	Skin	Melanoma
10	0.129	0.015	RT-4	Bladder carcinoma	Urinary tract	Carcinoma
	0.126	0.019	DAN-G	Human pancreas adenocarcinoma cell line	Pancreas	Adenocarcinoma
	0.100	0.008	SISO	Uterine cervical adenocarcinoma	Cervix	Adenocarcinoma
	0.202	0.115	J82	Bladder carcinoma	Urinary tract	Carcinoma
	0.074	0.027	SK-ES1	Ewing sarcoma	Bone	Sarcoma
	0.267	0.221	T98G	Glioblastoma	Brain	Carcinoma
	0.167	0.132	MIA PaCa-2	Pancreatic carcinoma	Pancreas	Carcinoma
	0.117	0.086	NCI-H647	Adenosquamous lung carcinoma	Lung	Carcinoma
	0.254	0.236	U-266	Plasma cell myeloma	Blood	Myeloma
	Non-tumor cell line prediction					
	0.392	0.036	HEK293	Embryonic kidney fibroblast	Kidney	-
	Cancer cell line prediction					
	0.624	0.012	MDA-MB-231	Breast adenocarcinoma	Breast	Adenocarcinoma
	0.572	0.015	OVCAR-3	Ovarian adenocarcinoma	Ovarium	Adenocarcinoma
	0.447	0.035	YAPC	Pancreatic carcinoma	Pancreas	Carcinoma
	0.397	0.022	SK-MES-1	Squamous cell lung carcinoma	Lung	Carcinoma
	0.314	0.030	AGS	Gastric adenocarcinoma	Stomach	Adenocarcinoma
	0.329	0.073	PC-9	Lung adenocarcinoma	Lung	Adenocarcinoma
	0.216	0.016	LNCaP	Prostate carcinoma	Prostate	Carcinoma
	0.288	0.100	5637	Urothelial bladder carcinoma	Urinary tract	Carcinoma
	0.193	0.015	HOS-TE85	Osteosarcoma	Bone	Sarcoma
	0.164	0.008	SK-MEL	Melanoma	Skin	Melanoma
11	0.129	0.015	RT-4	Bladder carcinoma	Urinary tract	Carcinoma
	0.122	0.021	DAN-G	Human pancreas adenocarcinoma cell line	Pancreas	Adenocarcinoma
	0.098	0.008	SISO	Uterine cervical adenocarcinoma	Cervix	Adenocarcinoma
	0.202	0.116	J82	Bladder carcinoma	Urinary tract	Carcinoma
	0.072	0.029	SK-ES1	Ewing sarcoma	Bone	Sarcoma
	0.264	0.228	T98G	Glioblastoma	Brain	Carcinoma
	0.167	0.131	MIA PaCa-2	Pancreatic carcinoma	Pancreas	Carcinoma
	0.114	0.096	NCI-H647	Adenosquamous lung carcinoma	Lung	Carcinoma
	Non-tumor cell line prediction					
	0.397	0.036	HEK293	Embryonic kidney fibroblast	Kidney	-

Continuation of the table

Molecule	Pa	Pi	Cell-line	Cell-line full name	Tissue	Tumor type
12	*Cancer cell line prediction*					
	0.563	0.019	MDA-MB-231	Breast adenocarcinoma	Breast	Adenocarcinoma
	0.508	0.020	OVCAR-3	Ovarian adenocarcinoma	Ovarium	Adenocarcinoma
	0.434	0.049	YAPC	Pancreatic carcinoma	Pancreas	Carcinoma
	0.394	0.024	SK-MES-1	Squamous cell lung carcinoma	Lung	Carcinoma
	0.304	0.037	AGS	Gastric adenocarcinoma	Stomach	Adenocarcinoma
	0.315	0.083	PC-9	Lung adenocarcinoma	Lung	Adenocarcinoma
	0.210	0.018	LNCaP	Prostate carcinoma	Prostate	Carcinoma
	0.192	0.015	HOS-TE85	Osteosarcoma	Bone	Sarcoma
	0.283	0.113	5637	Urothelial bladder carcinoma	Urinary tract	Carcinoma
	0.140	0.010	SK-MEL	Melanoma	Skin	Melanoma
	0.112	0.033	RT-4	Bladder carcinoma	Urinary tract	Carcinoma
	0.273	0.198	T98G	Glioblastoma	Brain	Carcinoma
	0.273	0.198	RKO	Colon carcinoma	Colon	Carcinoma
	0.082	0.017	SK-ES1	Ewing sarcoma	Bone	Sarcoma
	0.196	0.136	J82	Bladder carcinoma	Urinary tract	Carcinoma
	0.161	0.114	NCI-N87	gastric carcinoma	Stomach	Carcinoma
	0.094	0.047	DAN-G	Human pancreas adenocarcinoma cell line	Pancreas	Adenocarcinoma
	0.072	0.038	SISO	Uterine cervical adenocarcinoma	Cervix	Adenocarcinoma
	0.154	0.121	SAOS-2	Osteosarcoma	Bone	Sarcoma
	0.166	0.133	MIA PaCa-2	Pancreatic carcinoma	Pancreas	Carcinoma
	0.257	0.229	U-266	Plasma cell myeloma	Blood	Myeloma
	0.108	0.107	NSCLC	Non-small cell lung carcinoma	Lung	Carcinoma
	Non-tumor cell line prediction					
	0.304	0.057	HEK293	Embryonic kidney fibroblast	Kidney	-

Results and discussion

In this study, we have considered twelve benzimidazole derivative compounds because we are still conducting important studies on these molecules for their potential use as active pharmaceutical ingredients for the treatment of MS. Therefore, in this study, we thought it was necessary to examine these molecules in terms of biological activity. It was determined that the most toxic molecule was molecule 5 at 523.900 mg/kg in class 5 and molecule 3 at 2255.000 mg/kg was non-toxic when we examined all molecules in terms of Rat IP LD$_{50}$ (intraperitoneal administration route). The reason for the very high toxicity of molecule 5 is likely to be the -C$_6$H$_5$ bound at the -R$_2$ point. It is seen that a ranking is formed as 2>5>6>8>1>7> 11>12>10>4>9>3 when we rank the toxicity in molecules from the

strongest to the lowest. When we analyze the results in terms of Rat IV LD$_{50}$, it is seen that the most toxic molecule is molecule 5 with 157.600 mg/kg in class 4. Molecule 2 was found to have the lowest toxicity among all molecules as 371.900 mg/kg in class 5. The reason for the very high toxicity of molecule 5 is likely to be the -CH$_3$ bound at the -R$_1$ point. When we rank the Toxicity in molecules from the strongest to the lowest, it is seen that a ranking is formed as 5>8>10>3>7>9>6>12>1>4> 11>2. It is seen that the most toxic molecule is molecule 7 with 426.200 mg/kg in class 4 when we examined the results in terms of Rat Oral LD$_{50}$. Molecule 10 was found to have the lowest toxicity among all molecules at 3592.000 mg/kg in class 5. The reason for the very high toxicity of molecule 7 is likely to be the -CH$_3$ bound at the -R$_1$ point. When we rank the toxicity in molecules from the strongest to the lowest, it is seen that a ranking

is formed as 7>12>2>3>1>9>11>5>6>8>4>10. Finally, when we examine the results in terms of Rat SC LD$_{50}$, it is seen that the most toxic molecule is molecule 11 as 767.800 mg/kg in class 4. Molecule 6 was found to have no toxicity among all molecules as 4788.000 mg/kg. Graphical representation of the data obtained in Table 2 for rat acrute toxicity is demonstrated on Figure 2.
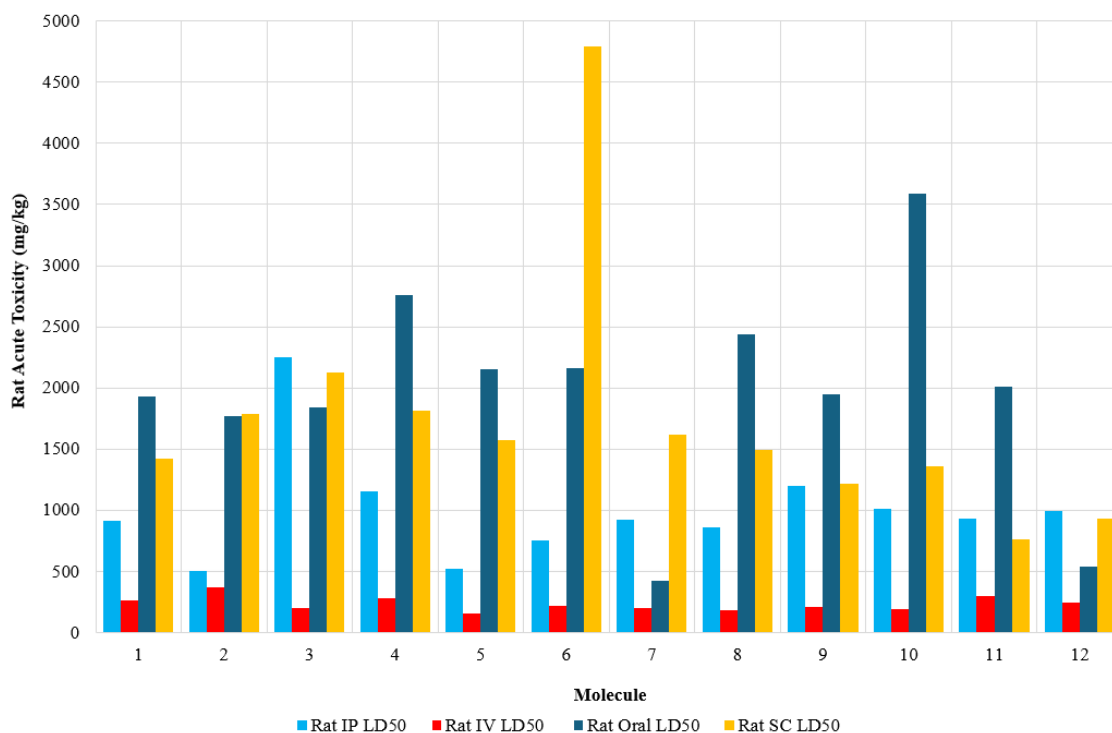
Figure 2 – Acute rat toxicity values of molecules

It was determined that molecules 1, 5, 6, and 9 did not show any adverse effect when we examined the molecules in terms of the adverse effect they showed. Among the other molecules, hepatotoxicity was the most adverse effect, followed by nephrotoxicity. The term "hepatotoxicity" describes a substance's capacity to harm the liver, including medications, chemicals, and natural compounds. The liver is an essential organ that produces crucial proteins, breaks down medications, and detoxifies blood. Hepatotoxic substances have the potential to cause liver harm, which can vary in severity from slight increases in liver enzymes to complete liver failure [41]. Seven different molecules showed hepatotoxicity effect (molecules 3, 4, 7, 8, 10, 11, and 12), and three different molecules (molecules 2, 4, and 8) showed nephrotoxicity effect. The term "nephrotoxicity" describes a substance's capacity to harm the kidneys. The kidneys are vital organs that filter waste materials out of the blood, control fluid balance, and preserve electrolyte levels. Nephrotoxicity is the ability of a chemical to damage kidney function, resulting in either chronic kidney disease (CKD) or acute kidney injury (AKI) [42]. It was determined that only molecule 4 showed an arrhythmia effect. Any irregularity in the heart's rhythm, such as beating too quickly, too slowly, or irregularly, is referred to as an arrhythmia [43]. Molecule 4 showed three different effects, molecule 8 showed two different effects, while molecules 2, 3, 4, 7, 8, 10, 11, and 12 showed only one effect. The highest Pa value was 0.422 for molecules 10 and 11, and the lowest Pa value was 0.273 for molecule 2. The highest Pi value was 0.266 in molecule 4, and the lowest Pi value was 0.110 in molecule 4. Graphical representation of the data obtained in Table 3 for adverse effects is presented on Figure 3.
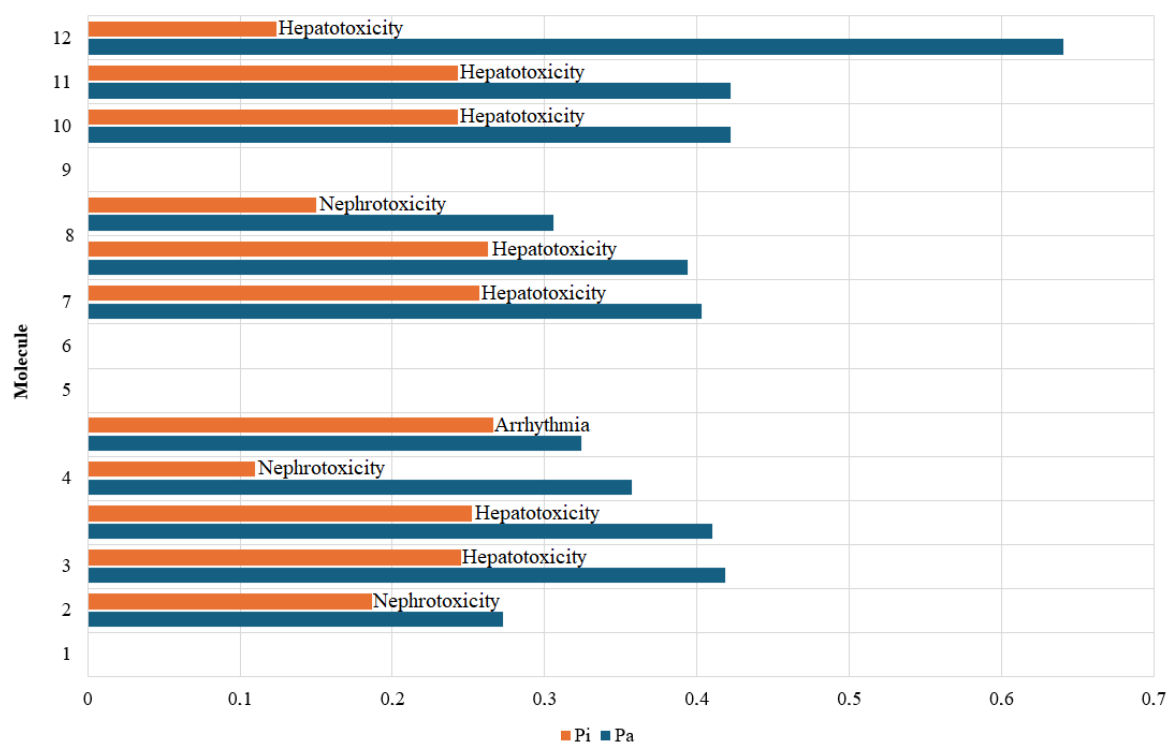
Figure 3 – Adverse effect values of molecules

Classifying antibacterial activity according to MIC (minimum inhibitory concentration) values is a widely used method for assessing the effectiveness of a substance on a bacterial species. MIC refers to the lowest concentration of antibiotic or antimicrobial agent required to stop the growth of a particular bacterium. The lower the MIC value, the stronger the antibacterial agent. The efficacy of an agent can be assessed by classifying MIC values according to certain ranges. This classification is usually done as follows: strong antibacterial activity (MIC≤1 µg/mL, this range indicates that the substance is effective even at very low concentrations, indicating a high antibacterial potential), moderate antibacterial activity (MIC>1 µg/mL and ≤10 µg/mL, this range indicates that the substance is still effective but at higher concentrations), weak antibacterial activity (MIC>10 µg/mL and ≤100 µg/mL, this range indicates that the antibacterial effect of the substance is weak and much higher concentrations are needed to be clinically effective), and very weak or no inhibitory effect (MIC>100 µg/mL, in this case, the substance is considered to have no or a very weak inhibitory effect on bacterial growth). When we examined the Antibacterial activity MIC values given in Table 4, it was found that molecule 2 showed the strongest antibacterial effect against Shigella sp. (MIC 0.96759

µg/mL), molecule 5 against Shigella sp. (MIC 0.87413 µg/mL), and molecule 1 against Shigella sp. (MIC 0.73073 µg/mL). Antibacterial effect of other molecules was moderate, weak, and very weak or there was no inhibitory effect. Information on strong, moderate, and weak antibacterial activity and MIC (µg/mL) values shown by the molecules is presented on Figure 4.

The term "antifungal activity" describes a substance's capacity to stop fungus growth or eradicate fungal organisms. A vast variety of organisms, including molds like *Aspergillus* species and yeasts like *Candida* species, are classified as fungi. These organisms can cause a variety of illnesses, especially in those with impaired immune systems [44]. Since fungal infections can range from minor skin infections to serious systemic disorders, antifungal activity is an essential part of treating fungal infections. Treatment plans are determined by the type of infection, the fungus present, and the general health of the patient. The efficiency of an antifungal medication is frequently gauged by its minimum inhibitory concentration (MIC) against particular fungi [45]. It is seen that most of the molecules we studied do not have antifungal activity. Molecules 1, 4 and 8 appear to have antifungal activity. Among these, molecule 4 showed the highest antifungal

activity against *Cryptococcus bacillisporus* with a value of 0.98135 µg/mL. The weakest antifungal activity was shown in molecule 1 with 20.00000 µg/mL against *Cryptococcus bacillisporus*. A visual representation of the data on antifungal activity is given in Figure 5.
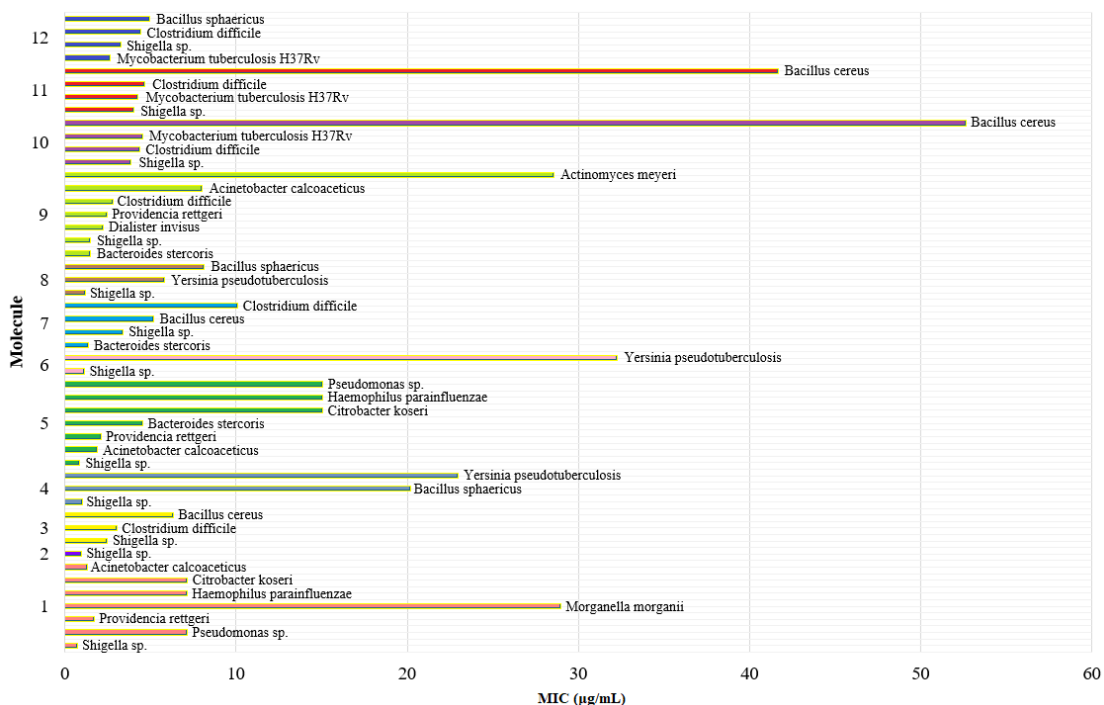
Figure 4 – Strong, moderate, and weak antibacterial activity and MIC values by the molecules
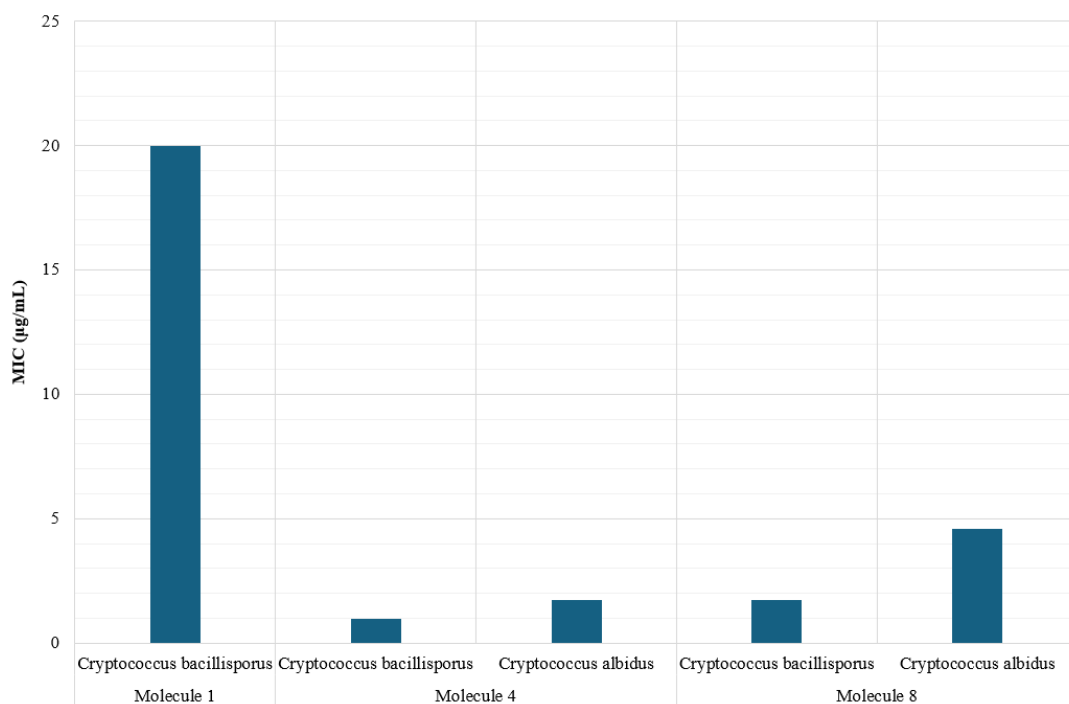
Figure 5 – Antifungal activity values of molecules

HIV Targets Prediction is the computational prediction of a compound's capacity to interact with particular HIV (human immunodeficiency virus) targets in PASS. Researchers working on drug discovery and development might benefit greatly from HIV Targets Prediction in PASS Online, which offers insights into possible interactions between chemical compounds and important HIV-related targets. This may hasten the discovery and development of novel antiviral medications intended to cure or prevent HIV infection [44]. The pIC_{50} value is a measure of the potency of a compound to inhibit a specific target, such as an HIV-associated protein or enzyme. Based on its size, which is correlated with the compound's potency in blocking HIV targets, pIC_{50} values are categorized (high potency (strong inhibitor) : pIC_{50} > 8, moderate potency (moderate inhibitor) : pIC_{50} between 6 and 8, low potency (weak inhibitor) : pIC_{50}

between 4 and 6, and very low potency or inactive : pIC_{50} < 4). Stronger inhibition and more potential as an antiviral agent are indicated by higher pIC_{50} values, which makes these compounds more desirable candidates for HIV medication development. As HIV targets, the molecules were found to play an active role in five different targets. Molecules 4, 6, 7, 8, 11, and 12 have moderate potency in protease (HIV-1) target, molecules 1, 2, 3, 5, 9, and 10 have moderate potency in protease (HIV-1), reverse transcriptase (HIV-1), integrase (HIV-1), and REV (HIV-1)), molecules 4, 6, 7, 8, 11, and 12 were found to have low potency in reverse transcriptase (HIV-1), integrase (HIV-1), and REV (HIV-1). Finally, it was concluded that molecules 1, 2, 4, 5, 6, 8, 9, 10, and 11 were inactive, while molecules 3, 7, and 11 were active in the target TAT (HIV-1). Visual representation of the data given in Table 6 is given in Figure 6.
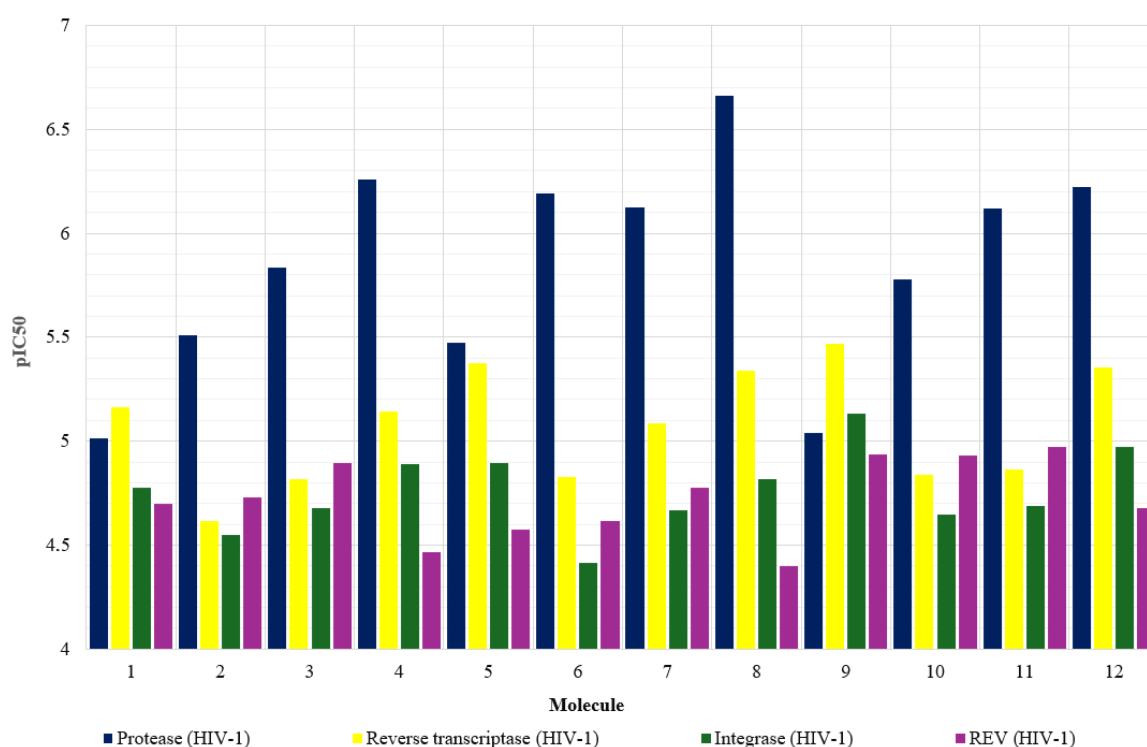
Figure 6 – HIV targets and pIC50 values of molecules

The ability of a material, usually a medication or natural molecule, to prevent viruses from replicating and spreading within a host organism is known as the antiviral effect. A crucial characteristic of substances or medications that prevent viral replication and aid in the management or eradication of viral illnesses is their antiviral effect [45]. This impact can be attained

via a number of strategies that target distinct phases of the viral life cycle, ultimately stopping the virus's replication and lessening the infection's severity or spread [46]. As can be seen in Table 7, all the molecules studied showed antiviral effects on specific viruses and proteins. The quantitative magnitude of this effect is given in this table with confidence

values. The antiviral effect is classified according to the confidence value as strong activity (confidence value > 0.7), moderate activity (confidence value between 0.5 and 0.7), low activity, (confidence value between 0.3 and 0.5), and very low activity (confidence value < 0.3). As can be seen from the confidence values given in Table 7, almost all of the molecules show low and very low antiviral activity. The highest antiviral effect was obtained in molecule

1 against dengue virus 2 with a confidence value of 0.5092 in the target protein genome polyprotein. The lowest antiviral effect was obtained in molecule 12 against human herpesvirus 6A (strain Uganda-1102) (HHV-6 variant A) (human blymphotropic virus) with a confidence value of 0.0009 in human herpesvirus 6 DNA polymerase target protein. A visual of the confidence values of the molecules with the target protein they show antiviral effect is given in Figure 7.
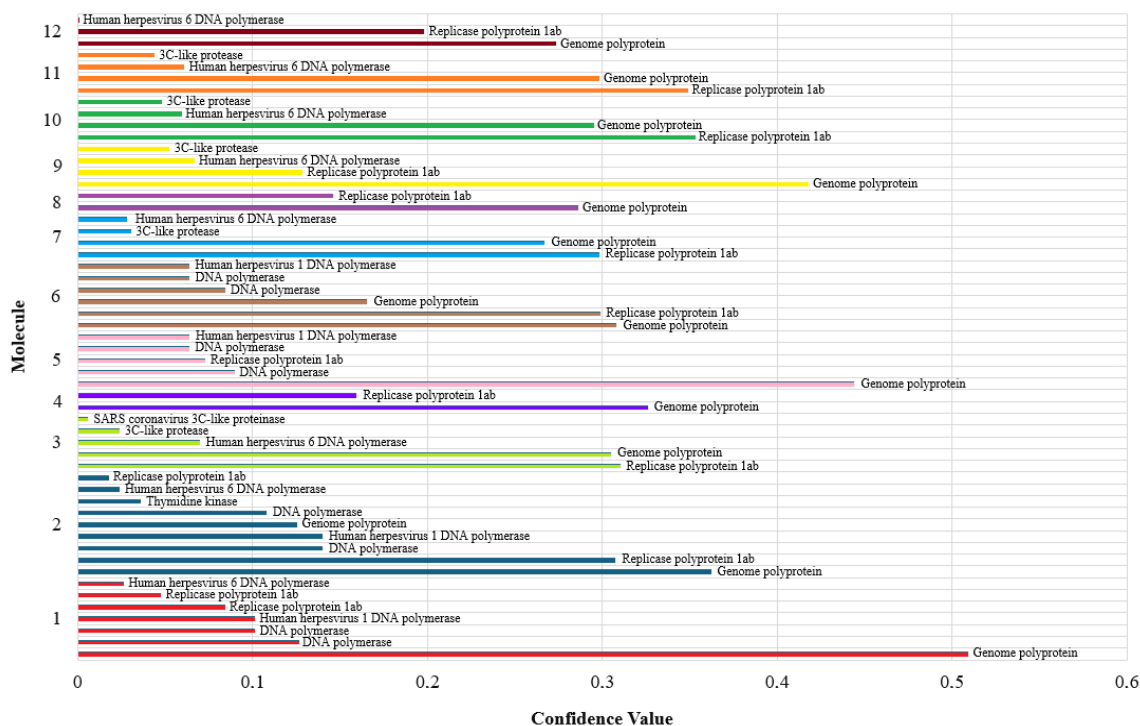
Figure 7 – Target proteins and confidence values of molecules with antiviral effects

Cancer cell lines are cells derived from human or animal tumors that can be grown in the laboratory [47]. The practice of forecasting how a specific substance or medication would influence different cancer cell lines is known as "cancer cell line prediction." This is a crucial component of oncology research and medication development since it enables researchers to assess a compound's possible effectiveness against various cancer cell types [48]. PASS (Prediction of Activity Spectra for Substances) Online is one tool that may be used to predict the activity of chemicals against different cancer cell lines. This tool offers probability scores for the chance that a substance would be effective against particular cancer cell lines, which are comparable to Pa and Pi values. Pa and Pi values give insight into the likelihood that a

compound will be effective against a specific cancer cell line [49]. If Pa is considerably greater than Pi (Pa > 0.7 and Pi < 0.3, for example), there is a good chance that the drug will be effective against the cancer cell line. These substances are seen to be excellent candidates for additional experimental confirmation. The prediction is less certain when Pa and Pi values are near to one another (Pa = 0.5 and Pi ≈ 0.5, for example). Although the forecast does not support the compound's candidacy, it may have some activity. To fully understand its potential, more testing might be necessary. There is less chance that the drug will be effective against the cancer cell line when Pa is low and Pi is high (e.g., Pa < 0.3 and Pi > 0.7). Generally speaking, these substances are not given as much priority for more research about

that particular activity [50]. As can be seen from the data given in Table 8, it is seen that the molecules have certain Pa and Pi values, although not very high, on the tumor types that the tissue has in many cell-line lines. These show us that the molecules have the potential to be effective on many cancer types.

Conclusion

As a result, seven different biological activities, including acute rat toxicity, adverse drug effects, antibacterial activity, antifungal activity, anti-HIV activity, antiviral activity, and cell line cytotoxicity, were calculated for twelve benzimidazole derivative compound examined here. Rat IP LD$_{50}$ (intraperitoneal administration toxicity measure), Rat IV LD$_{50}$ (intravenous administration toxicity measure), Rat Oral LD$_{50}$ (oral administration toxicity measure), and Rat SC LD$_{50}$ (subcutaneous administration toxicity measure) The toxicities of the molecules were generally not very low. It was determined that some of the molecules had side effects while others had no side effects. In terms of antibacterial activity, it was observed that generally the molecules had moderate antibacterial activity and very few had high antibacterial activity. While some of the molecules had antifungal activity, this effect was not observed in some of them. In terms of HIV targets, it was observed that they showed different qualities of activity. In terms of antiviral activity, they did not exhibit very strong activity, but all molecules showed a certain antiviral activity. Finally, it was observed that the molecules were active on many tumor types.

Conflict of interest

The author is aware of the article's content and declares no conflict of interest.

References

1.   Barot P.K., Nikolova S., Ivanov I., Ghate M.D. (2013) Novel research strategies of benzimidazole derivatives: a review. *Mini Rev. Med. Chem.*, 13(10), pp. 1421-1447.

2.   Al-rifaie D.A., Rasheed M.K., Meri M.A., Mustafa M.A. (2023) Synthesis and characterization of some benzimidazole derivatives derived from pharmaceutical compounds, and evaluation of their antibacterial and antifungal activity. *Lat. Am. J. Pharm.*, 42, pp. 229-233.

3.   Francesconi V., Rizzo M., Schenone S., Carbone A., Tonelli M. (2024) State-of-the-art review on the antiparasitic activity of benzimidazole-based derivatives: Facing malaria, leishmaniasis, and trypanosomiasis. *Curr. Med. Chem.*, 31(15), pp. 1955-1982.

4.   Chen M., Su S.J., Zhou Q., Tang X.M., Liu T.T., Peng F., He M., Luo H., Xue W. (2021) Antibacterial and antiviral activities and action mechanism of flavonoid derivatives with a benzimidazole moiety. *J. Saudi. Chem. Soc.*, 25(2), pp. 1-14. https://doi.org/10.1016/j.jscs.2020.101194.

5.   Divaeva L.N., Zubenko A.A., Morkovnik A.S., Sochnev V.S., Svyatogorova A.E., Klimenko A.I. (2024) Synthesis of new n-[β-(hetero)arylethyl]benzimidazole-2-carbothioamides and their analogues as anti-Infective agents and compounds with possible neuro(psycho)tropic and anticancer activity. *Russ. J. Gen. Chem.*, 94(2), pp. 341-351. https://doi.org/10.1134/S1070363224020105.

6.   Chikkula K.V., Sundararajan R. (2017) Analgesic, anti-inflammatory, and antimicrobial activities of novel isoxazole/pyrimidine/pyrazole substituted benzimidazole analogs. *Med. Chem. Res.*, 26(11), pp. 3026-3037. https://doi.org/10.1007/s00044-017-2000-0.

7.   Sagnou M., Mavroidi B., Shegani A., Paravatou-Petsotas M., Raptopoulou C., Psycharis V., Pirmettis I., Papadopoulos M.S., Pelecanou M. (2019) Remarkable brain penetration of cyclopentadienyl M(Co)$^{3+}$ (m=99mtc, re) derivatives of benzothiazole and benzimidazole paves the way for their application as diagnostic, with single-photon-emission computed tomography (spect), and therapeutic agents for alzheimer's disease. *J. Med. Chem.*, 62(5), pp. 2638-2650. https://doi.org/10.1021/acs.jmedchem.8b01949.

8.   Mishra G.P., Tripathy S., Pattanayak P. (2024) Novel urea substituted benzimidazole derivatives as anthelmintics: in silico and in vitro approaches. *Russ. J. Bioorg. Chem.*, 50(3), pp. 962-973. https://doi.org/10.1134/S1068162024030221.

9.   Van Oosten, M.J., Silletti S., Guida G., Cirillo V., Di Stasio E., Carillo P., Woodrow P., Maggio A., Raimondi G. (2017) A benzimidazole proton pump inhibitor increases growth and tolerance to salt stress in tomato. *Front. Plant Sci.*, 8, pp. 1-14. https://doi.org/10.3389/fpls.2017.01220.

10.   Shabana K., Salahuddin S., Mazumder A., Kumar R., Datt V., Tyagi S., Yar M.S., Ahsan M.J., Sarafroz M. (2024) Review on the discovery of new benzimidazole derivatives as anticancer agents: synthesis and structure-activity relationship (2010-2022). *Lett. Drug Des. Discov.*, 21(3), pp. 451-479.

11.   Güzel E., Çevik U.A., Evren A.E., Bostanci H.E., Gül U.D., Kayis U., Özkay Y., Kaplancikli Z.A. (2023) Synthesis of benzimidazole-1,2,4-triazole derivatives as potential antifungal agents targeting 14α-demethylase. *ACS Omega*, 8(4), pp. 4369-4384. https://doi.org/10.1021/acsomega.2c07755.

12.   Rostami H., Haddadi M.H. (2022) Benzimidazole derivatives: a versatile scaffold for drug development against helicobacter pylori-related diseases. *Fundam. Clin. Pharmacol.*, 36(6), pp. 930-943. https://doi.org/10.1111/fcp.12810.

13.   Krstulovic L., Rastija V., De Carvalho L.P., Held J., Rajic Z., Zivkovic Z., Bajic M., Glavas-Obrovac L. (2024) Design, synthesis, antitumor, and antiplasmodial evaluation of new 7-chloroquinoline-benzimidazole hybrids. *Molecules*, 29(13), pp. 1-20. https://doi.org/10.3390/molecules29132997.

14. Abdelhafiz A.H.A., Serya R.A.T., Lasheen D.S., Wang N., Sobeh M., Wink M., Abouzid K.A.M. (2022) Molecular design, synthesis and biological evaluation of novel 1,2,5-trisubstituted benzimidazole derivatives as cytotoxic agents endowed with ABCB1 inhibitory action to overcome multidrug resistance in cancer cells. *J. Enzyme Inhib. Med. Chem.*, 37(1), pp. 2710-2724.

15. Chintakunta R., Meka G. (2020) Synthesis, in silico studies and antibacterial activity of some novel 2-substituted benzimidazole derivatives. *Future J. Pharm. Sci.*, 6(1), pp. 1-6. https://doi.org/10.1186/s43094-020-00144-9.

16. Druzhilovskiy D.S., Rudik A.V., Filimonov D.A., Gloriozova T.A., Lagunin A.A., Dmitriev A.V., Pogodin P.V., Dubovskaya V.I., Ivanov S.M., Tarasova O.A., Bezhentsev V.M., Murtazalieva K.A., Semin M.I., Maiorov I.S., Gaur A.S., Sastry G.N., Poroikov V.V. (2017) Computational platform Way2Drug: from the prediction of biological activity to drug repurposing. *Russ. Chem. Bull.*, 66(10), pp. 1832-1841. https://doi.org/10.1007/s11172-017-1954-x.

17. Druzhilovskiy D., Rudik A., Filimonov D., Sastry G.N., Poroikov V. (2018) Way2drug platform – ligand-based approach to drug repurposing. *Abstr. Pap. Am. Chem. Soc.*, 256, pp. 452.

18. Güven O., Menteşe E., Emirik M., Sökmen B.B., Akyüz G. (2023) Benzimidazolone-piperazine/triazole/thiadiazole/furan/thiophene conjugates: Synthesis, in vitro urease inhibition, and in silico molecular docking studies. *Arch. Pharm.*, 356(11), pp. 1-14. https://doi.org/10.1002/ardp.202300336.

19. Chu I., Secours V.E., Valli V.E. (1982) Acute and sub-acute toxicity of octachlorostyrene in the rat. *J. Toxicol. Environ Health*, 10(2), pp. 285-296. https://doi.org/10.1080/15287398209530251.

20. Gebbers J.O., Lotscher M., Kobel W., Portmann R., Laissue J.A. (1986) Acute toxicity of pyridostigmine in rats – histological-findings. *Arch. Toxicol.*, 58(4), pp. 271-275.

21. Liu Z.Y., Dang K., Gao J.H., Fan P., Li C.Z., Wang H., Li H., Deng X.N., Gao Y.C., Qian A.R. (2022) Toxicity prediction of 1,2,4-triazoles compounds by QSTR and interspecies QSTTR models. *Ecotoxicol. Environ. Saf.*, 242, pp. 1-12. https://doi.org/10.1016/j.ecoenv.2022.113839.

22. Unnissa S.H., Rajan D. (2016) Drug design, development and biological screening of pyridazine derivatives. *J. Chem. Pharm. Res.*, 8(8), pp. 999-1004.

23. Fedorova E.V., Buryakina A.V., Zakharov A.V., Filimonov D.A., Lagunin A.A., Poroikov V.V. (2014) Design, synthesis and pharmacological evaluation of novel vanadium-containing complexes as antidiabetic agents. *PLoS One*, 9(7), pp. 1-11. https://doi.org/10.1371/journal.pone.0100386.

24. Wexler P. (2014) Encyclopedia of toxicology (3rd ed.), Cambridge, Massachusetts, ABD, Academic Press., pp. 638-642, ISBN: 978-0-12-386455-0.

25. Poroikov V.V., Filimonov D.A., Gloriozova T.A., Lagunin A.A., Druzhilovskiy D.S., Rudik A.V., Stolbov L.A., Dmitriev A.V., Tarasova O.A., Ivanov S.M., Pogodin P.V. (2019) Computer-aided prediction of biological activity spectra for organic compounds: the possibilities and limitations. *Russ. Chem. Bull.*, 68(12), pp. 2143-2154. https://doi.org/10.1007/s11172-019-2683-0.

26. Ivanov S.M., Lagunin A.A., Rudik A.V., Filimonov D.A., Poroikov V.V. (2018) Adverpred-web service for prediction of adverse effects of drugs. *J. Chem. Inf. Model.*, 58(1), pp. 8-11.

27. Lasure P.P., Munot N.M., Lawande S.S. (2012) Determination of antibacterial activity of punica granatum fruit. *Int. J. Pharm. Sci. Res.*, 3(11), pp. 4421-4424.

28. Li Y., Chen L., Han G.J., Zhou J.H., Zhao Y. (2014) Determination of antibacterial activity of aucubigenin and aucubin. *Asian J. Chem.*, 26(2), pp. 559-561.

29. Judd W.R., Martin C.A. (2009) Antifungal activity of nontraditional antifungal agents. *Curr. Fungal Infect. Rep.*, 3(2), pp. 86-95. https://doi.org/10.1007/s12281-009-0012-z.

30. Campoy S., Adrio J.L. (2017) Antifungals. *Biochem. Pharmacol.*, 133, pp. 86-96.

31. Meadows D.C., Gervay-Hague J. (2006) Source, Targeting HIV. *ChemMedChem.*, 1(1), pp. 16-29. https://doi.org/10.1002/cmdc.200500026.

32. Martrus G., Altfeld M. (2016) Immunological strategies to target HIV persistence. *Curr. Opin. HIV AIDS*, 11(4), pp. 402-408. https://doi.org/10.1097/COH.0000000000000289.

33. Puhl A.C., Demo A.G., Makarov V.A., Ekins S. (2019) New targets for HIV drug discovery. *Drug Discov. Today*, 24(5), pp. 1139-1147. https://doi.org/10.1016/j.drudis.2019.03.013.

34. Amvrosyeva T.V., Votyakov V.I., Vladyko G.V., Andreeva O.T., Vervetchenko S.G., Goretskaya I.S., Klimashevskaya L.M. (1992) On antiviral properties of official drugs. *Antibiot Khimioter*, 37(11), pp. 5-8.

35. Al-Khikani F.H.O., Almosawey H.A.S., Abdullah Y.J., Al-Asadi A.A., Hameed R.M., Hasan N.F., Al-Ibraheemi M.K.M. (2020) Potential antiviral properties of antifungal drugs. *J. Egypt Women Dermatol. Soc.*, 17(3), pp. 185-186. https://doi.org/10.4103/JEWD.JEWD_40_20.

36. Meghana S.K.V.S. (2023) Comparative analysis of antiviral properties of carbohydrates derivatives over commercial antiviral drugs. *Cardiometry*, 25, pp. 1577-1583.

37. Furuyama H., Arii S., Mori A., Imamura M. (2000) Role of E-cadherin in peritoneal dissemination of the pancreatic cancer cell line, Panc-1, through regulation of cell to cell contact. *Cancer Lett.*, 157(2), pp. 201-209. https://doi.org/10.1016/S0304-3835(00)00488-2.

38. Timoumi R., Amara I., Ayed Y., Ben Salem I., Abid-Essefi S. (2020) Triflumuron induces genotoxicity in both mice bone marrow cells and human colon cancer cell line. *Toxicol. Mech. Methods*, 30(6), pp. 438-449. https://doi.org/10.1080/15376516.2020.1758981.

39. Leonessa F., Coialbu T., Toma S. (1986) Different techniques for drug cytotoxicity evaluation on mcf-7 human-breast cancer cell-line. *Anticancer Res.*, 6(6), pp. 1291-1296.

40. Doki Y., Shiozaki H., Tahara H., Inoue M., Oka H., Iihara K., Kadowaki T., Takeichi M., Mori T. (1993) Correlation between e-cadherin expression and invasiveness *in-vitro* in a human esophageal cancer cell-line. *Cancer Res*., 53(14), pp. 3421-3426.

41. Timbrell J.A. (1983) Drug hepatotoxicity. *Br. J. Clin. Pharmacol.*, 15(1), pp. 3-14. https://doi.org/10.1111/j.1365-2125.1983.tb01456.x.

42. Walker R.J., Duggin G.G. (1988) Drug nephrotoxicity. *Annu. Rev. Pharmacol. Toxicol.*, 28, pp. 331-345.

43. Mandel W.J. (1992) Arrhythmias. *Curr. Opin. Cardiol.*, 7(1), pp. 1-2.

44. De Clercq E. (2002) New anti-HIV agents and targets. *Med. Res. Rev.*, 22(6), pp. 531-565.

45. James J.P., Jyothi D., Priya S. (2021) *In silico* screening of phytoconstituents with antiviral activities against sars-cov-2 main protease, nsp12 polymerase, and nsp13 helicase proteins. *Lett Drug. Des. Discov.*, 18(8), pp. 841-857. https://doi.org/10.2174/1570180818666210317162502.

46. Ng T., Cheung R., Wong J., Wang Y., Ip D., Wan D.C.C, Xia J. (2017) Antiviral activities of whey proteins. *Appl. Microbiol. Biotechnol.*, 99(17), pp. 6997-7008. https://doi.org/10.1007/s00253-015-6818-4.

47. Radicchi D.C., Melo A.S., Lima A.P.B., Almeida T.C., De Souza G.H.B., Da Silva G.N. (2022) Naringin: antitumor potential in silico and in vitro on bladder cancer cells. *Ars Pharm.*, 63(2), pp. 132-143. https://doi.org/10.30827/ars.v63i2.22430.

48. Suliman R.S., Alghamdi S.S., Ali R., Rahman I., Alqahtani T., Frah I.K., Aljatli D.A., Huwaizi S., Algheribe S., Alehaideb Z., Islam I. (2022) Distinct mechanisms of cytotoxicity in novel nitrogenous heterocycles: future directions for a new anti-cancer agent. *Molecules*, 27(8), pp. 1-22. https://doi.org/10.3390/molecules27082409.

49. Hosseini M.S., Hadadzadeh H., Mirahmadi-Zare S.Z., Farrokhpour H., Aboutalebi F., Morshedi D. (2023) A curcumin-nicotinoyl derivative and its transition metal complexes: synthesis, characterization, and in silico and *in vitro* biological behaviors. *Dalton Trans.*, 52(40), pp. 14477-14490. https://doi.org/10.1039/d3dt01351k.

50. Tarai S.K., Tarai A., Mandal S., Nath B., Som I., Bhaduri R., Bagchi A., Sarkar S., Biswas A., Moi S.C. (2023) Cytotoxic behavior and DNA/BSA binding activity of thiosemicarbazone based Ni(II) complex: bio-physical, molecular docking and DFT study. *J. Mol. Liq.*, 383, pp. 1-16. https://doi.org/10.1016/j.molliq.2023.121921.

Information about the author:
Fatih İslamoğlu – (corresponding author) – Professor, Recep Tayyip Erdoğan University, Faculty of Science and Arts, Department of Chemistry, 53100 Rize/Turkey, e-mail: fatih.islamoglu@erdogan.edu.tr

A. Bahmani [ID] , M.H. Rajaee [ID] , A. Ebadi [ID] ,
Z. Najafi [ID] , D. Dastan [ID] , G. Chehardoli * [ID]

Hamadan University of Medical Sciences, Hamadan, Iran
*e-mail: cheh1002@gmail.com

Novel 3-benzylbenzo[d]thiazol-2(3H)-iminium salts as potent DNA benzylating agents: design, synthesis, MTT assay, and DFT calculation

Abstract. New derivatives of 3-benzylbenzo[d]thiazol-2(3H)-iminium salt were developed, synthesized, and assessed for their cytotoxic effects on the MCF-7 cell line. Among them, two molecules, identified as 3g and 3i, demonstrated notable cytotoxic activity with IC_{50} values of 41.76 and 58.34 µmol/L respectively, compared to the reference drug Cis-platin, which has an IC_{50} of 22.36 ± 2.98 µmol/L. Subsequent DNA interaction docking studies were conducted with these compounds. The docking data revealed that both 3g and 3i effectively bind within the minor groove of DNA, showing a preference for interaction with AT-rich sequences over CG-rich sequences. These findings suggest that 3g and 3i are effective DNA-binding agents. Further analysis using Density Functional Theory (DFT) was performed to explore the potential of DNA benzylation by compound 3g. The DFT studies suggested that the benzylation of guanine bases by 3g could occur at room temperature. Nonetheless, further experimental investigations are necessary to validate this hypothesis. The DFT studies suggested that the benzylation of guanine bases by 3g could occur at room temperature. Nonetheless, further experimental investigations are necessary to validate this hypothesis.
Key words: 3-Benzylbenzo[d]thiazol-2(3H)-iminium salt, cytotoxic, DNA interaction, cancer, 2-Aminobenzothiazol.

Introduction

Benzothiazole (BTA) is a bicyclic heterocycle consisting of a 1,3-thiazole ring attached to a benzene ring. BTA is found in many natural products and is responsible for many medicinal and pharmacological properties [1]. BTA scaffold has a wide range of biological activities such as antidiabetic [2], fungicidal [3], antileishmanial [4], anti-Alzheimer [5], anticonvulsants [6], antituberculosis [7], antibacterial [8], and anthelmintic [9], etc., schematically presented on Figure 1.

Also, BTA derivatives exhibit prevalent and remarkable cytotoxic effects against some types of tumors and cancer cell lines e.g. human colon adenocarcinoma cell line (SW480), human cervical cancer cell line (HeLa), human liver carcinoma cells (HepG2) [10], nonsmall-cell lung, colon [11], human breast cancer cell line (MCF-7) [12], and hepatocellular carcinoma (HCC) [13] and so on. The

sentences are only a very small part of the biological applications of BTA derivatives. Therefore, researchers are very interested in synthesizing new derivatives based on BTA and evaluating their medicinal properties.

DNA benzylating agent can be defined as a compound capable of covalently attaching a benzyl group to the DNA nucleobases under the physiological conditions. In this reaction, compounds always behave as carbon electrophiles and some nitrogen or oxygen atoms of DNA nucleobases are nucleophiles [14, 15]. Both structure and dynamics of DNA are seriously changed by benzylation of its nucleobases. As a result, DNA strand undergoes structural deformations that affect both replication and/or transcription stages. Benzylation also induces the mispairing of the nucleobases by change of the natural hydrogen bonding between the bases. Therefore, benzylating agents can destroy cancer cells by damaging their DNA [16].
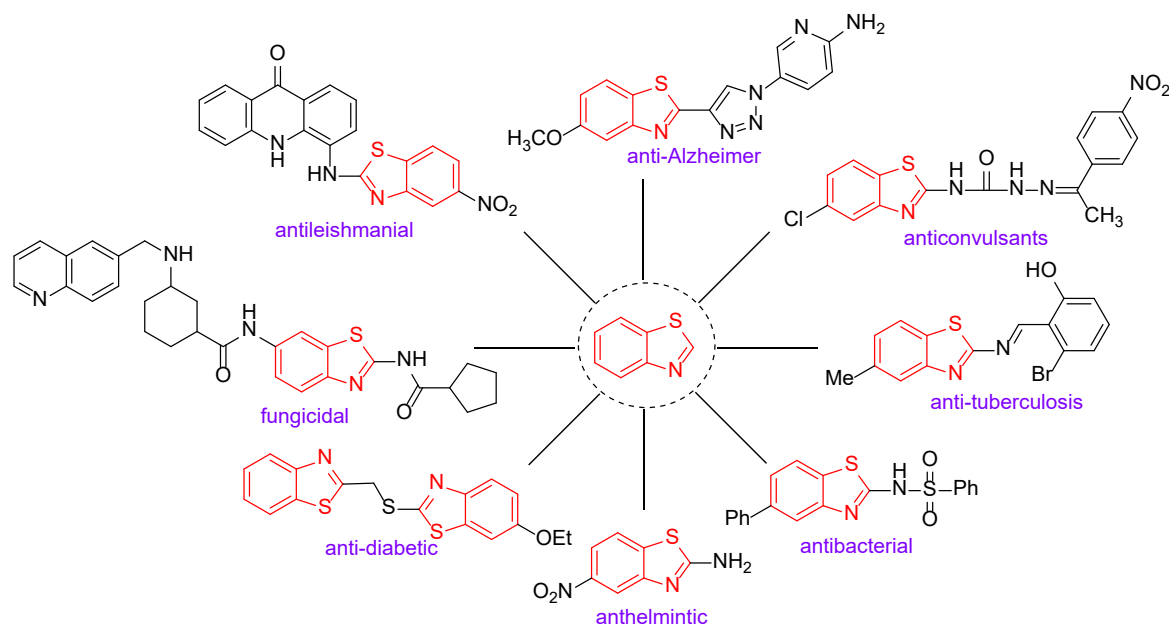
Figure 1 – Some biologically active compounds with benzothiazole scaffold

In continuation of our investigations on biologically active heterocyclic compounds [17-20], mainly the synthesis of cytotoxic compounds [21-23], new 3-benzylbenzo[*d*]thiazol-2(3*H*)-iminium salt derivatives are synthesized, characterized and evaluated for their cytotoxic activities.

Materials and methods

Chemistry
Synthesis of 3-benzylbenzo[d]thiazol-2(3H)-iminium salts: General procedure

In a 50 ml round bottom flask, a solution was prepared by dissolving 13.7 mmol of 2-aminobenzothiazole derivatives and 18.2 mmol of benzyl halide derivatives in 25 ml of n-butanol, to which one mmol of sodium iodide was subsequently added. This mixture was then subjected to reflux for a duration of 8 hours. Monitoring of the reaction's progress was conducted using thin layer chromatography (TLC) employing a solvent system composed of equal parts *n*-hexane and ethyl acetate. Following the reaction, the mixture was filtered to collect any solids, which were then washed with water and crystallized using methanol.

Spectral data were collected for the resulting products:

3a*: 3-Benzyl Benzo [d] Thiazol-2(3H)-Iminium Bromide*

^{1}H NMR (301 MHz, DMSO d$_6$) δ: 10.56 (2H, s), 8.06 (1H, d, *J* = 8.1 Hz), 7.55 (1H, d, *J* = 8.0 Hz), 7.26-7.38 (5H, d, *J* = 7.2 Hz), 5.66 (d, *J* = 7.9 Hz, 2H), 3.16 (2H, s). IR-KBr(cm^{-1}) *v*: 3263, 3078, 1663, 1558 and 1470; MS m/z (%): 320.0.

3b*: 3-(4-Fluorobenzyl) Benzo [d] Thiazol-2(3H)-Iminium Chloride*

^{1}H NMR (301 MHz, DMSO d$_6$) δ: 11.21 (2H, s), 8.04 (1H, d, *J* = 7.9 Hz), 7.60 (1H, d, *J* = 8.0 Hz), 7.18-7.42 (4H, d, *J* = 7.5 Hz), 5.66 (2H, d, *J* = 7.9 Hz), 3.16 (2H, s). IR-KBr(cm^{-1}) *v*: 1650, 1566.85 and 1472; MS m/z (%): 294.0.

3c*: 3-(4-Chlorobenzyl) Benzo [d] Thiazol-2(3H)-Iminium Chloride*

^{1}H NMR (301 MHz, DMSO d$_6$) δ: 11.06 (2H, s), 8.02 (1H, d, *J* = 8.1 Hz), 7.57 (1H, d, *J* = 8.0 Hz), 7.30-7.49 (4H, d, *J* = 7.2 Hz), 5.74 (2H, d, *J* = 7.9 Hz), 3.42 (2H, s). IR-KBr(cm^{-1}) *v*: 1644, 1564 and 1471; MS m/z (%): 310.0.

3d*: 3-(4-Methylbenzyl) Benzo [d] Thiazol-2(3H)-Iminium Chloride*

^{1}H NMR (301 MHz, DMSO d$_6$) δ: 11.39 (2H, s), 8.03 (d, *J* = 7.8 Hz, 1H), 7.66 (d, *J* = 7.7 Hz, 1H), 7.31-7.51 (d, *J* = 7.4 Hz, 4H), 7.17 (d, *J* = 7.7 Hz, 2H), 3.40 (2H, s), 2.30 (3H, s). IR-KBr(cm^{-1}) *v*: 3293, 1644, 1566 and 1469; MS m/z (%): 290.1.

3e*: 3-Benzyl-5-Methylbenzo [d] Thiazol-2(3H)-Iminium Bromide*

^{1}H NMR (301 MHz, DMSO d$_6$) δ: 10.39 (2H, s), 7.84 (1H, d, *J* = 7.7 Hz), 7.46 (1H, d, *J* = 7.7 Hz), 7.25-7.40 (5H, d, *J* = 7.3 Hz), 5.61 (2H, d, *J* = 7.7 Hz), 3.20 (2H, s), 2.42 (3H, s). IR-KBr(cm^{-1}) *v*: 3457, 1632, 1566 and 1487; MS m/z (%): 334.2.

***3f*: 3-(4-Fluorobenzyl)-5-Methylbenzo [d] Thiazol-2(3H)-Iminium Chloride**

^{1}H NMR (301 MHz, DMSO d$_6$) δ: 11.06 (2H, s), 7.83 (1H, d, J = 7.4 Hz), 7.51 (1H, d, J = 7.5 Hz), 7.18-7.42 (5H, d, J = 7.2 Hz), 5.75 (2H, d, J = 7.4 Hz), 4.02 (2H, s), 2.52 (3H, s). IR-KBr(cm^{-1}) v: 1637, 1566 and 1454; MS m/z (%): 308.2.

***3g*: 3-(4-Chlorobenzyl)-5-Methylbenzo [d] Thiazol-2(3H)-Iminium Chloride**

^{1}H NMR (301 MHz, DMSO d$_6$) δ: 11.01 (2H, s), 7.82 (1H, d, J = 7.5 Hz), 7.45 (1H, d, J = 7.4 Hz), 7.28-7.42 (4H, d, J = 7.4 Hz), 5.79 (2H, d, J = 7.6 Hz), 3.40 (2H, s), 2.52 (3H, s). IR-KBr(cm^{-1}) v: 1650, 1568 and 1490; MS m/z (%): 324.0.

***3h*: 5-Methyl-3-(4-Methylbenzyl) Benzo [d] Thiazol-2(3H)-Iminium Chloride**

^{1}H NMR (301 MHz, DMSO d$_6$) δ: 11.01 (2H, s), 7.81 (1H, d, J = 7.4 Hz), 7.43 (1H, d, J = 7.4 Hz), 7.31-7.16 (4H, d, J = 7.3 Hz), 5.67 (2H, d, J = 7.4 Hz), 3.38 (2H, s), 2.51 (6H, s). IR-KBr(cm^{-1}) v: 1647, 1574 and 1488; MS m/z (%): 304.1.

***3i*: 3-Benzyl-5-Ethoxybenzo [d] Thiazol-2(3H)-Iminium Chloride**

^{1}H NMR (301 MHz, DMSO d$_6$) δ: 10.41 (2H, s), 7.76 (1H, d, J = 7.5 Hz), 7.49 (1H, d, J = 7.4 Hz), 7.03-7.39 (5H, d, J = 7.4 Hz), 5.66 (2H, d, J = 7.5 Hz), 4.01 (2H, s), 2.53 (3H, t), 1.31 (2H, m). MS m/z (%): 320.

***3j*: 5-Ethoxy-3-(4-Fluorobenzyl) Benzo [d] Thiazol-2(3H)-Iminium Chloride**

^{1}H NMR (301 MHz, DMSO d$_6$) δ: 10.87 (2H, s), 7.88 (1H, d, J = 7.4 Hz), 7.48 (1H, d, J = 7.5 Hz), 7.04-7.37 (4H, d, J = 7.7 Hz), 5.69 (2H, d, J = 7.3 Hz), 4.03 (2H, s), 2.00 (3H, t), 1.31 (2H, m). IR-KBr(cm^{-1}) v: 1644, 1576 and 1490; MS m/z (%): 338.2.

***3k*: 5-Ethoxy-3-(4-Methylbenzyl) Benzo [d] Thiazol-2(3H)-Iminium Chloride**

^{1}H NMR (301 MHz, DMSO d$_6$) δ: 10.89 (2H, s), 7.68 (1H, d, J = 7.2 Hz), 7.47 (1H, d, J = 7.3 Hz), 7.02-7.23 (4H, d, J = 7.3 Hz), 5.66 (2H, d, J = 7.2 Hz), 4.02 (2H, s), 2.30 (t, 6H), 1.33 (2H, m). IR-KBr(cm^{-1}) v: 1648, 1563 and 1488; MS m/z (%): 334.

***3l*: 3-(4-Chlorobenzyl)-5-Ethoxybenzo [d] Thiazol-2(3H)-Iminium Chloride**

^{1}H NMR (301 MHz, DMSO d$_6$) δ: 10.98 (2H, s), 7.67 (1H, d, J = 7.4 Hz), 7.47 (1H, d, J = 7.4 Hz), 7.03-7.36 (4H, d, J = 7.2 Hz), 5.72 (2H, d, J = 7.3 Hz), 4.03 (2H, s), 2.53 (t, 6H), 1.34 (2H, m).

MTT assay

Studies on cell viability were conducted using the MCF-7 breast cancer cell line. These cells were cultured in DMEM high glucose medium supplemented with 10% Fetal Bovine Serum (FBS) and 1% penicillin-streptomycin, maintained in an environment of 95% humidity and 5% CO$_2$. The viability of the cells was assessed using an MTT assay. Initially, 1.0×10^4 MCF-7 cells were seeded in each well of a 96-well plate and allowed to incubate for 16 hours. Various concentrations of compounds (**3a-l**) ranging from 12.5 to 100 μM were then exposed to the cells for a duration of 72 hours. Subsequently, each well received an MTT solution at a concentration of 0.50 mg/ml, followed by an additional incubation period of 4 hours under the same conditions. After this period, the culture medium was removed, and the formazan precipitate was dissolved in 100 μL of pure DMSO. The absorbance was measured using a BMG Spectro Nano Elizabeth Reader at wavelengths of 570 nm and 630 nm, which correspond to formazan and background absorbance respectively. Cell viability was quantified using the formula: Cell viability % = [AT (sample) / AT (control)] × 100, where AT represents the adjusted absorbance (A570 – A30).

The mean viability percentage along with the standard deviation was calculated from three independent experiments. The IC$_{50}$ values were calculated using GraphPad Prism version 9.0 software.

Molecular docking studies

Docking simulations were accomplished by AutoDock 4.2 software according to the conditions mentioned in our previously reported paper [22].

DFT calculation

Density functional theory (DFT) calculations were done using the ORCA quantum chemistry package [24]. The structure of compound 3g, guanine, and Chlormethine were optimized with the BP86 functional applying RI approximation and a TZVP basis set together with a matching auxiliary basis set (TZV/J). Numerical frequency was calculated at the same level. Initial guess of the transition state (TS) was based on the S$_N$2 mechanism. Single point energy calculations were done with the PW6B95 method by applying Def2-TZVP basis set.

Results and discussion

Chemistry

The preparation reaction of 3-benzylbenzo[*d*]thiazol-2(3*H*)-iminium salt derivatives (**3a-l**) is shown on Figure 2. In the presence of NaI as catalyst, various 2-aminobenzothiazoles (1) and benzyl halides (2) react under the reflux of *n*-butanol to obtain the desired products **3a-l** (moderate to good yields).

New 3-benzylbenzo[*d*]thiazol-2(3*H*)-iminium salts were characterized by IR, ¹H NMR, and mass spectroscopy. Figure 3 presents the ¹H NMR spectrum of 3-benzyl-5-ethoxybenzo[*d*]thiazol-2(3*H*)-iminium bromide (**3i**) as a model compound. A triplet peak at 1.29-1.34 ppm corresponds to the -CH₃ group and a quartet peak at 3.99-4.06 ppm belongs to the CH₂ of ethyl group. The peak related to benzylic CH₂ appeared in the region of 5.66 ppm as a singlet and with integral 2. The peaks of the aromatic protons appeared

in 7.3 to 7.76 ppm as multiplets and with integral 8. The peak related to NH₂ protons appeared in the region of 10.41 ppm as a broad peak with integral 2. The use of D₂O solvent during spectroscopy caused the peak of this region to be removed, which proves that these peaks are related to hydrogens attached to N.

Although we expected the benzyl group to be attached to NH₂, this group was attached to the nitrogen of the benzothiazole ring. Products out of salt form were nowhere to be found.

3a: R₁=H , R₂=H, X= Br
3b: R₁=H , R₂=F, X= Cl
3c: R₁=H , R₂=Cl, X= Cl
3d: R₁=H , R₂=CH₃, X= Cl
3e: R₁=CH₃ , R₂=H, X= Br
3f: R₁=CH₃ , R₂=F, X= Cl
3g: R₁=CH₃ , R₂=Cl, X= Cl
3h: R₁=CH₃ , R₂=CH₃, X= Cl
3i: R₁=OEt , R₂=H, X= Br
3j: R₁=OEt , R₂=F, X= Cl
3k: R₁=OEt , R₂=CH₃, X= Cl
3l: R₁=OEt , R₂=Cl, X= Cl
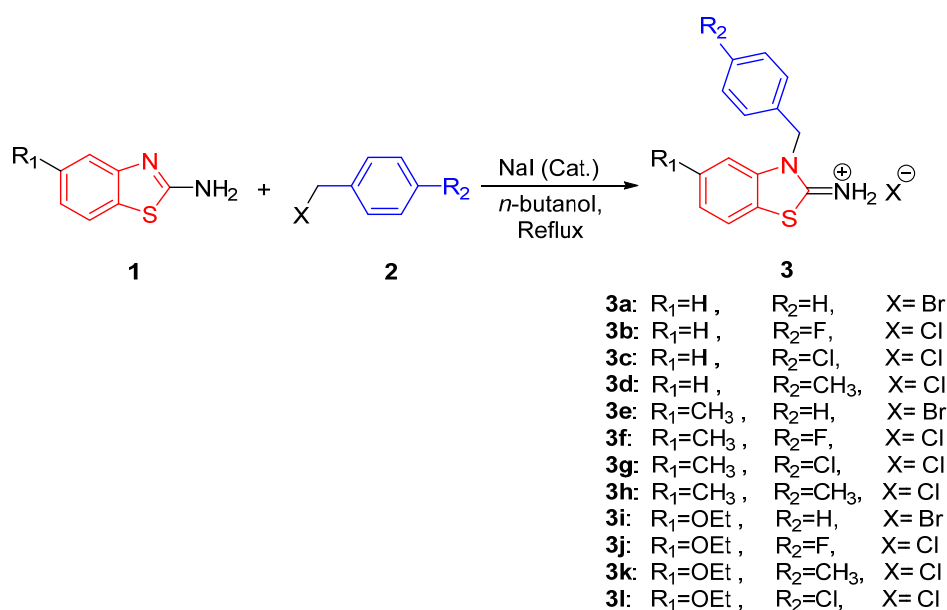
Figure 2 – Synthesis of 3-benzylbenzo[*d*]thiazol-2(3*H*)-iminium salt derivatives (3a-l)
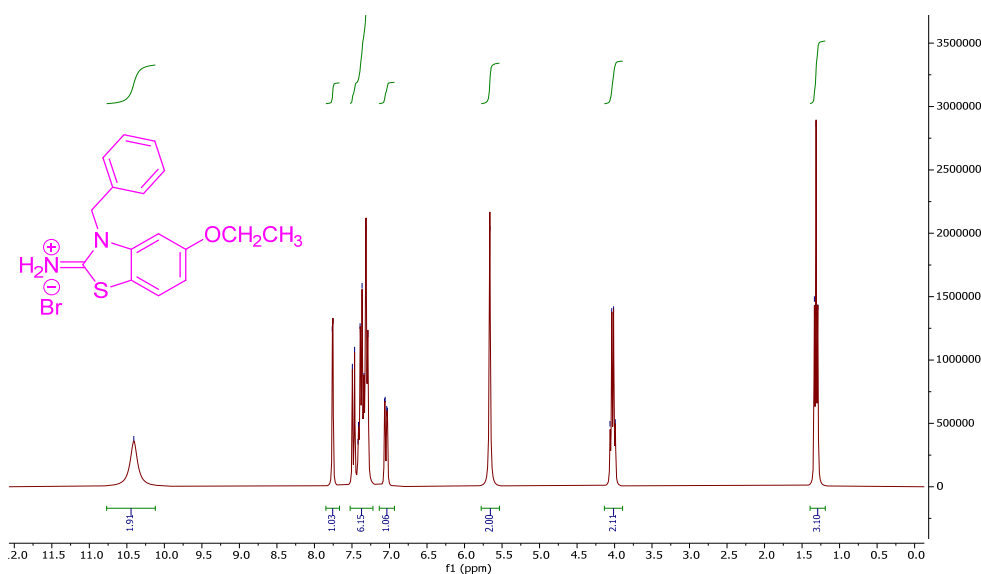
Figure 3 – ¹H NMR spectrum of 3-benzyl-5-ethoxybenzo[*d*]thiazol-2(3*H*)-iminium bromide (**3i**)

MTT assay

Table 1 details our findings on the antitumor efficacy of derivatives **3a-3l** of 3-benzylbenzo[*d*]thiazol-2(3*H*)-iminium salt against the MCF-7 human breast cancer cell line. Among these, only compounds **3g** and **3i** demonstrated notable activity, with IC_{50} values of 41.76 μmol/L and 58.34 μmol/L respectively, when compared to the reference anticancer drug Cis-platin, which has an IC_{50} value of 22.36 μmol/L. Specifically, the compound 3-(4-chlorobenzyl)-5-methylbenzo[d]thiazol-2(3*H*)-iminium chloride (**3g**), featuring a chlorine atom at the 4 position on the benzyl and a methyl group at the 5 position of the benzothiazole ring, showed a greater antiproliferative effect than 3-benzyl-5-ethoxybenzo[d]thiazol-2(3H)-iminium bromide (**3i**). The other derivatives did not exhibit significant cytotoxic effects, making it impractical to assess the impact of different substituents on the benzothiazole ring.

Molecular modeling studies

In silico study of the ligand-DNA interaction is one of the most essential aspects of medicinal chemistry researches with the aim of discovering and developing new kinds of anti-cancer drugs [25]. In this regard, we investigated the interactions of **3g** and **3i** with DNA.

Using docking software, we studied the binding of **3g** and **3i** with two DNA chains, 1CGC [decamer of the repeated Cytosine-Guanine d(CCGGCGCCGG)] and 1DNE [dodecamer of two repeats of Adenine-Thymine d(CGCGATATCGCG)] [26]. The results are shown in Table 2. These compounds interacted with the minor groove of DNA. Each amino group of these compounds had a hydrogen bond with the ribose ring of the DNA. The benzylic group was placed along the minor groove and participated in van der Waals interactions.

Table 3 shows the free energy DNA-binding values (ΔG) of the ligands. **3g** interacted more effectively than **3i** with the minor groove and penetrated the groove better. The affinity of both compounds to the AT-rich chain was higher than to the CG-rich chain. We compared the free energy binding values of **3g** and **3i** with pyriproxyfen [22]. The results showed that **3g** binds to 1DNA better than others. However, pyriproxyfen establishes a better binding with 1CGC than **3g** and **3i**.

Table 1 – The IC_{50} values of the complexes

Ligand	IC_{50} (μM)
3a	>100
3b	>100
3c	>100
3d	>100
3e	>100
3f	>100
3g	41.76 ± 2.26
3h	>100
3i	58.34 ± 2.59
3j	>100
3k	>100
3l	>100
Cis-platin	22.36 ± 2.98

Based on the results of docking, we concluded that 3-benzylbenzo[*d*]thiazol-2(3*H*)-iminium salt derivatives have the capability to form a stable ligand-DNA complex. Because of the positive charge, the hydrophilicities of the ligands are low (ClogP less than 0.5), and it increases the probability of interaction with the DNA chain rich in negative charge. Of course, the effect of the hydrophilicity of these derivatives in passing through the cell membrane should be evaluated biologically.

Table 2 – 3D and 2D interactions of two **3g** and **3i** with CG and AT-rich DNA chains
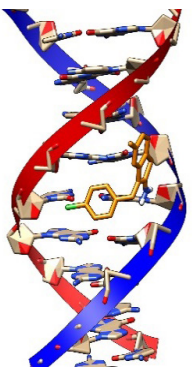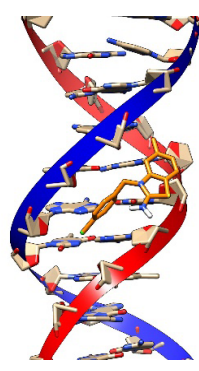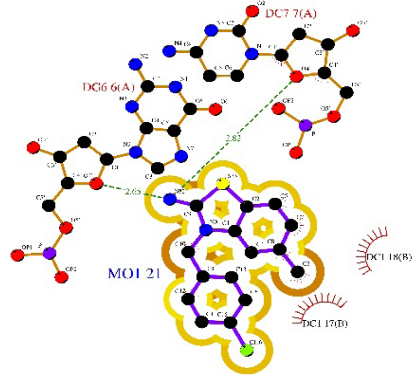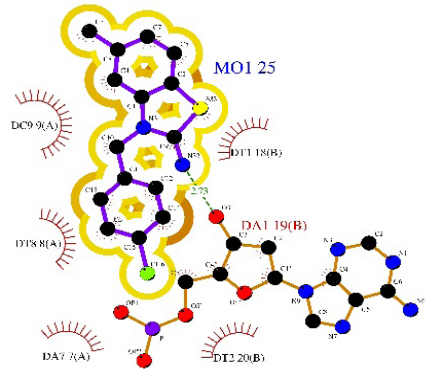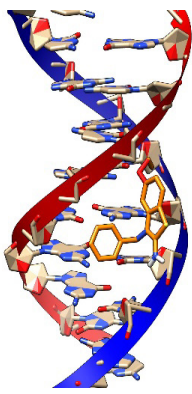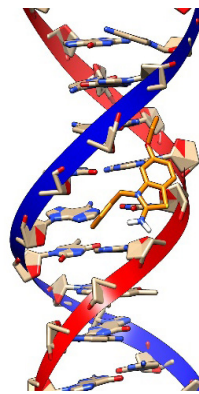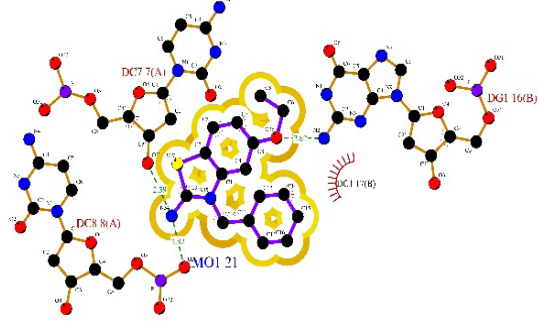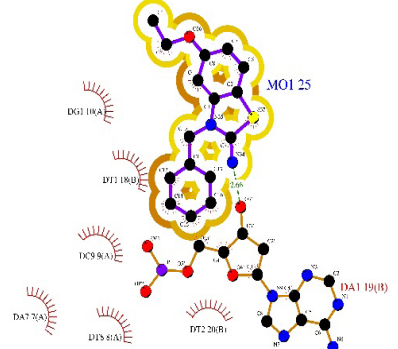
Ligand	1CGC	1DNE
3g		
3i		

Table 3 – Free energy (Kcal mol^{-1}) DNA-binding of **3g, 3i** and pyriproxyfen

Ligand	Strand rich in AT (1DNE)	Strand rich in CG (1CGC)
	Free energy of binding	Free energy of binding
3g	-6.96	-5.58
3i	-6.26	-4.98
Pyriproxyfen	-6.7	-7.4

Table 4 – Calculated LE amounts of **3g**, **3i** and pyriproxyfen

Ligand	Strand rich in AT (1DNE)	Strand rich in CG (1CGC)
	LE	LE
3g	0.36	0.29
3i	0.31	0.25
Pyriproxyfen	0.27	0.3

Ligand efficiency (LE) displays the ability of the ligands to interact to the receptor, which is calculated through the below equation [27]:

$$LE = \frac{\Delta G}{N}$$, N= Number of non-hydrogen atoms

Calculated LE values of **3g**, **3i** and pyriproxyfen (as a DNA-binding model) are shown in Table 4.

The LE calculated for **3g**-1DNE is 0.36 which is more than the LEs of compounds **3i** and pyriproxyfen, but LE calculated for **3g**-1CGC and **3i**-1CGC is lower than the LE of pyriproxyfen. These results show that compound **3g** has good ability to bind to AT-rich strand of DNA. After docking, this question occurred for us considering the structure of the products, will they be able to act as DNA benzylating agents? (Figure 4).
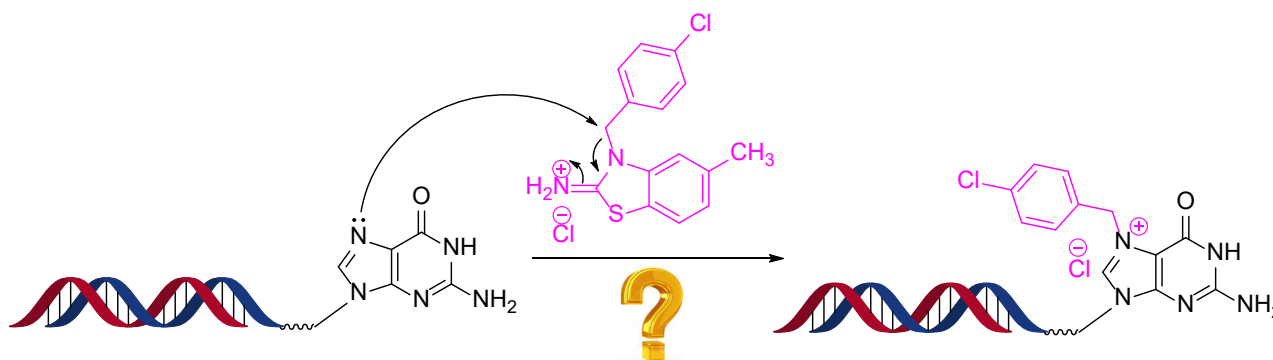
Figure 4 – Will the **3g** derivative be able to act as a DNA benzylating agent?

To answer this question, we performed DFT calculations on the compound **3g** as the most effective compound in the MTT test. DFT calculation resembled the S_N^2 attack of guanine N7 atom to benzylic carbon of compound **3g** (Figure 5).

Chlormethine, as aliphatic nitrogen mustard, was used for comparison. The transition state of the reaction was confirmed by single negative frequency. The energy of TS for the reaction of Chlormethine and guanine was 3.72 kcal/mol more stable than the starting material. The stability of transition state in comparison to starting material indicates the high reactivity of Chlormethine that is in accordance to the clinical activity of the drug. On the other hand, the TS of the compound **3g** located 18.59 kcal/mol upper than the compound and guanine. The obtained results indicated that reaction between compound 3g and guanine could take place in room temperature (activation energy less than ~20 kcal/mol) but in comparison to Chlormethine the reaction rate is slow.

Molecular study indicated that the designed compound **3g** could bind to DNA strands. Also, DFT calculation indicated that compound **3g** could alkylate the guanine in room temperature.
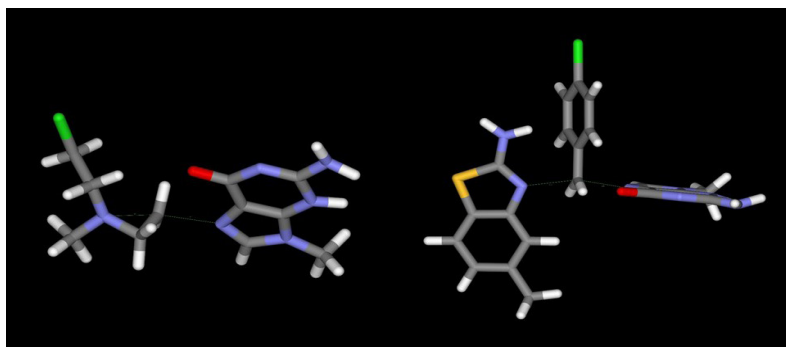
Figure 5 – TS of reaction between Chlormethine and compound 3g with guanine nucleobase.
In first case ring opening reaction leads to alkylation of guanine.
In second case, the benzylation of guanine takes places

Conclusion

We synthesized twelve new 3-benzylbenzo[*d*]thiazol-2(3*H*)-iminium salt derivatives. Then we used them in the MTT assay against the MCF-7 cell line (human breast cancer). Among all products, only two compounds **3g** and **3i** have significant cytotoxic effects against MCF-7 with IC$_{50}$ values of 41.76 and 58.34 μmol/L respectively, compared to the Cis-platin as an anti-cancer drug (IC$_{50}$ value 22.36 μmol/L). Then we performed molecular docking simulations on the DNA interactions of these ligands. Based on the results, these compounds can interact well with the minor groove of DNA. Of course, the interaction of the ligands with the AT-rich chain (1DNE) was better than the CG-rich chain (1CGC). Therefore, it can be concluded that **3g** and **3i** are suitable interactors with DNA. DFT calculation showed compound **3g** can benzylate the guanine base of DNA. However, Proving the DNA benzylation ability of these compounds requires experimental studies.

Acknowledgements

Conflict of interest

All authors are aware of the article's content and declare no conflict of interest.

References

1. Irfan A., Batool F., Zahra Naqvi S.A., Islam A., Osman S.M., Nocentini A., et al. (2020) Benzothiazole derivatives as anticancer agents. *J. Enzyme Inhib. Med. Chem.*, 35, pp. 265-279. https://doi.org/10.1080/14756366.2019.1698036.
2. Meltzer-Mats E., Babai-Shani G., Pasternak L., Uritsky N., Getter T., Viskind O., et al. (2013) Synthesis and mechanism of hypoglycemic activity of benzothiazole derivatives. J. Med. Chem., 56, pp. 5335-5350. https://doi.org/10.1021/jm4001488.
3. Liu Y., Wang Y., Dong G., Zhang Y., Wu S., Miao Z., et al. (2013) Novel benzothiazole derivatives with a broad antifungal spectrum: Design, synthesis and structure–activity relationships. *Med. Chem. Comm.*, 4, pp. 1551-1561. https://doi.org/10.1039/C3MD00215B.
4. Delmas F., Avellaneda A., Di Giorgio C., Robin M., De Clercq E., Timon-David P., et al. (2004) Synthesis and antileishmanial activity of (1, 3-benzothiazol-2-yl) amino-9-(10H)-acridinone derivatives. *Eur. J. Med. Chem.*, 39, pp. 685-690. https://doi.org/10.1016/j.ejmech.2004.04.006.
5. Wongso H., Ono M., Yamasaki T., Kumata K., Higuchi M., Zhang M.-R., et al. (2023) Synthesis and structure–activity relationship (SAR) studies of 1, 2, 3-triazole, amide, and ester-based benzothiazole derivatives as potential molecular probes for tau protein. *RSC Med. Chem.*, 14(5), pp. 858–868. https://doi.org/10.1039/D2MD00358A.
6. Siddiqui N., Rana A., Khan S.A., Bhat M.A., Haque S.E. (2007) Synthesis of benzothiazole semicarbazones as novel anticonvulsants—The role of hydrophobic domain. *Bioorg. Med. Chem. Lett.*, 17, pp. 4178-4182. https://doi.org/10.1016/j.bmcl.2007.05.048.
7. Suyambulingam J.K., Karvembu R., Bhuvanesh N.S., Enoch I.V.M.V., Selvakumar P.M., Premnath D., et al. (2020) Synthesis, structure, biological/chemosensor evaluation and molecular docking studies of aminobenzothiazole Schiff bases. *J. Adhes. Sci. Technol.*, 34, pp. 2590-2612. https://doi.org/10.1080/01694243.2020.1775032.
8. Ikpa C.B., Onoja S.O., Okwaraji A.O. (2020) Synthesis and antibacterial activities of benzothiazole derivatives of sulphonamides. *Acta Chem. Malays.*, 4, pp. 55-57. https://doi.org/10.2478/acmy-2020-0009.

9.   Gill R.K., Rawal R.K., Bariwal J. (2015) Recent advances in the chemistry and biology of benzothiazoles. *Arch. Pharm*., 348, pp. 155-178. https://doi.org/10.1002/ardp.201400340.

10.   Shi X.-H., Wang Z., Xia Y., Ye T.-H., Deng M., Xu Y.-Z., et al. (2012) Synthesis and biological evaluation of novel benzothiazole-2-thiol derivatives as potential anticancer agents. *Molecules*, 17, pp. 3933-3944. https://doi.org/10.3390/molecules17043933.

11.   Mortimer C.G., Wells G., Crochard J.P., Stone E.L., Bradshaw T.D., Stevens M.F., et al. (2006) Antitumor benzothiazoles. 26. 2-(3, 4-Dimethoxyphenyl)-5-fluorobenzothiazole (GW 610, NSC 721648), a simple fluorinated 2-arylbenzothiazole, shows potent and selective inhibitory activity against lung, colon, and breast cancer cell lines. *J. Med. Chem*., 49, pp. 179-185. https://doi.org/10.1021/jm050942k.

12.   Al-Sanea M.M., Hamdi A., Mohamed A.A., El-Shafey H.W., Moustafa M., Elgazar A.A., et al. (2023) New benzothiazole hybrids as potential VEGFR-2 inhibitors: design, synthesis, anticancer evaluation, and in silico study. *J. Enzyme Inhib. Med. Chem*., 38, pp. 2166036. https://doi.org/10.1080/14756366.2023.2166036.

13.   Baffy G. (2012) hepatocellular carcinoma in type 2 diabetes: more than meets the eye. *Am. J. Gastroenterol.*, 107, pp. 53-55. https://doi.org/10.1038/ajg.2011.390.

14.   Peterson L.A. (1997) *N*-Nitrosobenzylmethylamine Is Activated to a DNA Benzylating Agent in Rats. *Chem. Res. Toxicol.*, 10, pp. 19-26. https://doi.org/10.1021/tx9601014.

15.   Rasimas J.J., Dalessio P.A., Ropson I.J., Pegg A.E., Fried M.G. (2004) Active-site alkylation destabilizes human O6-alkylguanine DNA alkyltransferase. *Protein Sci.*, 13, pp. 301-305. https://doi.org/10.1110/ps.03319404.

16.   Avendaño, C. and Menéndez, J.C. (2015) Medicinal Chemistry of Anticancer Drugs. 2nd Edition, Amsterdam: Elsevier, 305 p.

17.   Babaee S., Chehardoli G., Akbarzadeh T., Zolfigol M.A., Mahdavi M., Rastegari A., et al. (2021) Design, Synthesis, and Molecular Docking of Some Novel Tacrine Based Cyclopentapyranopyridine-and Tetrahydropyranoquinoline-Kojic Acid Derivatives as Anti-Acetylcholinesterase Agents. *Chem. Biodivers*., 18, pp. e2000924. https://doi.org/10.1002/cbdv.202000924.

18.   Bahmani A., Najafi Z., Chehardoli G. (2022) Curcumin-Derived Heterocycles as Anticancer Agents. A Systematic Review. *Org. Prep. Proced. Int*., 54, pp. 493-510. https://doi.org/10.1080/00304948.2022.2094659.

19.   Chehardoli G., Bahmani A. (2021) Synthetic strategies, SAR studies, and computer modeling of indole 2 and 3-carboxamides as the strong enzyme inhibitors: a review. *Mol. Divers*., 25, pp. 535-550. https://doi.org/10.1007/s11030-020-10061-x.

20.   Najafi Z., Kamari-aliabadi A., Sabourian R., Hajimahmoodi M., Chehardoli G. (2022) Synthesis and molecular modeling of new 2-benzylidenethiobarbituric acid derivatives as potent tyrosinase inhibitors agents. *J. Chin. Chem. Soc*., 69, pp. 692-702. https://doi.org/10.1002/jccs.202100537.

21.   Ebadi A., Karimi A., Bahmani A., Najafi Z., Chehardoli G. (2024) Novel Xanthene-1, 8-dione Derivatives Containing the Benzylic Ether Tail as Potent Cytotoxic Agents: Design, Synthesis, In Vitro, and In Silico Studies. *J. Chem.*, 2024(1), pp. 6612503. https://doi.org/10.1155/2024/6612503.

22.   Ebadi A., Najafi Z., Pakdel-yeganeh H., Dastan D., Chehardoli G. (2022) Design, synthesis, molecular modeling and DNA-binding studies of new barbituric acid derivatives. *J. Iran. Chem. Soc.*, 19, pp. 3887-3898. https://doi.org/10.1007/s13738-022-02576-x.

23.   Mahdian M., Ebadi A., Bahmani A., Dastan D., Zolfigol M.A., Chehardoli G. (2023) Synthesis, Molecular Modeling, and Biological Evaluation of New N-(Benzo [d] thiazol-2-yl)-3-amino-but-2-enamide Derivatives as Cytotoxic Agents. *Org. Prep. Proced. Int*., 56, pp. 292-301. https://doi.org/10.1080/00304948.2023.2260727.

24.   Neese F. (2012) The ORCA program system. *WIREs Comput. Mol. Sci*., 2, pp. 73-78. https://doi.org/10.1002/wcms.81.

25.   Tavakolinia F., Baghipour T., Hossaini Z., Zareyee D., Khalilzadeh M.A., Rajabi M. (2012) Antiproliferative activity of novel thiopyran analogs on MCF-7 breast and HCT-15 colon cancer cells: synthesis, cytotoxicity, cell cycle analysis, and DNA-binding. *Nucleic Acid Ther*., 22, pp. 265-270. https://doi.org/10.1089/nat.2012.0346.

26.   Mary V., Haris P., Varghese M.K., Aparna P., Sudarsanakumar C. (2017) Experimental probing and molecular dynamics simulation of the molecular recognition of DNA duplexes by the flavonoid luteolin. *J. Chem. Inf. Model.*, 57, pp. 2237-2249. *doi:* 10.1021/acs.jcim.6b00747.

27. Hopkins A.L., Keserü G.M., Leeson P.D., Rees D.C., Reynolds C.H. (2014) The role of ligand efficiency metrics in drug discovery. *Nat. Rev. Drug Discov*., 13, pp. 105-121. https://doi.org/10.1038/nrd4163.

Information about authors:

Asrin Bahmani – PhD, Researcher, Department of Medicinal Chemistry, School of Pharmacy, Medicinal Plants and Natural Products Research Center, Hamadan University of Medical Sciences, Hamadan, Iran, e-mail: asrin.bahmani@gmail.com

Mohammad Hosein Rajaee – Pharm-D, Researcher, Department of Medicinal Chemistry, School of Pharmacy, Medicinal Plants and Natural Products Research Center, Hamadan University of Medical Sciences, Hamadan, Iran, e-mail: hosein.r101@gmail.com

Ahmad Ebadi – Associate Professor, Department of Medicinal Chemistry, School of Pharmacy, Medicinal Plants and Natural Products Research Center, Hamadan University of Medical Sciences, Hamadan, Iran, e-mail: ahmadebadie@gmail.com

Zahra Najafi – Associate Professor, Department of Medicinal Chemistry, School of Pharmacy, Medicinal Plants and Natural Products Research Center, Hamadan University of Medical Sciences, Hamadan, Iran, e-mail: najafi.zch@gmail.com

Dara Dastan – Associate Professor, Department of Medicinal Chemistry, School of Pharmacy, Hamadan University of Medical Sciences, Hamadan, Iran, e-mail: dara962@gmail.com

Gholamabbas Chehardoli – (corresponding author) – Professor, Department of Medicinal Chemistry, School of Pharmacy, Medicinal Plants and Natural Products Research Center, Hamadan University of Medical Sciences, Hamadan, Iran, e-mail: cheh1002@gmail.com

P.P. Majalekar * , P.J. Shirote

Shivaji University, Sangli, India
*e-mail: majalekarpriyanka@gmail.com

Enhanced compound selection using holistic virtual screening for gatifloxacin analogues to overcome dysglycemic effects

Abstract. Gatifloxacin, a fluoroquinolone-class antibacterial agent, is effective but has been associated with dysglycemic side effects, leading to the withdrawal of its oral formulation. Patients treated with gatifloxacin have shown notable decrease blood glucose level and after four days of treatment there will be increases in blood glucose levels. To mitigate this issue, novel gatifloxacin derivatives were designed and assessed for their efficacy and safety through in silico molecular docking studies. The derivatives aim to prevent dysglycemia by blocking human pancreatic alpha-amylase (PDB ID: 5TD4). These modifications are hypothesized to retain antibacterial effectiveness while minimizing blood glucose fluctuations. Using AutoDock, molecular docking of gatifloxacin and its derivatives with α-amylase (PDB ID: 5TD4) revealed binding energies, with gatifloxacin exhibiting a binding interaction of -7.1 Kcal/mol; meanwhile derivatives i) Gati I = -9.0 Kcal/mol, ii) Gati-II showed -8.2 Kcal/mol; iii) Gati III -8.5 Kcal/mol; iv) Gati IV = -9.3 Kcal/mol; v) Gati V = -8.9 Kcal/mol; vi) Gati VI = -7.6 Kcal/mol; Acarbose = -13.8 Kcal/mol. Unlike gatifloxacin, these derivatives demonstrated stronger binding interactions with 5TD4, potentially reducing dysglycemic risks. This study contributes to design the targeted antibacterial agents that minimize dysglycemia-related complications, thus enhancing clinical outcomes.

Key words: AUTODOCK, gatifloxacin, gatifloxacin derivatives, PDB ID: 5TD4, α-amylase, dysglycemic activity.

Introduction

Antibiotics are indispensable in virtually all modern medicine. The antibiotic era revolutionized the treatment of infectious diseases worldwide. Gatifloxacin is nothing but the synthetic broad-spectrum antibacterial scaffold possessing 8-methoxyfluoroquinolone [1]. As a quinolone antibiotic, gatifloxacin belongs to the fourth generation of fluoroquinolones [2]. It was first made available by Bristol-Myers Squibb in 1999 as Tequin® to treat respiratory tract infections. Gatifloxacin can be administered in oral, ophthalmic, or various aqueous solution forms for intravenous therapy [3,4].

Moreover, Allergan sells it under the Zymar® brand name as eye drops in the market for conjunctivitis. Gatifloxacin functions as an antibacterial agent by inhibiting bacterial enzymes namely topoisomerase II, and topoisomerase IV. Besides, DNA gyrase II also eradicate the bacteria growth. The mechanism is totally based on binding to DNA gyrase, an enzyme that permits the untwisting requisite to copy one DNA double helix into two, thus preventing bacterial DNA replication [5,6]. Notably, the medication exhibited 100-fold greater affinity for bacterial DNA gyrase than for human DNA gyrase. This broad-spectrum antibiotic is effective against not only gram-positive but also gram-negative bacteria [7]. These are useful in only for infections that are clearly caused by bacteria or that have been proven to be so [8].

Due to the substantial number of reports of adverse events pertaining to gatifloxacin-associated dysglycemia, there was a higher frequency of hyper- and hypoglycemic episodes in gatifloxacin-treated patients than in those receiving macrolide antibiotics [9]. Hence, the FDA withdrew approval for the use of gatifloxacin-containing non-opthalmic products. Therefore, gatifloxacin oral formulations (200 mg and 400 mg tablets) were banned due to dysglycemic conditions in India almost 2011 [10]. Gatifloxacin-associated dysglycemia events were reported in clinical studies, cohort episodes, case control trails, and post-marketing surveillance. However, in the case of oral formulation of gatifloxacin, hypoglycemia occurred in the first two days and hyperglycemia occurred 3-6 days after the administration of gatifloxacin. The onset of hyperglycemia occurs 3 to

10 days after the initiation of treatment, but this can be rectified by discontinuation of gatifloxacin therapy within 24 hours [11].

According to a literature survey, the reason behind dysglycemia has not been revealed. But the mechanism behind gatifloxacin's dysglycemic effects involves deregulation of key enzymes in glucose metabolism.

However, theoretically, dysglycemic events occur due to the targeted enzymes, namely α-amylase and α-glucosidase [12]. The salivary glands produce ptyalin, which is α-amylase. It's a metalloenzyme made of calcium that helps with digestion. From the exocrine cells of the pancreas, acinar cells secrete, produce, and transfer pancreatic amylase into the intestine. It plays a pivotal role by cleaving the internal α 1-4 glycosidic bonds of polysaccharides and hydrolyzing them into small-chain dextrins, namely glucose and maltose [13]. This allows the two important surface binding sites on the same face as the active site. It has been demonstrated that a second site with a tryptophan residue that a malto-oligosaccharide wraps around has a significant impact on soluble starch binding and hydrolysis, while the first site, which has two aromatic residues, is in charge of attachment to starch granules. Further, absorption of glucose single units facilitates through GLUT-1 and GLUT-2 transporters into the circulation system. Thus, affinity of gatifloxacin derivatives towards protein PDB ID: 5TD4 was assessed through molecular docking.

Consequently, the synthesis of gatifloxacin derivatives aims to mitigate dysglycemia while retaining the antibiotic's efficiency and potency. In this way, virtual screening of all six derivatives was carried out by selecting the protein PDB ID:5TD4 from the Protein Data Bank belongs to pancreatic α-amylase [14]. These derivatives may offer improved safety profiles and therapeutic benefits [15]. However, it is essential to conduct rigorous studies to validate the effectiveness and safety of these methods. The targeted modification of the chemical framework of gatifloxacin explored variations that overcome the deregulation of blood glucose level [16]. It is therefore hypothesized that gatifloxacin ester derivatives will be synthesized, with some bulky groups occupying the third position.

As per the literature review, plant isolated constituents namely quercetin, bergenin, kaempherol, betasitosterol, stigmasterol and lanosterol lower the blood glucose level and act as dibegon. This moiety act as carriers for all gatifloxacin derivatives. Phytosterol administration can enhance insulin circulation by promoting insulin secretion from pancreatic β-cells, thereby decreasing sugar level in circulation system [17]. Isolated lanosterol also exhibits glucose-lowering properties [18]. Stigmasterol may reduce intestinal glucose absorption and activate glycolytic and glycogenic processes, leading to decreased glycogenolysis and gluconeogenesis pathways [19].

Mechanically, quercetin lowers serum glucose levels primarily through its antioxidant effects and modulation of hepatic gene expression. By blocking α-glucosidase activity *in vitro*, quercetin also lowers blood sugar levels [20]. It has been discovered that isolated kaempferol inhibits α-amylase and α-glucosidase, which further reduces glucose [21].

The association of ligand-protein paired complexes and their potential interaction sites are investigated in the field of drug development using silico docking. Molecular modelling has been shown to be an effective technique for creating novel gatifloxacin drug candidates by comparing the interactions of active medications with those of ligand molecules when they become embedded inside proteins (PDB ID: 5TD4) (Figure 1) [22].

Figure 1 – Binding topology of 5TD4

PDB ID: 5TD4 is named as Human pancreatic α-amylase enzyme, which is a starch binding site; presented in Table 1.

Table 1 – Macromolecular content

Classification	Hydrolase
Organism(s)	*Homo sapiens*
Molecule	Pancreatic alpha-amylase
Chains	A, B, C, D, E, F
Sequence length	496
Expression system	*Komagataella pastoris*
Method	X-RAY DIFFRACTION
Resolution	2.30A°
Structure weight	59.66 kDa
Atoms count	4,352
Model residues count	496
Deposited residues count	496
Unique protein chain	6
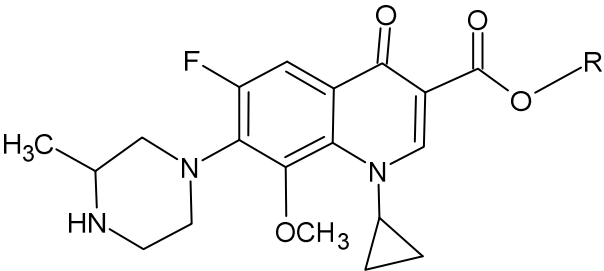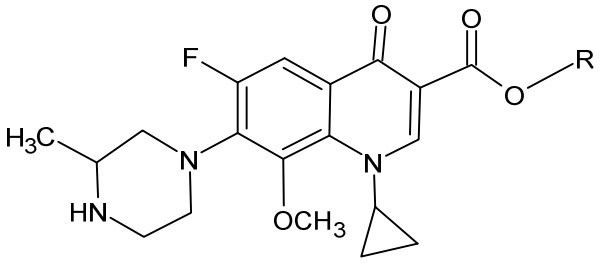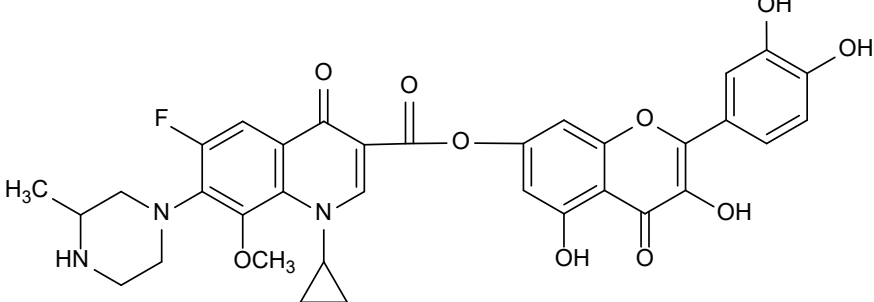
It includes D300N variant complexed with an octaose substrate.
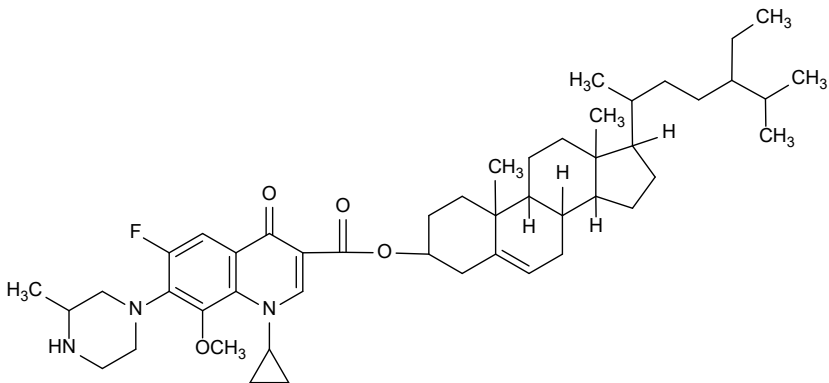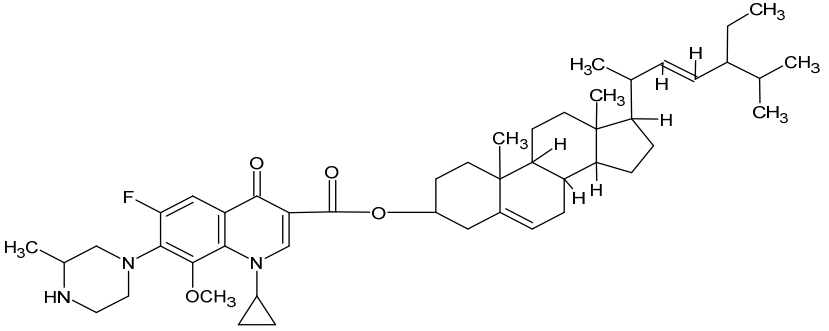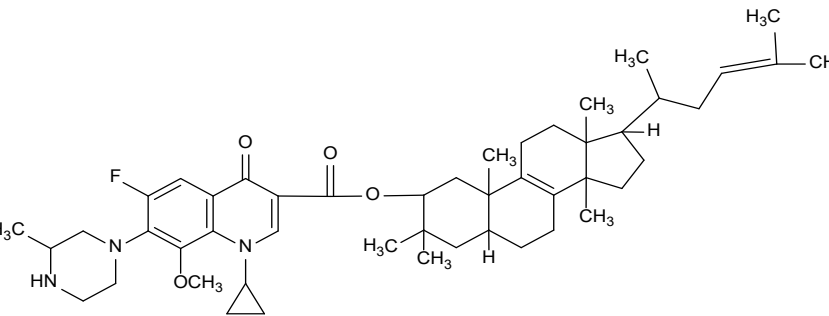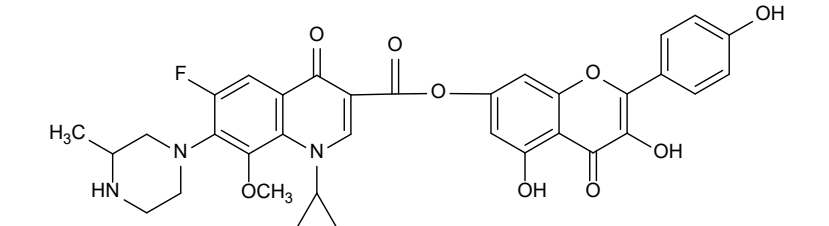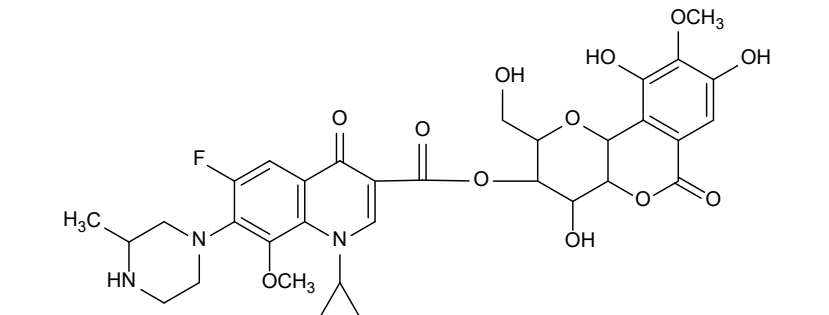
Materials and methods

In contemporary drug discovery, virtual screening serves as a crucial foundation and plays a vital role in identifying potential lead compounds. Finding the ideal ligand arrangement and placement within a receptor's binding site is the goal of molecular docking. In order to compute docking scores, AutoDock Vina was utilized to handle flexible ligands, giving priority to conformations and binding interactions that resembled those of the co-crystallized ligand.

Table 2 includes a list of the six gatifloxacin derivative structures.

Table 2 – Gatifloxacin scaffolds

Gati-II	
Gati-III	
Gati-IV	
Gati-V	
Gati-VI	

The following steps were performed on Autodock:

Three-dimensional macromolecular structures are made available through molecular docking, a technique allowing for careful examination of the binding region topology. Downloading various software packages was the first step in these docking procedures namely [23,24].

i. ChemDraw
ii. Pymol
iii. Bioviadiscovery
iv. Autodock 1.5.7
v. Mgltools 1.5.7 [25,26].

Based on the protein's lower resolution, the data's completeness, and the target enzyme accountable for pharmacological activity, the appropriate proteins were chosen from the Protein Data Bank. The selected proteins were downloaded as PDB ID:5TD4 dysglycemic activity [27].

1. Preparation of 3D Ligands:

a. ChemDraw software:

The ChemDraw software was used to draw ligand, and 'structure' tab was selected, which is available on the toolbar. Then I clicked on the 'check structure' and 'clean up' structures for errors if present, and finally clicked on '3D cleanup'. Thus, in MDL – output format, an established structural unit was verified in the form of "Ligand."

b. Pymol:

The verified ligand was opened, and the "file" and "Export structure" options were selected as the "Export molecule." The outcome window that resulted contained the same file stored in the "BIOVIA discovery file" format as "Ligand" [28].

2. Preparation of Protein:

a. BIOVIA:

The "Chemistry" option in the toolbar was used to open the downloaded protein and add polar hydrogen groups. The side window was simultaneously cleared of the heteroatoms and ligand groups. The modified protein has been stored as "Protein" as part of the "BIOVIA discovery file" in the "Protein Data Bank File" format, and amino acid attributes were copied to the configuration file on the right. [29].

3. AutoDock 1.5.7:

In addition to helping to dock ligands and proteins, AutoDock also predicts binding affinities for potential interactions by converting proteins and ligands into PDBQT files. Nine distinct positions of ligand and protein interactions were obtained by commanding the main docking folder's toolbar: dock.vina.exe.cmd–help (1st command), dock.vina.exe--configconFiguretext--loglog.text (2nd command),

and dock.vina_split.text.exe--inputligand.9out (3rd command). pdbqt. Lastly, the affinity was recorded in Kcal/mol. After dragging these nine positions into BIOVIA, the locations where Hydrogen-bond stacking with amino acids took place were examined. The results were verified by 2D image, 3D image, and H-bond interactions [30].

Results and discussion

This research work focused on different gatifloxacin building blocks as a good antibacterial scaffold that possesses less impact on blood glucose level. We designed six derivatives, namely Gati I to Gati VI, and analyzed their binding interaction with key targeted protein (5TD4) to understand their safety and efficacy profiles.

The parent gatifloxacin exhibited an affinity energy of -7.6 Kcal/mol towards this protein, indicating a strong interaction. Gatifloxacin exhibited condition based dysglycemia like hypoglycemia or hyperglycemic episodes. Hence, this study aimed to tweak its chemical structure, hoping to retain its antibacterial properties while overcoming its dysglycemic effects. The affinity energies of these derivatives were tested against the protein identified PDB ID: 5TD4. The derivatives showed reduced binding affinities: Gati I: -9.0 Kcal/mol; Gati II: -8.2 Kcal/mol; Gati III: -8.5 Kcal/mol; Gati IV: -8.9 Kcal/mol; Gati V: -8.9 Kcal/mol; Gati VI: -7.6 Kcal/mol. These lower binding affinities suggested that all derivatives interact more strongly with the 5TD4 protein compared to the parent gatifloxacin. The above increased affinity energies are reflecting minimum changes on blood glucose level than gatifloxacin treatment. Therefore, we are able to synthesize gatifloxacin derivatives in antibacterial armory by reducing the potential risk of blood glucose disturbance. Docking simulations of all the derivatives were carried out with PDB ID: 5TD4 for dysglycemic activity. The binding interactions gave 2D and 3D images, linked amino acids with H-bond interactions to ligands, and docking scores (Table 3, Figure 2).

Here, Gati I disclosed a potential target of 5TD4 and an affinity energy of -9.0 Kcal/mol (1st binding pose). Additionally, the 2nd binding pose had a -8.7 Kcal/mol affinity energy, and the lower and upper bound root square mean derivations were 30.528 and 34.969, respectively. The linked amino acids are Glu A:78, ARG A:20, VAL A:366, ARGA:72, GLY A:365, and ILEA:367 (Table 4, Figure 3).

Table 3 – Docking score with 5TD4 (Kcal/mol)

Sr. No.	Compounds	Affinity energy	Number of H-bond
1.	Gati I	-9.0	6
2.	Gati II	-8.2	2
3.	Gati III	-8.5	1
4.	Gati IV	-9.3	4
5.	Gati V	-8.9	3
6.	Gati VI	-7.6	2
7.	Gatifloxacin	-7.1	3
8.	Acarbose	-13.8	1
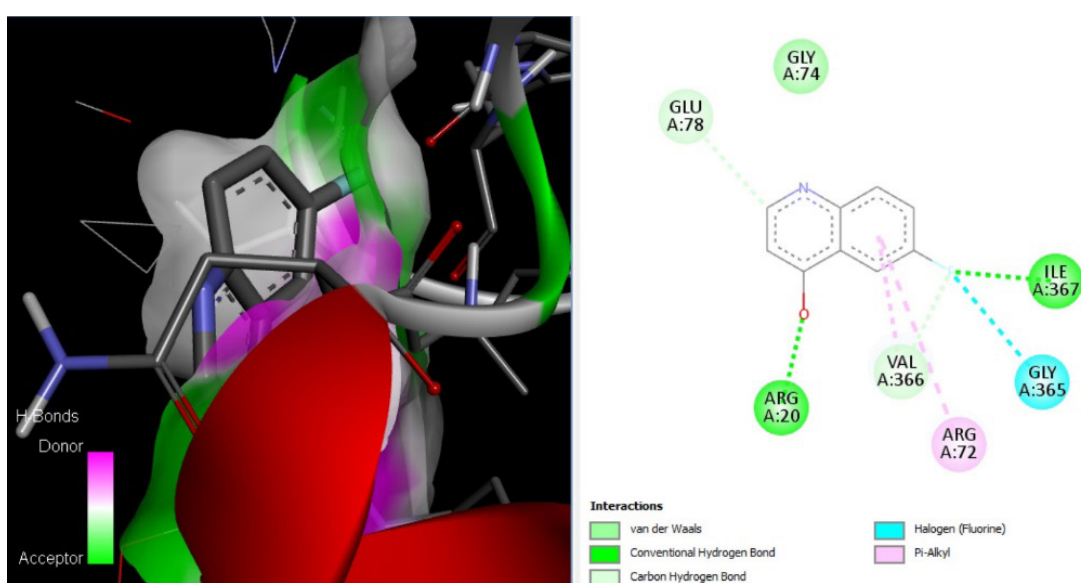
Figure 2 – 2D, 3D images – Gati I (PDB ID: 5TD4)

Table 4 – Docking score with binding interactions of Gati-I

Derivative	Binding energy (Kcal/mol)	Ligand	Linked amino acid	Distance	Type of interaction
Gati-I	-9.0	C atom of Pyridine	GLU A:78	1.89642	H bond
		O atom of pyridine ring	ARG A:20	3.02626	H bond
		Benzene ring	VAL A: 366	1.76012	H bond
		Benzene ring	ARG A:72	1.89824	H bond
		F atom	GLY A: 365	1.99998	H bond
		F atom	ILE A:367	3.36772	H bond
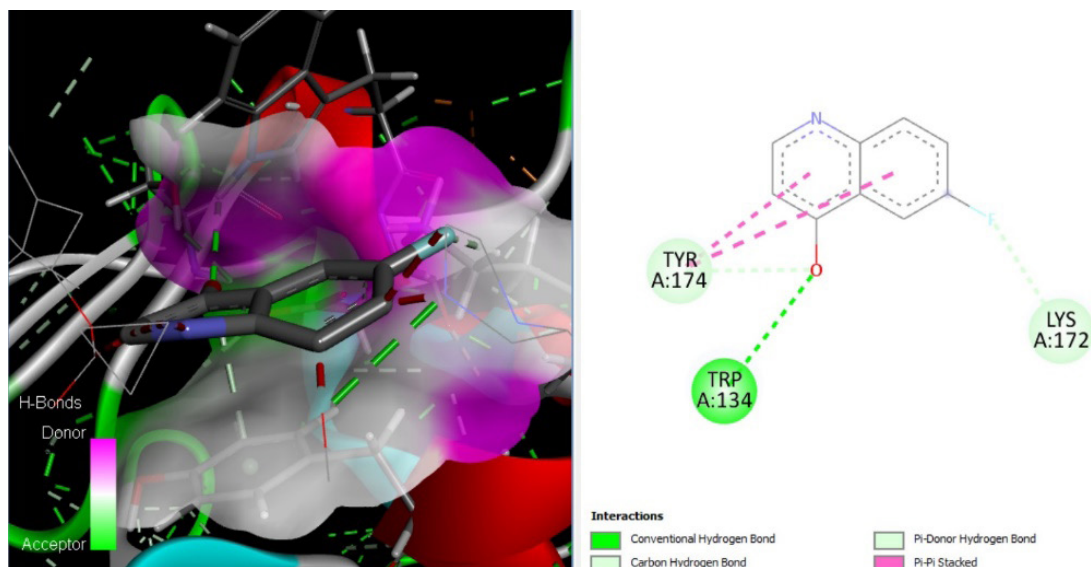
Figure 3 – 2D, 3D images – Gati II (PDB ID: 5TD4)

The second derivative, Gati II, had 1.093 and 1.770 distances from the lower & upper bounds limits (root square mean deviation), respectively, and showed binding affinities of -8.2 Kcal/mol (1st binding pose) and -8.1 Kcal/mol (2nd binding pose). The amino acids CYS A:70 and CYS A:115 demonstrated the predominant proteins' affinity energy for ligands (Table 5, Figure 4).

Table 5 – Docking score with binding interactions of Gati II

Derivative	Binding energy (Kcal/mol)	Ligand	Linked amino acid	Distance	Type of interaction
Gati-II	-8.2	Pyridine ring	CYS A:70	1.86493	Hydrophobic bond
		F atom	CYS A:115	1.93467	H bond
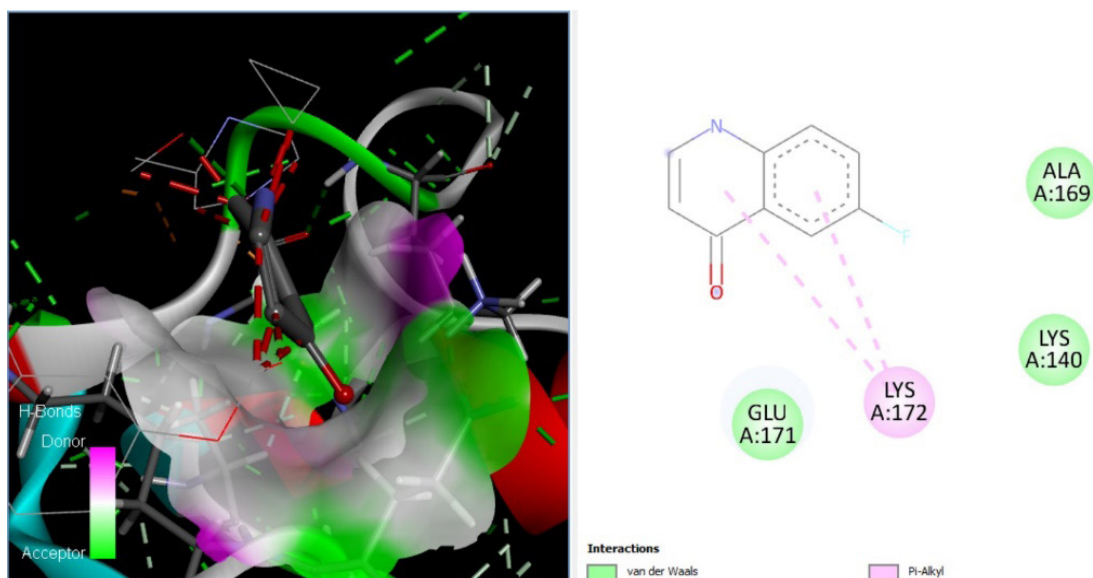
Figure 4 – 2D, 3D images – Gati III (PDB ID: 5TD4)

The free binding energy was estimated using the interaction between the 5TD4 protein and Gati III. The docking score was -8.5 Kcal/mol for the first binding pose and -8.4 Kcal/mol for the second binding pose, according to the lower bound (1.065) and upper bound (1.496) root mean square deviations. The ligand was docked onto protein sites by LYS A:172 (Table 6, Figure 5).

Table 6 – Docking score with binding interactions of Gati-III

Derivative	Binding energy (Kcal/mol)	Ligand	Linked amino acid	Distance	Type of interaction
Gati-III	-8.5	Benz pyrimidine ring	LYS A:172	2.52343	H bond
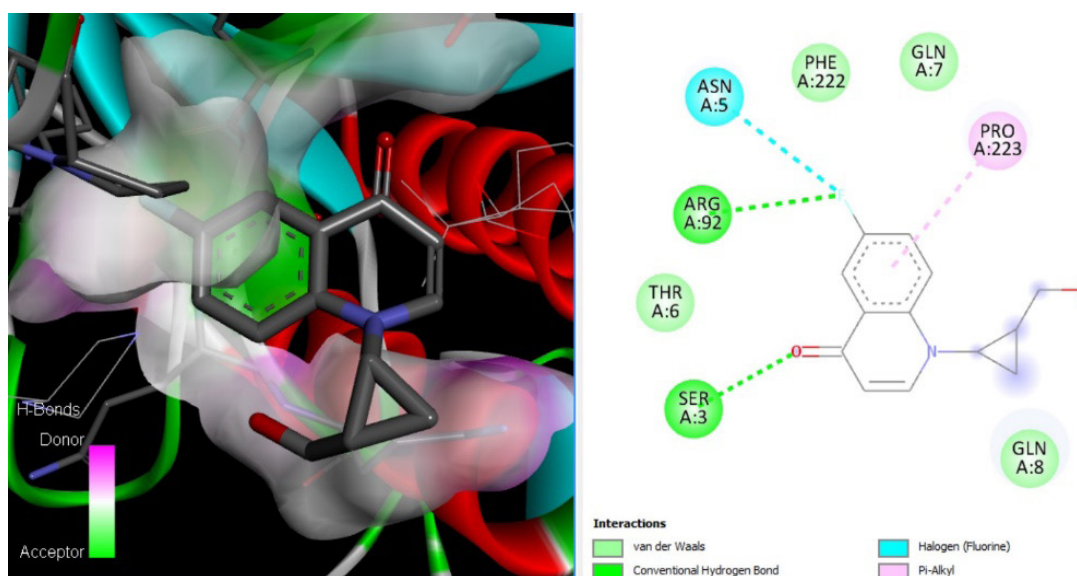
Figure 5 – 2D, 3D images – Gati IV (PDB ID: 5TD4)

Gati IV exhibited an affinity energy of -9.3 Kcal/mol in the primary binding pose and -9.3 Kcal/mol in the secondary pose, with corresponding root mean square deviations (RMSD) of 1.839 Å (lower) and 2.368 Å (upper). Potential interacting amino acid residues include ASN A:5, ARG A:92, SER A:3, and PRO A:223 (Table 7, Figure 6).

Table 7 – Docking score with binding interactions of Gati IV

Derivative	Binding energy (Kcal/mol)	Ligand	Linked amino acid	Distance	Type of interaction
Gati-IV	-9.3	F atom	ASN A:5	3.01834	H bond
		F atom	ARG A:92	3.24961	H bond
		O atom of ketone	SER A:3	2.95887	H bond
		Benzene ring	PRO A:223	2.98123	H bond
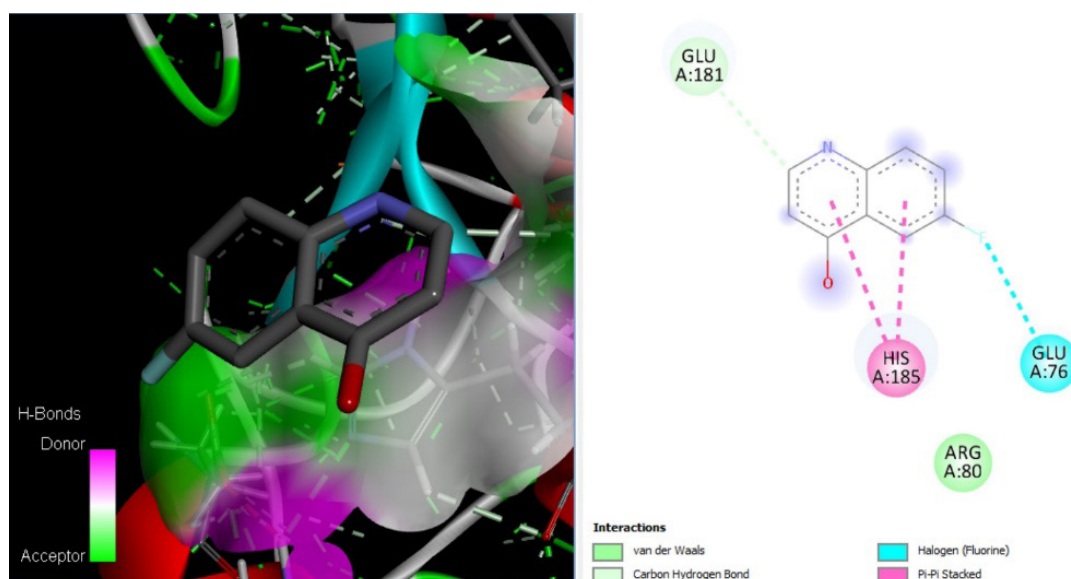
Figure 6 – 2D, 3D images – Gati V (PDB ID: 5TD4)

Gati V displayed significant dysglycemic activity at the 5TD4 protein target. In the first binding pose with 5TD4, Gati V showed a free binding energy of -8.9 Kcal/mol. The second binding pose exhibited a free binding energy of -8.8 Kcal/mol, with root-mean-square deviation (RMSD) values of 20.097 Å (lower bound) and 23.664 Å (upper bound). Notably, Gati V interacts with the receptor protein through binding with residues GLU A:181, HIS A:185, and GLU A:76 (Table 8, Figure 7).

Gati VI demonstrated a binding energy of -7.6 Kcal/mol in its primary binding pose, indicating potential as a monoamine oxidase inhibitor. The secondary binding pose exhibited a binding affinity of -7.5 Kcal/mol, with root mean square deviations (RMSD) of 16.572 Å (lower bound) and 19.558 Å (upper bound). The interacting amino acid residues are GLU A:181 and HIS A:185 (Table 9, Figure 8).

At PDB ID: 5TD4, gatifloxacin demonstrated a less binding interaction with the same protein. In particular, when Gatifloxacin interacted with 5TD4, it showed a free binding energy of -7.1 Kcal/mol for the first binding pose. With a lower bound root-mean-square deviation (RSMD) of 1.562 and an upper bound of 2.149, the second pose yielded a binding energy of -7.0 Kcal/mol. Gatifloxacin interacts with the amino acids PRO A:228, LEU A:214, and LYS A:227 to bind to the receptor protein (Table 10, Figure 9).

Table 8 – Docking score with binding interactions of Gati V

Derivative	Binding energy (Kcal/mol)	Ligand	Linked amino acid	Distance	Type of interaction
Gati V	-8.9	C atom of pyrimidine ring	GLU A:181	2.75787	H bond
		Benzene ring	HIS A:185	2.32565	H bond
		F atom of benzene ring	GLU A:76	2.92036	H bond
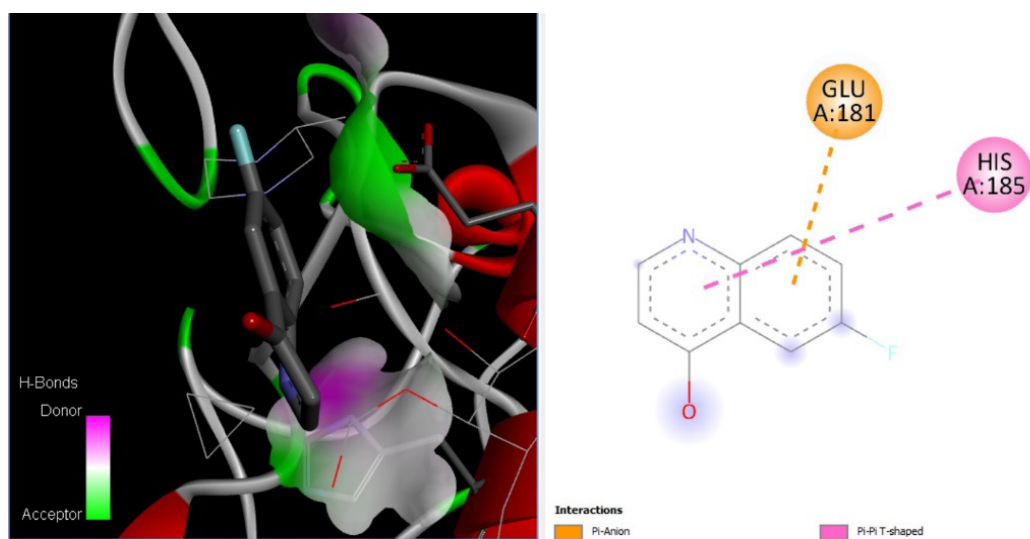
Figure 7 – 2D, 3D images – Gati VI (PDB ID: 5TD4)

Table 9 – Docking score with binding interactions of Gati VI

Derivative	Binding energy (Kcal/mol)	Ligand	Linked amino acid	Distance	Type of interaction
Gati VI	-7.6	Benzene ring	GLU A: 181	1.7	H bond
		F atom of benzene ring	HIS A: 185	2.0	H bond
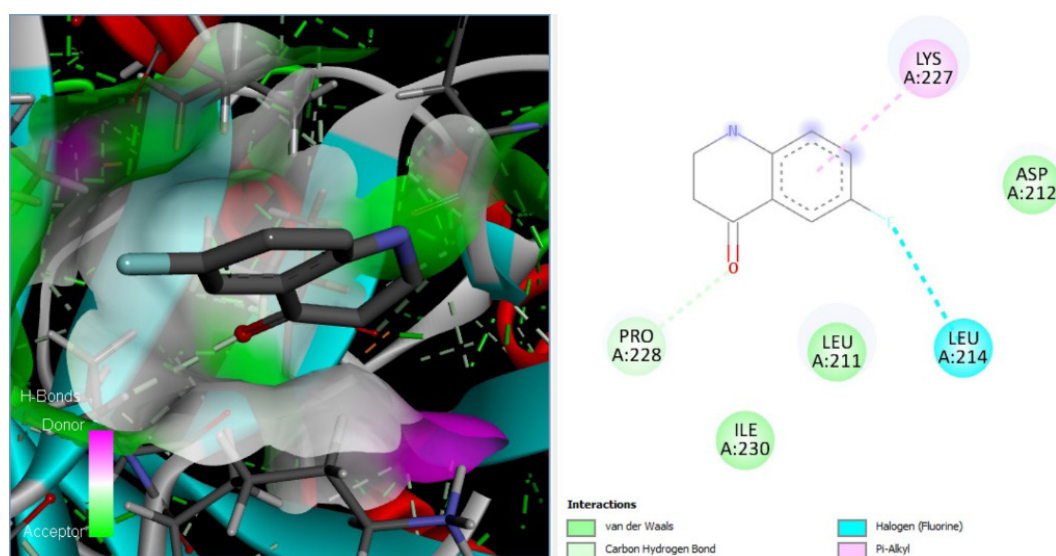
Figure 8 – 2D, 3D images – Gatifloxacin (PDB ID: 5TD4)

Table 10 – Docking score with binding interactions of Gatifloxacin

Standard	Binding energy (Kcal/mol)	Ligand	Linked amino acid	Distance	Type of interaction
Gatifloxacin	-7.1	Benzene ring	PRO A:228	1.73673	H bond
		F atom	LEU A: 214	2.03383	H bond
		Benzene ring	LYS A:227	2.90897	H bond
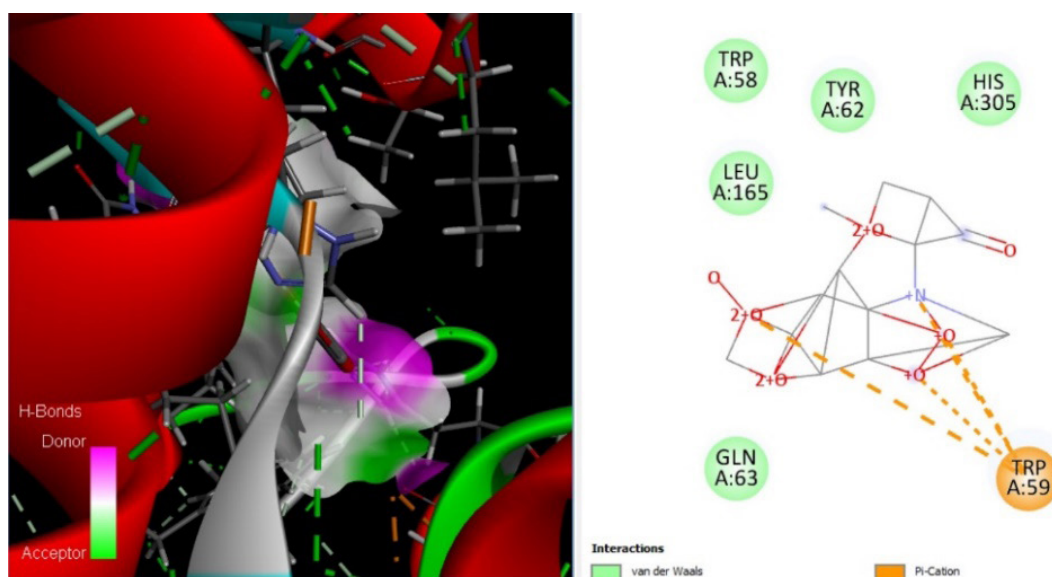
Figure 9 – 2D, 3D images – Acarbose (PDB ID: 5TD4)

At PDB ID: 5TD4, acarbose demonstrated strong dysglycemic action. In particular, while interacting with 5TD4, it showed an unrestrained binding power of -13.8 Kcal/mol for the initial binding position. With a lower limit of the root-mean-square deviation (RSMD) of 0.923 and an upper bound of 2.049, the second pose yielded an energy binding value of -13.6 Kcal/mol. Gatifloxacin interacts with the amino acid TRP A:59 to attach to the receptor protein (Table 11).

Table 11 – Docking score with binding interactions of Acarbose

Standard	Binding energy (Kcal/mol)	Ligand	Linked amino acid	Distance	Type of interaction
Acarbose	-13.8	Quaternary N atom	PRO A:228	1.73673	H bond

Conclusion

This discovery successfully enlighted that gatifloxacin derivatives (Gati I to Gati VI) contribute a maximum affinity energy towards the 5TD4 protein. The increased affinity energy is less significant to induce dysglycemic effects. Thus, finding gives a safer alternative to gatifloxacin, retaining antibacterial efficacy while minimizing the risk of adverse effects on blood glucose levels. So, this research encountered a promising avenue for developing improved antibacterial agents with enhanced safety profiles.

Acknowledgments

Conflict of interest

All authors are aware of the article's content and declare no conflict of interest.

References

1.   Fish D., North D. (2001) Gatifloxacin, an advanced 8-methoxy fluoroquinolone. *Pharmacother.,* 21(1), pp. 35-59. https://doi.org/10.1592/phco.21.1.35.34440.

2.   Kishii R., Takei M., Fukuda H., Hayashi K., Hosaka M. (2003) Contribution of the 8-methoxy group to the activity of gatifloxacin against type ii topoisomerases of streptococcus pneumonia. *J Antimicrob Agents and Chemother.,* 47(1), pp. 77-81. https://doi.org/10.1128/aac.47.1.77-81.2003.

3.   Fung-Tomc J., Minassian B., Kolek B., Washo T., Huczko E., Bonner D. (2000) In vitro antibacterial spectrum of a new broad-spectrum 8-methoxy fluoroquinolone, gatifloxacin. *J Antimicrob Chemother.*, 45(40), pp. 437-446. https://doi.org/10.1093/jac/45.4.437.

4.   Stein G. (2000) The methoxy fluroquinolones: Gatifloxacin and moxifloxacin. *J Infections Med.*, 17(8), pp. 564-570.

5.   Franca S., Carvalho C. (2002) Effectiveness, safety and tolerability of gatifloxacin, a new 8- methoxy fluoroquinolone, in the treatment of outpatients with community-acquired pneumonia: a Brazilian study. *Braz J Infect Dis.*, 6(4), pp. 157-163. https://doi.org/10.1590/S1413-86702002000400002.

6.   Grasela D. (2003) Clinical pharmacology of gatifloxacin, a new fluoroquinolone. *Clin Infect Dis.*, 31, suppl. 2, pp. S51-S58. https://doi.org/10.1086/314061.

7.   Dubreuil L., Behra-Miellet J., Neut C., Calvet L. (2003) In vitro activity of gatifloxacin, a new fluoroquinolone, against 204 anaerobes compared to seven other compounds. *Clin Microb Infect.,* 9(11), pp. 1133-1138. https://doi.org/10.1046/j.1469-0691.2003.00773.x.

8.   Jones R., Croco M., Pfaller M., Beach M., Kulger K. (1999) Antimicrobial activity evaluations of gatifloxacin, a new fluoroquinolone: contemporary pathogen results from a global antimicrobial resistance surveillance program (SENTRY, 1997). *Clinical Microb Infect.,* 5(9), pp. 540–546. https://doi.org/10.1111/j.1469-0691.1999.tb00432.x.

9.   Cunha B. (1998) Quinolones: Clinical use and formulary considerations. *Adv Ther.*, 15(5), pp. 277-287.

10. Gajjar D., Kollia G., Lacreta F. (2000) Effect of multiple- dose gatifloxacin or ciprofloxacin on glucose homeostasis and insulin production in patients with noninsulin-dependent diabetes mellitus maintained with diet and exercise. *Pharmacother.*, 20(6Pt2), pp. 76-86. https://doi.org/10.1592/phco.20.8.76S.35182.

11. Note: Determination that TEQUIN (Gatifloxacin) was withdrawn from sale for Reasons of Safety Effectiveness by the Department of Health and Human Services, FDA (US), Docket no. FDA, 2006, 0081.

12. Kaur N., Kumar V., Nayak S., Wadhwa P., Kaur P., Sahu S. (2021) A-amylase as molecular target for treatment of diabetes mellitus: a comprehensive review. *Chem Biology and Drug Design.*, 98(4), pp. 539-560. https://doi.org/10.1111/cbdd.13909.

13. Ben E., Asuquo A., Owo A. (2019) The role of serum alpha-amylase and glycogen synthase in the anti-diabetic potential of terminalia catappa aqueous leaf extract in diabetic wistar rats. *Asian J Res Med Pharm Sci.*, 6(2), pp. 1-11. https://doi.org/10.9734/ajrimps/2019/v6i230096.

14. Butterworth P., Warren F., Ellis P. (2011) Human α-amylase and starch digestion: An interesting marriage. *Starch – Stärke.*, 63(7), pp. 395-405. https://doi.org/10.1002/star.201000150.

15. Park-wyllie L., Juurlink D., Kopp A., Shah B., Stukel T., Stumpo C., Dresser L., Low D., Mamdani M. (2006) Outpatient gatifloxacin therapy and dysglycemia in older adults. *J New England Med.*, 354(13), pp. 1352. https://doi.org/61. 10.1056/NEJMoa055191.

16. Baker S., Hangii M. (2002) Possible gatifloxacin-induced hypoglycemia. *Annals of Pharmacother.*, 36(11), pp. 1722-1726. https://doi.org/10.1345/aph.1A480.

17. Ponnulakshmi R., Shyamaladevi B., Vijayalakshmi P., Selvaraj J. (2016) In silico and in vivo analysis to identify the antidiabetic activity of beta sitosterol in adipose tissue of high fat diet and sucrose induced type-2 diabetic experimental rats. *Toxicol Mech Methods.,* 29(4), pp. 276-290. https://doi.org/10.1080/15376516.2018.1545815.

18. Bagri P., Ali M., Aeri V., Bhowmik M. (2016) Isolation and antidiabetic activity of new lanostenoids from the leaves of psidium guajava l. *Int J Pharm Sci.,* 8(9), pp. 14-18. http://dx.doi.org/10.22159/ijpps.2016v8i9.10425.

19. Wang J., Huang M., Yang J. (2017) Anti-diabetic activity of stigmasterol from soybean oil by targeting the GLUT4 glucose transporter. *Food Nutrition Res.,* 61(1), pp. 1-14. https://doi.org/10.1080/16546628.2017.1364117.

20. Bulea M., Abdurahmand A., Nikfara S., (2019) Antidiabetic effect of quercetin: A systematic review and meta-analysis of animal studies. *Food Chem Toxicol.,* 125, pp. 494-502. https://doi.org/10.1016/j.fct.2019.01.037.

21. Ibitoye O., Uwazie J., Ajiboye T. (2018) Bioactivity-guided isolation of kaempferol as the antidiabetic principle from Cucumis sativus L. fruits. *J Food Biochem.,* 42(3), pp. 1-7. https://doi.org/10.1111/jfbc.12479.

22. Cowen P., Browning M. (2015) What has serotonin to do with depression? *World Psychiatry.*, 14(2), pp. 158-160. https://doi.org/10.1002/wps.20229.

23. Omran Z. (2024) Design, synthesis of new gatifloxacin derivatives as antibacterial activity. *J Res Chem.*, 5(1), pp. 19-27. https://doi.org/10.22271/reschem.2024.v5.i1a.112.

24. Sriram D., Fisher L., Yogeeswari P., Aubry A. (2006) Gatifloxacin derivatives: synthesis, antimycobacterial activities, and inhibition of Mycobacterium tuberculosis DNA gyrase. *Bioorgan Med letters.*, 16(11), pp. 2982-2985. https://doi.org/10.1016/j.bmcl.2006.02.065.

25. Mesaik M. (2010) Synthesis, characterization, antibacterial, antifungal, and immunomodulating activities of gatifloxacin derivatives. *Med Chem Res.*, 19, pp. 1210-1221. https://doi.org/10.1016/j.molstruc.2010.01.036.

26. Mauro V., Maurı F., Saraiva A., Marcus V., Cristiane F., Vicenteb F., Lourenc M. (2007) Synthesis and antitubercular activity of lipophilic moxifloxacin and gatifloxacin derivatives. *Bioorgan Med Chem Letters.*, 17(20), pp. 5661-5664. https://doi.org/10.1016/j.bmcl.2007.07.073.

27. Forli S., Huey R., Pique M., Sanner M., Goodsell D., Olson A. (2016) Computational protein ligand docking and virtual drug screening with the AutoDock suite. *Natural Protocols.,* 11(5), pp. 905-919. https://doi.org/10.1038/nprot.2016.051.

28. Trott O., Olson A. (2010) AutoDock Vina: improving the speed and accuracy of docking with a new scoring function, efficient optimization and multithreading. *J Computer Chem.,* 31(2), pp. 455-461. https://doi.org/0.1002/jcc.21334.

29. Seeliger D., Groot B. (2010) Ligand docking and binding site analysis with pymol and autodock/vina. *J Computer Aided Drug Design.,* 24, pp. 417-422. https://doi.org/10.1007/s10822-010-9352-6.

30. Desai K., Hajoori M., (2019) Molecular docking studies of novel nitrophenyl inhibitor against saldose reductase. *Int J Res Reviews.,* 6(2), pp. 92z-95z. https://doi.org/10.1371/journal.pone.0138186.

Information about authors:

Priyanka Majalekar – (corresponding author) – M. Pharm., Assistant Professor, Appasaheb Birnale College of Pharmacy, Sangli, India, e-mail: majalekarpriyanka@gmail.com

Pramodkumar Shirote – PhD, Principal Investigator, Dr. Bapuji Salunkhe Institute of Pharmacy, Miraj, Sangli, India, e-mail: padmpramod@reffimail.com

F. Hamedi [ID] , A. Naghipour * [ID] ,

E. Ghasemian Lemraski [ID] , S. Taghavi Fardood [ID]

Ilam University, Ilam, Iran
*e-mail: a.naghipour@ilam.ac.ir

Synthesis, characterization and catalytic activity in Suzuki-Miura and Mizoroki-Heck coupling reactions of trans-dichloro bis(4'-bromobiphenyl-4-yl)diphenylphosphine palladium(II) complex

Abstract. In this research palladium (II) chloride, $PdCl_2$, reacts with (4'-bromobiphenyl-4-yl) diphenylphosphine compound, $Br(C_6H_4)_2P(C_6H_5)_2$, to give trans-$PdCl_2L_2$ [L: $Br(C_6H_4)_2P(C_6H_5)_2$] complex. trans-dichloro bis(4'-bromobiphenyl-4-yl)diphenylphosphine palladium(II) complex has been characterized by elemental analysis, FT-IR, ^1H, ^{31}P and ^{13}C NMR. The catalytic performance of this complex has been rigorously evaluated and compared in the context of Suzuki-Miyaura and Mizoroki-Heck coupling reactions. It is noteworthy that under specific optimal conditions, including solvent type, base type, base quantity, catalyst quantity, and temperature, this complex serves as an efficient and suitable catalyst for the synthesis of biphenyl aryl halide derivatives. The resulting yield in these processes strongly supports the efficacy of this complex as a catalyst.
Key words: Phosphine, palladium, NMR analysis, Suzuki&Heck, coupling reactions, aryl halides.

Introduction

The ability to tune both the electronic and steric properties of phosphine ligands lie behind their importance in the development of effective homogeneous and hetrogeneous catalysts, thus in recent years, the synthesis of phosphine ligands has attracted the attention of many chemical researchers due to their structure, unique characteristics and reactivity as well as the chemistry of their metal complexes. Organic chemistry that inspires the design of new phosphines with various structures and tuning their properties includes studies of the reactivity of phosphines, especially those based on the attack of a nucleophile on the carbon atom of an electrophilic substrate [1].

The utilization of an extensive array of trivalent phosphorus ligands in the realm of transition metal catalysis persists as a pivotal driver in the realm of conventional P-C-bonded phosphines. Concurrently, the domain of organocatalytic processes finds itself in a rapid state of proliferation within the annals of organic chemistry. This, in turn, serves as the wellspring of inspiration for the conception of novel phosphines, each possessing an assortment of structural attributes, inviting the meticulous refinement of their intrinsic properties [2]. What is certain tri-phenylphosphine with IUPAC name: triphenylphosphane is a common organophosphorus compound with the formula $P(C_6H_5)_3$ that is frequently abbreviated as PPh_3 or Ph_3P. It is widely used in organic and organometallic compound synthesis because it is an effective reducing agent as well as a neutral ligand. This ligand binds well to most transition metals, especially those in the middle and late transition metals of groups 7–10. In terms of steric bulk [3].

Transition metal-catalyzed cross-coupling reactions of organic electrophiles with organometallic reagents represent one of the most important ways for the formation of carbon-carbon and carbon-heteroatom bonds, respectively [4]. A variety of organometallic reagents and organic halides, including aryl, alkyl, allyl, alkenyl and alkynyl groups, can be applied [5]. The advantages of cross-couplings over classical organic reactions are the easily accessible and inexpensive starting materials, versatile coupling methods, high productivity and selectivity as well as the tolerance concerning various functional groups and shorter reaction sequences [6].

In addition, C-C cross-coupling reactions are useful tools for the synthesis of complex structures, fine chemicals and natural products. However, the success of these transformations is highly dependent on the applied transition metal catalyst [7].

Generally, phosphines are widely used as a ligand for nickel or palladium catalysts in cross-coupling reactions. They are also effective ligands for rhodium, iridium and gold catalysts and used in catalytic reactions such as hydrogenation and cyclization reactions. The ability to fine-tune the reaction conditions (temperature, solvents, ligands, bases and other additives) of palladium catalysts makes palladium catalysis an extremely versatile tool in organic chemical synthesis [8].

As catalysts, typically late transition metals (*e. g.* Ni, Pd, Cu) are used and especially palladium attracted much attention during the last 50 years [9]. The advantages of palladium compared to other metals are its *non*-toxicity, its insensitivity toward oxygen and moisture and its tolerance toward numerous functional groups [10]. So, in our project, Pd is one of the most efficient metal elements in the field of catalytic processes and is commonly used as one of the most powerful tools for the formation of carbon-carbon bonds in the synthesis of organometallic compounds. Therefore, palladium-catalysed C-C cross-coupling reactions, especially the Suzuki and Heck reactions, have played an important role in chemical research at both industrial and laboratory scales. The Suzuki reaction is important to organic chemistry because it forms carbon-carbon bonds allowing the synthesization of various organic molecules and the Heck reaction, generally defined as the substitution of a vinylic hydrogen with an aryl, vinyl, or benzyl group, is widely regarded as one of the premier synthetic tools for the construction of new C–C bonds [11-15].

In this research paper, our investigation revolved around the synthesis of a novel phosphino Pd(II) complex, denoted as $PdCl_2L_2$ [L: $Br(C_6H_4)_2P(C_6H_5)_2$]. What is evident in this process is the use of cheap and available raw materials, performing organic reactions in shorter times compared to previous methods, and observing the principles of green chemistry and atomic economy. We thoroughly characterized this complex utilizing a variety of analytical techniques, including FT-IR, ^{1}H, ^{31}P and ^{13}C NMR spectroscopy. Furthermore, we explored the catalytic performance of the synthesized complex in carbon-carbon coupling reactions, specifically focusing on the Suzuki and Heck reactions.

Materials and methods

The present investigation employed chemicals and reagents sourced from Merck, Aldrich, and Fluka. Melting points were determined using the IA9100 device by Electrothermal (England). The FT-IR spectra were acquired using a Bruker Vertex 70, utilizing potassium bromide pellets. NMR spectra were obtained on a 400 MHz Bruker spectrometer in $CDCl_3$ or DMSO as the solvent at room temperature. TLC was performed utilizing Merck silica gel 60 F254 plates that were pre-coated with a thickness of 0.25 mm.

Synthesis of (4'-bromobiphenyl-4-yl)diphenylphosphine, $Br(C_6H_4)_2P(C_6H_5)_2$ ligand : 10 mmol of 4,4'-dibromo-1,1'-biphenyl was dissolved in 190 mL of dry diethyl ether under a nitrogen atmosphere. Then, 10 mmol of n-butyl lithium was slowly added to the solution at -10°C, and the mixture was stirred for 2 h. In the following, the mixture was stirred for 1h at room temperature. Afterward, 10 mmol of chlorodiphenylphosphine was added to the solution at -10°C, and the mixture was stirred for 9 h. Following this, the mixture was stirred for a period of 2 hours at room temperature. Upon the completion of the stirring process, dehydrated diethyl ether was added to the mixture. The product (4'-bromobiphenyl-4-yl)diphenylphosphine was subsequently isolated and underwent purification using dichloromethane. This process yielded 84.69% of the product in the form of a white powder, as shown in Scheme 1. **^{1}H NMR:** (250 MHz, $CDCl_3$, ppm) δ: 7.88 – 7.65 (m, 1H), 7.65 – 7.52 (m, 1H), 7.52 – 7.30 (m, 1H). **^{13}C NMR:** (63 MHz, $CDCl_3$, ppm) δ: 143.43, 143.38 – 131.82 (m), 131.81 – 128.45 (m), 26.95 (d, J = 12.3 Hz), 122.59. **^{31}P NMR:** (101MHz, $CDCl_3$, ppm) δ: 28.99, -5.87 (d, J = 6.5 Hz). (Figure 1). **FT-IR (υ, cm^{-1}):** 3468, 3417, 2924, 2857, 1629, 1498, 1459, 1379, 1107, 1061, 990, 806, 622, 538, 496.

Synthesis of trans-dichlorobis (4'-bromobiphenyl-4-yl)diphenylphosphine palladium(II) complex as catalyst: 100 mg of (4'-bromobiphenyl-4-yl)diphenylphosphine was dissolved in 2 mL of dichloromethane. Then, 21.2 mg palladiu(II) chloride, 0.5 mL acetone and 5 mL dichloromethane were added to the solution and the mixture were stirred at room temperature for 24 h. The separated solid was filtered off and washed with 2 mL methanol and 60 mL dichloromethane to give dichlorobis (4'- bromobiphenyl-4-yl)diphenylphosphine palladium(II) as a yellow powder [16, 19-22]. Yield: 63% (Scheme 2). **^{1}H NMR:** (300 MHz, $CDCl_3$) δ 7.75 (ddt, J = 15.4, 10.2, 4.4 Hz, 11H), 7.65 – 7.52 (m, 8H), 7.52 – 7.36 (m, 15H), 7.33 (s, 1H), 1.49 – 1.24 (m, 4H), 0.92 (q, J = 7.2 Hz, 2H). **^{13}C-NMR:** (75 MHz, $CDCl_3$) δ: 141.44, 138.58, 135.08 (d, J = 6.2 Hz), 134.62 (t, J = 6.2 Hz), 131.58, 130.23, 129.05, 128.78 – 126.93 (m), 126.02, 121.83, 77.01,

76.59, 76.16. **^{31}P-NMR:** (121 MHz, CDCl$_3$) δ: 32.42, 29.01, 23.00 (d, J = 3.1 Hz). (Figure 2). **FT-IR(υ, cm^{-1}):** 3440, 3052, 2924, 2856, 1706, 1661, 1588, 1471, 1429, 1378, 1185, 1094, 995, 844, 806, 741, 691, 518.

General method for Suzuki cross-coupling reaction: In a typical method, a mixture of aryl halide (0.25 mmol), phenylboronic acid (0.30 mmol), Potassium carbonate (0.375 mmol), 0.0012 g of dichloro bis(4'-bromobiphenyl-4-yl) diphenylphosphine palladium(II) complex as catalyst and 2 mL dimethylformamide as solvent was heated at 80°C using an oil bath for a suitable time. The reaction progress was monitored using TLC (n-hexane). After removing the solvent, an adequate amount of ethyl acetate was added to the mixture and poured into the separatory funnel containing distilled water. After separating the organic phase, the ethyl acetate was allowed to drain from the reaction vessel.

General method for Heck cross-coupling reaction: In a typical method, a mixture of aryl halide (0.25 mmol), n-butyl acrylate (0.30 mmol), Potassium carbonate (0.375 mmol), 0.0012 g of dichlorobis (4'-bromobiphenyl-4-yl)diphenylphosphine palladium(II) complex as catalyst and 2 mL dimethylformamide as solvent was heated at 80°C using an oil bath. The reaction was monitored by employing TLC with a mobile phase consisting of a 9:1 combination of n-hexane and ethyl acetate. After the reaction was completed, the reaction mixture was allowed to cool to room temperature. Following removing the solvent, an appropriate amount of ethyl acetate was added to the mixture and poured into the Separatory funnel containing hot distilled water. After separating the organic phase, the ethyl acetate was allowed to drain from the reaction vessel.

Results and discussion

NMR analysis For the (4'-bromobiphenyl-4-yl)diphenylphosphine ligand. In the ^{31}PNMR signal, Phosphorus resonance has appeared as a distinct single signal in the -5.87 ppm region. The position of the obtained signal compared to the signal of phosphorus (related to the free chlorodiphenylphosphine ligand with δ= -6 ppm) indicates the formation of a new bond between the phosphorus atom with the carbon atom, which has caused the phosphorus signal to shift to a down field by reducing the electron density on the phosphorus atom. The signal seen in 28.99 ppm is related to (4'-bromobiphenyl-4-yl) diphenylphosphine oxide. The data show that the desired organic ligand has been synthesized with a high percentage of purity (95%) (Figure 1) [19, 20].
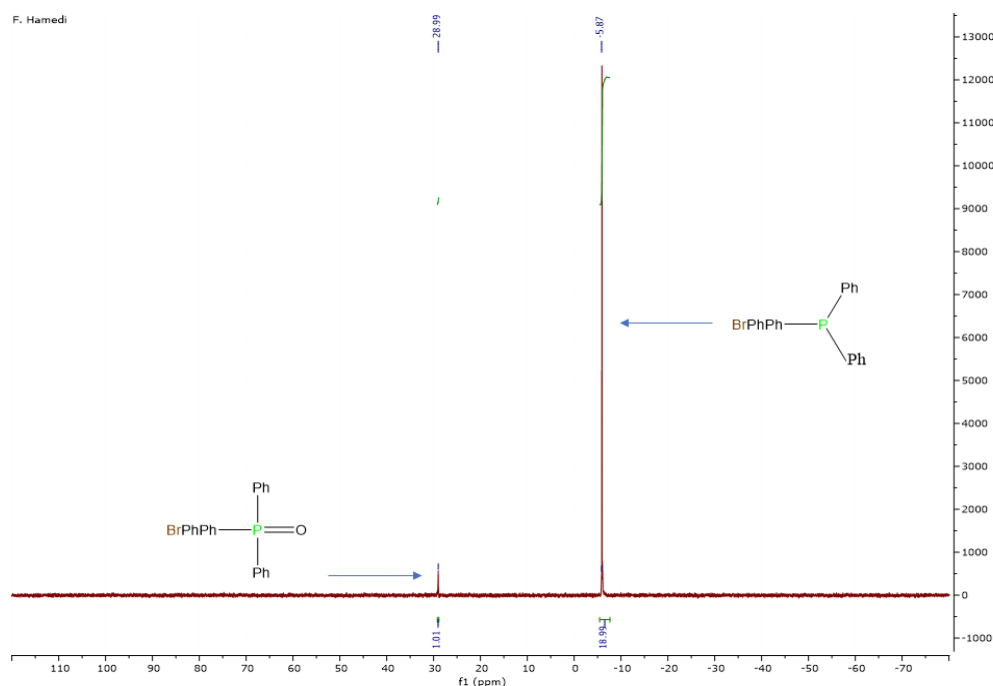
Figure 1 – ^{31}P NMR spectra of a (4'-bromobiphenyl-4-yl)diphenylphosphine ligand

In the ^{1}HNMR spectrum, the peak in the δ= 7.26 ppm region is related to the CDCl$_3$ solvent. In this spectrum, hydrogens of aromatic rings have appeared as multiple peaks in the δ= 7.772-7.399 ppm region (Scheme 1).

NMR analysis For the trans-dichlorobis(4'-bromobiphenyl-4-yl)diphenylphosphine alladium(II) complex. The ^{31}PNMR signals indicated a mixture of trans- PdCl$_2$L$_2$, (4'-bromobiphenyl-4-yl)diphenylphosphine oxide and cis- PdCl$_2$L$_2$ (δ=

32.42, 29.01, 23.00 ppm) respectively. It is clear that the signal corresponding to (4'-bromobiphenyl-4-yl) diphenylphosphine oxide remained unchanged, indicating that this compound did not react with PdCl$_2$L$_2$ (Figure 2) [16-23].

Based on the literature, an equilibrium mixture of the the trans and cis (trans/cis: 10/1) show that the phosphine ligands are predominantly (91%) coordinate in a trans configuration about the ion center (Scheme 2).
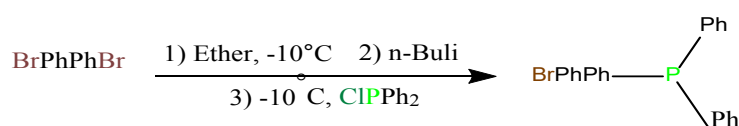
Scheme 1 – Synthesis of (4'-bromobiphenyl-4-yl)diphenylphosphine ligand
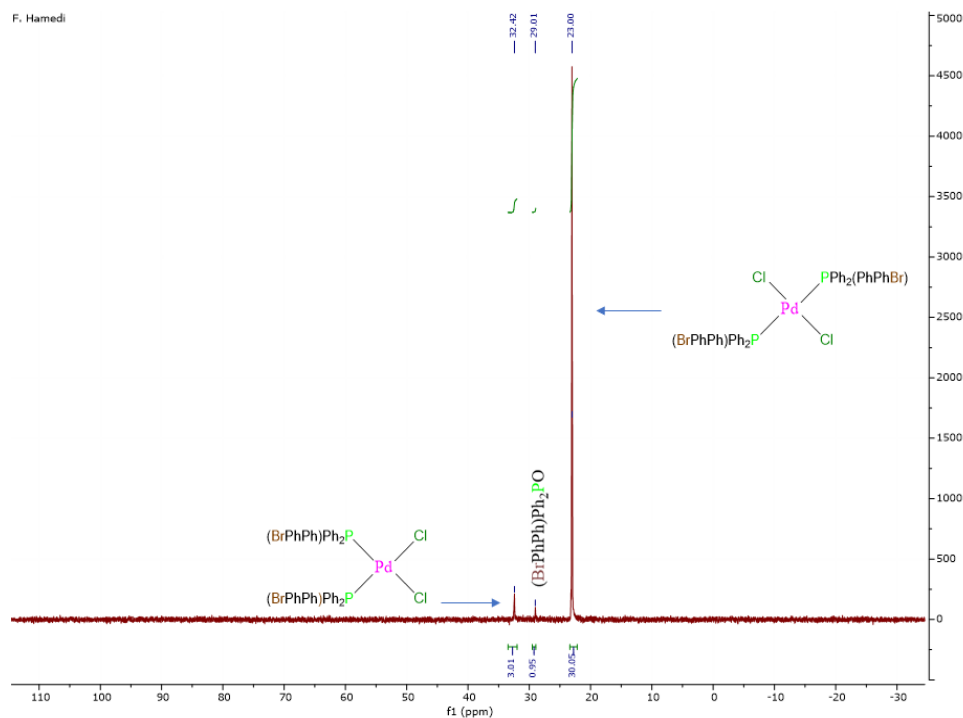
Figure 2 – ^{31}P-NMR spectra of
dichlorobis(4'-bromobiphenyl-4-yl)diphenylphosphine palladium(II) as catalyst
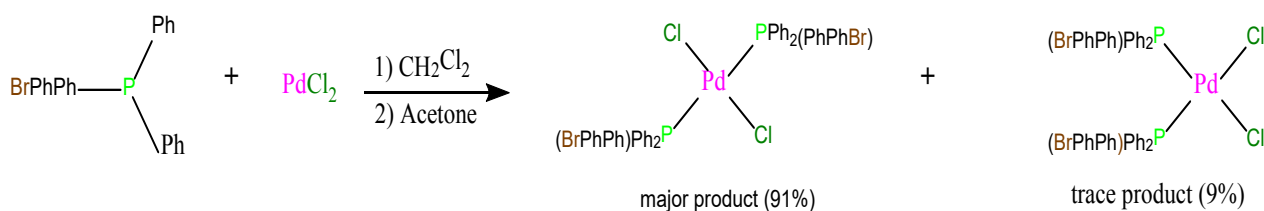
Scheme 2 – Synthesis of trans-dichlorobis(4'-bromobiphenyl-4-yl)diphenylphosphine palladium(II) complex

FT-IR analysis for the (4'-bromobiphenyl-4-yl)diphenylphosphine ligand: Aromatic compounds have characteristic infrared bands in five separate regions of the mid-infrared spectrum. The vibrational frequencies corresponding to the stretching of the C-H bonds in aromatic compounds are seen in the spectral region between 3100 and 3000 cm^{-1} (in this paper: 2924 cm^{-1}), This difference makes it possible to separate these bands from those due to aliphatic C-H groups, which appear at frequencies below the threshold of 3000 cm^{-1}. In the 2000-1700 cm^{-1} spectral region, a series of complex combination and overtone bands appear, showing a correspondence between the configuration of these overtone bands and the pattern of substitutions on the benzene ring (in this paper: not found). Skeletal vibrations, representing C=C stretching, absorb in the 1650 – 1430 cm^{-1} range (in this paper: 1629 and 1498 cm^{-1}). The C–H bending bands appear in the regions 1275 – 1000 cm^{-1} (in-plane bending) (in this paper: 1107, 1061 and 990 cm^{-1}), and 900 – 690 cm^{-1} (out-of-plane bending) (in this paper: 806 cm^{-1}). The vibrations associated with out-of-plane bending in aromatic compounds give rise to robust and distinctive bands, the intensity of which corresponds to the number of hydrogen atoms in the ring. Consequently, these bands can be used to elucidate the pattern of substitutions on the aromatic ring. The absorption regions for C–X stretching (X = F, Cl, Br or I) in organic halogen compounds observed in the 800 – 400 cm^{-1} range (in this paper: 622, 538 and 494 cm^{-1}). The absorption regions for aromatic P–C stretching appear in the 1450 – 1430 cm^{-1} range (in this paper: 1459 cm^{-1}) [24, 25].

FT-IR analysis for the trans-dichlorobis(4'-bromobiphenyl-4-yl)diphenylphosphine palladium(II) complex: Based on what was said above: The C–H stretching bands of aromatic compounds appeared in the 3052cm^{-1}, the overtone bands observed in the 1706cm^{-1}, the C=C stretching appear in the 1588 and 1471cm^{-1}, the C–H bending bands appeared in the 1185 and 1094cm^{-1}, the out-of-plane bending observed in the 691cm^{-1} (v_{P-C}, vs), the C–X stretching appear in the 691cm^{-1} and the aromatic P–C stretching appeared in the 1429cm^{-1} (v_{P-Ph}, s) [24-26].

Catalytic study-Suzuki cross-coupling reactions: The catalytic activity of the Pd complex was evaluated in the C–C coupling reactions of aryl halides with phenylboronic acid. Initial experiments were carried out to investigate the interaction between iodobenzene and phenylboronic acid. The aim was to fine-tune the reaction parameters, which included choice of solvent, choice of base, amount of catalyst and temperature.
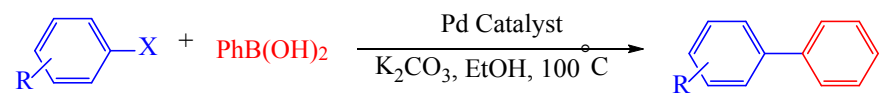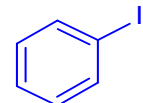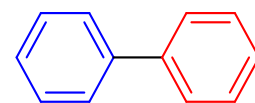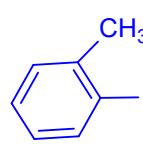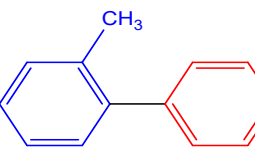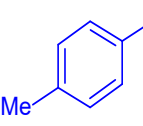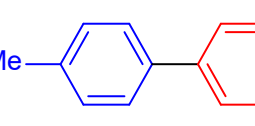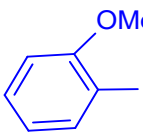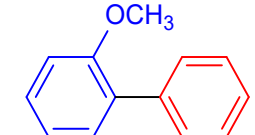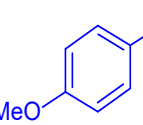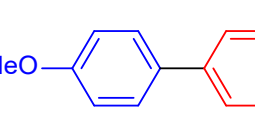
The results are presented in Table 1. During the preliminary refinement phase, we focused on evaluating the effect of a protic solvent on the reaction. Consequently, the prototypical reaction was carried out in a number of solvents, namely DMF, EtOH, i-PrOH and PEG. Among the range of non-aqueous solvents investigated, EtOH emerged as the frontrunner, providing superior yields of the coupled product (Table 1, entries 1–4). For the next stage, various inorganic bases were selected for investigation. Notable among these were K$_2$CO$_3$, Na$_2$CO$_3$, KOH and NaOH, each chosen to assess their influence on the desired reaction (Table 1, entries 5-8). As can be seen from the tabulated data, K$_2$CO$_3$ proved to be the optimum base for the reaction, giving the highest yield. In the third step, the reactions were carried out at different temperatures (as listed in Table 1, entries 9-11). In particular, the reduction in reaction temperature correlated with a decrease in yield, accompanied by an intrinsic increase in reaction time. Consequently, the optimum temperature was found to be 100°C, which provided a suitable optimum temperature. In the next stage, attention shifted to the amount of catalyst used. As predicted, the degree of variation in catalyst dosage had a pronounced effect on catalyst performance. Remarkably, an optimal amount was found to be 0.0007g of Pd complex, a revelation underlined by the data in Table 1 (entries 12-13). Conversely, a decrease in catalyst amount resulted in correspondingly lower yields, confirming the catalytic importance (Table 1, entry 4). As described in Table 4, the yield of biphenyl (Table 1, entry 10) could not be significantly increased by increasing the amount of catalyst to 0.0020 g. Therefore, from an economic point of view, 0.0007g of catalyst was identified as the optimum catalyst loading.

The optimized conditions are: 0.0518g of K$_2$CO$_3$ as base, 0.0007g of Pd complex as catalyst at 100°C in EtOH as solvent. Following the optimization of the experimental parameters, we embarked on an evaluation of the catalytic efficacy of the palladium complex towards a range of aryl halides. The results of these evaluations are summarized in Table 2. Various aryl iodides (Table 2, entries 1-5), bromides (Table 2, entries 6-7) and chlorides (Table 2, entries 8-9) were involved in successful reactions with phenylboronic acid in this study. In each case, the resulting yields ranged from good to excellent yields.
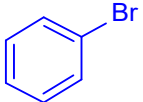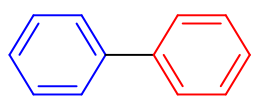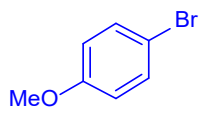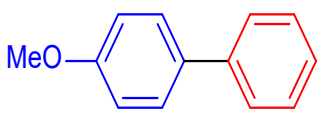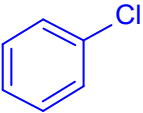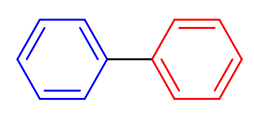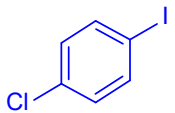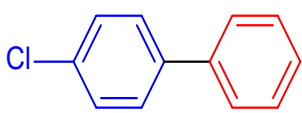
Table 1 – Optimization of reaction conditions for Carbon-Carbon cross coupling of iodobenzene with $PhB(OH)_2$

Entry	Catalyst (g)	Base	Base amount (g)	Solvent	θ (°C)	Time (min)	Yield[a] (%)
1	0.0012	K_2CO_3	0.0518	DMF	80	40	45
2	0.0012	K_2CO_3	0.0518	EtOH	80	40	90
3	0.0012	K_2CO_3	0.0518	PEG	80	40	50
4	0.0012	K_2CO_3	0.0518	i-PrOH	80	40	60
5	0.0012	K_2CO_3	0.0518	EtOH	80	40	90
6	0.0012	Na_2CO_3	0.0397	EtOH	80	40	70
7	0.0012	KOH	0.0210	EtOH	80	40	80
8	0.0012	NaOH	0.0149	EtOH	80	40	75
9	0.0012	K_2CO_3	0.0518	EtOH	60	40	65
10	0.0012	K_2CO_3	0.0518	EtOH	80	40	90
11	0.0012	K_2CO_3	0.0518	EtOH	100	40	95
12	0.0007	K_2CO_3	0.0518	EtOH	100	40	95
13	0.0020	K_2CO_3	0.0518	EtOH	100	40	92

Table 2 – The optimal conditions for the Suzuki C-C coupling of aryl halides

Entry	Aryl halide	Product	Time (min)	Yield (%)[b]	Melting point (°C) Measured	Melting point (°C) literature
1			40	95	68	[27]
2			27	90	Pale yellow liquid	[27]
3			25	93	45-47	[28]
4			30	90	Pale yellow liquid	[29]
5			20	96	86-88	[28]

6	Br (benzene)	biphenyl	40	90	68	[27]
7	MeO—C6H4—Br	MeO—biphenyl	30	89	86-88	[28]
8	Cl (benzene)	biphenyl	50	85	68	[27]
9	Cl—C6H4—I	Cl—biphenyl	70	75	80	[30]

Catalytic study-Heck cross-coupling reactions: Following an investigation of the Suzuki reaction with various aryl halides using a Pd complex as a catalyst, our aim was to evaluate the catalytic efficacy of the aforementioned catalyst in Heck coupling reactions.

Therefore, we studied the effect of non-aqueous protic solvents, inorganic bases, different amounts of optimum base, different amounts of catalyst and various temperature on the model reaction involving iodobenzene and n-butyl acrylate catalyzed by a Pd complex (Table 3). In the initial phase of optimization, a comprehensive investigation was carried out to measure the influence of various solvents, including DMF, EtOH, i-PrOH and PEG. In particular, polyethylene glycol (PEG) demonstrated superior solvent properties when compared to the other solvents investigated. Furthermore, the use of polyethylene glycol (PEG) as a solvent resulted in a significant increase in production efficiency, reaching a remarkable maximum of 95%. (Table 3, entry 1-4). The next stage was to explore the implications of using different bases in the context of the Heck reaction carried out in the PEG solvent. The selection included K_2CO_3, Na_2CO_3, NaOH and KOH, each of which was carefully evaluated (Table 3, entries 5-8). Based on the data presented in Table 3, K_2CO_3 was identified as the optimal base of choice. Moving on to the third step, a meticulous exploration of different amounts of the optimal base, ranging from 0.0518 g to 0.1036 g, was carried out for this reaction. In particular, 0.1036 g of K_2CO_3 was found to be the optimal dosage (Table 3, entries 9-11). The next step involved a meticulous examination of different amounts of catalyst, ranging from 0.0007g to 0.0020g, in search of the optimum performance of the reaction. Notably, 0.0012 g of catalyst appeared to be the optimal choice (Table 3, entries 12-14). In the fifth progression, a substantial augmentation in the reaction's progress was obtained by increasing the temperature from 80 to 120°C (Table 3, entries 15–17).

Table 3 – Optimizing conditions for the C-C coupling of iodobenzene with n-butyl acrylate

Entry	Catalyst (g)	Base	Base amount (g)	Solvent	θ (°C)	Time (min)	Yield[a] (%)
1	0.0012	K_2CO_3	0.0518	DMF	80	20	25
2	0.0012	K_2CO_3	0.0518	ETOH	80	20	35
3	0.0012	K_2CO_3	0.0518	PEG	80	20	95
4	0.0012	K_2CO_3	0.0518	i-PrOH	80	20	20
5	0.0012	K_2CO_3	0.0518	PEG	80	20	95
6	0.0012	Na_2CO_3	0.0397	PEG	80	20	50
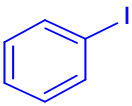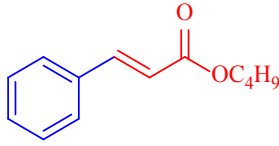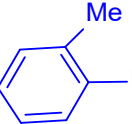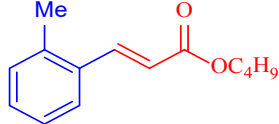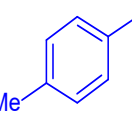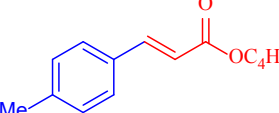
Entry	Catalyst (g)	Base	Base amount (g)	Solvent	θ (°C)	Time (min)	Yield[a] (%)
7	0.0012	KOH	0.0210	PEG	80	20	45
8	0.0012	NaOH	0.0149	PEG	80	20	70
9	0.0012	K_2CO_3	0.0518	PEG	80	20	90
10	0.0012	K_2CO_3	0.0691	PEG	80	16	91
11	0.0012	K_2CO_3	0.1036	PEG	80	10	95
12	0.0007	K_2CO_3	0.1036	PEG	80	20	85
13	0.0012	K_2CO_3	0.1036	PEG	80	10	95
14	0.0020	K_2CO_3	0.1036	PEG	80	8	95
15	0.0012	K_2CO_3	0.1036	PEG	80	10	95
16	0.0012	K_2CO_3	0.1036	PEG	100	7	96
17	0.0012	K_2CO_3	0.1036	PEG	120	5	98
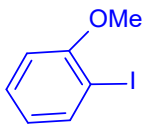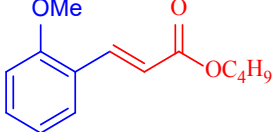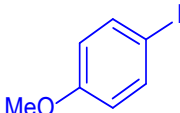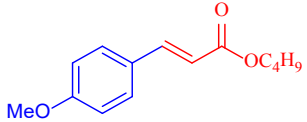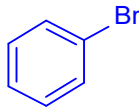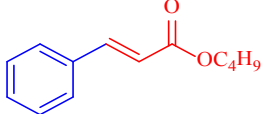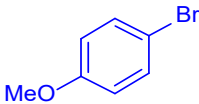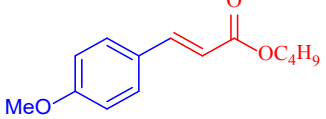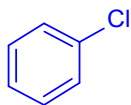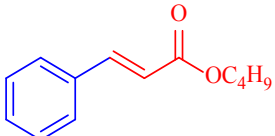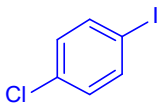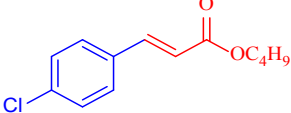
The reaction with activated aryl halides was easily carried out at 120°C. Therefore, the reaction temperature was maintained at 120°C, which was determined to be the optimum temperature. As Table 3 reveals, the optimal conditions involved using a Pd complex (0.0012 g) within a PEG medium, with 0.1036 g of K_2CO_3 as the base, all operating at 120°C. Following the fine-tuning of these reaction parameters, we expanded the capabilities of this catalytic system to facilitate the reaction of n-butyl acrylate with a diverse range of aryl halides, encompassing both electron-donating and electron-withdrawing groups. The outcomes under these optimized conditions are presented in Table 4.

Table 4 – Heck C-C coupling of aryl halides under ideal conditions

Entry	Aryl halide	Product	Time (min)	Yield (%)[b]	Melting point (°C) Measured literature
1			5	98	Pale yellow liquid [27]
2			19	89	Pale yellow liquid [28]
3			6	90	Pale yellow liquid [28]

4	OMe, I	OMe OC_4H_9	40	87	Pale yellow liquid [31]
5	I, MeO	MeO OC_4H_9	20	95	Pale yellow liquid [32]
6	Br	OC_4H_9	25	90	Pale yellow liquid [32]
7	Br, MeO	MeO OC_4H_9	35	85	Pale yellow liquid [31]
8	Cl	OC_4H_9	85	80	Pale yellow liquid [29]
9	I, Cl	Cl OC_4H_9	25	80	Pale yellow liquid [23]

In all cases, we obtained high yields, ranging from good to excellent.

Conclusion

In this study, we prepared the trans-Pd(II) ion catalyst and systematically characterized its structure using NMR and FT-IR. Furthermore, the transe-Pd(II) ion complex was employed as a highly efficient and precisely defined catalyst for the facilitation of Suzuki and Heck cross-coupling reactions involving various aryl halides, leading to the production of corresponding products with yields ranging from moderate to excellent. Notably, the catalyst exhibited remarkable activity.

Conflict of interest

All authors are aware of the article's content and declare no conflict of interest.

References

1. Schlatzer T., Breinbauer B. (2021) Synthesis of hydrophilic phosphorus ligands and their application in aqueous-phase metal-catalyzed reactions. *Adv. Synth. Catal.*, 363(3), pp. 668-687. https://doi.org/10.1002/adsc.202001278.

2. Musina E., Balueva A., Karasik A. (2019) Phosphines: preparation, reactivity and applications. O*rganophosphorus Chemistry.*, 48, pp. 1-63. https://doi.org/10.1039/9781788016988-00001.

3. Spessard G.O., Miessler G.L. (2016) Organometallic chemistry: 3rd ed. New York: Oxford University Press, 849 p. ISBN 978-0-19-934267-9.

4. Chadwick J.C., Duchateau R., Freixa Z., Van Leeuwen P.W.N.M. (2011) Homogeneous Catalysts: Activity-Stability-Deactivation. Weinheim: Wiley-VCH, 418 p. ISBN 978-3-527-32329-6.

5. Xue L., Lin Z. (2010) Theoretical aspects of palladium-catalysed carbon-carbon cross-coupling reactions. *Chem. Soc. Rev.*, 39, pp.1692-1705. https://doi.org/10.1039/B814973A.

6. Baerns M. (2004) Basic principles in applied catalysis. Berlin, Heidelberg, New York: Springer-Verlag, 558 p. ISBN 978-3-642-07310-6.

7. Beller M., Bolm C. (2008) Transition metals for organic synthesis: building blick and fine chemicals: 2nd ed. Weinheim: Wiley-VCH, 1344 p. ISBN 978-3-527-61940-5.

8. Crabtree R.H. (2014) The organometallic chemistry of the transition metals: 6th ed. New Jersey: John wiley & Sons, 522 p. ISBN 978-1-11-813707-6.

9. Shi W., Liu C., Lei A. (2011) Transition-metal catalyzed oxidative cross-coupling reactions to form C-C bonds involving organometallic reagents as nucleophiles. *Chem. Soc. Rev.*, 40, pp. 2761-2776. https://doi.org/10.1039/C0CS00125B.

10. Milde B. (2012) (Ethynyl-)ferrocenyl phosphine palladium complexes and (bis-)phosphinoimidazol(e/ium) compounds and their application in homogeneous catalysis. Technische Universität Chemnitz, Fakultät für aturwissenschaften, 239 p.

11. Wang Y., Luo J., Liu Z. (2013) Salicylaldoxime-functionalized poly(ethylene glycol)-bridged dicationic ionic liquid ([salox-PEG$_{1000}$-DIL][BF$_4$]) as a novel ligand for palladium-catalyzed Suzuki–Miyaura reaction in water. *Appl. Organomet. Chem.*, 27(10), pp. 601-605. https://doi.org/10.1002/aoc.3038.

12. Tabrizi L., Zouchoune B., Zaiter A. (2020) Theoretical and experimental study of gold(III), palladium(II), and platinum (II) complexes with 3-((4-nitrophenyl)thio)phenylcyanamide and 2,2′-bipyridine ligands: Cytotoxic activity and interaction with 9-methylguanine. *Inorg. Chim. Acta.*, 499, p. 119211. https://doi.org/10.1016/j.ica.2019.119211.

13. Zhou B., Wang H., Cao Z.Y., Zhu J.W., Liang R-X., Hong X., Jia Y.X. (2020) Dearomative 1,4-difunctionalization of naphthalenes via palladium-catalyzed tandem Heck/Suzuki coupling reaction. *Nature communications*, 11(1), p. 4380. https://doi.org/10.1038/s41467-020-18137-w.

14. Naghipour A., Ghorbani-Choghamarani A., Babaee H., Hashemi M., Notash B. (2017) Crystal structure of novel polymorph of trans-dichloro(triphenylphosphine) palladium(II) and its application as a novel efficient and retrievable for the amination of aryl halides and stille crocc-couplhng reactions. *J. Organomet. Chem.*, 841, pp. 31-38. https://doi.org/10.1016/j.jorganchem.2016.10.002.

15. Naghipour A., Ghorbani□Choghamarani A., Babaee H., Notash B. (2016) Synthesis and X□ray structural characterization of a bidendate phosphine (dppe) palladium (II) complex and its application in Stille and Suzuki cross□coupling reactions. *Appl. Organomet. Chem.*, 30(12), pp. 998-1003. https://doi.org/10.1002/aoc.3533.

16. Knight L.K., Freixa Z., Leeuwen P.W.N.M.V., Reek J.N.H. (2006) Supramolecular trans-coordination phosphine ligands. *Organometallics.*, 25, pp. 954-960. https://doi.org/10.1021/om050865r.

17. Martin L.L., Jacobson R.A. (1971) The Crystal and molecular structure of cis-dichlorobis(dimethylphenylphosphin) palladium(II). *Inorg. Chem.* 1971, 10(8), pp. 1795-1798.

18. Zasukhin D.S., Kostyukov I.A., Kasyanov I.A., Kolyagin Yu.G., Ivanova I.I. (2021) ^{31}P NMR spectroscopy of adsorbed probe molecules as a tool for the determination of the acidity of molecular sieve catalysts (a review). *Petrol. Chem.*, 61(8), pp. 875-894. https://doi.org/10.1134/S0965544121110232.

19. Tastawiecka E., Flis A., Stankevic M., Grekuk M., Stowik G., Gac W. (2018) P-Arylation of secondary phosphine oxides catalyzed by nickel-supported nanoparticles. *Org. Chem. Front.*, 5(13), pp. 2079-2085. https://doi.org/10.1039/C8QO00356D.

20. Albright T.A., Freeman W.J., Schweizer E.E. (1975) Nuclear magnetic resonance studies. IV. The carbon and phosphorus nuclear magnetic resonance of phosphine oxides and related compounds. *J. Org. Chem.*, 40(23), pp. 3437-3441.

21. Duckmanton P.A., Blake A.J., Love J.B. (2005) Palladium and rhodium ureaphosphine complexes: exploring structural and catalytic consequences of anion binding. *Inorg. Chem.*, 44(22), pp.7708-7710. https://doi.org/ 10.1021/ic051110f.

22. Lu X.X., Tang H.S, Ko C.C., Wong J.K.Y., Zhu N., Yam V.W.W. (2005) Anion-assisted trans-cis isomerization of palladium(II) phosphine complexes containing acetanilide functionalities through hydrogen bonding interactions. *Chem. Commun.*, 12, pp. 1572-1574. https://doi.org/10.1039/B418202B.

23. Celepci D.B. (2020) Novel *cis*-[PdCl$_2$(NHC)(PPh$_3$)] complex: synthesis, crystal structure, spectral investigations, DFT and NCI studies, prediction of biological activity. *J.Coord. Chem.*, 73(4), pp. 525-543. https://doi.org/10.1080/00958972.2020.1732360.

24. Stuart B. H. (2004) Infrared Spectroscopy: Fundamentals and Applications. John Wiley & Sons., 245 p. ISBN 0-470-85428-6.

25. Nakamoto K. (2009) Infrared and Raman Spectra of Inorganic and Coordination Compounds, Part B: Applications in Coordination, Organometallic, and Bioinorganic Chemistry. John Wiley & Sons., 416 p. ISBN 978-0-471-74493-1.

26. Al-Jibori S.A., Ulghafoor M.A., Karadag A., Aydin A., Akbas H., Ruiz S.G. (2019) Synthesis, characterization and anti-tumor activity of Pd(II) complexes with 4,5-benzo-3H-1,2-dithiole-3-thione. *Transition Met. Chem.*, 44, pp. 575-583. https://doi.org/ 10.1007/s11243-019-00314-6.

27. Ghorbani-Choghamarani A., Naghipour A., Babaee H., Notash B. (2016) Synthesis, crystal structure study and high efficient catalytic activity of di-μbromo-trans–dibromobis[(benzyl)(4-methylphenyl)(phenyl)phosphine] dipalladium(II) in Suzuki–Miyaura and Heck–Mizoroki C–C coupling reactions. *Polyhedron.*, 119, pp. 517-524. https://doi.org/10.1016/j.poly.2016.08.040.

28. Naghipour A., Fakhri A. (2016) Heterogeneous Fe$_3$O$_4$@chitosan-Schiff base Pd nanocatalyst: Fabrication, characterization and application as highly efficient and magnetically-recoverable catalyst for Suzuki–Miyaura and Heck–Mizoroki C–C coupling reactions. *Catal. Commun.*, 73, pp. 39-45. https://doi.org/10.1016/j.catcom.2015.10.002.

29. Pathan S., Patel A. (2012) Heck coupling catalyzed by Pd exchanged supported 12-tunstophosphoric acid – an efficient ligand free, low Pd-loading heterogeneous catalyst. *RSC Adv.*, 2(1), pp. 116-120. https://doi.org/10.1039/C1RA00687H.

30. Moradi Z., Ghorbani-Choghamarani A. (2021) Design and synthesis of Fe_3O_4@SiO_2@KIT-6@DTZ-Pd^0 as a new and efficient mesoporous magnetic catalyst in carbon-carbon cross-coupling reactions *Sci. Rep.*, 11(1), p. 23967. https://doi.org/10.1038/s41598-021-03485-4.

31. Zhu Q., Nie F., Feng J., Li Y., Wang X., Xu Y. (2016) ChemInform abstract: palladium-catalyzed synthesis of novel O-heterocycles by Domino Suzuki coupling-Michael addition reaction. *ChemInform.*, 47(35), pp. 919-923. https://doi.org/10.1002/chin.201635118.

32. Chen T., Gao J., Shi M. (2006) A novel tridentate NHC–Pd (II) complex and its application in the Suzuki and Heck-type cross-coupling reactions. *Tetrahedron*, 62(26), pp. 6289-6294. https://doi.org/10.1016/j.tet.2006.04.034.

Information about authors:

Farhang Hamedi – PhD Student, Department of Chemistry, Faculty of Science, Ilam University, Ilam, Iran, e-mail: f.hamedi@ilam.ac.ir

Ali Naghipour – (corresponding author) – Associate Professor, Dr., Department of Chemistry, Faculty of Science, Ilam University, Ilam, Iran, e-mail: a.naghipour@ilam.ac.ir

Ensieh Ghasemian Lemraski – Associate Professor, Dr., Department of Chemistry, Faculty of Science, Ilam University, Ilam, Iran, e-mail: e.ghasemian@ilam.ac.ir

Saeid Taghavi Fardood – Assistant Professor, Dr., Department of Chemistry, Faculty of Science, Ilam University, Ilam, Iran, e-mail: s.taghavi@ilam.ac.ir

D.B. Wadave * , S.C. Daswadkar

Dr. D. Y. Patil College of Pharmacy, Maharashtra, India
*e-mail: dishawadave1999@gmail.com
(Received 26 June 2024; received in revised form 21 July 2024; accepted 27 July 2024)

Molecular docking study of 2,4-disubstituted thiazole derivatives as antiulcer activity

Abstract. In this study, 2,4-disubstituted thiazole derivatives were used to create an antiulcer agent. These compounds were chosen based on molecular properties and a drug-likeness score, ensuring their suitability for oral absorption. The molecular docking of 2,4-disubstituted thiazole derivatives was performed using AutoDock Vina ver. 1.1.2. The thiazole derivatives were constructed using Cambridge's ChemDraw Ultra 8.0 software. The program Chem 3D Ultra 8.0 was used to convert 2D structures to 3D structures. Thiazole derivatives were docked into the H2 blocker, with nizatidine binding at the active site (PDB ID: 2XZB) as the target protein obtained from the protein data bank. The current study reported anti-ulcer activity of newly synthesized derivatives with electron releasing and electron withdrawing groups on thiazole derivative. The study provided potential derivatives exhibiting significant anti-ulcer activity with fast onset and extended duration of action, which is the most promising expectation of any anti-ulcer agent, especially when administered in conjunction with complaint-specific therapy.
Key words: Antiulcer, 2,4-disubstituted thiazole derivative, 2XZB, AutoDock Vina, ChemDraw.

Introduction

One of the most common chronic gastrointestinal disorders is peptic ulcer.causes resulting from an imbalance in blood flow, mucus, bicarbonate, prostaglandin, acid, pepsin, and bile. Factors related to heredity, alcohol, drugs, smoking, and *Helicobacter pylori* are causes of imbalance. A peptic ulcer is a lesion that appears on the mucosa of the stomach or duodenum and is caused by exposure of the mucosal epithelium to acid and pepsin. The continuous lining of the epithelium breaks when there is an imbalance between aggressive and protective to mucosal damage in peptic ulcers [1]. Around 10% of people worldwide suffer from peptic ulcers. Peptic ulcer disease is thought to affect 5-10% of the general population. Duodenal peptic ulcers account for about 19 of every 20 cases. An estimated 15,000 deaths are attributed to peptic ulcers annually. According to the most recent WHO data, 68,108 deaths in India were related to peptic ulcer disease in 2020, accounting for 0.80% of all deaths. India is ranked 42nd in the world with an age-adjusted death rate of 6.24 per 100,000 people [2]. The 2,4-disubstituted thiazole derivatives became important class in the field of medicinal chemistry due to their various pharmacological and biological activities such as antitumor [3], antiinflammatory [4], anticonvulsant [5], anticancer, antioxidant [6], anti-microbial [7], antibacterial, antifungal [8], antidiabetic [9].

Materials and methods

Preparation of target protein X-ray structure. The target protein was chosen to be the crystal structure of the H2 blocker in which nizatidine bound at the active site (PDB ID: 2XZB), which was obtained from http://www.pdb.org.

Design of 2,4 disubstituted derivatives. The three steps in the development of an innovative drug are (a) pharmacophore determination, (b) pharmacophore substituent variation, and (c) pharmacophore list determination. 2,4-disubstituted thiazole is the anti-ulcer agent used in this study and is pharmacophore-like. -F, -CF_3, -NO_2, -CH_3, -Br, -$N(CH_3)_2$, -NH_2, -OCH_3, and other substituents are among the several designated for the design of novel analogs (Figure 1).
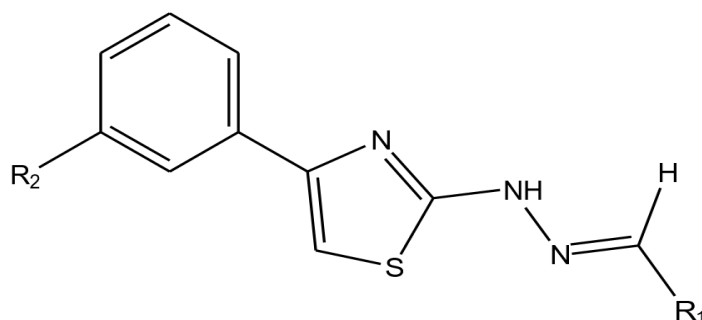
Figure 1 – Structure of 2,4-disubstituted thiazole derivative

Ligands preparation. Cambridge Soft's ChemDraw Ultra 8.0 program was used to haggard the structures of 2,4-disubstituted Thiazole derivatives like TZ6, TZ16, and TZ-17. By using the Chem 3D Ultra 8.0 tool, the 2D structures of the suggested ligand were transformed into a 3D structure. By applying a termination RMS gradient of 0.001 KCal/mol for extreme up to 1000 iterations, the semi-empirical PM3 technique was used to optimize the proposed ligand and minimize its energy. The resultant PBD arrangement was saved and could be read by the AutoDock Vina software. Following that, the Swiss ADME tool was used to determine the drug-likeness attribute.

Molecular docking studies. Molecular docking is the computational modeling of a ligand interacting with a receptor or target protein; it aids in predicting the ligand's binding to the target protein to determine its activity and affinity. A molecular docking method such as AutoDock Vina ver. 1.1.2 was used to evaluate the interaction between H2 blocker and thiazole derivatives. The target protein that we used was the X-ray crystal structure of the H2 blocker where nizatidine bound at the active site (PDB ID: 2XZB) [10], which was obtained from http://www.pdb.org. The ligands were redocked into their binding pocket within the H2 blocker x-ray crystal structure to obtain the docked pose and RMSD, which served as an authentication step for the docking procedure prior to ligand examination. The Discovery Studio software version 3.1.0.11157 was utilized to investigate the molecular interaction between the newly designed ligands and the target protein. Table 1 contains the tabulated interactions and docking scores. The ligands' active site of binding in an H2 blocker, in conjunction with the interacting amino acids.

Results and discussion

Molecular docking enables virtual screening, a computational method that finds new bioactive compounds in huge chemical libraries. By guiding drug-receptor interactions, these techniques help designers of new drugs by providing insight into the relationship between ligands and target proteins. Small molecules are identified with the help of computer-aided drug design, which places and scores them in the active site of the target protein. Using AutoDock Vina Version 1.1.2, molecular docking simulations were run for thiazole derivatives in this study, with the target protein being 2XZB. Based on the ligand binding position and fitness function scores, the program determined the optimal docking poses. The optimal ligand binding position was assessed using RMSD. The docking scores, which indicate the binding energy needed for the target protein to interact with ligands, demonstrated stability and were suggestive of compound activity (Figure 1).

Table 1 lists the thiazole derivatives' binding energy values. A total of twenty derivatives showed docking scores between -8.9 and -9.3 kcal/mol. When compared to the standard compound nizatidine, the thiazole derivatives displayed higher docking scores.

The proposed 2,4-disubstituted thiazole derivatives had an approximate docking score of -7.7–-9.3 kcal/mol. Ten derivatives of 2,4-disubstituted thiazole had higher docking scores than nizatidine (-8.2), which was used as the standard compound. The derivative TZ-16 had a higher binding energy (-9.3) than the other 2,4-disubstituted thiazole derivatives.

The interaction of probable derivatives with the target protein structure was determined and visualized using the Discovery Studio visualizer, as shown in Figures 2-3.

Table 1 – The thiazole derivatives' binding energy values

Ligand	Binding Affinity (kcal/mol)	Ligand	Binding Affinity (kcal/mol)
TZ-1	-9.8	TZ-11	-8.8
TZ-2	-8.5	TZ-12	-8.6
TZ-3	-9	TZ-13	-8.8
TZ-4	-9.2	TZ-14	-9.3
TZ-5	-8.6	TZ-15	-9
TZ-6	-8.8	TZ-16	-9.4
TZ-7	-9	TZ-17	-8.9
TZ-8	-8.4	TZ-18	-8.4
TZ-9	-9	TZ-19	-8.9
TZ-10	-8.5	TZ-20	-9.1
Std	-8.6	-	-
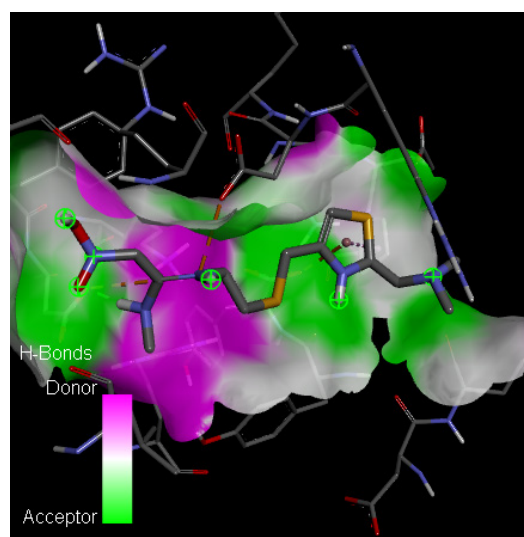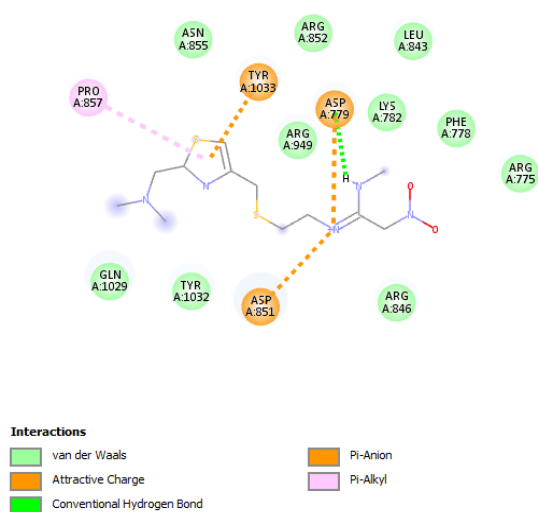
Figure 2 – 3D and 2D figures about the interaction of Nizatidine with 2XZB target protein
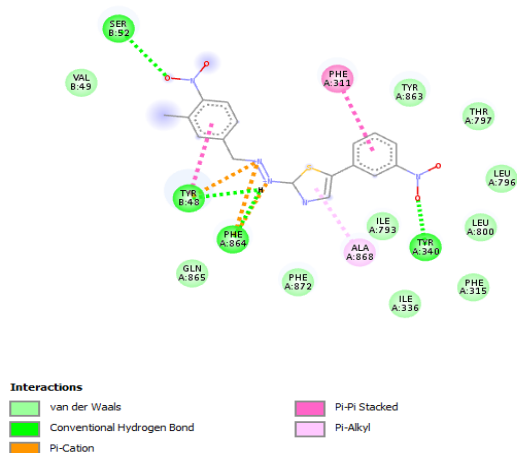
Figure 3 – 3D and 2D figures about the interaction of TZ-1with 2XZB target protein

Conclusion

This study analyzed 20 molecular structures of 2,4 disubstituted thiazole derivatives with aldehyde groups attached to their rings. These compounds were then docked to determine how they interact with the 2XZB protein structure. The docking scores were used to identify ligands that had a high affinity for 2XZB. The results showed that twenty derivatives had higher docking scores than nizatidine, indicating stronger binding energy and interaction with the target protein. As a result, these compounds have the potential to act as powerful antiulcer agents. However, additional studies involving synthesis and in vitro evaluations are required to determine their true antiulcer activity.

Conflict of interest

All authors are aware of the article's content and declare no conflict of interest.

References

1.   Narayanan M., Reddy K.M., Marsicano E. (2018) Peptic ulcer disease and Helicobacter pylori infection. *Missouri medicine*, 115(3), pp. 219. https://www.ncbi.nlm.nih.gov/pmc/articles/PMC6140150/.

2.   Behrman S.W. (2005) Management of complicated peptic ulcer disease. *Archives of surgery*, 140(2), pp. 201-208. https://doi.org/10.1001/archsurg.140.2.201.

3.   Arshad M.F., Alam A., Alshammari A.A., Alhazza M.B., Alzimam I.M., Alam M.A., Mustafa G., Ansari M.S., Alotaibi A.M., Alotaibi A.A., Kumar S. (2022) Thiazole: A versatile standalone moiety contributing to the development of various drugs and biologically active agents. *Molecules*, 27(13), pp. 3994. https://doi.org/10.3390/molecules27133994.

4.   Krishnan P.G., Prakash K.G., Sekhar K.C. (2019) Synthesis, characterization and anti-inflammatory activity of certain novel 2, 4-disubstituted 1, 3-thiazole derivatives. *Rasāyan Journal of Chemistry*, 1(12), pp. 1. http://dx.doi.org/10.31788/RJC.2019.1215069.

5.   Petrou A., Fesatidou M., Geronikaki A. (2021) Thiazole ring – a biologically active scaffold. *Molecules*, 26(11), pp. 3166. https://doi.org/10.3390/molecules26113166.

6.   An T.N., Kumar M.A., Chang S.H., Kim M.Y., Kim J.A., Lee K.D. (2014) Synthesis, anticancer and antioxidant activity of novel 2, 4-disubstituted thiazoles. *Bull. Korean Chem. Soc.*, 35(6), pp. 1619. https://doi.org/10.5012/bkcs.2014.35.6.1619.

7.   An T.N., Phuong P.T., Quang N.M., Son N.V., Cuong N.V., Tan L.V., Tri M.D., Alam M., Tat P.V. (2020) Synthesis, docking study, cytotoxicity, antioxidant, and anti-microbial activities of novel 2, 4-disubstituted thiazoles based on phenothiazine. *Current Organic Synthesis*, 17(2), pp. 151-159. https://doi.org/10.2174/1570179417666191220100614.

8.   Arora P., Narang R., Nayak S.K., Singh S.K., Judge V. (2016) 2, 4-Disubstituted thiazoles as multitargated bioactive molecules. *Medicinal Chemistry Research*, 25, pp. 1717-1743. https://doi.org/10.1007/s00044-016-1610-2.

9.   Gujjarappa R., Kabi A.K., Sravani S., Garg A., Vodnala N., Tyagi U., Kaldhi D., Gupta S., Malakar C.C. (2022) Overview on Biological Activities of Thiazole Derivatives. InNanostructured Biomaterials: Basic Structures and Applications. Singapore: Springer Singapore, pp. 101-134. https://doi.org/10.1007/978-981-16-8399-2_5.

10.   Noor A., Qazi N.G., Nadeem H., Khan A.U., Paracha R.Z., Ali F., Saeed A. (2017) Synthesis, characterization, anti-ulcer action and molecular docking evaluation of novel benzimidazole-pyrazole hybrids. *Chemistry Central Journal*, 11, pp. 1-3. https://doi.org/10.1186/s13065-017-0314-0.

Information about authors:

Disha B. Wadave – (corresponding author) – master's student, Pharmaceutical Chemistry, Dr. D.Y. Patil College of Pharmacy, Akurdi Pune, India, e-mail: dishawadave1999@gmail.com

Shubhangi C. Daswadkar – PhD, Associate Professor, Dr. D. Y. Patil College of Pharmacy, Akurdi Pune, India, e-mail: shubhangidaswadkar@dyppharmaakurdi.ac.in

A.E. Johns [1]* , P.M. Radhamany[2]

[1] St. Thomas College, Kozhencherry, Kerala, India
[2] University of Kerala, Thiruvananthapuram Kariavattom, Kerala, India
*e-mail: adheenajohns123@gmail.com

Phytochemical Screening, HPTLC and FT-IR analysis of methanolic bark extract of *Syzygium stocksii* (Duthie) Gamble – a critically endangered taxon in Myrtaceae

Abstract. *Syzygium* is a large genus with numerous species in the Family Myrtaceae. The genus *Syzygium* is a treasure trove of phytochemicals with immene therapeutic potential. *Syzygium stocksii* (Duthie) Gamble syn. *Syzygium travancoricum*, a critically endangered plant collected from Thrissor District in Kerala, India. The present study aims at the preliminary phytochemical screening, HPTLC and FT-IR analysis of the plant. Qualitative phytochemical studies revealed the presence of alkaloids, phenolics, flavonoids, tannins, and terpenoids. The preliminary phytochemical screening results revealed the presence of more constituents on the methanolic bark extract, and hence, this was further subjected to an HPTLC analysis to determine the number of compounds in the crude extract. FTIR analysis was also conducted to identify the major functional groups in the compounds in the extract. From this study, it can be concluded that *Syzygium stocksii* contains various bioactive compounds. This study calls for the importance of excavating the phytochemical and pharmacological potential of this relatively unexplored species.
Key words: *Syzygium stocksii*, preliminary phytochemical screening, HPTLC, FTIR.

Introduction

The genus *Syzygium*, part of the Myrtaceae family, is the largest woody genus of flowering plants, comprising 1,200 to 1,800 species found across the Old-World tropics and subtropics [1]. Myrtaceae plants are well-known for their rich supply of medicinally valuable volatile oils, which are widely used in traditional medicines throughout various ethnobotanical practices in tropical regions [2]. Numerous phytochemical studies have been conducted on various *Syzygium* species, such as *Syzygium cumini*, *S. jambos*, *S. malaccense*, *S. guineense*, and *S. caryophyllatum* [3,4].

Among the species, *Syzygium stocksii* (Duthie) Gamble (syn. *Syzygium travancoricum* Gamble) remains relatively unexplored despite its significant ethnopharmaceutical importance. This fruit tree, classified as critically endangered under the IUCN Threatened Species category, is reported to have only around 200 trees remaining in the Western Ghats according to the IUCN Red List (2010, 2012, 2013). *Syzygium stocksii* is an evergreen tree that can grow up to 25 meters in height with white flowers, typical of the Myrtaceae family. While many studies have evaluated the phytopharmacological properties of other *Syzygium* species, research on *Syzygium stocksii* is still sparse.

Materials and methods

Plant material and sample preparations. Leaves, bark, fruit pulp, and seeds of *S. stocksii* were collected from Thrissur district, Kerala, India. A voucher specimen (KUBH 10252) was prepared, identified and deposited at the Department of Botany, University of Kerala. For phytochemical analysis, bark, leaves, fruit pulp and seeds were separately dried at below 40°C. The powdered samples were sequentially extracted with hexane, ethyl acetate, acetone, methanol, and water in the increasing polarity with the Soxhlet apparatus. The extracts were filtered through Whatman No.1 filter paper and the solvents were evaporated under reduced pressure. Dried extracts obtained were stored at 4°C until further analysis.

Preliminary phytochemical screening. Qualitative phytochemical analyses were done for establishing a profile of the given extract for its chemical composition. The following tests were performed on extracts to detect various phytoconstituents present in them [6-8]:

Detection of alkaloids. Stirred 50 mg solvent free extract with few ml of dilute hydrochloric acid and filtered. The filtrate was tested carefully with various alkaloid reagents as follows.

Mayer's test. To a few ml of filtrate, one or two drops of Mayer's reagent were added through the side of the test tube. A white or creamy precipitate indicates the test as positive.

Dragendorff's test. To a few ml of filtrate, 1 or 2 ml of Dragendorff's reagent was added. A prominent yellow precipitate indicates the test as positive.

Detection of anthocyanins. The addition of 10% NaOH to the extract resulted in a blue coloration, indicating the presence of anthocyanins. Similarly, the addition of concentrated sulfuric acid produced a yellowish orange colour, further confirming the presence of anthocyanins.

Detection of coumarins. To the extract, addition of alcoholic KOH or NaOH resulted yellow colouration appears which will disappear on adding concentrated HCl indicating the presence of coumarins.

Detection of flavonoids. Three different methods were employed to determine the presence of flavonoids in the plant samples. For the alkaline reagent test, the extract was treated with a few drops of NaOH solution, resulting in the formation of an intense yellow colour. This yellow colour disappeared upon the addition of a dilute acid, confirming the presence of flavonoids. To a portion of the aqueous filtrate of the extract, 5 ml of dilute ammonia solution was added, followed by concentrated sulfuric acid. The appearance of a yellow coloration in the extract indicates the presence of flavonoids. A portion of the filtrate was heated with 10 ml of ethyl acetate over a steam bath for 3 minutes. The mixture was filtered and 4 ml of filtrate was shaken with 1 ml of dilute ammonia solution. Yellow coloration indicates the presence of flavonoids.

Detection of glycosides. Fifty milligrams of the extract were hydrolysed with concentrated hydrochloric acid for 2 hours on a water bath. After filtration, the hydrolysate was subjected to Bontrager's test [9]. To 2 ml of the filtered hydrolysate, 3 ml of chloroform was added and shaken. The chloroform layer was then separated, and 10% ammonia was added to it. The appearance of a pink colour indicated the presence of glycosides.

Detection of phenolic compounds. Ferric chloride test. Dissolved 50mg of extract in 5ml of distilled water and to which few drops of neutral 5% ferric chloride solution was added. Dark green colour indicates the presence of phenolic compounds.

Gelatin test. The extract (50mg) was dissolved in 5ml of distilled water and added 2ml of 1% solution of gelatin containing 10% sodium chloride to it. White precipitate indicates the presence of phenolic compounds.

Detection of saponins. Froth test. The extracts were diluted with distilled water to a total volume of 20 ml and shaken in a graduated cylinder for 15 minutes. The formation of a foam layer over 1cm indicates the presence of saponins [10].

Foam test. A total of 0.5 g of the extract was shaken with 2 ml of water. The persistence of foam for ten minutes indicated the presence of saponins.

Detection of Steroids. Libermann-Burchrd's test. Added 2 ml of acetic anhydride to 0.5 g extract of each sample with 2 ml of sulphuric acid. The colour change from violet to blue or green indicates the presence of steroids.

Detection of tannins. Gelatin test. To the extract, 1% gelatin solution containing sodium chloride was added. The formation of a white precipitate indicated the presence of tannins. Additionally, the extract was treated with ferric chloride, and the appearance of a dark blue or greenish-black color further confirmed the presence of tannins.

Detection of terpenoids. Salkowski test. Mixed 5 ml of the extract with 2 ml of chloroform and carefully added 3 ml of concentrated sulphuric acid to form a layer. A reddish-brown coloration at the interface was formed to show a positive result for the presence of terpenoids.

Detection of quinone. The extract is mixed with concentrated sulphuric acid; the resulting red colour indicates the presence of quinone.

Detection of carbohydrates and reducing sugar. Dissolved small quantities of the filtrate in 4ml of distilled water and filtered. The filtrate was subjected to Fehling's test. The extract was treated with Fehling's reagent A & B. The appearance of reddish-brown colour precipitate indicates the presence of reducing sugar. For the Benedict's test, the extract was treated with Benedict's reagent. Appearance of reddish orange colour precipitate indicates the presence of reducing sugar.

Detection of iridoids. The extract was added to 1 ml of reagent (10 ml acetic acid, 0.2% $CuSO_4$ and 0.5 ml conc. HCl). The mixture was heated over a small flame. The development of a light blue colour indicates the presence.

High Performance Thin Layer Chromatography Analysis (HPTLC). A number of solvent systems were tried and a system which gave the maximum resolution was ethyl acetate: methanol (5:0.8) and

was selected as the solvent system for the extract. The extracts were applied as different tracks of different concentrations of width 8 mm each on silica gel 60 F 254 pre-coated aluminium sheets through CAMAG micro litre syringe using Automatic TLC Sampler 4 (ATS4). After sample application the plate was introduced vertically in a CAMAG developing chamber (10 cm × 10 cm) pre-saturated with the mobile phase selected. The developed chromatogram was air dried to evaporate solvents from the plate and the plate was kept in CAMAG Vizualizer and the images were captured under UV light at 254 nm and 366 nm. The plate was scanned at 254 nm and 366 nm using TLC Scanner 4 and the fingerprint profiles were documented. The R f values and finger print data were recorded with winCATS software associated with the scanner. The plate was derivatised using vanillin-sulphuric acid reagent, heated at 105^0C by placing on CAMAG TLC plate heater till the colour of the bands appeared. Then the plate was visualized under white light and the chromatograms were documented. The plate was scanned at 575 nm and the R_f values and finger print data were documented.

Fourier Transformed Infrared Spectroscopy (FTIR) Analysis. About 1mg of the dried methanolic extract was encapsulated in 10 mg of KBr pellet in order to prepare translucent sample discs. The powdered sample of the extract was loaded in FTIR spectroscope (Shimadzu, Japan), with a scan range from 400 to 4000 cm^{-1} with a resolution of 4 cm^{-1}. The spectral data was taken on an Agilent Cary 630 FTIR spectrometer based on the ATR (Attenuated Total Reflection) method. This was done to determine the functional groups in the plant extract.

Results and discussion

The results of the preliminary phytochemical analysis, as presented in Tables 1-4, indicate the presence of alkaloids, phenols, terpenoids, and flavonoids in the leaves, bark, fruit pulp, and seeds. Among the solvents tested – hexane, ethyl acetate, acetone, distilled water, and methanol – methanol extracts revealed the highest number of phytochemicals, while hexane extracts showed the least. Different plant parts, including leaves, bark, fruit, and seeds, were found to contain multiple phytochemical compounds, many of which are recognized for their beneficial roles in medical sciences.

Table 1 – Preliminary phytochemical screening of the leaves of *Syzygium stocksii*

Phytochemical constituents	Hexane	Ethyl acetate	Acetone	Methanol	Distilled water
Alkaloids	-	-	-	+	-
Anthocyanins	-	-	-	+	-
Coumarins	+	+	+	+	-
Flavonoids	-	-	+	+	+
Glycosides	-	-	+	+	+
Phenols	-	+	+	+	+
Saponins	-	-	-	+	+
Steroids	-	-	-	-	-
Tannins	-	+	+	+	+
Terpenoids	-	-	-	+	-
Quinones	-	-	-	-	-
Reducing sugar	-	-	-	-	+
Carbohydrates	-	-	-	-	+
Iridoids	+	-	-	-	-
Note: "+"indicates the presence of phytochemical; "-" indicates the absence of phytochemical					

Table 2 – Preliminary phytochemical screening of the bark of *Syzygium stocksii*

Phytochemical constituents	Hexane	Ethyl acetate	Acetone	Methanol	Distilled water
Alkaloids	-	-	-	+	-
Anthocyanins	-	-	-	+	-
Coumarins	+	+	+	+	-
Flavonoids	-	-	+	+	+
Glycosides	-	-	+	+	+
Phenols	-	+	+	+	+
Saponins	-	-	+	+	+
Steroids	-	-	-	+	-
Tannins	-	+	+	+	+
Terpenoids	-	-	-	+	-
Quinones	-	-	-	-	-
Reducing sugar	-	-	+	-	+
Carbohydrates	-	-	+	-	+
Iridoids	-	-	-	-	-
Note: "+"indicates the presence of phytochemical; "-" indicates the absence of phytochemical					

Table 3 – Preliminary phytochemical screening of the fruit pulp of *Syzygium stocksii*

Phytochemical constituents	Hexane	Ethyl acetate	Acetone	Methanol	Distilled water
Alkaloids	-	-	-	+	+
Anthocyanins	-	-	-	-	+
Coumarins	+	+	+	+	-
Flavonoids	-	-	+	+	+
Glycosides	-	-	+	+	-
Phenols	-	+	+	+	+
Saponins	-	-	-	+	-
Steroids	-	-	-	-	-
Tannins	-	+	+	+	+
Terpenoids	+	+	+	+	+
Quinones	-	-	-	-	-
Reducing sugar	-	-	-	+	-
Carbohydrates	-	-	+	+	+
Iridoids	-	-	-	-	-
Note: "+"indicates the presence of phytochemical; "-" indicates the absence of phytochemical					

Table 4 – Preliminary phytochemical screening of the seeds of *Syzygium stocksii*

Phytochemical constituents	Hexane	Ethyl acetate	Acetone	Methanol	Distilled water
Alkaloids	-	-	-	+	+
Anthocyanins	+	-	-	-	-
Coumarins	+	+	-	+	-
Flavonoids	-	-	+	+	+

Continuation of the table

Phytochemical constituents	Hexane	Ethyl acetate	Acetone	Methanol	Distilled water
Glycosides	-	-	+	+	+
Phenols	-	+	+	+	+
Saponins	-	+	+	+	+
Steroids	-	-	-	-	-
Tannins	-	+	+	+	+
Terpenoids	-	-	+	+	+
Quinones	-	-	-	+	-
Reducing sugar	-	-	-	+	-
Carbohydrates	-	-	-	+	-
Iridoids	-	-	-	-	-
Note: "+"indicates the presence of phytochemical; "-" indicates the absence of phytochemical					

Alkaloids exhibit a wide range of medicinal properties and have various applications, including antiparasitic, antiplasmodial, anticorrosive, antioxidative, antibacterial, anti-HIV, and insecticidal activities [11]. Phenolics and flavonoids are also well-documented for their extensive pharmacological activities [12]. Additionally, terpenoids, a class of isoprenoids, are known to possess numerous biological activities [13]. The detection of these compounds in different plant parts highlights the potential for further phytochemical research.

To determine the number of compounds, HPTLC analysis was performed on the methanolic extract of the bark. Since most plant constituents react with vanillin–sulphuric acid to produce coloured zones, this spray reagent was used to detect the presence of phytochemicals in the *S. stocksii* methanolic bark extracts. The R_f values and colour reactions of the compounds were compared. Identical colours and R_f values under the same experimental conditions indicated the presence of similar compounds. The chromatograms of *Syzygium stocksii* bark extract at UV 254 nm and 366 nm revealed that all sample constituents were clearly separated without any tailing and diffuseness. The HPTLC chromatogram of ethanolic extract recorded at 254 nm, 366 nm and after derivatization with vanillin – sulphuric acid at 575 nm was depicted on Figure 1.

The HPTLC fingerprint profiles, R_f values, and area obtained for extracts after scanning at UV 254 nm, 366 nm, and after derivatization with vanillin sulphuric acid are given in Figures 2, 3 and 4 and Tables 5, 6 and 7, respectively.

Under UV short   Under UV long   Under white light after derivatisation
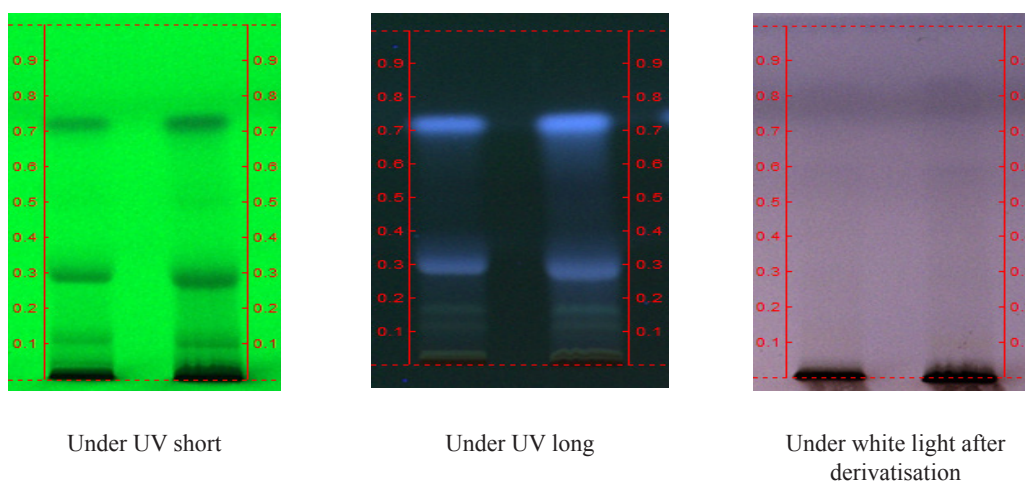
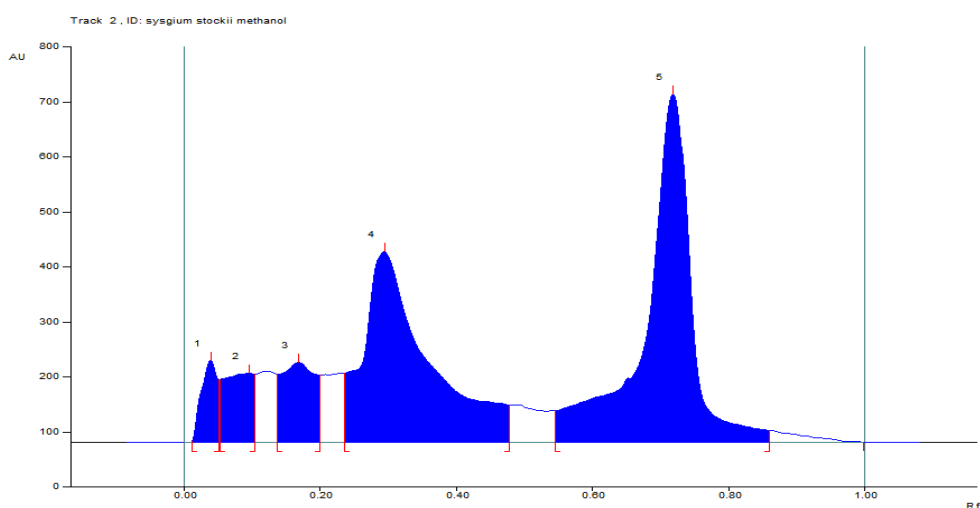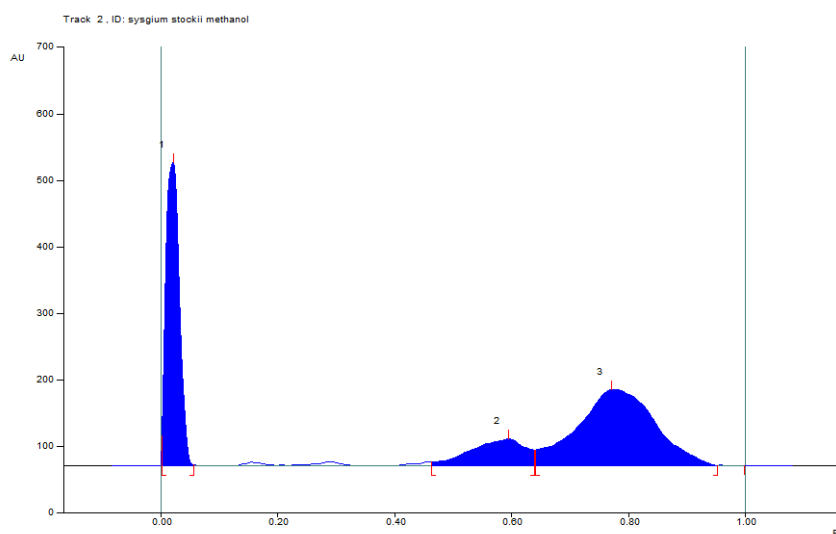**Figure 1** – HPTLC chromatogram of methanolic extract of *Syzygium stocksii* bark
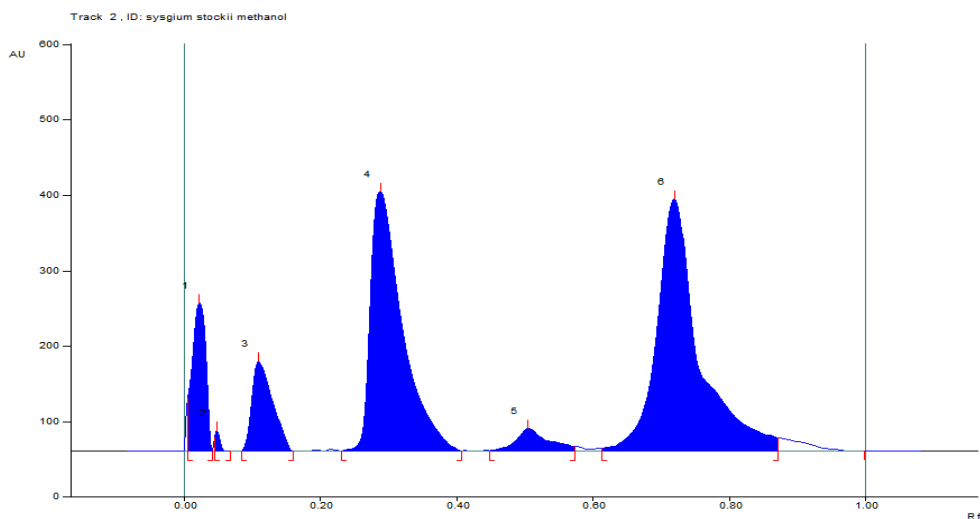
Figure 2 – HPTLC fingerprint of *Syzygium stocksii* bark at 254 nm

Table 5 – HPTLC peak table of methanolic extract of *Syzygium stocksii* at 254 nm

Peak	Start Position	Start Height	Max Position	Max height	Max %	End Position	End Height	Area	Area%
1	0.00 Rf	69.6 AU	0.02 Rf	195.8 AU	18.67%	0.04 Rf	0.4 AU	2761.0 AU	8.76%
2	0.05 Rf	16.9 AU	0.05 Rf	26.7 AU	2.55%	0.07 Rf	0.0 AU	134.3 AU	0.43%
3	0.09 Rf	0.4 AU	0.11 Rf	118.4AU	11.29%	0.16 Rf	0.0 AU	2478.8 AU	7.86%
4	0.23 Rf	0.0 AU	0.29 Rf	343.9 AU	32.78%	0.41 Rf	0.2 AU	10932.6 AU	34.67%
5	0.45 Rf	0.6 AU	0.50 Rf	30.1 AU	2.87%	0.57 Rf	5.8 AU	993.2 AU	3.15%
6	0.61 Rf	3.8AU	0.72 Rf	334.0 AU	31.84%	0.87 Rf	17.5 AU	4234.3 AU	45.14%

Figure 3 – HPTLC fingerprint of *Syzygium stocksii* bark at 366 nm

Table 6 – HPTLC peak table of methanolic extract of *Syzygium stocksii* at 366 nm

Peak	Start Position	Start Height	Max Position	Max height	Max%	End Position	End Height	Area	Area %
1	0.01 Rf	1.7 AU	0.04 Rf	149.4 AU	10.66%	0.05 Rf	14.0 AU	2456.9 AU	3.89%
2	0.05 Rf	114.3 AU	0.10 Rf	126.1 AU	9.00%	0.10 Rf	23.9 AU	3884.0 AU	6.14%
3	0.14 Rf	124.5 AU	0.17 Rf	145.1 AU	10.36%	0.20 Rf	22.7 AU	5034.5 AU	7.96%
4	0.24 Rf	125.9 AU	0.29 Rf	346.7AU	24.74%	0.48 Rf	67.9 AU	22909.3 AU	36.23%
5	0.55 Rf	57.5 AU	0.72 Rf	633.9 AU	45.24%	0.86 Rf	21.8 AU	28944.9 AU	45.78%

Figure 4 – HPTLC fingerprint of *Syzygium stocksii* bark at 575 nm

Table 7 – HPTLC peak table of methanolic extract of *Syzygium stocksii* at 575 nm

Peak	Start Position	Start height	Max position	Max height	Max %	End position	End height	Area	Area%
1	0.00 Rf	45.3AU	0.02 Rf	455.6AU	74.61%	0.06 Rf	1.8AU	7464.2AU	36.04%
2	0.46 Rf	5.4 AU	0.60 Rf	40.4 AU	6.62%	0.64 Rf	23.7AU	2608.2AU	12.59%
3	0.64 Rf	23.8AU	0.77 Rf	114.6AU	18.76%	0.95 Rf	0.4 AU	10639 AU	51.37%

The chromatograms observed under UV light at 254 nm and 366 nm revealed clear separation of all sample constituents. In the methanolic extract of the bark, six peaks were identified, indicating the presence of at least six different components. At 254 nm, one of the components, with an Rf value of 0.87, occupied 45.15% of the total area. After derivatization with vanillin–sulphuric acid reagent, five peaks were observed at 366 nm and three peaks at 575 nm, suggesting further differentiation of the components.

FTIR support a material's ability to absorb light by analyzing how different molecular compounds respond to an infrared beam. This interaction helps determine the composition of the material under investigation. The FTIR spectrum in this study, presented in Figure 5, reveals several distinct absorption bands. A broad band is observed in the single-bond region, while a peak at 3214.40 cm^{-1} confirms the presence of ammonium ions. In the triple-bond region, a peak at 2038.73 cm^{-1} suggests the presence of cyanide and thiocyanate ions, while

a peak at 1983.29 cm⁻¹ may indicate alkynes. The strong C=O stretching at 1718.75 cm⁻¹ suggests the presence of formates or unsaturated esters. The peak at 1604 cm⁻¹ points to C-C stretching and N-H bending, indicating conjugated alkenes and amines.
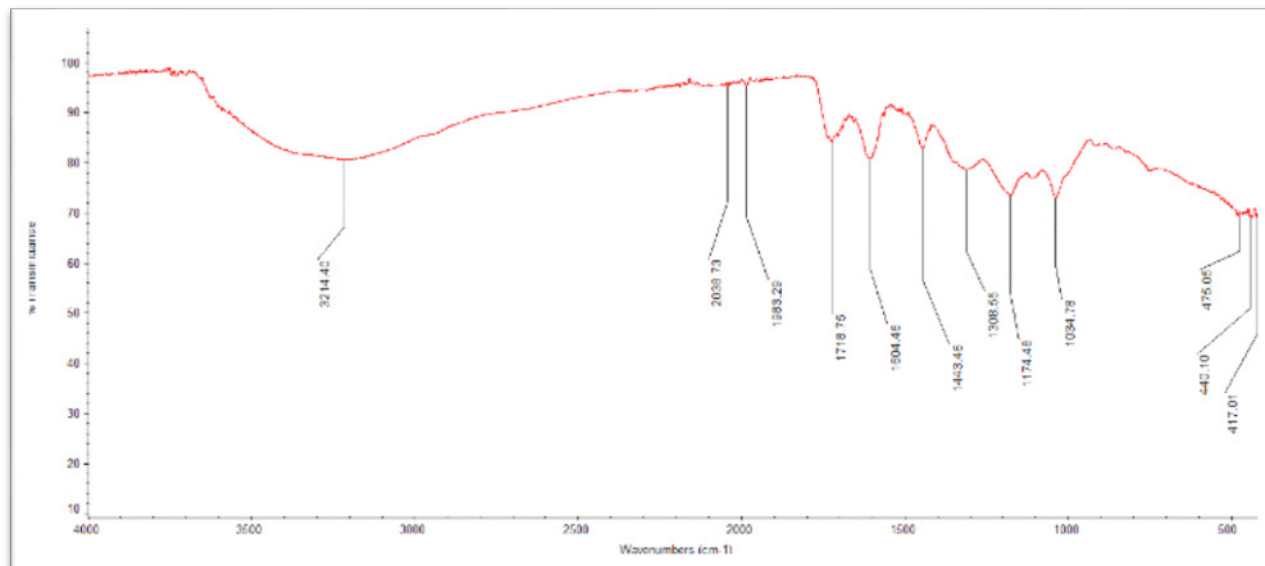
Figure 5 – FTIR Spectra of methanolic bark extract of *Syzygium stocksii* extract

Further, a peak at 1443.46 cm⁻¹ suggests the presence of carbonate ions, while the peak at 1308.55 cm⁻¹ corresponds to strong S=O and C-O stretching, pointing to sulphones and aromatic esters. Strong C=O stretching at 1174.48 cm⁻¹ indicates esters, and the peak at 1034.78 cm⁻¹ suggests the presence of S=O in sulphoxide ions. Three additional peaks in the fingerprint region, at 475.05 cm⁻¹, 440.10 cm⁻¹, and 417.01 cm⁻¹, were also observed. The fingerprint of a sample can be seen in an infrared spectrum, where the absorption peaks signify the frequencies of vibrations between the atoms that make up the substance [14]. All materials are made up of diverse combinations of atoms, hence no two compounds will have the same infrared spectrum. It can also lead to the identification of distinct type of material [15].

Conclusion

The preliminary phytochemical analysis is crucial for identifying compounds that contribute to the biopotential and traditional medicinal uses of *Syzygium stocksii*. The analyses conducted reveals the chemistry of the plant compounds in the bark of the plant.This study provides insights into the phytochemicals present in the plant, all of which play a significant role in treating various ailments. Further in-depth pharmacological and phytochemical characterization is essential to confirm its therapeutic potential.

Conflict of interest

All authors are aware of the article's content and declare no conflict of interest.

References

1. Pawar A. P., Patil V. K., Patil M. D., Rane A. D., Mhaiske V. M., & Tripath V. D. (2023). Distribution and phenology of *Syzygium stocksii* (Duthie) Gamble, an endangered tree species in South Konkan. *Indian Journal of Ecology,* 50(4), pp. 963-968. https://doi.org/10.55362/IJE/2023/3996.

2. Mitra S.K., Irenaeus T.K.S., Gurung M.R. and Pathak P. (2012). Taxonomy and importance of Myrtaceae. *Acta Horticulturae*, 959, pp. 23-34. https://doi.org/10.17660/ActaHortic.2012.959.2.

3. Chandra A.S., Siril E.A., Radhamany P.M. (2020) Phytochemical profile of *Syzygium caryophyllatum* (L.) Alston. *International Journal of Botany Studies*, 5, 6, pp. 599-602.

4. Aung E.E., Kristanti A.N., Aminah N.S., Takaya Y., Ramadhan R. (2020) Plant description, phytochemical constituents and bioactivities of *Syzygium genus*: A review. *Open Chemistry*, 18, 1, pp. 1256-1281. https://doi.org/10.1515/chem-2020-0175.

5. Roby T.J., Joyce J., Nair P.V. (2013) *Syzygium travancoricum* (Gamble)-a critically endangered and endemic tree from Kerala, India- threats, conservation and prediction of potential areas; with special emphasis on Myristica swamps as a prime habitat. *International Journal of Science*, 2, 6, pp. 1335-1352.

6. Evans W.C. (1997) Pharmacognosy 13th Edition. London: Balliere, Tindall, pp. 23-54.

7. Gupta R., Gabrielsen B., Ferguson F.M. (2005) Nature's medicines: traditional knowledge and intellectual property management. Case studies from the National Institutes of Health (NIH), USA. *Curr. Drug Discov. Technol.*, 2, pp. 203-219.

8. Harborne J.B. (1973) Phytochemical methods. London: Chapman and Hall Ltd., pp. 49-188.

9. Harborne J.B. (1973) Phytochemical methods, a guide to modern techniques of plant analysis. London: Chapman and Hall Ltd., pp. 12-236.

10. Iyengar M.A. (1995) Study of Crude Drugs. 8th edition, India, Manipal: Manipal Power Press.

11. Kurek Joanna. (2019) Introductory Chapter of Alkaloids – Their Importance in Nature and for Human Life, ed. by Joanna Kurek. IntechOpen, 2019. https://doi.org/10.5772/intechopen.85400.

12. Tungmunnithum D., Thongboonyou A., Pholboon A., Yangsabai A. (2018) Flavonoids and Other Phenolic Compounds from Medicinal Plants for Pharmaceutical and Medical Aspects: AnOverview. *Medicines (Basel,Switzerland)*, 5, 3, p. 93. https://doi.org/10.3390/medicines5030093.

13. Perveen S. (2018) "Introductory Chapter: Terpenes and Terpenoids". Terpenes and Terpenoids, edited by Shagufta Perveen, Areej Al-Taweel. IntechOpen. https://doi.org/10.5772/intechopen.79683.

14. Nisreen A., Eltahir M. A., Siddig A. A., Siddig, Hajir Adam (2013) Structure and physical properties of flowering plants of the genus hibiscus, *Sudan Medical Monitor*, 8, 3, pp. 135-139.

15. Siddig M. A., Abdelgadir A. E., Elbadawi A. A., Mustafa E. M., & Mussa, A. A. (2015) Structural characterization and physical properties of Syzygium cumini flowering plant. *International Journal of Innovative Research in Science, Engineering and Technology,* 4, 5, pp. 2694-2700, https://doi.org/10.15680/IJIRSET.2015.0405006.

Information about authors:

Adheena Elza Johns – (corresponding author) – M.Sc., Assistant Professor, Department of Botany, St.Thomas College, Kozhencherry, Kerala, India, e-mail: adheenajohns@gmail.com

Radhamany Puthuparambil Madhavan – Dr., Emeritus Professor, Department of Botany, University of Kerala, Kariavattom, Thiruvananthapuram, Kerala, India, e-mail: radhamany_m@rediffmail.com

A. Ydyrys [1*] , G. Askerbay [1] , Zh. Ashirova [1] ,

J. Jielile [2] , M. Ilesbek [1]

[1]Al-Farabi Kazakh National University, Almaty, Kazakhstan
[2]Xinjiang Medical University, Ürümqi, Xinjiang, China
*e-mail: ydyrys.alibek@gmail.com
(Received 30 April 2024; received in revised form 21 June 2024; accepted 12 July 2024)

Green synthesis of silver nanoparticles using plant leaf extraction and phytochemical profile and biological potential of *Artemisia schrenkiana*

Abstract. This study explores the green synthesis of silver nanoparticles utilizing plant leaf extraction from *Artemisia schrenkiana* and evaluates their potential anticancer activity against liver cancer cells *in vitro*. One such method is the use of plant leaf extraction, which has shown promising results in the synthesis of silver nanoparticles. The use of *A. schrenkiana*, a plant native to Kazakhstan, for the green synthesis of silver nanoparticles is particularly intriguing. *A. schrenkiana* has been found to contain bioactive compounds that have potential anticancer properties. The green synthesis of silver nanoparticles using plant leaf extraction of *A. schrenkiana* presents an opportunity for sustainable and eco-friendly production methods. The process involves the utilization of environmentally friendly methods for nanoparticle synthesis, utilizing the natural properties of plant extracts. The synthesized nanoparticles are then tested for their efficacy in inhibiting the growth of pancreatic and liver cancer cells in laboratory settings. The findings shed light on the potential of these silver nanoparticles as a promising candidate for cancer therapy, emphasizing their biocompatibility and eco-friendly synthesis route.

Key words: *Artemisia schrenkiana,* medicinal plants, AgNO$_3$ solution, absorption spectra**,** green synthesis, leaf extraction, silver nanoparticles.

Introduction

Medicinal plants possess potent healing properties, offering safety, efficacy, environmental friendliness, and minimal side effects, thus driving a growing demand worldwide [1]. According to the World Health Organization (WHO), traditional medicine encompasses practices, methods, and accumulated knowledge derived from life experiences, including plant, animal, and mineral-based remedies, spiritual therapies, and disease treatment techniques. Utilizing natural products for therapeutic purposes dates back to early medical practices [2].

Presently, medicines derived from plant sources are extensively utilized for treating and preventing various diseases, with their variety continually expanding [3, 4]. Herbal remedies offer distinct advantages over synthetic drugs, including pleasant effects and low toxicity. However, in modern Kazakhstan, the potential of medicinal plants from the domestic flora remains underexplored, despite their significance in producing essential medications, cosmetics, and dietary supplements [5, 6].

Humanity has long recognized the significance of plants, not only for their nutritional value but also for their medicinal properties, which have been utilized in the treatment of diseases for thousands of years. Many wild plants harbor rich reservoirs of raw materials in nature. However, the rapid depletion of forest land due to anthropogenic pressures, unplanned development, and excessive exploitation of cultivated plants has led to a decline in their numbers and the extinction of numerous species in nature. This loss of biodiversity and the extinction of endemic species have serious implications [7-9]. To address this challenge, growing medicinal plants in botanical gardens or agricultural fields has emerged as an alternative strategy to obtain more raw materials [10, 11]. Currently, many scientists are dedicated to cultivating medicinal plants using various methods, including organic cultivation without the use of fertilizers or agricultural chemicals, as well as utilizing agricultural byproducts as biogums [12]. The study of *Artemisia* plants is particularly significant due to the presence of a myriad of biologically active substances, which hold immense potential for

agricultural and pharmaceutical industries. However, excessive exploitation of these resources not only depletes plant reserves but also poses a threat to ecosystem destruction [13].

Natural plant extracts play a crucial role in green synthesis processes due to their sustainability and environmental friendliness [14]. Green synthesis minimizes adverse environmental impacts by avoiding the use of toxic chemicals and the generation of hazardous byproducts, unlike conventional chemical synthesis methods [15]. Silver nanoparticles synthesized from plant extracts are particularly advantageous for various biological applications, including wound healing, drug delivery, and imaging, owing to their non-toxic and biocompatible nature [16, 17]. Moreover, these nanoparticles exhibit potent antibacterial properties against a wide range of pathogens, including viruses, bacteria, and fungi [18]. The antibacterial activity of green-synthesized silver nanoparticles may be further enhanced by the presence of phytochemicals and biomolecules in plant extracts [19].

A. schrenkiana, commonly known as Schrenk's wormwood, is a member of the *Asteraceae* family and the *Artemisia genus* [20]. This versatile plant thrives in diverse ecosystems across Eastern Kazakhstan, including the Altai Mountains, salty steppes of the Central Tien-Shan Mountains, and the shores of forests and salt lakes. Its adaptability allows it to flourish in various climatic zones, such as deserts, semi-deserts, forests, wetlands, and rocky mountain surfaces [21]. *A. schrenkiana* is a cross-pollinated plant with very small seeds, weighing between 0.2-0.4 grams per thousand grains [22].

In the Center for Scientific Research of Medicinal Plants at Al-Farabi Kazakh National University, laboratory studies were conducted for the first time on the dried whole parts of the plant species *A. schrenkiana* in the East Kazakhstan region. These studies encompassed investigations into the humidity, ash content, extractive substances, organic acids, coumarins, polysaccharides, quantitative content of flavonoids, and macro-microelements such as quercetin (lead, cadmium, zinc, copper, nickel, iron, manganese, sodium, potassium) [23]. These trace elements play a crucial role in *A. schrenkiana*, comprising components of the plant's enzymes and vitamins. Additionally, the effects of *A. schrenkiana* plant extract on insulin, glucose, and HOMA-IR serum levels in diabetic rats were studied [24]. Despite its significance, this plant remains one of the few plants that have not been extensively studied in Kazakhstan.

This research aims to delineate the characteristics of the plant community in the territory where *A. schrenkiana* grows, particularly in the Urzhar District of the Abai region of Kazakhstan. Furthermore, the study aims to investigate the synthesis of silver nanoparticles (AgNPs) using plant leaf extracts, specifically from *A. schrenkiana*. This process entails harnessing the biochemical compounds present in the plant extract as both reducing and stabilizing agents in AgNPs synthesis. Concurrently, this research focuses on analyzing the phytochemical composition of *A. schrenkiana*, which involves identifying and characterizing the bioactive compounds present in the plant extract, such as flavonoids, phenolic compounds, terpenoids, and alkaloids. Additionally, the study evaluates the biological potential of *A. schrenkiana* by conducting various biological assays to assess its antioxidant and membrane-stabilizing properties.

Materials and methods

Preparation of the plant extract for chemical composition. *A. schrenkiana* specimens were collected in the southeastern region of Kazakhstan (Urzhar districts) in 2022 and dried following standard procedures for medicinal plants. Plant materials were acquired from a local pharmacy and identified by Dr. Alibek Ydyrys and Raushan Kaparbay. Specimens (*A. schrenkiana*—No. 2-36857) were deposited at the Biomedical Research Centre, Al-Farabi Kazakh National University, Almaty, Kazakhstan. The plants were crushed and powdered using a laboratory mill. The determination of biologically active substances in the plant extract was conducted at the laboratories of Akdeniz University Faculty of Science (Antalya, Turkey). As previously described [28], 20 mL of 80% methanol was added to a 2.00 g plant sample, followed by extraction in an orbital shaker for 1 hour. The tube was centrifuged at 5000 rpm for 5 minutes, and the liquid phase was collected by filtering the solution. This process was repeated three times by adding 5 mL of 80% methanol to the residual part in the tube. The resulting extracts were transferred to a 50 mL volumetric flask and diluted to volume.

Determination of total phenolics. The total phenolic contents of the plant samples were determined spectrophotometrically according to the method of Spanos and Wrolstad [29, 30]. For this purpose, 100 μL of the extracted plant samples were mixed with 900 μL of deionized water, 4 mL of Na_2CO_4 solution (75 g/L), and 5 mL of 0.2 N Folin-Ciocalteu reagent. The mixture was incubated in darkness for 2 hours,

and the absorbance was measured at 765 nm using a spectrophotometer (Shimadzu UV-Vis 160A, Japan). The results were calculated as gallic acid equivalent [31].

Determination of total flavonoids. The total flavonoid contents of the plant samples were determined spectrophotometrically according to the method of Uysal et al. [32]. To achieve this, 1 mL of the extracted sample was mixed with 4 mL of deionized water and 0.3 mL of $NaNO_2$ solution (5%). After 5 minutes, 0.6 mL of $AlCl_3$ solution (10%) was added, followed by 2 mL of NaOH (4%) after another 5 minutes. The total volume was adjusted to 10 mL with deionized water, and the absorbance was measured at 510 nm using a spectrophotometer (Shimadzu UV-Vis 160A, Japan). The results were calculated as catechin equivalent.

Antioxidant activity. The antioxidant activity was determined by the DPPH (2,2-biphenyl-1-picrylhydrazyl) radical scavenging method. The DPPH radical solution (1 mm) was prepared by diluting the analysis with methanol after extraction. Different volumes of plant sample extracts (20-40-60-80-100 µL) were added to test tubes containing 600 µL of DPPH solution, and the total volume was adjusted to 6 mL with methanol. The tubes were vortexed and incubated in darkness at room temperature for 15 minutes. The absorbance values were measured at 517 nm using a spectrophotometer, and the percentage inhibition values were calculated accordingly.

% Inhibition=[(ADPPH–Aextract)/ADPPH] x 100

Certain inhibition values were plotted on a graph depicting the sample volume values, and a linear regression analysis was conducted to establish a curved equation dependent on the sample. The EC50 value was then calculated based on this equation. The determination of the DPPH (1/IC50) value involved converting the reverse value to milligrams for the new plant, which inhibits 50% of the 1 g DPPH radical [33].

Preparation of the plant extract for estimation of lipid peroxidation in liver microsomes. The estimation of total phenolic and flavonoid content. The total phenolic content was determined using the Folin-Ciocalteu reagent technique [36]. Similarly, the total flavonoid concentrations were evaluated colorimetrically using rutin as the reference [37].

The estimation of lipid peroxidation in liver microsomes. Lipid peroxidation (LPO) was determined by measuring malondialdehyde content as thiobarbituric acid-reacting substances (TBARS) using the Ohkawa et al. method [38].

The isolation of rat erythrocytes. Rat erythrocytes were isolated following euthanasia and centrifugation, and the erythrocyte pellets were used immediately for osmotic resistance testing after rinsing [39].

The estimation of the osmotic resistance of erythrocytes. The osmotic resistance of erythrocytes (ORE) was assessed by treating isolated erythrocytes with a hypotonic solution of NaCl and measuring hemoglobin absorbance in the supernatant to determine the extent of hemolysis [40-43].

Green synthesis of silver nanoparticles. AgNPs are now created using a variety of physical, chemical, and biological techniques. However, the most significant techniques are biological ones, including green synthesis, sometimes referred to as "eco-friendly" techniques. *A. schrenkiana* specimens were collected from the open spaces of Urzhar, Kazakhstan. Figure 1 shows crisp digital photos of the *A. schrenkiana* leaves. After giving the collected leaves a good rinse with running tap water and then with distilled water, they were allowed to air dry for two weeks at room temperature in the shade. The air-dried leaves were then put to storage in plastic bags for later usage after being ground into a powder using an electronic blender. Twenty grams of the final powder sample and one hundred milliliters of distilled water were combined to create the leaf broth solution. For thirty minutes, the mixture was agitated at 80-90 °C with a magnetic stirrer. Following cooling, the mixture was filtered using Whatman Filter Paper No. 1 and regular filter paper. The leftover extract was kept at 4 °C for further use, and the filtrates were used in the tests.

Figure 1 – *Artemisia schrenkiana* Ledeb

Biosynthesis of silver nanoparticles. The filtered plant extract was stored at 4 °C for use in another research. 6 mL of 0.01 mM prepared $AgNO_3$ solution (Merck, Germany) was incubated with 6 mL of *A. schrenkiana* extract for 5 minutes at 30 °C while being constantly stirred in order to produce silver nanoparticles (AgNPs). To make a stock solution of 1 mM $AgNO_3$, 0.17 g of $AgNO_3$ was dissolved in 100 mL of distilled water in a volumetric flask. Every solution within the volumetric flasks was covered with a black covering and kept in a dark place for storage. Next, using a magnetic stirrer, 90 mL of the aqueous $AgNO_3$ solution was combined dropwise with 10 mL of plant extract, and the combination was stirred for 25 minutes at room temperature.

Study of optical properties of AgNPs by UV-Vis spectrometry. To verify the AgNP production, the UV–vis spectra were taken at various times. After 24 hours, the totally reduced solution was centrifuged using a Sorvall ST 8R centrifuge, with the settings set at 9000 rpm for 20 minutes at 25 °C. After discarding the supernatant liquid, the particle was again dispersed in distilled water [44-47]. To get rid of anything that clung to the silver nanoparticles' surface, the centrifugation procedure was performed three times.

Statistical data analysis. Statistical analysis was performed using the GraphPad Prism 6.0 Program (GraphPad Software, San Diego, CA, USA). Data were statistically analyzed using comparative and descriptive statistical techniques. The results of three separate experiments were provided as the mean standard deviation (SD). The correlation between extract concentration and lipid peroxidation was assessed, along with the degree of hemolysis. The Pearson correlation coefficient was generated using a nonlinear regression equation, with significance set at $p \leq 0.05$, and the T-criterion was used to determine the reliability of the registered changes in the indices.

Results and discussion

Phytochemical profile and biological potential of A. schrenkiana. Biologically active substances found in plants serve as crucial indicators of plant quality, shaping their properties and overall value. The quantity and quality of these compounds are influenced by a multitude of internal and external factors. Variations in geographical growth areas and climatic conditions can lead to a diverse array of chemical compounds within the same plant species, thereby shaping the properties and diversity of biologically active compounds.

The collected plant materials of *A. schrenkiana* were carefully dried in shaded outdoor areas, ensuring

purity and the absence of fungi, while quantitatively and qualitatively assessing factors such as humidity and the quantity of extractive substances.

Minerals play a vital role in both plant and human life, with their composition in medicinal plants estimated through ash content analysis. Research indicates that mineral content can range from 3-25% depending on the type of raw material. In the case of *A. schrenkiana*, analysis revealed an ash content of 5.7% and humidity of 5.36% in the above-ground parts of the plant. Furthermore, it was determined that the surface part of the plant contains essential compounds such as amino acids, carbohydrates, polyphenols, flavonoids, and carotenoids (Table 1).

Table 1 – Quantitative composition of biologically active compounds (quantitative composition, mg/g of dry matter)

Metabolites	Amount of biologically active substances, %
Extractive substances	29.57±0.10
Amino acids	1.45±0.16
Coumarins	0.135±0.31
Carbohydrates	2.32±0.4
Flavonoids	3.8±0.11
Tannin	10.06±0.02
Alkaloids	1.0±0.31
Phenols	2.83±0.22

Extractives refer to the weight of the dry residue obtained by evaporating the dried powder of *A. schrenkiana* individually with 80% ethanol alcohol. According to the research findings, this plant contained extractive substances at a concentration of 29.57%, along with amino acids at 1.45%. A total of 12 amino acids were identified in the extract of *A. schrenkian*a, of which 8 are considered essential amino acids. The quantities of amino acids determined in the plant extract using the capillary electrophoresis system "Capel 105M" are presented in Table 1 (chromatogram).

As depicted in Table 2, it can be observed that the content of non-essential amino acids, specifically leucine + isoleucine, is relatively high, at 190.0 mg/l. Additionally, arginine, histidine, methionine, and threonine were determined to be present at levels of 25.0 mg/l, 23.0 mg/l, 12.0 mg/l, and 15.0 mg/l, respectively. Among the 13 different amino acids identified, 8 types (leucine, isoleucine, lysine, methionine, threonine, phenylalanine, arginine, histidine) are considered non-essential amino acids.

Table 2 – Number of amino acids determined in *A. schrenkiana* plant extract

No.	Time	Component	Height	Start	End	Area	Conc., mg/l	% of amino acids
1	6.198	arginine	0.505	6.167	6.233	22.02	25.0	0.103±0.041
2	8.522	lysine	0.157	8.483	8.563	3.495	1.70	0.007±0.002
3	8.652	tyrosine	0.102	8.570	8.697	3.948	4.10	0.017±0.005
4	9.025	phenylalanine	0.140	8.945	9.087	6.859	6.50	0.027±0.008
5	9.243	histidine	0.396	9.123	9.335	24.95	23.0	0.095±0.047
6	9.493	leucine + isoleucine	9.190	9.335	9.590	524.5	190.0	0.781±0.203
7	9.632	methionine	0.468	9.590	9.708	14.29	12.0	0.049±0.017
8	9.802	proline	0.198	9.708	9.838	8.101	5.00	0.021±0.005
9	9.893	threonine	0.711	9.843	9.967	22.44	15.0	0.062±0.025
10	10.237	serin	0.051	10.198	10.302	2.143	1.10	0.005±0.001
11	10.367	alanine	0.316	10.302	10.443	10.7	4.50	0.018±0.005
12	10.867	glycine	0.204	10.832	10.918	3.677	1.30	0.005±0.002

According to our research findings, *A. schrenkiana* contains various compounds, including coumarins (0.135%), carbohydrates (2.32%), sucrose (0.30g/100g), fructose (11.02g/100g), and tannins (10.06%). Additionally, the plant exhibited a relatively low level of polyphenols (265.01±1.2mg GAE/g), while the total quantitative number of flavonoids, determined by standard colorimetric analysis, was notably high (142.1±2.1mg CAE/g).

The DPPH radical scavenging activity of these plants ranged from 0.45 µg/ml to 5.01 µg/ml (EC50) respectively. The crude methanolic extracts of *A. schrenkiana* showed antioxidant activity, with (EC50) values of (3.7 µg/ml) respectively.

Yields of essential oils are 0.37 % for *A. schrenkiana*. The main components of *A. schrenkiana* essential oil were Camphene – 3.65%, 1,8-Cineole – 29.05%, γ-Terpinene – 0.30%, p-Cymene – 1.08%, α-Thujone – 0.35%, Camphor – 44.79%, Bornyl acetate – 0.93%, Terpinene-4-ol – 1.16%, Borneol – 4.26%, Carvone – 0.70%, β-Oplopenone – 1.57%, Spathulenol – 3.76%, and Unidentified compounds – 8.40%.

The properties of plant extracts. The results of the analysis of the IC50 for plant extracts, total flavonoids, and concentration of polyphenolic components are shown in Table 3. These findings provide an evaluation of certain biochemical characteristics of *A. schrenkiana*, a plant or material under investigation for possible health advantages.

Based on the estimation of membrane-stabilizing attributes linked to the IC50 values, the most significant membrane-stabilizing effects of *A. schrenkiana* may be identified. The plant extracts from *A. schrenkiana* were arranged according to the amount of flavonoids and phenolic compounds they contained. The knowledge acquired was in line with studies on plant extracts' antioxidant and membrane-stabilizing properties.

The Impact of Herbal Extracts of A. schrenkiana. Table 4 illustrates that the *A. schrenkiana* extract exhibited the best membrane-protective qualities. Plant ethanolic extracts efficiently decreased erythrocyte hemolysis at concentrations ranging from 0 to 100 g dry substance/mL. At a concentration of 5 g/mL, erythrocyte fragility therefore dropped by as much as 50.9 ± 0.9% and 93.1 ± 1.2%. The antihemolytic action of plantains varies with dosage.

Table 3 – Lipid peroxidation and membrane-stabilizing properties of several *A. schrenkiana* plant extracts (mean ± standard deviation (SD), *n* = 3)

Species	Total Polyphenols (μg GAE/mg)	Total Flavonoids (μg RE/mg)	Lipid Peroxidation IC50 (μg/mg protein)	Membrane Stabilizing Properties IC50 (μg/ mL of RBC)
A. schrenkiana	342.1 ± 2.1	265.1 ± 1.2	3.4 ± 0.07*	195.1 ± 7.0*
Note: A log dosage concentration–inhibition curve was used to calculate the 50% inhibitory concentration (IC50) values in μg/ mL. The concentration of total flavonoids and polyphenols was given as the mean ± SD of studies conducted in triplicate. Values represented as mean ± SE (*n* = 3). *p* value (***): very highly significant; (**): highly significant; (*): significant.				

Table 4 – Influence of herbal extracts of the *A. schrenkiana* on the osmotic resistance of the erythrocyte membrane. Note: mean ± SD, *n* = 3. The extent of hemolysis was calculated as the percentage of total hemolysis caused by 0.1% Na_2CO_3

Species	Extract Concentration (μg Dry Substance/mL ES)					
	0	5	10	50	100	IC50
A. schrenkiana	100	93.± 1.2*	86.3 ± 3.4**	53.9 ± 5.7***	50.9 ± 0.9*	50 μg <
Note: The data are expressed as the mean ± SD (*n* = 3). Values represented as mean ± SE (*n* = 3). *p* value (***): very highly significant; (**): highly significant; (*): significant.						

Nevertheless, it was discovered that at concentrations higher than 10 g/mL, the protective benefits of *A. schrenkiana* extracts on erythrocyte membranes were strengthened. After the research results were analyzed, it was shown that all plant extracts could maintain membranes and lessen hemolysis of red blood cells. Most of the extracts had a considerable impact on the stability of erythrocyte membranes; however, the concentration needed to achieve a 50% effect was outside the range that was investigated. On erythrocyte membranes, *A. schrenkiana* had a significant effect of stabilizing the membrane.

Herbal extracts were used to preincubate the erythrocyte suspension prior to testing it in a hypoosmotic NaCl solution. Osmotic resistance was measured using the degree of hemolysis. Nearly all of the extracts reduced cell hemolysis in a dose-dependent manner throughout the concentration range of 0–100 g/mL, as Table 4 illustrates. With a 42.2% reduction in hemolysis, respectively, these results unambiguously validated the antihemolytic effect of *A. schrenkiana* extracts. The extracts of *A. schrenkiana* also showed anti-hemolytic activity at concentrations of 100 g/mL, lowering erythrocyte hemolysis by 50.9 ± 0.9%.

Table 5 describes the results of studies on the effect of plant extracts on lipid peroxidation processes in the microsomal fraction of liver membranes. It is widely known that raw materials obtained from plant raw materials have beneficial properties for humans and contain many compounds. Medicinal plants contain various categories of phytochemicals that are organic sources of antioxidants.

Table 5 – Effect of *A. schrenkiana* herb extracts on the liver microsome's degree of lipid peroxidation

Species by common name	Extract Concentration (μg Dry Substance/mg Protein)					
	0	250	500	1250	2500	IC50
A. schrenkiana	100	81.5 ± 3.2*	26.6 ± 3.7**	19.4 ± 2.5**	14.5 ± 2.9*	392 μg
Note: *n* = 3, mean ± SD. In comparison to the control group, the data are presented as the mean ± SD (*n* = 3); * indicates *p* < 0.05; ** indicates *p* < 0.01; and *** indicates *p* < 0.001. *A. schrenkiana* rxy = −0.9736.						

Analyzing the data, it can be concluded that the membrane protective effect and antioxidant properties of extracts are not manifested to the same extent in the same plant species. This is primarily due to the different mechanisms of action of bioactive substances in plants on membranes.

Green synthesis of silver nanoparticles. This study examined various amounts of *A. schrenkiana* leaves extract from 10 ml with 100 ml aqueous solution of AgNO$_3$ (1 mM) in order to standardize the nanoparticles manufacturing technique. The color of the AgNO$_3$ solution rapidly changed from light yellowish to dark brown after 30 minutes due to the dissolution of the 15 ml leaf extract (Figure 2).

In contrast, other samples underwent color changes after 2–8 hours of incubation in a dark room, and the control sample remained colorless.

Additionally, the results of UV-visible spectrophotometers, which displayed a spectrum of surface plasmon resonance (SRP) ranging from 300 to 360 nm of absorption band, validated the production of AgNPs in the solution (Fig 3). It should be mentioned, nevertheless, that 1.5 ml of fruit extract in 100 ml of AgNO$_3$ solution was also used to create AgNPs. In fact, a more pronounced and intense absorption band at 360 nm was visible in the SPR spectra of AgNPs produced from the increased concentration of leaf extract (Figure 3).
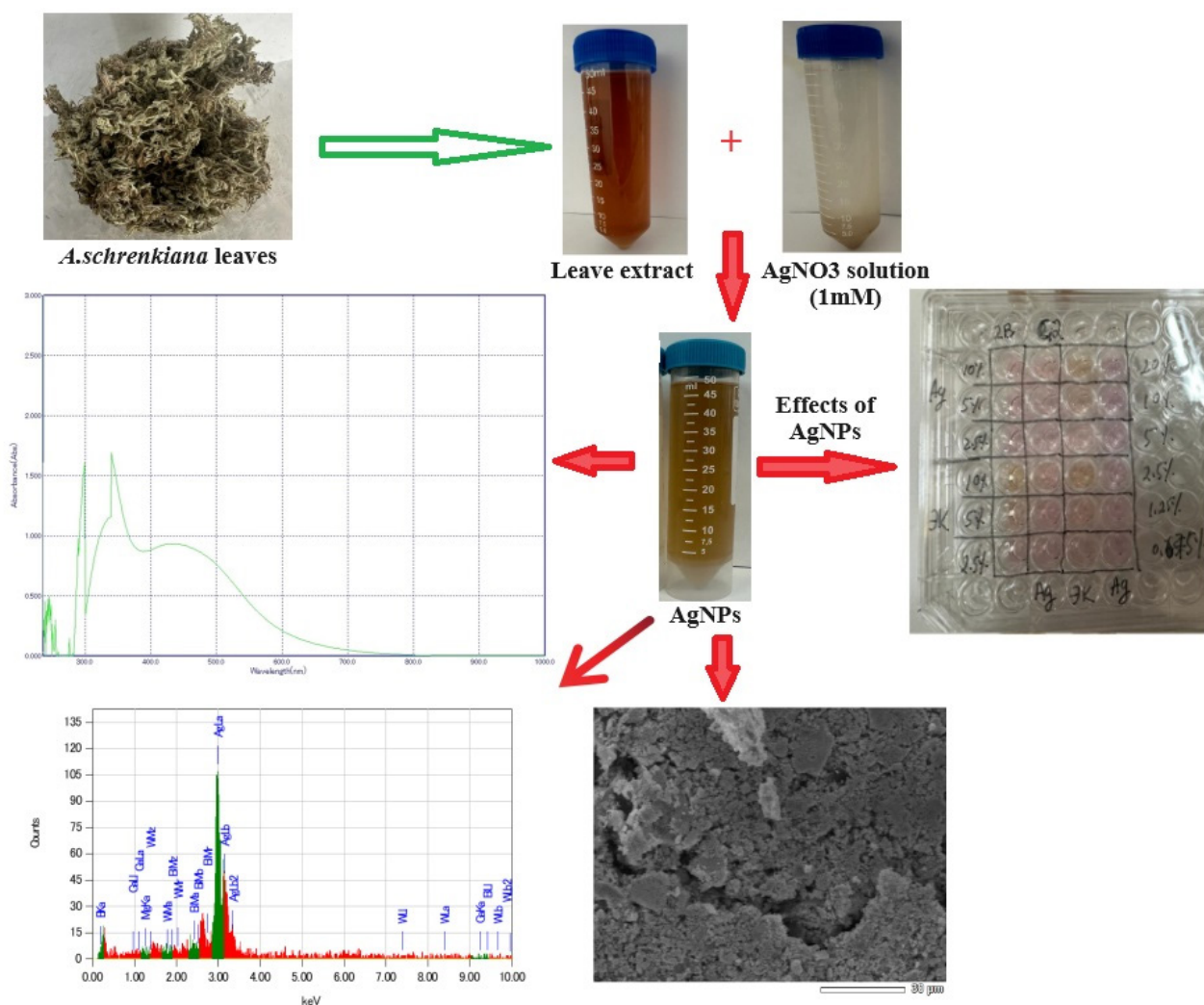
Figure 2 – Schematic diagram for biosynthesis of AgNPs using leaves extract of *A. schrenkiana*
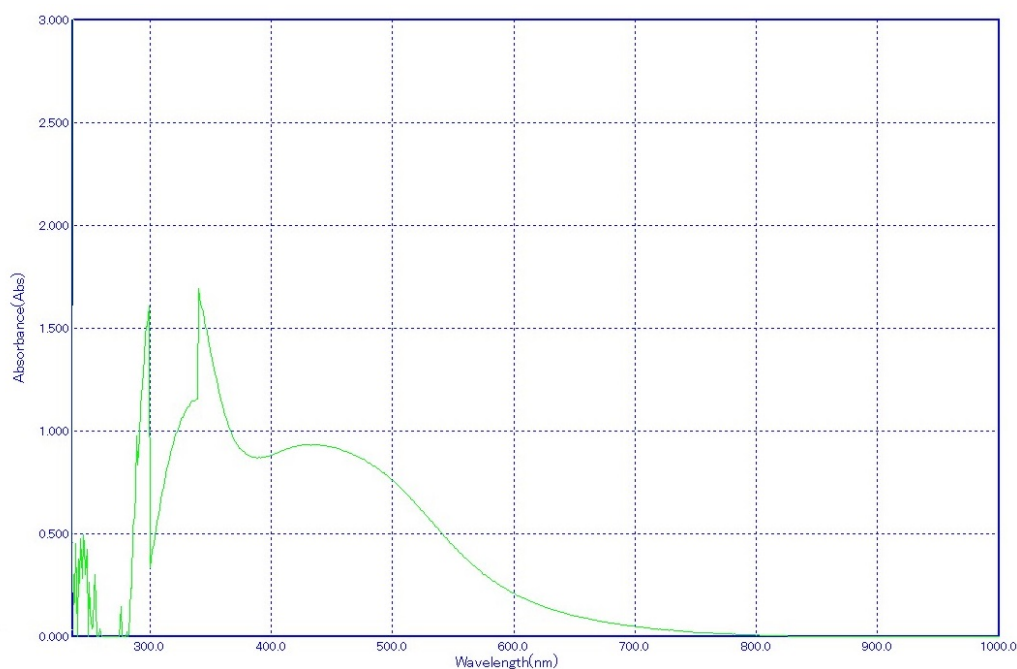
Figure 3 – Absorption spectra of extract of *A. schrenkiana* leaves

Additionally, the results of the UV-vis spectra demonstrated that the reaction mixture's absorbance intensity increased with time, and the solution remained stable after 24 hours of incubation, indicating that the creation of the nanoparticles in solution had been completed. As a result, the AgNPs mediated by the blend of 100 ml $AgNO_3$ solution and 15 ml leaf extract were freeze-dried and utilized in subsequent research.

Study of optical properties of AgNPs by UV-Vis spectrometry. The final stage was using 100% ethanol. Morphological studies and size examination of the synthesized AgNPs were conducted by a field-emission scanning electron microscope and a transmission electron microscopy. The SEM image (Figure 4) and the TEM images both demonstrated that the majority of AgNPs were extremely mono-dispersed in spherical forms.

The SAED pattern's brilliant circular spots indicated the (1.04), (1.65), and (1.49) planes and confirmed the particles' crystalline structure. These statistics agree with the findings of the XRD. The AgNPs' size distributions ranged from 0.60 to 1.65

nm. Additionally, the presence of the silver element in the produced AgNPs was verified using the EDX equipment.

Anticancer activity against pancreatic and liver cells lines in vitro. The MTT assay (Sigma Aldrich, Germany) was used to examine the inhibitory effects of manufactured nanoparticles and A. ciniformis extract on the proliferation of liver cancer cells. For a whole day, the liver cancer cell was exposed to varying concentrations (0.75, 1.25, 2.5, 5, 10, 20μg/mL) of both commercial and biological silver nanoparticles. At a dose of 20 μg/mL, the greatest inhibitory effect on the growth of liver cancer cells was found; this effect was statistically significant when compared to the control group ($p < .001$).

When comparing the bioavailability percentage of commercial and phytosynthesized silver nanoparticles at 10 and 20 μg/mL to the untreated cells, there was no significant difference ($p > .05$) (Figure 5). Biological and commercial nanoparticles with a 20 μg/mL bioavailability of 78% and 91%, respectively.
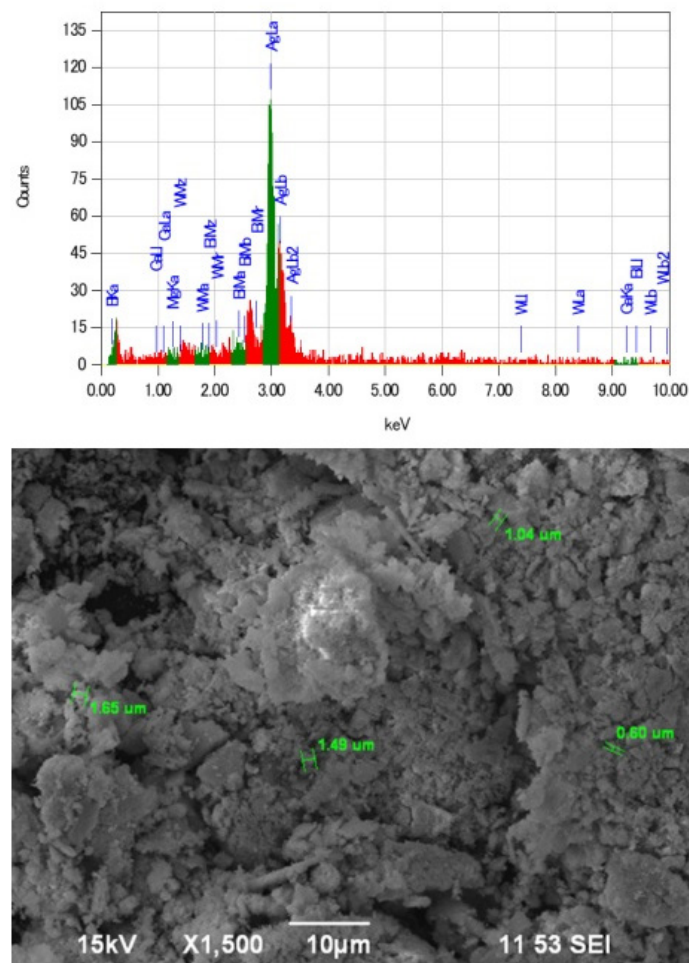
Figure 4 – EDX spectrum of the synthesized AgNPs. A strong peak at 3 keV indicates the existence of Ag
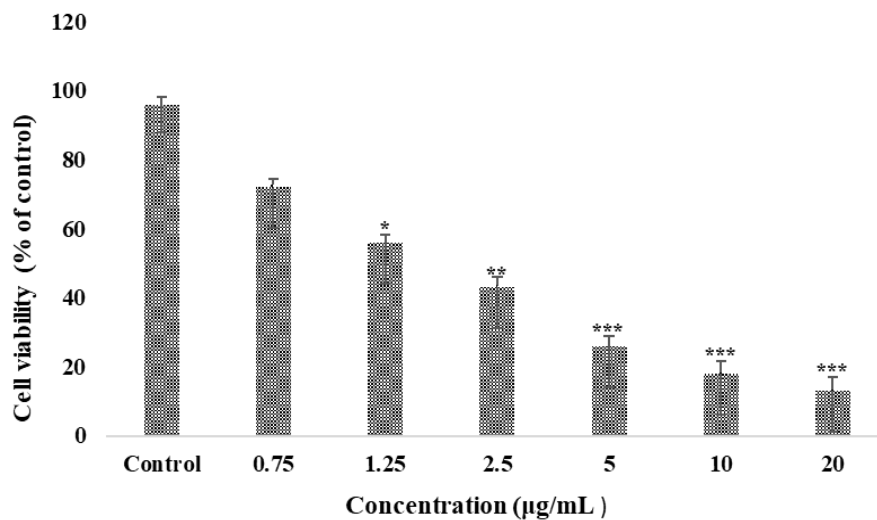
Figure 5 – Cell viability of liver cancer cells following treatment with biosynthesized AgNPs
after 24 (results are reported as viability in comparison with control group; $p \leq 0.001^{***}$, $p \leq 0.01^{**}$, $p \leq 0.05^{*}$).

Using varying AgNP concentrations, the colorimetric MTT test was used to assess the cytotoxicity of AgNPs. The findings showed that the cytotoxicity of AgNPs was dose dependant and that they had the greatest inhibitory effect on liver cancer cells at doses of 10 μg/mL and 20 μg/mL ($p < .001$). Moreover, 2.5 μg/mL was determined to be the IC50 of AgNPs. Furthermore, the identical quantities of AgNPs were applied to liver cancer cells for a duration of 24 hours. The cytotoxicity of AgNPs against normal liver cancer cells revealed that these cells were less susceptible to AgNPs' effects (IC50 = 10 μg/mL). Figure 5 displays the outcomes of liver cancer cell survival after 24 hours. Following treatment with AgNPs, the morphological alterations in liver cancer cells were examined. AgNPs treatment of liver cancer cells resulted in wrinkling, rounding, and membrane bulging, all of which are signs indicating the AgNPs will probably cause the cancer cells to undergo apoptosis.

Conclusion

In conclusion, *A. schrenkiana* emerges as a significant medicinal plant, particularly in the context of the domestic flora of Kazakhstan. Through comprehensive phytochemical analysis, it has been revealed to contain a rich array of biologically active compounds, including extractive substances, coumarins, carbohydrates, tannins, amino acids, flavonoids, and phenolic compounds [43]. These constituents contribute to its pharmacological properties, which encompass antioxidant, anti-inflammatory, antimicrobial, and anticancer activities. Overall, *A. schrenkiana* represents a promising avenue for the development of novel therapeutic and preventive drugs, offering potential solutions for addressing various health challenges. Continued investigation into this plant species holds the promise of uncovering new avenues for drug discovery and development, ultimately benefiting both traditional and modern healthcare systems.

AgNPs made by green synthesis from plant extracts seem to be more suitable for clinical applications than those made by physical or chemical means. Furthermore, the green synthesis of AgNPs is an easy, secure, economical, and environmentally beneficial process. Green AgNPs appear to be some promising anti-cancer drugs as a result. To ascertain their biocompatibility and adverse effects in animal samples, more investigation is necessary. The current study's findings demonstrated that green AgNPs produced by *A. schrenkiana* have anti-metastatic effects on liver cancer cells, and that these effects are achieved by causing the cancer cells to undergo apoptosis. As a result, biosynthesized nanoparticles may be applied as cancer-fighting chemotherapeutic drugs.

Acknowledgments

Conflict of interest

All authors are aware of the article's content and declare no conflict of interest.

References

1. Che C-T., George V., Ijinu T.P., Pushpangadan P. and Andrae-Marobela K. (2017) Traditional medicine. *In Pharm*. pp. 15-30. https://doi.org/10.1016/B978-0-12-802104-0.00002-0.

2. Berganayeva G., Kudaibergenova B., Litvinenko Y., Nazarova I., Sydykbayeva S., Vassilina G., Izdik N., Dyusebaeva M. (2023) Medicinal plants of the flora of Kazakhstan used in the treatment of skin diseases. *Molec.*, 28(10), pp. 4192. https://doi.org/10.3390/molecules28104192.

3. Houwati N., Alibek Y., Tuleuhanov S., Ablaikhanova N., Gulishayia D., Yueerlin M. & Baishanbo A. (2017) Study on the effect of the Kazakh Traditional Medicine Kezimuk granules to the immunologic function of cyclophosphamide induced immunosuppressed mice. *Int. J. Biol. Chem.,* 10(1), pp. 50-56.

4. Ydyrys Y., Serbayeva A., Dossymbetova S., Akhmetova A. and Zhuystay A. (2020) The effect of anthropogenic factors on rare, endemic plant species in the Ile Alatau. *E3S Web of Conferences* 2020; 222(2), 05021.

5. Posadino M., Giordo R., Pintus G., Mohamme S.A., Orhan I.E., Fokou P.V., Alibek Y. & Cho W.C., et al. (2023) Medicinal and mechanistic overview of artemisinin in the treatment of human diseases. *Biomed. and Pharma.*, 163, pp. 114866. https://doi.org/10.1016/j.biopha.2023.114866.

6. Akzhigitova Z., Dyusebaeva M.A., Tokay T., et al. (2020) Phytochemical Study of *Bergenia crassifolia*. *Chem Nat Compd*., 56, pp. 912–914. https://doi.org/10.1007/s10600-020-03184-y.

7. Ydyrys A., Yeszhanov B., Baymurzaev N., Sharakhmetov S., Mautenbaev A., Tynybekov B. and Baidaulet T. (2020) Technology of landscaping in arid zones by using biohumus from sheep wool. *E3S Web of Conferences*. 169(2), 02012.

8. Ivashchenko A.A., Mukhitdinov N., Abidkulova K.T., Ametov A., Tashev A. and Ydyrys A. (2021) Floristic analysis of plant communities with the participation of a narrow tien shan endemic, *taraxacum kok-saghyz* l.e.rodin. *For. Ideas*., 27(1), pp. 195-209.

9. Ydyrys A., Abdolla N., Seilkhan A.S., Masimzhan M. and Karasholakova L. (2020) Importance of the geobotanical studying in agriculture (with the example of the Sugaty region). *E3S Web of Conferences*. 222(1), 04003.

10. Begenov A.B., Mukhitdinov N.M., Ametov A.A., Nazarbekova S.T., Kuatbayev A., Tynybekov B. and Abidkulova K.T. (2014) Assessment of the current status of populations of Kazakh rare plants (*Berberis iliensis* M.Pop.). *Wor. App. Sci. J.*, 30(1), pp. 105-109.

11. Ydyrys A., Mukhitdinov N., Ametov A., Tynybekov B., Akhmetova A., Abidkulova K. (2013) The states of coenpopulations of endemic, relict and rare species of plant *Limonium michelsonii* and their protection, *Wor. App. Sci. J.*, 26, pp. 934-940. https://doi.org/10.5829/idosi.wasj.2013.26.07.13525.

12. A. B. Akhmetova, N. M. Mukhitdinov, A. Ydyrys, A. A. Ametov, Z. A. Inelova and M. Öztürk. (2018) Studies on the root anatomy of rubber producing endemic of Kazakhstan, *Taraxacum Kok-Saghyz* L.E. Rodin. *Journal of Animal and Plant Sciences*, 28(5), pp. 1400-1404.

13. Askarova M., Medeu A., Medeu A. & Arslan M. (2018) Assessment of the Current Plant Diversity Status in Kazakhstan. *Vegetation of Central Asia and Environs*. pp. 303-320.

14. Dyusebaeva M.A., Berillo D.A., Berganayeva A.E., Berganayeva G.E., Ibragimova N.A., Jumabayeva S.M., Kudaibergenov N.Z., Kanapiyeva F.M., Kirgizbayeva A.A., Vassilina G.K. (2023) Antimicrobial activity of silver nanoparticles stabilized by liposoluble extract of *Artemisia terrae-albae*. *Processes*, 11, pp. 3041. https://doi.org/10.3390/pr11103041.

15. Jasrotia R., Verma A., Nidhi A.V., Ahmed J., Fazil M., Khanna V. & Kandwal A. (2024) Nanocrystalline Co/Ga substituted $CuFe_2O_4$ magnetic nanoferrites for green hydrogen generation. *Int. J. Hydrogen Energy*, 52, pp. 1194-1205.

16. Azat S., Arkhangelsky E., Papathanasiou T., Zorpas A.A., Abirov A. & Inglezakis V.J. (2023) Synthesis of biosourced silica–Ag nanocomposites and amalgamation reaction with mercury in aqueous solutions. *Comptes Rendus. Chimie.*, 23(1), pp. 77-92.

17. Sindhu M., Sharma R., Saini A., Khanna V. & Singh G. (2024) Nanomaterials mediated valorization of agriculture waste residue for biohydrogen production. *Int. J. Hydrogen Energy*, 52, pp. 1241-1253.

18. Khezerlou A., Alizadeh-Sani M., Azizi-Lalabadi M. & Ehsani A. (2018) Nanoparticles and their antimicrobial properties against pathogens including bacteria, fungi, parasites and viruses. *Microbial pathogenesis*, 123, pp. 505-526.

19. Habeeb Rahuman H.B., Dhandapani R., Narayanan S., Palanivel V., Paramasivam R., Subbarayalu R. & Muthupandian S. (2022) Medicinal plants mediated the green synthesis of silver nanoparticles and their biomedical applications. *IET nanobiotechnology*, 16(4), pp. 115-144.

20. Bukenova E.A., Bassygarayev Z.M., Akhmetova A.B., Altybaeva N.A., Zhunusbayeva Z.K. and Ydyrys A. (2019) Development of the method of obtaining the endogenic biostimulator from wheat green spike glumes. *Res on Cro*., 20(1). https://doi.org/10.31830/2348-7542.2019.030.

21. Ydyrys A., Masimzhan M.T., Abdullah N., Abdrasulova Zh., Sryakhil S. (2022) A feature of the essential oil *Artemisia schrenkiana* Ledeb plant community growing in the south-east of Kazakhstan. *Bulletin of the L.N. Gumilyev Eurasian National University* Series Biological Sciences., 141(4), pp. 24-36.

22. Seilkhan A., Syraiyl S., Turganova G., Satbayeva E. and Erkenova N. (2021) Determination of laboratory seed yield of *Artemisia schrenkiana* Ledeb and Chorispora bungeana Fisch. *IOP Conference Series: Earth Environ. Sci.*, 699(1). https://doi.org/10.1088/1755-1315/699/1/012014.

23. Syraiyl S., Ydyrys A., Ahmet A., Aitbekov R. and Imanaliyeva M.T. (2022) Phytochemical composition and antioxidant activity of three medicinal plants from southeastern Kazakhstan. *Inter. J. Biol. Chem.*, 15(1), pp. 73-78.

24. Syrayil S., Abdolla N. and Erkenova N. (2020) Effect of *Artemisia schrenkiana* ledeb plant extract on insulin, glucose and Homa-ir serum levels in diabetic rats. *Asta. Med. Jour.*, 106(4), pp. 257-262.

25. Ydyrys A., Mukhitdinov N., Abbas A., Mukhitdinova Z., Ametov A., Tynybekov B. & Abidkulova K. (2014) The states of coenpopulations of endemic, relict and rare species of plant *Ferula iliensis* and their protection. *Journal of Biotechnology*, 185, pp. 32-33.

26. Abdulina S.A. (2014) List of vascular plants of Kazakhstan / ed. R.V. Camelina. Almaty: 1998, 187 p.

27. Czerepanov S.K. (2007) Vascular plants of Russia and adjacent states (the former USSR). Cambridge University Press, 516 p. ISBN 9780521044837.

28. Alibek Y., Abdolla N., Masimzhan M., Abdrasulova Z., Syraiyl S. (2023) Cultivation and resource of *Artemisia schrenkiana* (L.) for increased pharmaceutical perspective. *Res. on Cr.*, 24(1), pp. 171-178. https://doi.org/10.31830/2348-7542.2023.ROC-881.

29. Cemeroglu B. (2010) Gıda analizleri [Food analysis] Ankara: Gida teknolojisi derneği yayinlari, 682 p.

30. Spanos G.A., Wrolstad R.E. (1990) Influence of processing and storage on the phenolic composition of Thompson seedless grape juice. *J. Agri. and Food Chem.*, 38, pp. 1565-1571. https://doi.org/10.1021/jf00097a030.

31. Ena A., Pintucci C., Carlozzi P. (2012). The recovery of polyphenols from olive mill waste using two adsorbing vegetable matrices. *J Biotech.*, 157, pp. 573–577.

32. Baharatlar, Çeşniler ve Tıbbi Bitkiler-Uçucu Yağ Muhtevasının Tayini (hidrodistilasyon yöntemi). Türk Standartları Enstitüsü, Ankara. Anonim 2011; TSE EN ISO 6571.

33. Uysal B.F., Çinar O. (2020) Kültür koşullarında yetiştirilen farklı origanum spp. türlerinin bazı verim ve kalite parametreleri, Derim. 37 (1), pp. 10-17.

34. Spanos G., Wrolstad R.E. (1990) Phenolics of apple, pear and white grape juices and their changes with processing and storage. *J Agric Food Chem*., 40, pp. 1478–1487.

35. Ydyrys A., Zhaparkulova N., Aralbaeva A., Mamataeva A., Seilkhan A., Syraiyl S. & Murzakhmetova M. (2021) Systematic analysis of combined antioxidant and membrane-stabilizing properties of several lamiaceae family Kazakhstani plants for potential production of tea beverages. *Plants*, 10(4), https://doi.org/10.3390/plants10040666.

36. Di Meo S., Reed T.T., Venditti P., Victor V.M. (2016) Role of ROS and RNS Sources in Physiological and Pathological Conditions. *Oxidative Med. Cell. Longev*., 1245049. https://doi.org/10.1155/2016/1245049.

37. Ohkawa H., Ohishi N., Yagi K. (1979) Assay for lipid peroxides in animal tissues by thiobarbituric acid reaction. *Anal. Biochem*., 95, pp. 351–358. https://doi.org/10.1016/0003-2697(79)90738-3.

38. Zhamanbaeva G.T., Murzakhmetova M.K., Tuleukhanov S.T., Danilenko M.P. (2014) Antitumor Activity of Ethanol Extract from Hippophae rhamnoides L. Leaves towards Human Acute Myeloid Leukemia Cells In Vitro. *Bull. Exp. Biol. Med*., 158, pp. 252–255. https://doi.org/10.1007/s10517-014-2734-3.

39. Singleton V.L., Orthofer R., Lamuela-Raventós R.M., Lester P. (1990) Analysis of total phenols and other oxidation substrates and antioxidants by means of Folin-Ciocalteu reagent. *Methods Enzymol*., 299, pp. 152–178.

40. Murzakhmetova M., Moldakarimov S., Tancheva L., Abarova S., Serkedjieva J. (2008) Antioxidant and prooxidant properties of a polyphenol-rich extract from *Geranium sanguineum* L. *in vitro* and *in vivo*. *Phytother. Res.*, 22, pp. 746–751. https://doi.org/10.1002/ptr.2348.

41. Pires, S. M., Reis, R. S., Cardoso, S. M., Pezzani, R., Paredes-Osses, E., Seilkhan, A., ... & Sharifi-Rad, J. (2023). Phytates as a natural source for health promotion: A critical evaluation of clinical trials. *Frontiers in Chemistry*, 11, pp. 1174109. https://doi.org/10.3389/fchem.2023.1174109.

42. Ijaz S., Iqbal B.A., Abbasi Z., Ullah T., Yaseen S. (2023) Rosmarinic acid and its derivatives: Current insights on anticancer potential and other biomedical applications. *Biomed. Pharm*., 162, pp. 114687. https://doi.org/10.1016/j.biopha.2023.114687.

43. Syraiyl S., Ydyrys A., Askerbay G. and Aitbekov R. (2024) Chemical composition and biological uses of *Artemisia schrenkiana* Ledeb. *BIO Web Conf.* 100:04039. https://doi.org/10.1051/bioconf/202410004039.

44. Imanaliyeva, M., Kyrbassova, E., Aksoy, A., Vardar, M. C., Sadyrova, G., Parmanbekova, M., ... & Tynybekov, B. (2024). Ecological Monitoring of G. olivieri Griseb Populations, A Medicinal and Food Plant. *ES Food & Agroforestry*, 17, pp. 1245.

45. Aitbekov, R., Zhamanbayeva, G., Aralbaeva, A., Zhunussova, G., Zhumina, A., Zhusupova, A., ... & Ydyrys, A. (2024). Pharmacological Composition of Thymus Serpyllum and Its Components. *ES Food & Agroforestry*, 17, pp. 1244. http://dx.doi.org/10.30919/esfaf1244.

46. Ashirova, Z. B., Kuzhantaeva, Z. Z., Abdrassulova, Z. T., Shaimerdenova, G. Z., & Atanbaeva, G. K. (2021). Studying phytochemical features of three Asteraceae herbs growing wild in Kazakhstan. *Floresta e Ambiente*, 28(4), e20210060. https://doi.org/10.1590/2179-8087-floram-2021-0060.

47. Ashirova, Z. Z., Kuzhantaeva, Z. Z., Rakhimova, Z. S., Kuraspayeva, A. Z., Abdrassulova, Z. T., & Shaimerdenova, G. Z. (2018). Changes in the taxonomy based on phytochemistry of the species of the Rose family (Rosaceae). *Journal of Pharmaceutical Sciences and Research*, 10(12), pp.3261.

Information about authors:

Alibek Ydyrys – (corresponding author) – PhD, Professor, Biomedical Research Centre, Al-Farabi Kazakh National University, Almaty, Kazakhstan, e-mail: ydyrys.alibek@gmail.com

Gulnaz Askerbay – 2nd year PhD student, Faculty of biology and biotechnology, Al-Farabi Kazakh National University, Almaty, Kazakhstan, e-mail: askerbaygulnaz1@gmail.com

Zhadyra Ashirova – PhD, Al-Farabi Kazakh National University, Almaty, Kazakhstan, e-mail: zhadyra.ashirova@kaznu.edu.kz

Jiasharete Jielile – PhD, Professor, Department of Orthopaedics Centre, First Teaching Hospital of Xinjiang Medical University, Urumqi, Xinjiang Uygur Autonomous Region, China, e-mail: jiasharete jielilej@foxmail.com

Marzhanay Ilesbek – 1st year PhD student, Faculty of Biology and Biotechnology, Al-Farabi Kazakh National University, Almaty, Kazakhstan, e-mail: milesbek01@gmail.com

S. Satayeva [1] , F. Akhmetova [1*] , S. Yermukhanova [1] ,

G. Gubaidullina [1] , A. Abdrakhmanova [2] , M. Ibrayeva [3] ,

M. Ozturk [4] , T. Utepova [2]

[1]Zhangirkhan West-Kazakhstan Agrarian Technical University, Uralsk, Kazakhstan
[2]M. Utemisov West Kazakhstan University, Uralsk, Kazakhstan
[3]Yessenov University, Aktau, Kazakhstan
[4]Mugla Sıtkı Koçman University, Mugla, Turkey
*e-mail: firuza.92@mail.ru

Use of local raw materials to obtain glass used in glazing of ceramic products

Abstract. Glass is one of the widely used materials in the construction industry and in everyday life. The year-on-year growing demand for various types of glass products pushes the glass-making industries to increase their production volumes and not to lower their quality levels. The scientific and technical progress in glass extraction has gradually expanded the area of its effective use. In recent years, significant changes have taken place in the glassmaking technique. New production methods and ways of improving existing technological processes appeared, and new areas of glass application began to open. The chemical composition of the product was changed, and different types of glass were made. In this regard, the study of the method of obtaining glass with different properties is one of the most important issues. In order to prepare the composition of colored glass used in the production of various products, colored glass was obtained in laboratory conditions. Physico-chemical properties of the obtained colored glass were studied in order to determine the area of application. Based on the research results, the obtained colored glass can be used for decorative purposes.

Key words: colored glass, glass charge, sand, soda, slaked lime, thermal stability, chemical stability.

Introduction

Glass is an amorphous material obtained by cooling the melt. Raw materials used in glass production are conditionally divided into basic and auxiliary. Main raw materials for glass production: quartz sand, soda, dolomite, feldspar, calcium carbonate, etc.; and auxiliary raw materials include bright color givers, decolorizers, dyes, quenchers, oxidizers (carbon substances) [1-3].

Quartz sand is the main material used in the introduction of silica into the composition of glass. Silica SiO_2 is the main component of silicate glass. The main requirement for sand is to have a large amount of SiO_2 in it, and a very small number of impurities (including iron oxides). The silica content of the sand used in glass baking should not be less than 95%. In addition, the sand contains additives that change the color of the glass mass during the glass baking process. Such additives include iron oxide, titanium, vanadium, chromium oxides. The amount of these additives should be very small. Pure quartz glass is obtained from quartz sand. It requires a temperature of 1850-1950 ºC. That is, the melting temperature of sand is very high and requires a long time [4-7].

That's why other additives are added in order to reduce the melting point of sand in glass production [8]. It includes naturally occurring chalk, marble, feldspar, etc. In addition to minerals, synthetic additives can also be used. These additives give different properties to the glass.

The presence of alkali metal oxides (Na_2O, K_2O) in the glass reduces its thermal and chemical stability, reduces its mechanical and dielectric properties. It also reduces melt viscosity and glass baking temperature. The amount of alkali metal oxides in the glass does not exceed 14-15%. Sodium oxide is introduced using soda ash and sodium sulfate, and potassium oxide is introduced using potash and

saltpeter. Calcined soda is the main material used in the introduction of sodium oxide into glass. A white powder that dissolves well in water. During the glass baking process, soda decomposes into sodium oxide and carbon dioxide. Sodium sulfate Na_2SO_4 is difficult to decompose during glass baking. That is why carbon reducers (coal, sawdust) are added to the charge. The purpose of adding sodium sulfate to the charge is not to replace soda ash, but to facilitate the glass baking process. Potash K_2CO_3 consists of 68.2% K_2O and 31.8% CO_2. An artificial white compound that dissolves easily in water. Calcined potash is used in glass production. The use of potassium oxide instead of sodium oxide increases the transparency and gloss of the glass. Coloration of glass depends on the type of dye, its concentration, properties and oxidation-reduction conditions. One type of dye can color the glass in different colors depending on the process conditions and concentration. Chromium, manganese, iron, cobalt, nickel, copper, selenium, cadmium, uranium, sulfur, tellurium compounds are used as dyes to give color to glass [9-13].

Thermal properties of glass describe its ability to change as a result of heating or cooling. These properties include thermal stability, heat capacity, thermal conductivity, and thermal expansion of glass [14].

The thermal stability of the glass depends on its homogeneity and the state of the surface layer. If the glass is poorly annealed (after heat treatment), the thermal stability is low because the stress is not evenly distributed on its surface. Therefore, determining the thermal stability of glass is one of the methods of controlling the quality of glass firing. As a result of annealing the glass, its surface layer is without any defects. This increases the thermal stability of the product by 1.5-2 times. Annealing and fusible acid treatment eliminate defects in the surface layer of glass and increase its thermal stability [15].

When determining thermal stability, a sample of a glass product is heated to a certain temperature, and the heated sample is placed in cold water and its change is observed [16].

Materials and methods

Sand from the Karatobe deposit in the West Kazakhstan region was used as local raw material. A batch was prepared from the raw material from the Karatobe deposit and glass was obtained.

Determination of the thermal stability of the glass was carried out according to the Standard 25535-2013. Methods for determining the thermal

stability of glass according to the standard are based on determination by heating and cooling the glass, considering the temperature difference of the heating and cooling medium.

The test is carried out on a finished product or sample with a size of 150x150 mm. Samples that have not undergone preliminary mechanical and heat treatment are taken for testing. Before the test, the samples are kept for 30 minutes in the test place at a temperature of not less than 18 ºC.

Equipment required for testing:

1) Hot water tank. The water in the tank should be changed regularly. The temperature variation of the water in the tank should not exceed 1 ºC. The volume of water should be 2 times more than the volume of the samples to be tested.

2) An electric oven heated up to 350 ºC with the ability to change the temperature. The deviation of the oven temperature from the set temperature should not exceed 1 ºC.

3) Cool water tank. The water in the tank needs to be replaced. Water temperature variation should not exceed 1 ºC. The volume of water in the tank should be 5 times more than the size of the samples.

4) A device for measuring temperature with a measurement error of ±1 ºC.

5) Sample transport containers.

6) Holders used to transport specimens.

The temperature of the test place should not be lower than 18 ºC. The temperature of the cold water in the tank should be between 5 ºC and 27 ºC. During the test, the temperature of the heating and cooling medium is determined considering the purpose of the test and the possible thermal stability of the sample.

When calculating the composition of the charge according to the specified glass composition, the composition of the charge is calculated per 100 g of net weight of sand or 100 g of net weight of glass. Usually, in practice, the composition of the charge is calculated per 100 g of net weight of glass. During such calculations, the theoretical yield of glass, losses during the glass melting process and the theoretical composition of glass are calculated. The theoretical composition of glass differs from the specified composition of glass due to the influence of contamination of raw materials. Chemically pure materials are used so that the theoretical and specified composition of the glass is the same. In this case, the theoretical and established composition of glass does not differ from each other. But it differs from the composition of the glass, which is determined by chemical analysis and depends on the conditions of the glass melting process.

*Calculation of charge composition from chemically pure raw materials*

The composition of raw materials used in the production of glass containing SiO_2 75%, CaO 10%, Na_2O 15% is given: sand SiO_2 100%, slaked lime $Ca(OH)_2$ 100%, soda Na_2CO_3 100%.

Calculation of the composition of the charge per 100 g of glass (Table 1).

Determination of the amount of sand:

$$100 \text{ g sand} ----- 100\% \ SiO_2$$
$$x \text{ g sand} ----- 75\% \ SiO_2$$
$$x = \frac{100*75}{100} = 75 \text{ g } SiO_2$$

Determination of the amount of slaked lime. Slaked lime decomposes during the process:

$$Ca(OH)_2 = CaO + H_2O$$
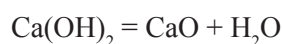
$$100\%: 74.09 \text{ g } Ca(OH)_2 ----- 56.08 \text{ g CaO}$$
$$y \text{ g } Ca(OH)_2 ----- 10\% \text{ CaO}$$
$$y = \frac{74,09*10}{56,08} = 13.21 \text{ g } Ca(OH)_2$$

Determining the amount of soda. Sodium oxide passes through the glass according to the following reaction:

$$Na_2CO_3 = Na_2O + CO_2$$
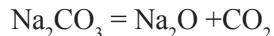
$$100\%: 105.98 \text{ g } Na_2CO_3 ----- 61.98 \text{ g } Na_2O$$
$$z \text{ g } Na_2CO_3 ----- 15\% \ Na_2O$$
$$z = \frac{105,98*15}{61,98} = 25.65 \text{ g } Na_2CO_3$$

Considering that 5% of Na_2O evaporates during the process, 25.65×1.05=26.93 g of soda is obtained.

Table 1 – Theoretical composition of glass to obtain 100 g of glass

Batch composition		The amount of oxides passing into the glass, %		
Raw material	Mass, g	SiO_2	Na_2O	CaO
Sand	75.00	75.00	-	-
Soda	26.93	-	15	-
Slaked lime	13.21	-	-	10
Total	115.14	75	15	10

Results and discussion

In order to obtain colored glass, color-giving compounds were added to the composition of the charge prepared according to the calculated glass composition. When producing colored glass, not only metal oxides, but also salts of the color-giving metal were used as a color-giving compound. The coloring compounds used to obtain colored glass during the work are listed in Table 2.

Table 2 – Coloring compounds that give color to glass

Coloring compounds	Amount (%)	Color
CuO	0.1-0.2	Blue
MnO_2	0.01-0.05	Purple
S	1-2	Black
Cr_2O_3	0.05-0.1	Green
$CoCl_2 \cdot 6H_2O$	0.09-0.1	Blue
$NiSO_4 \cdot 7H_2O$	0.1-0.2	Brown

During the process of glass extraction, glass batches of two different compositions were placed in crucibles and placed in a furnace with the required temperature. After the temperature reached the desired level, the glass baking process continued for 20-30 minutes. As a result of the process, colored glass was obtained from the charge of the first composition between 800-900 ºC. And the glass from the charge of the second composition was ready at 1000-1100 ºC. Further analysis of physico-chemical properties of obtained glasses of two different compositions was carried out.

During the determination of the thermal stability of the glass in the first composition, the possible thermal stability started from 90 ºC. After that, during each repetition, the temperature of the furnace increased by 10 ºC. As a result, when the temperature reached 140 ºC, changes in the appearance of the glass were observed. When the temperature was 160ºC, the glass sample was divided into particles (Table 3).

Table 3 – The result of determining the thermal stability of colored glass in the first composition

Temperature, ºC		The condition of the sample
furnace	water	
100	18	unchanged
120	18	unchanged
130	18	unchanged
140	18	irritation was observed
150	18	the edge began to crack
160	18	divided into parts

Based on the results of the analysis, the thermal stability of colored glass in the first composition was determined:

$$\Delta T = 160 \text{ ºC} - 18 \text{ ºC} = 142 \text{ ºC}$$

According to this method, work was carried out to determine the thermal stability of colored glass in the second composition. As a result, changes in the appearance of the glass were observed at 160 ºC. And at 200 ºC, the glass was divided into particles. Based on the result, the thermal stability of colored glass in the second composition was determined (Table 4).

Table 4 – The result of determining the thermal stability of the glass in the second composition

Temperature, ºC		The condition of the sample
furnace	water	
100	18	unchanged
120	18	unchanged
140	18	unchanged
160	18	unchanged
170	18	unchanged
180	18	irritation was observed
190	18	the edge began to crack
200	18	divided into parts

Thermal stability of glass in the second composition:

$$\Delta T = 200 \text{ ºC} - 18 \text{ ºC} = 182 \text{ ºC}$$

Based on the results of determining the chemical stability of the glass in the first composition, it was determined that it belongs to the third hydrolytic class, calculating the amount of hydrochloric acid used for titration (Table 5).

Table 5 – The result of determining the chemical stability of glass in the first composition

Chemical stability	Hydrolytic class
Volume of HCl solution, ml	
0.9	3

Based on the results of determining the chemical stability of the glass in the second composition, it was determined that it belongs to the third hydrolytic class, calculating the amount of hydrochloric acid used for titration (Table 6).

Table 6 – The result of determining the stability of the glass in the second composition

Chemical stability	Hydrolytic class
Volume of HCl solution, ml	
1.5	3

Conclusion

According to the conducted research, the following conclusion was made: colored glass was obtained as a result of the addition of compounds that give color to the prepared charge. Colored glass of the first composition was ready at 800-900 ºC, and glass of the second composition at 1000-1100 ºC; physico-chemical properties of obtained colored glasses were studied. According to the thermal and chemical stability of the glass, it was determined that the thermal stability of the glass in the first composition is between 140-160 ºC, and it belongs to the 3rd hydrolytic class according to its chemical stability. The thermal stability of the glass in the second composition is about 180-200 ºC, its chemical stability belongs to the 3rd hydrolytic class.

In the course of determining the area of application of the obtained colored glass, the possibility of using it as a glaze used in the coating of ceramic products was considered.

Conflict of interest

All authors have read and are familiar with the content of the article and have no conflict of interest.

References

1. C. Bedon, X. Zhang, F. Santos, D. Honfi, M. Kozłowski, M. Arrigoni, L. Figuli, D. Lange. (2018) Performance of structural glass facades under extreme loads – design methods, existing research, current issues and trends. *Construct. Build. Mater*., 163, pp. 921-937. https://doi.org/10.1016/j.conbuildmat.2017.12.153.

2. Silva, J. de Brito, P.L. Gaspar. (2011) Service life prediction model applied to natural stone wall claddings (directly adhered to the substrate). *Construct. Build. Mater*., 25(9), pp. 3674-3684. https://doi.org/10.1016/j.conbuildmat.2011.03.064.

3. Ferreira, A. Silva, J. de Brito, I.S. Dias, I. Flores-Colen. (2021) Definition of a condition-based model for natural stone claddings. *J. Build. Eng*., 33, pp. 101643. https://doi.org/10.1016/j.jobe.2020.101643.

4. Sala R., Deom, J.-M. (2010) Medieval tortkuls of northern tienshan and mid-low syrdarya, in: Masanov, N.E. (Ed.), Proceedings of the International Conference in Commemoration of N.E. Masanov, Almaty 22–23 April 2010, pp. 263-286.

5. Baibosynov K.B., Baipakov K.M., Lobas D.A. (2002) Tortkuli (3), in: Svod Pamyatnikov Istorii i Kul'tury Respubliki Kazahstan. Jambylskaya Oblast'. Almatry: RGP "NIPI PMK", p. 350

6. Martínez Ferreras V., Fusaro A., Gurt Esparraguera J.M., Arino ˜ Gil E., Pidaev S.R., Angourakis A. (2019) The islamic ancient termez through the lens of ceramics: a new archaeological and archaeometric study. *Iran*, 58(2), pp. 250-278. https://doi.org/10.1080/05786967.2019.1572430.

7. Matin M., Tite M., Watson O. (2018). On the origins of tin-opacified ceramic glazes: New evidence from early Islamic Egypt, the Levant, Mesopotamia, Iran, and Central Asia. *J Archaeol Sci*., 97, pp. 42-66. https://doi.org/10.1016/j.jas.2018.06.011.

8. Yeleuov M., Akymbek Y., Chang C. (2014) Sphero-conical vessels of Aktobe medieval ancient settlement. *Life Sci. J*., 11, pp. 384-387. https://doi.org/10.7498/aps.63.224101.

9. Buildings and climate change: status, challenges, and opportunities. United Nations Environment Programme. European Commission DG ENV: News Alert, issue 71, 2007.

10. T.L. Bergman, A.S. Lavine, F.P. Incropera, D.P. Dewitt. (2011) Introduction to heat transfer, 6 ed. United States of America: John Wiley & Sons, Inc., 960 p. ISBN 0470501960.

11. M.A. Shameri, M.A. Alghoul, K. Sopian, M.F.M. Zain, O. Elayeb. (2011) Perspectives of double skin façade systems in buildings and energy saving. *Renew. Sustain. Energy Rev*., 15(3), pp. 1468-1475. https://doi.org/10.1016/j.rser.2010.10.016.

12. C. Pereira, J. de Brito, J.D. Silvestre. (2018) Contribution of humidity to the degradation of façade claddings in current buildings. *Eng. Fail. Anal*., 90, pp. 103-115. https://doi.org/10.1016/j.engfailanal.2018.03.028.

13. W. Ochen, F.M. D'Ujanga, B. Oruru, P.W. Olupot. (2021) Physical and mechanical properties of porcelain tiles made from raw materials in Uganda. *Results in Materials*, 11, pp. 100195. https://doi.org/10.1016/j.rinma.2021.100195.

14. K. Dana, S.K. Das. (2008) Enhanced resistance to thermal cycling of slag-containing vitrified porcelain tiles. *Ind. Ceram*., 28(2), pp. 121-124.

15. T. Kopar, V. Ducman. (2002) Characterisation of frost damage to ceramic tiles in Slovenia. *Tile & brick international,* 18(5), pp. 314–317. https://plus.cobiss.net/ cobiss/si/en/bib/770151.

16. M. Tite, R. Mason. (1994) The beginnings of islamic stonepaste technology. *Archaeometry,* 36, pp. 77-91. https://doi.org/10.1111/j.1475-4754.1994.tb01066.x.

Information about authors:

Safura Satayeva – Candidate of Chemical Sciences, Ass. Professor, Zhangirkhan West-Kazakhstan Agrarian Technical University, Uralsk, Kazakhstan; e-mail: sataeva_safura@mail.ru

Firuza Akhmetova – (corresponding author) – Master of Technical Sciences, Senior Lecturer, Zhangirkhan West-Kazakhstan Agrarian Technical University, Uralsk, Kazakhstan; e-mail: firuza.92@mail.ru

Svetlana Yermukhanova – Master of Technical Sciences, Senior Lecturer, Zhangirkhan West-Kazakhstan Agrarian Technical University, Uralsk, Kazakhstan; e-mail: svetok_88-88@mail.ru

Gulkhan Gubaidullina – Candidate of Chemical Sciences, Zhangirkhan West-Kazakhstan Agrarian Technical University, Uralsk, Kazakhstan; e-mail: ggulkhan@mail.ru

Aibarsha Abdrakhmanova – Master of Technical Sciences, senior lecturer of M. Utemisov West Kazakhstan University, Uralsk, Kazakhstan; e-mail: aibarsha--61@mail.ru

Manshuk Ibrayeva – PhD, Senior Lecturer, Yessenov University, Aktau, Kazakhstan; e-mail: nykmukanova@mail.ru

Mehmet Ozturk – Professor, Department of Chemistry, Mugla Sıtkı Koçman University, Mugla, Turkey; e-mail: mehmetsadettin@gmail.com

Tilekshi Utepova – 1ˢᵗ year master student, Utemisov West Kazakhstan University, Uralsk, Kazakhstan, e-mail: tlekshi.utepova@mail.ru

A.G. Gappar * , A.K. Kipchakbayeva

Al-Farabi Kazakh National University, Almaty, Kazakhstan
*e-mail: gappar2018@mail.ru

Chemical composition and potential pharmacological properties of field horsetail extract based on GC-MS analysis

Abstract. The *Equisetaceae* family, particularly the species *Equisetum arvense*, has long attracted the attention of researchers due to its ancient origins and various applications in traditional medicine. Field *Equisetum arvense* has been used to treat inflammation, wounds, infections, and urinary tract diseases. In this study, a phytochemical analysis of the *Equisetum arvense* extract was conducted using gas chromatography-mass spectrometry (GC-MS) to examine its chemical composition and assess its wound-healing properties. The *Equisetum arvense* extract was obtained through percolation with ethanol, followed by treatment with diethyl ether and chloroform to isolate nonpolar compounds. Final purification of the extract was carried out using aluminum oxide. The GC-MS method revealed a variety of compounds, including terpenes and fatty acids. Among these were components with anti-inflammatory, antibacterial, and antioxidant properties that may aid in accelerating wound healing. The primary components of the extract associated with wound-healing effects include quercetin, kaempferol, and β-sitosterol. The phytochemical analysis confirmed significant antioxidant properties in the extract, which may help protect tissues from oxidative stress that occurs during wound healing. The identified antibacterial compounds may help prevent wound infections and accelerate tissue regeneration. Thus, the *Equisetum arvense* extract, processed with chloroform and diethyl ether, represents a promising source of bioactive compounds with potential for application in the development of wound-healing agents.

Key words: *Equisetum arvense*, quercetin, kaempferol, β-sitosterol, antioxidant properties, wound-healing effect.

Introduction

In the past decade, interest in natural plant extracts with therapeutic properties has significantly increased. This trend is driven by a growing number of studies focused on identifying safe and effective alternatives to synthetic drugs, which can cause side effects and possess high toxicity with prolonged use. One promising source of natural compounds is *Equisetum arvense*. *E. arvense* are perennial, spore-bearing, herbaceous plants and ancient vascular plants in the class *Equisetopsida*, represented in modern flora by the single genus *Equisetum*. There are over 30 species of horsetail, distributed worldwide except for Australia, New Zealand, and tropical Africa [1,2].

Field *Equisetum* is a widespread weed. It grows in fields, meadows, wastelands, ravines, roadside ditches, and on road slopes. The specific name *arvensis* refers to its habitat. Among all species of *Equisetum*, *E. arvense* is the officially recognized medicinal plant. It grows in meadows, spruce forests, light coniferous forests, lime, aspen, pine-birch, birch, and mixed forests. It prefers floodplain forests, riverbanks, and shrub thickets. As a weed, it frequently occurs in fields and gardens. It can also be found along roadsides, on railway embankment slopes, near ditches, and in sandy and clay pits and excavations. In crops, it is quite abundant and is considered one of the most difficult-to-eradicate rhizomatous weeds [3-5].

Equisetum arvense has been traditionally used to treat various conditions, including inflammation, infections, and urinary tract disorders. However, its potential to accelerate wound healing has garnered particular interest and requires detailed scientific investigation.

Traumatic skin injuries, such as wounds, burns, and ulcers, present a significant medical challenge, especially when the healing process is hindered by factors such as infections or chronic illnesses. Developing new plant-based treatments to promote tissue regeneration has both theoretical and practical importance. Bioactive plant components, such as flavonoids, phenolic acids, and terpenes, have

demonstrated anti-inflammatory, antioxidant, and antimicrobial properties, which may aid the healing process.

Literature indicates that *Equisetum arvense* extracts contain several compounds with potential wound-healing properties. However, the chemical composition and mechanisms of action of these extracts in wound healing remain inadequately studied. Gas chromatography-mass spectrometry (GC-MS) offers a precise method for identifying the chemical compounds in the extract and assessing their biological activities. This opens up new possibilities for developing phytopreparations based on field horsetail that could effectively promote tissue regeneration.

The aim of this study is to investigate the chemical composition of *Equisetum arvense* extract, obtained through percolation and treated with chloroform, diethyl ether, and aluminum oxide, followed by an evaluation of its wound-healing properties.

Materials and methods

For this study, *Equisetum arvense* leaves were collected in the summer of 2023 from Shelek village, Almaty region, Kazakhstan, at coordinates [43.600817, 78.217464] (Figure 1). The plant material was identified by botanists and certified as corresponding to the *Equisetum arvense* species.
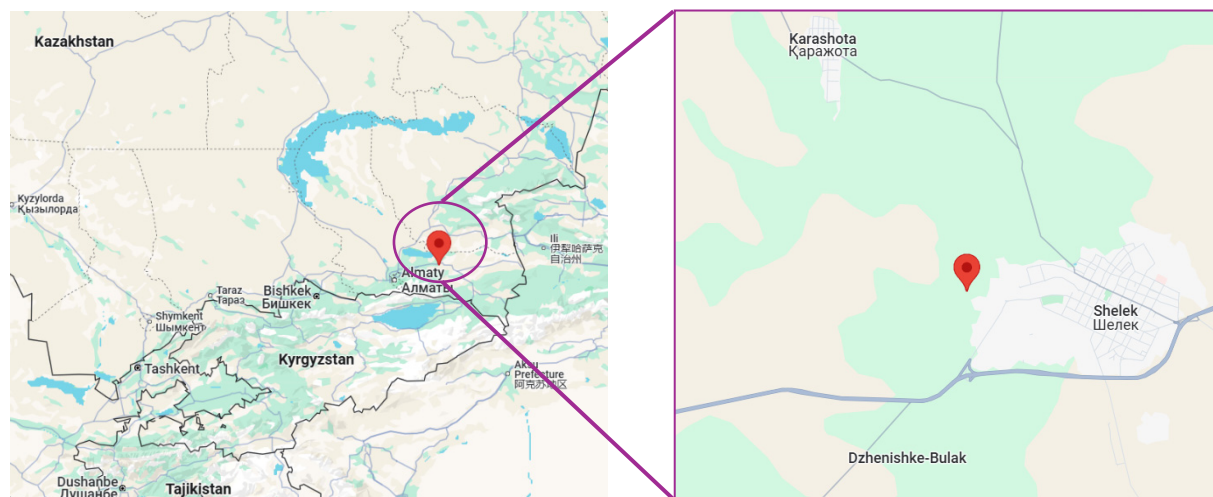
Figure 1 – The coordinates used for collecting field horsetail leaves

Extraction was conducted using ethanol (Talgar-Spirt, Kazakhstan) and other organic solvents, including chloroform (Baza 1 Khimreaktivov, Russia) and diethyl ether. Activated aluminum oxide was used for extract purification.

The component composition of the plant extract was analyzed on a TRACE 1310 gas chromatograph (Thermo Fisher Scientific, USA) equipped with a TSQ 8000 triple quadrupole mass spectrometric detector (Thermo Fisher Scientific, USA). Chromatographic separation was carried out using a TG-5SILMS capillary column (30 m × 0.25 mm × 0.25 μm). Helium was used as the carrier gas with a constant flow of 1 mL/min. The initial temperature of the column thermostat was set at 70°C with a 2-minute hold, then increased to 200°C at a rate of 5°C/min with a 1-minute hold, and then to 285°C at 10°C/min with a 10-minute hold, followed by cooling back to the starting temperature of 70°C. The injector temperature was set at 250°C, and the mass spectrometric detector temperature at 260°C. The extract was injected in a volume of 1 μL in split mode (split ratio 1:10). The ionization mode was EI at 70 eV, with the ion source temperature at 230°C, and the scan range set to m/z 50-550 in Full scan mode. The chromatography process was controlled using XCalibur software. Bioactive compounds from two extractions were identified based on GC retention time using a library of reference mass spectra and NIST software (National Institute of Standards & Technology) for GC-MS data.

Results and discussion

To extract bioactive compounds from *Equisetum arvense*, solvents were selected, and extraction conditions optimized. To improve the extraction process, the effects of the raw material-to-solvent ratio, extraction time, and temperature were examined. The optimal extraction conditions were found to be 70% ethanol (1:8 raw material-to-extractant ratio, 2 hours, room temperature), yielding up to 60% bioactive compounds (biologically active complex).

The moisture content of the aerial part of *Equisetum arvense* was 5.44%, and ash content was 2.7%. The higher concentration of extractives at 70% ethanol is attributed to increased solubility of bioactive compounds at higher ethanol concentrations, enhancing extraction efficiency. This is influenced by various factors, including solubility of bioactive compounds, extraction intensity, and cell structure dissociation.

The most common biologically active complex groups in *Equisetum arvense* include coumarins (1.8%), free organic acids (1.83%), and saponins (1.2%), all essential components of the plant. *Equisetum arvense* contains coumarins, which have anti-inflammatory and anticoagulant properties and positively affect blood circulation. Free organic acids, such as malic and citric acids, aid digestion and possess antimicrobial properties. Saponins act as natural surfactants and have immunomodulatory and anti-inflammatory effects. Quantitative analysis revealed small amounts of flavonoids (0.62%) and alkaloids (0.5%).

Our chemical study revealed that *Equisetum* species vary in chemical composition, which may explain differences in their pharmacological properties. *Equisetum arvense* contains phenolic compounds (flavonoids, phenolcarboxylic acids) in quantities of 1.5% or higher [6]. More than 35 macro- and microelements were also detected, with maximum concentrations for manganese (30.39 µg/g), iron (16.5 µg/g), and zinc (11.4 µg/g). Iron, zinc, and manganese play significant roles in human health. Iron is essential for hemoglobin, necessary for oxygen transport throughout the body, and participates in metabolic processes and immune function. Zinc is vital for growth and development, immune system function, hormone formation, and the health of skin, hair, and nails. Manganese is part of many enzymes necessary for metabolism, anti-inflammatory processes, and antioxidant defense. All these elements are crucial

for maintaining human health and proper body functioning.

Among the macroelements, potassium (701 µg/g), calcium (130 µg/g), and magnesium (700 µg/g) showed the highest concentrations. Potassium, calcium, and magnesium are also vital in the human body. Potassium is involved in regulating osmotic pressure, muscle and nerve function, maintaining a healthy heart rhythm, and controlling blood pressure. Calcium is a primary component of bones and teeth, necessary for normal muscle function, nerve impulse transmission, and blood clotting. Magnesium plays an essential role in over 300 biochemical reactions in the body, including protein and nucleic acid synthesis, muscle and nerve function, heart rhythm regulation, and maintaining healthy bone tissue metabolism. All these macronutrients are important for human health and proper body function [7].

The volatile components of *Equisetum arvense* were first studied using GC-MS, which identified twenty-five compounds. The primary components were cucurbitacin b, 25-desacetoxy-, rapamycin, Z,Z-2,5-Pentadecadien-1-ol, ergosta-5,22-dien-3-ol, acetate and geranyl isovalerate . The components of lipophilic extraction were identified by comparing the retention time and total mass spectra with the corresponding data from the Wiley275 and NIST98 libraries. The content of individual substances is calculated from the peak area, without the use of calibration coefficients with programmed automatic integration. Components with concentrations above 0.005% and a probability of matching mass spectra of more than 80% are taken into account. The repetition of the definitions is threefold.

The disc diffusion method was used to assess the antimicrobial activity of the oil against several microorganisms, including bacteria (*Staphylococcus aureus, Escherichia coli, Klebsiella pneumoniae, Pseudomonas aeruginosa*, and *Salmonella enteritidis*) and fungi (*Aspergillus niger* and *Candida albicans*). Dilution of horsetail essential oil at a 1:10 ratio demonstrated high antimicrobial activity against all tested strains [8].

These compounds were isolated for their diuretic, antioxidant, vasorelaxant, germination-inhibiting, antinociceptive, and anti-inflammatory effects.

In the ethanolic extract of *Equisetum arvense*, 25 bioactive phytochemical compounds were identified and characterized based on peak area, retention time, molecular weight, and formula (Table 1, Figure 2). These chemical components may prove beneficial in various herbal medicines, such as anti-inflammatory,

analgesic, antipyretic, cardiotonic, and anti-asthmatic drugs. Horsetail has traditionally been used for baths in treating rheumatic conditions, gout, as well as in the treatment of tumors and bone fractures in Europe. The plant is rich in sterols, ascorbic acid, phenolic acids, and flavonoids. Studies have shown that it possesses anti-inflammatory, antimicrobial, and analgesic properties.

Table 1 – Bioactive phytochemical compounds in the ethanol extract of field horsetail

No.	Compound	Molecular formula	RT	Content, %
1	Cucurbitacin b, 25-desacetoxy-	$C_{30}H_{44}O_6$	0.06	13.21
2	Rapamycin	$C_{51}H_{79}NO_{13}$	0.06	6.40
3	Z,Z-2,5-Pentadecadien-1-ol	$C_{15}H_{28}O$	5.44	30.46
4	Ergosta-5,22-dien-3-ol, acetate	$C_{30}H_{48}O_2$	0.06	7.94
5	Geranyl isovalerate	$C_{15}H_{26}O_2$	4.78	6.35
6	5-(Prop-2-enoyloxy)pentadecane	$C_{18}H_{34}O_2$	5.01	5.96
7	4-Dimethyl(dichloromethyl)silyloxypentadecane	$C_{18}H_{38}Cl_2OSi$	5.01	5.38
8	5-Cyclopropylcarbonyloxypentadecane	$C_{19}H_{36}O_2$	5.01	21.85
9	Acetamide, 2,2,2-trifluoro-	$C_2H_2F_3NO$	3.42	82.43
10	DL-Homocystine	$C_8H_{16}N_2O_4S_2$	6.09	6.31
11	d-Mannose	$C_6H_{12}O_6$	6.90	7.70
12	Hydroxylamine	H_3NO	1.58	93.89
13	6-(1-Methylethyl)-4,4,6-trimethyltetrahydro-1,3-oxazin-2-thione	$C_{10}H_{19}NOS$	3.18	10.88
14	Pterin-6-carboxylic acid	$C_7H_5N_5O_3$	3.74	6.96
15	Z,Z-2,5-Pentadecadien-1-ol	$C_{15}H_{28}O$	5.44	30.46
16	d-Glucopyranose, 4-O-б-D-galactopyranosyl-	$C_{12}H_{22}O_{11}$	8.18	8.42
17	Melibiose	$C_{12}H_{22}O_{11}$	12.62	5.37
18	Desulphosinigrin	$C_{10}H_{17}NO_6S$	13.68	9.51
19	N-Hydroxymethyl fluoroacetamide	$C_3H_4F_3NO2$	3.42	11.99
20	Benz[e]azulen-3(3aH)-one	$C_{17}H_{24}O_5$	0.16	6.74
21	Trichloromethane	$CHCl_3$	2.11	27.81
22	Pregan-20-one,2-hydroxy-5,6-epoxy-15-methyl-	$C_{22}H_{34}O_3$	4.78	9.00
23	DL-Cystine	$C_6H_{12}N_2O_4S_2$	3.67	7.02
24	1-Nitro-б-d-arabinofuranose, tetraacetate	$C_{13}H_{17}NO_{11}$	6.09	6.56
25	Carbon dioxide	CO_2	1.52	27.93
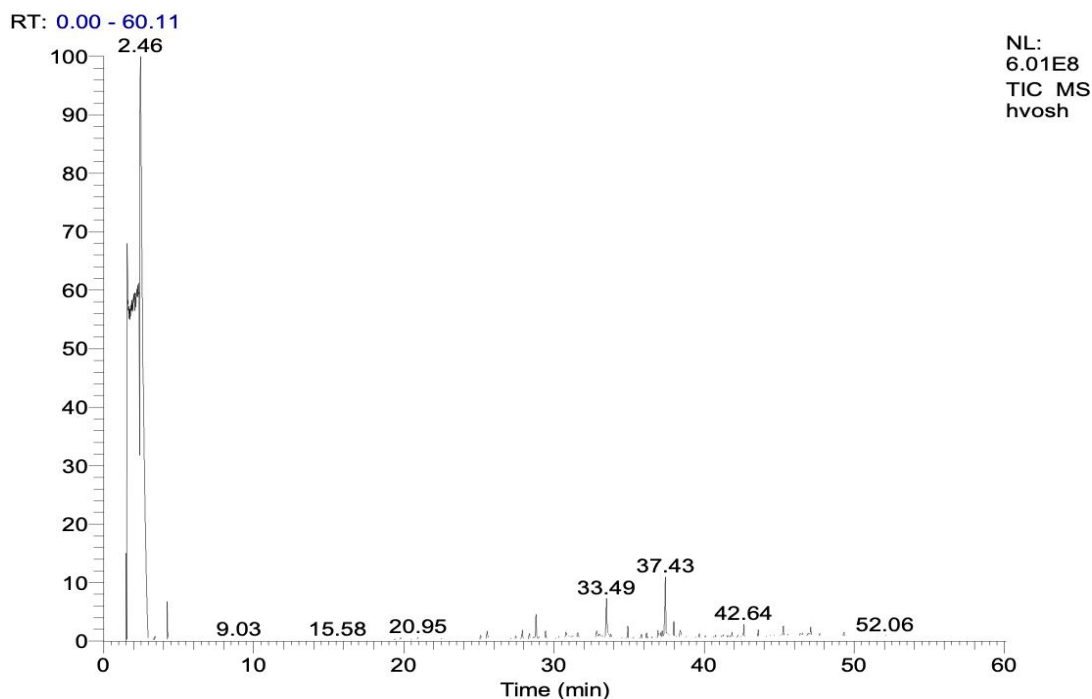
Figure 2 – Chromatogram of the GC-MS analysis of field horsetail extract *(Equisetum arvense)*

Equisetum arvense is particularly high in silicon, which is believed to significantly contribute to its medicinal properties, especially in bone diseases, while also providing diuretic, antioxidant, vasorelaxant, and sprouting-inhibitory effects, as well as antinociceptive and anti-inflammatory properties [9-15]. Acetylated flavonoid glycosides are common across all species of horsetail [16]. Studies on the antioxidant activity of field horsetail extracts have shown strong protective effects against free radicals, lipid peroxidation, and other oxidative agents [17].

Noteworthy phytochemicals found in horsetail include isobauerenol, taraxerol, germanicol, ursolic acid, oleanolic acid, and betulinic acid – the latter being a pentacyclic compound with known anticancer activity [18-20].

Conclusion

The findings of this study highlight the significance of *Equisetum arvense* extract in developing potential wound-healing agents based on natural components. Through phytochemical analysis using gas chromatography-mass spectrometry (GC-MS), a variety of bioactive compounds were identified, including phenolic acids and terpenes. These compounds demonstrated antioxidant, anti-inflammatory, and antibacterial properties, which

contribute to wound healing by protecting tissues from oxidative stress and preventing infection.

Key components of the extract that support its wound-healing effects include quercetin, kaempferol, and β-sitosterol. Quercetin and kaempferol are known for their potent antioxidant properties, which help reduce oxidative stress and protect cells from damage caused by free radicals. In addition, β-sitosterol exhibits anti-inflammatory effects, reducing tissue inflammation and thereby accelerating regeneration. These bioactive compounds also play a role in modulating the immune response, promoting cell proliferation, and enhancing collagen synthesis, which are essential steps in wound healing.

The extract's additional applications include its use as a diuretic and vasorelaxant, underscoring its broad therapeutic potential. The plant's high silicon content is also believed to support bone health by promoting tissue mineralization and strengthening bone structure. This property is particularly important in the treatment of bone fractures and conditions such as osteoporosis. Furthermore, the anti-inflammatory and antioxidant properties of the extract may provide significant relief in conditions related to chronic inflammation, such as arthritis.

In conclusion, *Equisetum arvense* extract may be a promising raw material for creating agents that accelerate wound healing and have a general strength-

ening effect on the body. Given its wide spectrum of beneficial effects, including its role in improving skin regeneration, reducing inflammation, and supporting bone health, the extract shows substantial potential in both therapeutic and preventive healthcare. Further research is needed to investigate the biochemical mechanisms of the identified compounds and their potential application in clinical practice. Such studies will help refine the development of targeted, effective phototherapeutic products for wound care and broader health applications.

Conflict of interest

All authors are aware of the article's content and declare no conflict of interest.

References

1. Botirov E.K., Bonacheva V.M., Kolomiets N.E. (2021). Chemical composition and biological activity of metabolites of the *Equisetum* L. genus plants. *Chemistry of Plant Raw Materials*, 1, pp. 5-26.

2. Buzuk G.N., & Elyashevich E.G. (2010). Pharmacognostic characteristics of field horsetail *Equisetum arvense* L. Literature review. *Pharmacy Bulletin*, 2(48), pp. 65-72.

3. Kolomiyets N.E. (2006) Plants of the Genus Equisetum. *Pharmacy*, 3, pp. 46-48.

4. Kurkin, V.A. (2007) Pharmacognosy: Textbook for the students of pharmaceutical universities. Samara: Samara State Medical University and Ofort, pp. 827-832.

5. Goncharova T.A. (2004) Encyclopedia of medicinal plants. Herbal treatments, 1, M., pp. 88-90.

6. Kolomiets N. E., Kalinkina G. I., & Bondarchuk R. A. (2008). Plants of the horsetail genus (*Equisetum* L.): promising sources of new medicinal drugs. *Educ. Bull. Consciousness*, 10(9), pp. 392-393.

7. Kolomiets N.E., Ageeva L.D., Abramets N.Yu. (2014). Elemental composition of species of the *Equisetum* L. genus. *Fundamental Research*, 8-6, pp. 1418-1421.

8. Radulović N, Stojanović G, Palić R. (2006) Composition and antimicrobial activity of *Equisetum arvense* L. essential oil. *Phytother Res*., 20(1), pp. 85-8. https://doi.org/10.1002/ptr.1815.

9. Altameme H. J., Hameed I. H., Abu-Serag N. A. (2015) Analysis of bioactive phytochemical compounds of two medicinal plants, *Equisetum arvense* and *Alchemila vulgaris* seeds using gas chromatography-mass spectrometry and Fourier-transform infrared spectroscopy. *Malaysian Applied Biology Journal*, 44 (4), pp. 47–58.

10. D'Agostino M., Dini A., Pizza C., Senatore F., Aquino R. (1984) Sterols from *Equisetum arvense*. *Boll Soc Ital Biol Sper*., 60(12), pp. 2241-5.

11. Broudiscou L.P., Papon Y., & Broudiscou A.F. (2000). Effects of dry plant extracts on fermentation and methanogenesis in continuous culture of rumen microbes. *Animal Feed Science and Technology*, 87, pp. 263-277.

12. Dos Santos J.G. Jr., Blanco M.M., Do Monte F.H., Russi M., Lanziotti V.M., Leal L.K., Cunha G.M. (2005) Sedative and anticonvulsant effects of hydroalcoholic extract of *Equisetum arvense*. *Fitoterapia*, 76(6), pp. 508-13. https://doi.org/10.1016/j.fitote.2005.04.017.

13. Aramwit P., Sangcakul A. (2007) The effects of sericin cream on wound healing in rats. *Biosci Biotechnol Biochem*., 71(10), pp. 2473-2477. https://doi.org/10.1271/bbb.70243.

14. Duke J., Bogenschutz J., du Cellier J., Duke P. (2002) Handbook of medicinal herbs, 2nd ed. Boca Raton, FL: CRC Press, 896 p. ISBN 9780429126581.

15. Do Monte F.H., dos Santos J.G. Jr., Russi M., Lanziotti V.M., Leal L.K., Cunha G.M. (2004) Antinociceptive and anti-inflammatory properties of the hydroalcoholic extract of stems from *Equisetum arvense* L. in mice. *Pharmacol Res*., 49(3), pp. 239-243. https://doi.org/10.1016/j.phrs.2003.10.002.

16. Nosrati Gazafroudi K., Mailänder L.K., Daniels R., Kammerer D.R., Stintzing F.C. (2024). From stem to spectrum: phytochemical characterization of five *Equisetum* species and evaluation of their antioxidant potential. *Molecules*, 29(12), p. 2821. https://doi.org/10.3390/molecules29122821.

17. Mimica-Dukic N., Simin N., Cvejic J., Jovin E., Orcic D., Bozin B. (2008). Phenolic compounds in field horsetail (*Equisetum arvense* L.) as natural antioxidants. *Molecules*, 13(7), pp. 1455-1464. https://doi.org/10.3390/molecules13071455.

18. Raghda Makia, Khulood W. Al-Sammarrae, Mohammad M.F. Al-Halbosiy and Mohammed H. Al-Mashhadani. (2022) Phytochemistry of the *Genus Equisetum* (*Equisetum arvense*). *GSC Biological and Pharmaceutical Sciences*, 18(02), pp. 283-289. https://doi.org/10.30574/gscbps.2022.18.2.0059.

19. Weber R. (2005). Equisetites aequecaliginosus sp. nov., ein Riesenschachtelhalm aus der spättriassischen Formation Santa Clara, Sonora, Mexico. *Revue de paléobiologie*, 24(1), pp. 331-364.

20. Sandhu N.S., Kaur Sarabjit, Chopra Divneet (2010). *Equisetum arvense*: pharmacology and phytochemistry-a review. *Asian journal of pharmaceutical and clinical research*, 3(3), pp. 146-150.

Information about authors:

Ablaikhan G. Gappar – (corresponding author) – master's student, Al-Farabi Kazakh National University, Almaty, Kazakhstan, e-mail: gappar2018@mail.ru

Aliya K. Kipchakbayeva – PhD, Senior Lecturer, Al-Farabi Kazakh National University, Almaty, Kazakhstan, e-mail: aliya_k85@mail.ru

Content